Schweizerische Eidgenossenschaft
Confédération suisse
Confederazione Svizzera
Confederaziun svizra

Eidgenössisches Departement für Umwelt, Verkehr, Energie und Kommunikation UVEK
Département fédéral de l'environnement, des transport, de l'énergie et de la communication DETEC
Dipartimento federale dell'ambiente, dei trasporti, dell'energia e delle communication DATEC

Bundesamt für Strassen
Office fédéral des routes
Ufficio federale delle Strade

Updated normative bridge load models to account for actual traffic effects and reliability demands across structure types

Révision du modèle de charge pour les ponts routiers en considérant les effets du trafic actuel et les exigences de fiabilité des différences entre les systèmes structuraux

Überarbeitung des Lastmodells für Brücken zur Berücksichtigung des heutigen Strassenverkehr Einwirkungen und der Anforderungen an die Zuverlässigkeit für verschiedene Bauwerkstypen

Ecole Polytechnique Fédérale de Lausanne
Prof. Alain Nussbaumer
Prof. Aurelio Muttoni
Dr Paola Miglietta
Dr Qianhui Yu
Dr Xhemsi Malja
Dr Adem Karasu

Eidgenössische Technische Hochschule Zürich
Prof. Andreas Taras
Stefan Martinolli

Research project BGT_20_02C_03
at the request of the Federal Roads Office FEDRO
August 2026 | 1830

Der Inhalt dieses Berichtes verpflichtet nur den (die) vom Bundesamt für Strassen unterstützten Autor(en). Dies gilt nicht für das Formular 3 "Projektabschluss", welches die Meinung der Begleitkommission darstellt und deshalb nur diese verpflichtet. Bezug: Schweizerischer Verband der Strassen- und Verkehrsfachleute (VSS)

Le contenu de ce rapport n'engage que les auteurs ayant obtenu l'appui de l'Office fédéral des routes. Cela ne s'applique pas au formulaire 3 « Clôture du projet », qui représente l'avis de la commission de suivi et qui n'engage que cette dernière. Diffusion : Association suisse des professionnels de la route et des transports (VSS)

The content of this report engages only the author(s) supported by the Federal Roads Office. This does not apply to Form 3 'Project Conclusion' which presents the view of the monitoring committee. Distribution: Swiss Association of Road and Transportation Experts (VSS)

La responsabilità per il contenuto di questo rapporto spetta unicamente agli autori sostenuti dall'Ufficio federale delle strade. Tale indicazione non si applica al modulo 3 "conclusione del progetto", che esprime l'opinione della commissione d'accompagnamento e di cui risponde solo quest'ultima. Ordinazione: Associazione svizzera dei professionisti della strada e dei trasporti (VSS)

Updated normative bridge load models to account for actual traffic effects and reliability demands across structure types

Révision du modèle de charge pour les ponts routiers en considérant les effets du trafic actuel et les exigences de fiabilité des différences entre les systèmes structuraux

Überarbeitung des Lastmodells für Brücken zur Berücksichtigung des heutigen Strassenverkehr Einwirkungen und der Anforderungen an die Zuverlässigkeit für verschiedene Bauwerkstypen

École Polytechnique Fédérale de Lausanne
Prof. Alain Nussbaumer
Prof. Aurelio Muttoni
Dr Paola Miglietta
Dr Qianhui Yu
Dr Xhemsi Malja
Dr Adem Karasu

Eidgenössische Technische Hochschule Zürich
Prof. Andreas Taras
Stefan Martinolli

Research project BGT_20_02C_03
at the request of the Federal Roads Office FEDRO
August 2026 | 1830

Imprint

Research centre and project team

Project management
Prof. Alain Nussbaumer

Members
Prof. Aurelio Muttoni
Prof. Andreas Taras
Stefan Martinolli
Dr Paola Miglietta
Dr Qianhui Yu
Dr Adem Karasu
Dr Xhemsi Malja

Advisory commission

President
Dr Hans Rudolf Ganz

Members
Prof. Ursula Freundt
Dr Armand Fürst
Ehfried Kölz
Dr Dimitrios Papastergiou
Dr Rudolf Vogt

Applicant
Federal Roads Office FEDRO

Source

The document can be downloaded free of charge from
https://www.mobilityplatform.ch/

August 2026

Table of contents

Table of contents **5**

List of illustrations **7**

List of tables **12**

List of abbreviations/symbols **14**

Summary **15**

Zusammenfassung **24**

Résumé **34**

1 Introduction **43**
1.1 Problem statement 43
1.1.1 Normative bridge traffic load models: historical background 43
1.1.2 Summary of critical review of LM1 47
1.2 Objectives of research 48
1.3 Scope and limitation of research 48

2 Methodology **51**

3 From WIM data to traffic modelling **53**
3.1 Selection of WIM data 53
3.2 Modelling of traffic 55
3.2.1 Traffic modelling semi-probabilistic method 55
3.2.2 Traffic modelling probabilistic method 57
3.2.3 Heavy vehicle lane distribution in JAM traffic simulation 57
3.2.4 Modifications to the algorithms for JAM traffic simulation 60

4 Design action effect on generic bridge types based on traffic simulation **61**
4.1 Generic bridge types representative of FEDRO 61
4.1.1 Transversal systems (Figure 14) 62
4.1.2 Longitudinal systems (Figure 15) 63
4.1.3 Cases investigated 63
4.2 Global action effects: longitudinal shear and bending results 65
4.2.1 Single lane analysis results 65
4.2.2 Double lane analysis results 66
4.2.3 Local action effects: transverse shear, bending and punching 69

5 Proposition of a new load model **71**
5.1.1 Investigated configurations of load models based on the analysis of WIM data 71
5.1.2 Definition of the New Load Model 1 (NLM1) for the first lane 72
5.1.3 Optimization of NLM1 including traffic on the second lane 74
5.1.4 Other considerations in developing New Load Model 1 (NLM1) 79
5.2 Summary of the proposed New Load Model 1 (NLM1) 85

6 Full probabilistic analysis on generic and specific bridge types 89
6.1 Introduction 89
6.2 Input parameters for the full-probabilistic analysis.....90
6.2.1 Probabilistic representation of action effects.....90
6.2.2 Probabilistic distribution of the sectional resistance 90
6.3 Results from the load model calibration 92
6.3.1 Evaluation of action sided model uncertainty 93
6.3.2 Performance of proposed load model 95
6.4 Interpretation of the results 99
6.4.1 Accuracy of existing load models 102
6.5 Second Lane analysis.....104

7 Implementation of a general procedure for updating traffic using the new load model (approach by Levels-of-Approximation) 107
7.1 Introduction 107
7.2 Limits of application..... 110
7.3 LoA I and II, workflows for deterministic examination 111
7.4 LoA III and IV, workflow for probabilistic examination 112

8 Conclusions.....117

9 Research needs 121

Bibliography 123

10 Appendix A: load model code development 129
10.1 Introduction 129
10.2 Design of new structures 129
10.2.1 Traffic load models on road bridges in the Eurocode 129
10.2.2 Traffic loads on bridges, Switzerland..... 134
10.2.3 Dynamic factors 135

11 Appendix B: Comparative study on the possible configurations for new load model..... 139
11.1 Action effect data analysis of selected cases (single lane), leading to possible configurations of normative load model..... 139
11.2 Action effect data analysis of selected cases 142
(double lane)..... 142
11.3 Application of the single lane load models..... 144
11.4 Comparisons between load models (double lane)..... 146

12 Appendix C: full-probabilistic analyses and input variables 149
12.1 Introduction to full-probabilistic analysis..... 149
12.1.1 Basic definitions..... 149
12.1.2 Consideration regarding the sensitivity factors 151
12.1.3 Application of full-probabilistic analysis for calibration of load model 153
12.2 Probabilistic description of input variables..... 159
12.2.1 Permanent loads 160
12.2.2 Probabilistic representation of resistance functions..... 163

12.2.3 Propositions for resistance model and action effects determination uncertainties 164
12.2.4 Probabilistic distributions of resistance functions 166

13 Appendix D: Further bridge-specific full- and semi-probabilistic analyses 175
13.1 Introduction 175
13.2 Uncertainty in the scatter of the resistance functions 175
13.3 Investigation of parametric bridges 177
13.3.1 Swiss bridge data base 177
13.3.2 Additional investigated parametric bridges 180
13.3.3 Structural models of bridges 181
13.4 Skewed frame bridges 183
13.5 Influence of number of spans 185

14 Appendix E: Benchmark cases of WIM data for traffic simulations 187
14.1 Analysis of traffic and inputs of traffic 187
14.2 Benchmark cases 193

Use of Data 194

Project conclusion 195

List of illustrations

Figure 1: Methodology followed for establishing a new Load Model (Note: ILs stands for Influence lines) 18
Figure 2: The New Load Model 1 (NLM1) for evaluation of existing bridges, presented in code format with the characteristic code values of the loads (the design values are obtained using: $\alpha_{i,act}$ =1.00 $\alpha_{i,act} = 1.00$, γ_F = 1.50 $\gamma_F = 1.50$) 20
Figure 3: Comparison of the total load on lane 1 (slow lane) on a strip of length according to the different editions of the SIA code series 44
Figure 4: Comparison of the total load on bridges of lengths between 20 and 80 m according to the different editions of the SIA code series (Vogel et al., 2009), a) roadway width 9 m, b) roadway width 12 m 45
Figure 5: Load model 1 from SIA 261:2020 46
Figure 6: Methodology followed for establishing a new Load Model 51
Figure 7: Workflow for calibration of load model (full-probabilistic illustrated) 52
Figure 8: Map of Switzerland with location of WIM stations 54
Figure 9: Qualitative fitting of a normal distribution using the assumed tail percentiles represented by the red dots. 56
Figure 10: Example of a weekly maxima histogram: positive moment at mid-span for a simply supported box-girder bridge with a span of 30m (unidirectional traffic); Fitting and tail goodness of fit performed using a Normal, Lognormal and a GEV distribution. 57
Figure 11: Heavy vehicle distribution in JAM analysis and resulting action effect E_d (a) for single lane and (b) for double lane for the cases 1 and 2. 58
Figure 12: Vehicle distribution between lanes with REL at Denges (a) Heavy vehicle lane change, (b) all vehicles flow rates comparison. Extracts from (Fénart et al., 2016) 60
Figure 13: Bridge longitudinal structural types in Switzerland a) with year of construction b) with span length (Ammann et al., 2024) 62
Figure 14: Transverse sections of investigated generic bridge types (units in meters) 62
Figure 15: Longitudinal systems of investigated generic bridge types 63
Figure 16: Ratio between single lane codified design action effect with $\alpha_{act,unique}$ = 0.6 and the design action effect from direct WIM and JAM analysis (refer to Table 3 for more detailed explanation of definition of bridge types and internal forces) 66
Figure 17: Ratio between double lane design action effect $E_{d,2l}$ (Option 1) and single lane design action effect E_d from direct WIM and JAM analysis 66
Figure 18: Ratio between double lane codified design action effect with $\alpha_{Q1,act}$ =$\alpha_{q1,act}$ = 0.60, $\alpha_{Q2,act}$ =$\alpha_{q2,act}$ = 0.30 and the double lane design action effect from direct WIM and JAM analysis (Option 1) 67
Figure 19: Ratio between double lane design action effect $E_{d,2la}$ (Option 2) and single lane design action effect E_d from direct WIM and JAM analysis (refer to **Figure 20:** for plot legend) 68

Figure 20: Ratio between double lane codified design action effect with $\alpha_{Q1,act}$ $=\alpha_{q1,act}$ = 0.60, $\alpha_{Q2,act}$ $=\alpha_{q2,act}$ = 0.30 and the double lane design action effect from direct WIM and JAM analysis (Option 2) 68
Figure 21: Design loads from WIM data strip analysis on a single lane, up to 4.4m 70
Figure 22: Design loads from WIM data strip analysis on a single lane, up to 20m 70
Figure 23: Investigated configurations of load models for the fist lane (*ls* is the bridge length, l_{q1} is the distribution length of the Uniformly Distributed Load 1 (UDL1) 71
Figure 24: (a) Proposal of New Load Model 1 (NLM1) for first lane based on optimization of design action effects for generic bridge types, (b) Comparison as ratio between NLM1 design action effect and the design action effect from simulations (direct WIM and JAM analysis) 73
Figure 25: Workflow to determine the parameters of NLM1 (the dynamic amplification DAF and modelling γ_{sd} factors are dealt with in paragraph 5.1.4) 74
Figure 26: NLM1 for first and second lanes, design values of the loads (careful the load values are in kN and kN/m and are design action effect from simulations, the dynamic amplification DAF and modelling γ_{sd} factors are dealt with in paragraph 5.1.4) 75
Figure 27: Ratio between action effects obtained using the double lane design values from NLM1 and from simulations, $E_{d,2l}$ (Option 2), for an optimised second distributed & second lane load (a) q_{2di} = 4.67 kN/m², (b) q_{2di} = 4.5 kN/m² and (c) q_{2di} = 4.34 kN/m²; please note that the dynamic amplification factor and the partial factor covering uncertainties in calculating action effects is not included yet 76
Figure 28: Example of local verifications (a) and comparison between LM1 (b) and NLM1(c) 78
Figure 29: Example of resulting $\varphi_{ULS,cap}$ curves for bending moment of concrete bridges 81
Figure 30: Resulting DAF found for the different cases of generic bridge types computed based on $\varphi_{ULS,cap}$ (capped DAF curves from REAL-LAST (Vorwagner et al., 2024)) 82
Figure 31: Comparison between the NLM1 action effects (with DAF $\varphi i, 1_{\varphi_{d,1}}$, without γ_{sd}) and the design action effects from the simulations, multiplied by the capped $\varphi_{ULS,cap}$ curve values from REAL-LAST) 83
Figure 32: Proposition of new load model 1 (NLM1) for evaluation of existing bridges, presented in code format with the corresponding **characteristic code values** of the loads ($\alpha i, act = 1.00, \gamma Sd = 1.00, \gamma F = 1.50$ and dynamic amplification factors included for ease of use) 84
Figure 33: Workflow to determine the loads of the new load model 1 (NLM1) for evaluation of existing bridges, with the final examination values displayed 85
Figure 34: Proposition of new load model 1 (NLM1) for evaluation of existing bridges, presented in code format with the **characteristic code values** of the loads ($\alpha i, act = 1.00, \gamma F = 1.50, \gamma Sd$ and dynamic amplification factors included for ease of use) 86
Figure 35: Description of probabilistic resistance function 92

Figure 36: Design value of model uncertainty of action effects 93
Figure 37: Comparison between global design value and station-wise design value 94
Figure 38: Difference between full-probabilistic results and semi-prob calibrated load model 96
Figure 39: Traffic sensitivity factor based on full-probabilistic analysis 97
Figure 40: Sensitivity factors for 1-year traffic selecting $\gamma sd = 1.05$ 98
Figure 41: Sensitivity factors for 1-year traffic, selecting $\gamma sd = 1.10$ 99
Figure 42: Reliability index based on calibrated NLM1 100
Figure 43: Influence of load ratio on sensitivity factors 101
Figure 44: Error between NLM1 and target reliability 101
Figure 45: Relative error between NLM1 and target reliability – weighted by sensitivity factors 102
Figure 46: Accuracy of LM1 from EN 1991-2 based on full-probabilistic analysis 103
Figure 47: Second lane full-probabilistic analysis: increased traffic & highest stations 105
Figure 48: Second lane full-probabilistic analysis: distributed traffic & highest stations 105
Figure 49: Second lane full-probabilistic analysis: increased traffic & second highest stations 105
Figure 50: Second lane full-probabilistic analysis: distributed traffic & second highest stations 105
Figure 51: Integration of the LoAs of traffic load model in the examination procedure of SIA 269:2011 110
Figure 52: LoA I and II, workflow for standard bridge types 111
Figure 53: LoA I and II, workflow for special bridge types 112
Figure 54: LoA III and IV, workflow for all bridge types 113
Figure 55: Target values for moment M0 - 2 lanes, adapted from (Sedlacek & al., 2008) 131
Figure 56: Target values for moment M0 - 1 lane, adapted from (Sedlacek & al., 2008) 132
Figure 57: Load model 1, highlighting the differences between EN and SIA (from EN 1991-2: 2004) 134
Figure 58: Load model 1, highlighting the differences between EN and SIA (Bez et al., 1987) 135
Figure 59: Dynamic amplification factors, from Eurocode background (Sedlacek & al., 2008) 136
Figure 60: Pie charts showing the truck types responsible for the tandem axles block maxima and the influence of the observation time for each block (single lane analysis) 140
Figure 61: Histograms of shear weekly bloc maxima for a box-girder bridge of (a) 4m and (b) 10m considering a single lane; pie charts showing vehicles distribution in the tail values further than 3 standard deviations (3σ) 140
Figure 62: Different variations of load models for fist lane (ls is the bridge length, l_{q1} is the length of UDL 1) 141

Figure 63: Axle loads for maximum shear cases in WIM analysis of box girder bridges with spans of (a) 4m, (b) 10m, (c) 20m and (d) overlapping plots of all cases 141
Figure 64: Axle loads for maximum bending in WIM analysis of box girder bridges with spans of (a) 4m, (b) 10m, (c) 20m and (d) overlapping plots of all cases 142
Figure 65: Strip analysis of the average axle group load (axles can be located on one or both lanes) 143
Figure 66: Design loads from WIM data strip analysis on two lanes, up to 4.4 m 144
Figure 67: Single span cases, positions of the concentrated and UDL corresponding to the maximum load effects for the four candidate load models (PM in the figures) and the SIA LM1 145
Figure 68: Three span case, positions of the concentrated and UDL corresponding to the maximum load effects (hogging moment) for the four candidate load models and the SIA LM1 145
Figure 69: Required second lane load ratio r_{Lane2} for NLM1 to achieve exactly the double lane action effect *Ed,2l* (Option 1) 146
Figure 70: Required second lane load ratio r_{Lane2} for NLM1 to achieve exactly the double lane action effect *Ed,2la* (Option 2) (refer to Figure 71 for legends of plot) 147
Figure 71: Ratio between double lane design action effect with NLM1, r_{Lane2} = 0.3 and the double lane action effect *Ed,2l* (Option 1) 147
Figure 72: Ratio between double lane design action effect with NLM1, r_{Lane2} = 0.5 and the double lane action effect *Ed,2la* (Option 2) (refer to Figure 71 for legends of plot) 148
Figure 73: Influence of ratio of scatter on reliability index 151
Figure 74: Influence of ratio of scatter on sensitivity factors 152
Figure 75: Required sensitivity factor dependent on observed time frame (for $\beta = 3.8$) 153
Figure 76: Proposed approach for the calibration of the load model 155
Figure 77: Applied procedure for extrapolation of probabilistic distribution of traffic action effects 158
Figure 78: Transformation of sensitivity factor between time frames (n=50) 159
Figure 79: Probabilistic representation of permanent loads 160
Figure 80: Ratio between approximated and calculated self-weight 161
Figure 81: Probabilistic bending resistance of T-beam section 168
Figure 82: Probabilistic bending resistance composite girder 169
Figure 83: Probabilistic distribution of concrete shear resistance 170
Figure 84: Distribution of concrete shear resistance, including the model uncertainty 171
Figure 85: Probabilistic distribution of shear resistance: composite section 172
Figure 86: Influence of the choice of probabilistic resistance parameters on the traffic calibration for load ratios a) $\chi = 0.5$ and b)) $\chi = 0.25$ 174
Figure 87: Envelope curve for concrete shear resistance functions 175
Figure 88: Accuracy of different concrete shear resistance failure modes (left: JCSS, right: EN 1992-1-1:2023) 176
Figure 89: Envelope curve for composite shear resistance functions 177
Figure 90: Distribution of erection of Swiss highway bridges 178
Figure 91: Distribution of span length for single span girder bridges 178
Figure 92: Distribution of span length for multi-span girder bridges 178

Figure 93: Distribution of span length for frame bridges 179
Figure 94: Distribution of span length for slab bridges 179
Figure 95: Distribution of span length for concrete and prestressed concrete bridges 179
Figure 96: Distribution of span length for steel-concrete composite bridges 179
Figure 97: Parametric portal frame bridge 180
Figure 98: Parametric T-beam girder bridge 180
Figure 99: Parametric box girder bridge 181
Figure 100: Parametric composite bridge 181
Figure 101: SOFiSTiK bridge models of frame bridge (left) and composite bridge (right) 181
Figure 102: Difference between full-probabilistic results and semi-prob calibrated load model 182
Figure 103: Reliability index based on calibrated NLM1 for further bridges 182
Figure 104: Influence lines of portal frames and the influence of inclined bridges 184
Figure 105: Influence line of second lane for frame bridges 184
Figure 106: Second lane full-probabilistic analysis: Portal frame bridges, distributed traffic 185
Figure 107: Second lane full-probabilistic analysis: Portal frame bridges, increased traffic 185
Figure 108: Comparison of bending moment influence line 185
Figure 109: Comparison of simple vs. multi-span systems 186
Figure 110: Sample of statistical analysis of data from the Ceneri traffic 2018, heavy vehicle type 113a 187
Figure 111: GVW distribution of each heavy vehicle type from the Ceneri traffic 2018 189
Figure 112: Heavy vehicles axle or axle groups spacings distributions for all types from the Ceneri traffic 2018 190
Figure 113: Heavy vehicles axle or axle groups weights distributions, all types combined, from the Ceneri traffic 2018 191
Figure 114: Axle groups weights linear relationships for all types from the Ceneri traffic 2018 192

List of tables

Table 1: Selected WIM stations/years 54
Table 2: Bridge longitudinal structural types in Switzerland (Vogel et al., 2009) 61
Table 3: Summary of generic bridge types investigated 64
Table 4: definition of the special vehicles representing the different types of mobile cranes 69
Table 5: Parameters investigation for the load configuration PM4 for the first lane 72
Table 6: investigated failure modes 91
Table 7: selected probabilistic resistance parameters 92

Table 8: Treatment of the uncertainty sources on action and action effects in function of the LoA 115
Table 9: Adjustment factors for design of new bridges in some EU countries, adapted from (Skokandić & et al., 2020) 133
Table 10: Model uncertainties for the calculation of action effects 162
Table 11: Probabilistic material and geometric parameters 163
Table 12: Overview resistance model uncertainties 164
Table 13: Model uncertainty for concrete bending moment resistance 165
Table 14: Model uncertainty for concrete shear resistance with reinforcement 165
Table 15: Model uncertainties for the calculation of action effects 166
Table 16: Summary of parametric bridge models 180
Table 17: GVW distribution parameters of heavy vehicles from the Ceneri traffic 2018 188

List of abbreviations/symbols

Art.	Article
DAF	Dynamic Amplification Factor, φ_{act}, φ_{dyn}. The common but overused term is used. However a better term describing what this factor covers is ADR for Allowable Dynamic Ratio (E. J. O'Brien et al., 2010)
E.g.	For example
i.e.	In extenso, at full length
ILs	Influence lines
HV	Heavy vehicle, all vehicles with a total weight above 6 t (this report) or above 10 t (Eurocodes). This difference stems from a detailed analysis comparing SARTC (Swiss10 classification) and WIM data, which showed that setting the limit at 6 tons is the best way to eliminate many misclassifications of vehicles such as delivery vans or small trucks (Sjaarda et al., 2022)
JAM	Jammed traffic condition
LM1	Load Model 1 from SIA261 for vertical traffic loads
NLM1	New load model 1
PUN	Pannenstreifenumnutzung (German acronym for REL)
R-BAU	Réutilisation Bande Arrêt d'Urgence (French acronym for REL)
REL	Repurpose of Emergency Lane
UDL	Uniform Distributed Load
Vol.	Volume
WIM	Weigh-in-motion
E_{sim}, $E_{d,sim}$	Computed E_{sim} distribution and $E_{d,sim}$ design value of action effects (from simulations using direct WIM, $E_{d,WIM}$ or JAM, $E_{d,JAM}$ at design level)
$E_{d,mod}$	Load model computed value of the action effects, design level
$E_{d,WIM}$	Direct simulation of traffic from flowing to congested (minimum speed of about 30 km/h) conditions on the influence lines,), design level
$E_{d,JAM}$	Simulation of synthetic traffics based on WIM data in jammed conditions on the influence lines,), design level
x_k	Characteristic value. For the action effect E_k, the characteristic value has a return period of 1000 years and corresponds to a 10% for a 100-year service life
x_d	Design value and, by extension, value at design level as well as examination value since the focus of the report is existing bridges
α_E	Sensibility factor of action effects in semi- and full-probabilistic analyses
α_i	Adjustment factor for load model LM1, as specified in SIA 261:2020 and EN 1991-2:2004
$\alpha_{i,act}$	Updated adjustment factor, or to simplify adjustment factor since the focus of the report is existing bridges
β_{tgt}	Annual, if not specified in index, target reliability value
γ_{sd}	Partial factor of action effects model uncertainty. Also, model uncertainty of (computing) action effects, or model uncertainty in the calculation of action effects. Composed of: $\gamma_{sd,Q}$, partial factor for uncertainty in modelling actions $\gamma_{sd,S}$, partial factor for uncertainty in determining internal forces

Summary

Introduction

Problem statement

A more efficient use of resources is being called across all domains, imposing the need to identify and remove unaccounted conservatism in design. Since 1892, Switzerland's traffic load requirements for designing new road bridges have been defined and updated regularly to account for the evolution of traffic and heavy vehicles. It is only from the introduction of code SIA 160:1956 onwards that traffic loads represented by actual vehicles have been replaced by a combination of uniformly distributed and concentrated load(s) which replicates the real traffic and the relative action effects. This work focuses only on the effects of vertical loads.

For designing new bridges, the economic and ecological cost of considering traffic loads larger than currently present on the road network can be considered a sustainable choice in the long term, since a resistance reserve allows for changes of use and to face potential innovation in transport technology.
However, for existing bridges, in the optics of sustainable decision making, the following considerations should be made:

- In general, the level of conservatism induced by current design/evaluation standards is not uniform between various structural systems. This inconsistency leads to a non-uniform conservatism within the existing bridge stock;
- When assessing existing bridges, hidden conservatism leads to unnecessary, time consuming, and costly retrofits, reinforcements, or other interventions, which are not in the interest of the society.

The points presented above are further confirmed by issues observed in practice with the current existing structures examination codes (SIA 269: 2011 series), that have resulted in an increased number of mandates for site-specific traffic analyses linked to bridge structural safety evaluations. While significant progress has been made on the load-bearing resistance calculation of bridge structural members, comparatively little effort has been directed to investigate traffic loads in order to remove conservatism. To this purpose, a critical analysis of the Load Model 1 (LM1) of the current design codes needs to be performed to identify LM1's shortcomings; alternatives to updating the traffic load model adjustment factors $\alpha_{i,act}$, see SIA 269/1:2011, should also be investigated, including the influence of the Repurpose of Emergency Lane (REL).
To this purpose, the main aim of this research is to identify reserves in terms of action effects due to traffic loads in road bridges and develop a New, improved Load Model (NLM1) to implement in future codes. Other aspects such as treatment of dynamic effects, the impact of overloaded and special vehicles are also discussed.

Objectives of research

The research needs and objectives for this project can be summarized as follows:

1. Historical review of the bases and development of LM1 in EN 1991-2:2004;
2. Overview of WIM data treatment and classification from the FEDRO database, including more recent data (from 2022) not included in previous projects. Algorithms overview for performing traffic simulations based on these data to develop and calibrate a new load model (NLM1) for assessing existing road bridges.
3. Better understanding of the critical traffic load situations in terms of probabilistic action effects on one and two lanes (valid for both existing and new bridges) for typical bridge types of the FEDRO existing bridges database.
4. Definition of a new load model (NLM1) to better describe the governing types of truck(s), including special vehicles, and their action effects for local and global verifications both for short and long span bridges (up to 80 m). Clarification of which uncertainties in action effects calculation are covered by the partial model factor γ_{Sd} and by the treatment of dynamic effects.
5. Extension of the model to double-lane traffic with reasonable assumptions, including the influence of the REL.
6. Propose a general procedure for quantifying the safety reserves between the action effects obtained using the current LM1, or other load models proposed by the SIA 269/1:2011, and those obtained by performing simulations using WIM data.
7. Establish a framework for regularly updating traffic assumptions to allow accounting for its evolution, with the corresponding revision of design and examination structural codes every 25 years (in link with objective 2 and allowing for the use of "trains of loads" to simulate various scenarios by selecting the specific traffic loads).

Fundamental information

Background on Load Models

The current Load Model 1 (LM1) according to SIA 261:2020 is presented in Figure 5, where the adjustment factors α_{Qi} and α_{qi} are nationally defined parameters (as in EN 1991-2:2002). The main difference between the LM1 of EN 1991-2:2002 and the SIA 261:2020 is that there is no axle load group on the 3rd lane. In addition, the EN proposes three more load models, whereas the Swiss code proposes only a second load model (for special and exceptional vehicles). From this point forward, in this document, LM1 according to EN 1991-2:2002 and according to SIA 261:2020 will be considered as equivalent and referred to simply as LM1.

The recent FEDRO research report 82001 (Documentation ASTRA 82001, 2025; Sjaarda et al., 2022) uses detailed analyses of carefully processed WIM measurements to identify which heavy vehicles and load cases are responsible for the largest action effects.

The current LM1 can be updated to cover determinant traffic load cases maintaining a combination of uniformly distributed loads and concentrated axles loads, especially for the examination of existing structures. At the origin of this research, the following issues with LM1 were identified:

- The concentrated load Q appears to be too large and the tandem axles are also too close (1.2 m);

- The distributed load q leads to values of action effects that are excessive for long spans;
- The treatment of the dynamic effects as being directly included as a single dynamic amplification factor in the characteristic load values does not represent reality, since it should depend on the type of load;
- It is unclear how γ_{Sd}, the partial load factor expected to account for uncertainties in the calculation of action effects, is determined, as well as which other uncertainties it is supposed to cover;
- The standardised sensitivity factor $\alpha_E = 0.7$ is an upper bound and thus introduces an additional level of conservatism, as shown for a large number of scenarios for example by fib (fib Model Code 2010);
- SIA261 does not consider actions due to special vehicles currently circulating on the road network (SIA261-10.3.4), however, SIA269/1 accounts for them when defining the updated adjustment factors (see notes of Table 1 of SIA269/1:2011);
- A non-uniform reliability level across various bridge types has been observed both in practice and research works, see (A. Fürst, personal communication, April 2021);
- The updated adjustment factors $\alpha_{i,act}$ for LM1 according to SIA 269/1:2011 are limited to legally allowed traffic and only account for traffic growth until 2025;
- The definitions for certain bridge types, such as short bridges, are unclear, and studies like those performed by Meystre et al. (2014) are not considered.

Importance of Weigh-in-motion (WIM) Data

Modern approaches use probabilistic methods and Weigh-in-Motion (WIM) data to account for variability and extreme scenarios. WIM technology is crucial for this research, because of its ability to provide detailed data on axle weights, vehicle configurations, and traffic flow patterns. In over 25 years, Switzerland has built a robust WIM database, offering high-quality data for model calibration through probabilistic methods that account for variability and extreme scenarios. Selected WIM data meet 3 main criteria, such as:

1. Representativeness of the FEDRO road network, which ensures the data reflects the variety of traffic conditions and vehicle types across the network;
2. Measurement quality, which guarantees accurate and reliable recordings of weights and axle configurations;
3. Long-term stability to provide consistent data over extended periods for robust analysis.

Methodology

In order to successfully evaluate the critical traffic combinations on road bridges, it is important to properly treat the joint occurrence of extreme loads, the occurrence of various traffic types (i.e. flowing, congested, jammed) and the influence of the different structural system configurations. Such analyses are first performed on a single lane and then extended to cover the case of two lanes. To this purpose, the FEDRO's WIM database is analysed, sorted, and a relevant set of traffic data is selected.
To develop the new load model, simulations are performed using 3 main load types, see Figure 1. Considering a single lane, the following load combinations are considered:

1. A concentrated or axle load for local verifications;

2. Groups of axles loads for local and global verifications of typical slab bridges;
3. A sequence of axles that represents a line of vehicles for global verifications of multiple spans or longer spans. This idealized configuration is then extended to the additional lanes; the joint presence of axles and heavy vehicles and multiple lanes are accounted for on various bridge types.

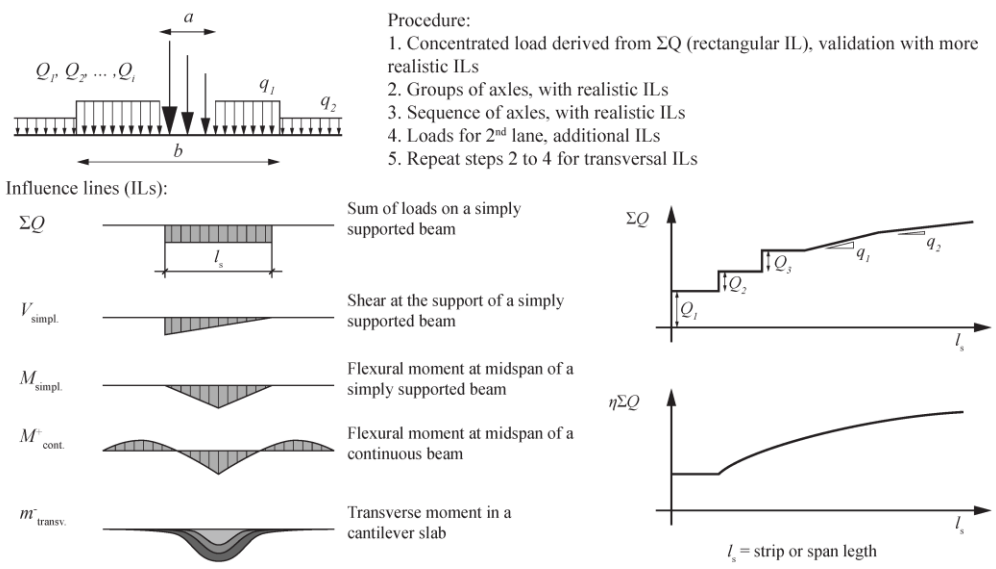

Figure 1: Methodology followed for establishing a new Load Model (Note: ILs stands for Influence lines)

The calibration of the new Load Model for the above 3 main load types, including their interactions and correlations, is performed and can be a combination of semi-probabilistic or full probabilistic modelling. The calibration procedure is summarized in the following points:

- Selection of relevant lane configurations from the WIM data and definition of the bridges population (systems, spans, ...);
- Calculation of the various distributions of action effects (E_{sim}) and, for fully probabilistic modelling, calculation of the corresponding resistances distributions;
- Definition of a new load model configuration and corresponding design actions effects calculation ($E_{d,mod}$);
- Deployment of reliability analyses (for semi-probabilistic a fixed importance factor α_E = 0.7 is assumed, as defined in (EN 1990:2021 Eurocode - Basis of Structural and Geotechnical Design, 2021) and in Appendix C of (SIA 269/1, 2011) ;
- Comparison of the actions effects ($E_{d,mod}$ and $E_{d,sim}$) for the bridges population in semi-probabilistic analyses;
- Comparison of reliability indexes (β and β_{tgt}) for the bridges population in full-probabilistic analyses;
- Optimization of the model values for the configuration of the new load model to achieve an optimized configuration with respect to selected population of bridges, $E_{d,mod}$ / $E_{d,sim}$ must be on the safe side $E_{d,mod}$ / $E_{d,sim}$ >1.0, as close as possible to unity, as uniform as possible, and minimizing variance;
- Critical review the optimized new load model from a practical point of view, privileging ease of implementation, usability and integration in current codes of practice, as well as adaptability in view of potential additional lanes with heavy traffic.

The general procedure for quantifying the reserves between the normative LM1 or an updated load model for the SIA 269/1 code and simulations of the actual loads and load effects is achieved by providing detailed guidance:

- Adhering to the examination procedure outlined in SIA 269:2011;
- Addressing the different types of FEDRO structures where LM1 would prove to be overly conservative;
- Following the stepwise approach to deterministic and probabilistic verifications, ensuring practical applicability. Thereby, the Levels of Approximation (LoA) approach will be introduced and used.

The advantage of this approach is that it represents a general framework and it is suitable to be updated considering new knowledge on current and future traffic evolution. Given its general validity, lower Levels of Approximation (LoA) can be defined by making conservative assumptions on higher LoAs. These assumptions can also be based on deterministic analysis, which are often used in practical cases.

Results

The results show that the proposed *New Load Model* 1, which will be denoted from now on as NLM1, represents a significant advancement compared to the current LM1, offering a more accurate, reliable and practical approach to load modeling for road bridges. Figure 2**Fehler! Verweisquelle konnte nicht gefunden werden.** shows the NLM1 configuration, where the relative location of $Q_{k,1}$ within $q_{1k,1}$ should be chosen to achieve the maximum action effect and the location of $Q_{k,2}$ is free. The reader is referred to § 5.2 for more information. The optimization of NLM1 is performed in several stages, first from simulations without including any dynamic amplification factor (DAF) φ_{dyn} nor model uncertainty of action effects γ_{sd}. Those are investigated separately and added explicitly, see § 5.1.4, allowing these factors to be adjusted for specific cases or if new findings indicate these values should be revised. The characteristic code values in Figure 2 are however given for ease of use as $E_{di,act}/\gamma_F$.
While the NLM1 has been calibrated to maximize the use of resources in existing bridges and improve sustainability, it could also be employed for the design of new bridges with additional validation and calibration.

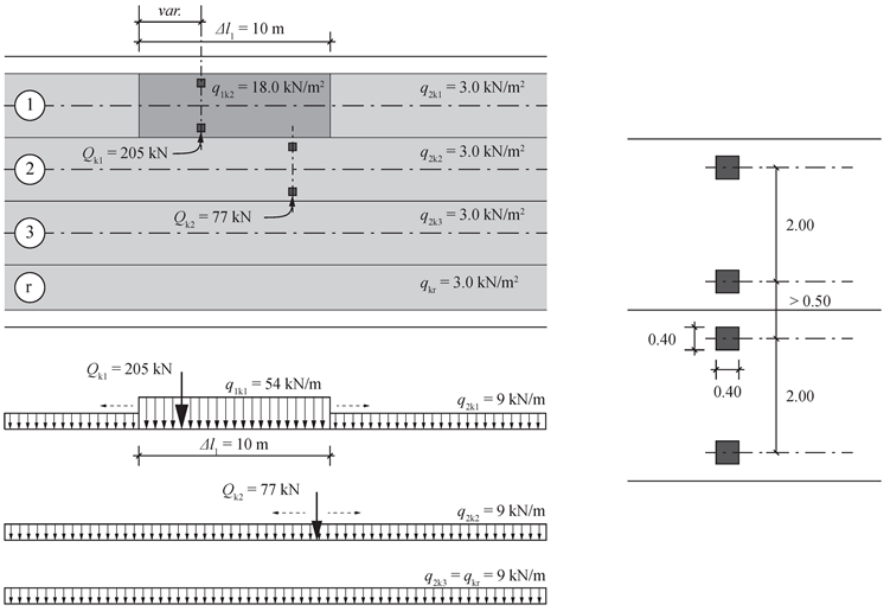

① $Q_{k,1}$ = 205 kN $q_{1k,1}$ = 18 kN/m² $q_{2k,1}$ = 3.00 kN/m²

where the relative location of $Q_{k,1}$ (*var*) within $q_{1k,1}$ should be chosen to achieve the maximum action effect

② $Q_{k,2}$ = 77 kN $q_{2k,2}$ = 3.00 kN/m²

③ $q_{2k,3}$ = 3.00 kN/m²

q_{kr} = 3.00 kN/m²

Figure 2: The New Load Model 1 (NLM1) for evaluation of existing bridges, presented in code format with the characteristic code values of the loads (the design values are obtained using: $\alpha_{i,act}$ =1.00, γ_F = 1.50)

Concerning the development on the NLM1, the following points can be highlighted:

- **Calibration process**: key parameters, such as distributed load magnitudes and axle group configurations, are calibrated iteratively using the methodology described above. This process is possible thanks to the availability of WIM data which provided a robust basis to calibrate the parameters of the model and reflect the actual traffic conditions.
- **Future traffic considerations**: despite many similarities, in the study for ASTRA 82001 (Papastergiou et al., 2025), the presence of REL was studied but only to fix a unique actualized factor (step 0). In this research, in order to propose a generically valid New Load Model a different philosophy was followed, namely to cover well the different highway lane patterns with two heavy traffic lanes, the worse being indeed with a REL. Future traffic increase is considered :
  - When two lanes with heavy traffic are simulated, with the increase in number of heavy vehicles of 67% compared to today and with their distribution among lanes;
  - For more lanes (3rd, 4th ...) by increasing the Uniform Distributed Load (UDL) from 2.25 to 3.00kN/m² compared to the current LM1.

  These cover uncertainties about future heavy traffic developments, such as increase in heavy traffic in different lanes, in traffic congestion, as well as the necessity to include bridges with bidirectional traffic on multiple lanes. The horizon 2050 was set because regular review of traffic development need to be made. They however may lead in certain cases to NLM1 being less favorable than ASTRA 82001. Thus the

conformity factors from verification using NLM1 can be lower than those found using ASTRA 82001. If a comparison is to be made between both, it should be done between results from Step 0 with REL ($\alpha_{act,unique}$ = 0.60) and those from the NLM1. Nevertheless, it was not the objective of NLM1 to be more economical (i.e. less conservative) but to reach a more uniform safety level, to be more versatile and thus allow for extrapolation, whereas ASTRA 82001 cannot be applied outside its applicability limits.

- **Single-lane model results**: for single-lane traffic scenarios, the NLM1 achieves a more uniform safety margin in action effects than the current model the LM1. In fact, the NLM1 shows a consistent performance independently of the span while the LM1 tends to be overly conservative for short and large spans (<15m and > 30m) while the safety margin largely reduces for medium spans (15-30 m).
- **Multi-lane model results**: double-lane traffic conditions further demonstrate the higher accuracy of the NLM1, as it accounts for the joint presence of heavy vehicles. However, the probabilistic approach ensures that reliability targets are met without excessive safety margin. Key performance indicators, such as uniform reliability indices and reduced variance in action effects, underscore the model's effectiveness. The NLM1 covers all extreme scenarios of double lane traffic with a large percentage of heavy vehicles on the 2nd lane. It covers cases with REL (i.e. 2 lanes transformed into 3 lanes) as well as construction works situations (i.e. with 2+2 bidirectional traffic on one bridge, with restriction only 2 lanes with heavy traffic);
- **Special vehicles scenarios**: the NLM1 better covers scenarios involving special vehicles, such as mobile cranes or overloaded trucks[1], that are not sufficiently covered in traditional load models. The flexibility of NLM1 allows for adjustments based on real-world traffic patterns with, on the 1st lane, its large distributed load over 10 m.
- **Consistency between Levels of Approximation (LoA's)**: the same reliability levels are achieved with both semi-probabilistic and full probabilistic analyses, and are consistent across various spans and bridge types. For semi-probabilistic analyses, the main factor in the calibration process is the sensitivity factor of the traffic action effects $\alpha_{E,Traffic}$. This study demonstrates that a value of $\alpha_{E,Traffic}$ in accordance with current standards is conservative however acceptable for road bridges and heavy vehicle traffic.
- **Full-probabilistic reliability analysis**: an algorithm is proposed to allow calibrating the load model using full-probabilistic analyses. These analyses show that the NLM1 provides a more uniform safety margin with respect to previous load models. Furthermore, it enables further improvements of the load model by investigating the reduction in the scatter of the action effect side model uncertainties. Finally, full-probabilistic analyses allow to calibrate the model for specific case studies involving other or special bridge types.
- **Dynamic factors and multi-lane effects:** dynamic amplification factors and multi-lane effects are implemented in an explicit manner, significantly improving the accuracy of the action effect predictions and allowing to update them as additional knowledge on these factors becomes available.

[1] Overloaded axles or total weights, where the authors recommend that the number of offenders must be kept to a minimum through more checks (by the police or technical equipment)

- **Overcoming limitations of current models**: limitations of the LM1 for evaluation, such as the inability to capture complex traffic scenarios or varying bridge geometries, are effectively addressed by the NLM1, ensuring that it is well-suited for evaluating existing bridges and making it suitable for designing new ones.

Recommendations for Future Research

During the course of the project, several topics were raised that were outside the scope of research, they are listed below:

- Further development of the NLM1 to extend its applicability and draft application rules for other traffic load effects, i.e. fatigue, acceleration, braking, centrifugal and transversal forces;
- Additional research should be performed to allow the use of NLM1 for retaining walls in accordance with Swiss codes (SIA 261, 2020) and (SIA 269/1, 2011). In fact, the current LM1 might result in overly conservative action effects requiring costly interventions;
- Extend the WIM database to include additional traffic scenarios, underrepresented bridge types, and geographic regions. It is advised to maintain the current network of WIM stations and data collection to allow investigating traffic development in time for specific sites;
- Prediction of the future traffic loads accounting for the impact of emerging technologies, such as electric heavy vehicles, autonomous vehicles and changes in freight patterns. Traffic evolution will impact both design of new bridges and examination of existing ones. In fact, current models primarily account for current traffic conditions. Recall that the NLM1 takes into account the use of the REL and an increase in heavy traffic;
- Dynamic effects and related uncertainties need to be better investigated and modeled using more refined techniques to accurately consider their influence on action effects, especially for specific scenarios including special vehicles which might lead to excessive conservatism;
- The sensitivity factor for traffic action effects in semi-probabilistic approaches, $\alpha_{E,Traffic}$ currently equal to 0.7, should be better investigated and alternative values should be proposed to reduce conservatism mostly in existing bridges;
- Full probabilistic reliability analysis should be extended to include a wider range of bridge types, non-linear combination of correlated action effects and bridge collapse. Also, a differentiation between failure modes would enhance reliability calculations;
- In probabilistic reliability analyses, the NLM1 proposed by this work has been compared using the current EN 1992-1-1:2004 to compute the resistance side. However, comparisons should also be performed using the new generation EN 1992-1-1:2023, which was shown to have a lower scatter in the resistance formulas;
- Interactions between various action effects, such as the Moment-Axial Load interaction close to the support of a beam, should be investigated. In this work, the maximal action effects are considered independently from each other according to preliminary investigations that indicated that separately maximizing each action effect is generally the most conservative case. However, there is no guarantee that this is the case for all geometric configurations and bridge types. Also, the level of additional conservatism derived by considering action effects separately should be determined;

- Development of simplified tools for practitioners, such as training programs, user-friendly tools, and workflows to facilitate the application of advanced load modeling techniques in a transparent manner. Allowing semi-probabilistic and probabilistic evaluation in practice is also critical to ensure quick adoption by engineers and policymakers.

Zusammenfassung

Einleitung

Problemstellung

Eine effizientere Nutzung von Ressourcen wird in allen Bereichen – so auch in der Baubranche – gefordert, was die Notwendigkeit mit sich bringt, ungerechtfertigte Sicherheitszuschläge in der Bemessung von Tragwerken zu identifizieren und zu beseitigen. Seit 1892 werden in der Schweiz die Anforderungen an die Verkehrslasten für die Bemessung neuer Brücken definiert und regelmäßig aktualisiert, um der Entwicklung des Verkehrs und des Schwerverkehrs Rechnung zu tragen. Erst seit der Einführung der Norm SIA 160:1956 werden die durch reale Fahrzeuge repräsentierten Verkehrslasten durch eine Kombination aus gleichmässig verteilter Belastung und Einzellasten ersetzt, die den realen Verkehr und die entsprechenden Einwirkungen nachbilden. Diese Arbeit konzentriert sich ausschließlich auf die Auswirkungen vertikaler Belastungen.

Bei der Bemessung neuer Brücken können die wirtschaftlichen und ökologischen Kosten, die durch die Berücksichtigung von Verkehrslasten entstehen, die über die derzeit im Strassennetz vorhandenen Lasten hinausgehen, langfristig als nachhaltige Entscheidung betrachtet werden, da eine Widerstandsreserve Nutzungsänderungen ermöglicht und potenzielle Innovationen in der Verkehrstechnik berücksichtigt.
Bei bestehenden Brücken sollten jedoch im Hinblick auf eine nachhaltige Entscheidungsfindung folgende Überlegungen angestellt werden:

- Im Allgemeinen sind vorhandene Sicherheitsreserven, die aus den aktuellen Normen für die Bemessung und Bewertung hervorgehen, nicht einheitlich für verschiedene Tragwerke. Diese Inkonsistenz führt zu einer uneinheitlichen Sicherheitsbewertung innerhalb des bestehenden Brückenbestands.
- Bei der Beurteilung bestehender Brücken führt versteckter Konservativismus zu unnötigen, zeitaufwändigen und kostspieligen Nachbesserungen, Verstärkungen oder weiteren Erhaltungsmassnahmen, die nicht im Interesse der Gesellschaft liegen.

Die oben dargelegten Aspekte werden durch in der Praxis beobachtete Probleme mit den aktuellen Normen Erhaltung von Tragwerken (Reihe SIA 269: 2011) weiter bestätigt, die zu einer steigenden Zahl von Aufträgen für standortspezifische Verkehrsanalysen im Zusammenhang mit der Bewertung der Tragsicherheit von Brücken geführt haben. Während bei der Widerstandsberechnung von Brückenbauwerken erhebliche Fortschritte erzielt wurden, wurden vergleichsweise wenig Anstrengungen zur Untersuchung von Verkehrslasten unternommen, um vorhandenen Konservatismus zu reduzieren. Zu diesem Zweck sollte eine kritische Analyse des Lastmodells 1 (LM1) der aktuellen Bemessungsnormen durchgeführt werden, um Mängel in der Bemessung mithilfe von LM1 zu identifizieren; Alternativen zur Aktualisierung der Anpassungsfaktoren des Verkehrslastmodells, $\alpha_{i,act}$, siehe SIA 269/1:2011, sollten ebenfalls untersucht werden; und einschliesslich der Auswirkungen der Pannenstreifenumnutzung (PUN).

Entsprechend besteht das Hauptziel dieses Forschungsberichtes darin, Reserven hinsichtlich der Einwirkungen von Verkehrslasten auf Brücken zu ermitteln und ein neues, verbessertes Lastmodell (NLM1) zu entwickeln, das für künftigen Normen Anwendung finden soll. Weitere Aspekte wie die Behandlung dynamischer Einwirkungen sowie die Auswirkungen von überladenen und Sonderfahrzeugen werden ebenfalls erörtert.

Forschungsziele

Die Forschungsbedürfnisse und -ziele für dieses Projekt lassen sich wie folgt zusammenfassen:

1. Historischer Rückblick auf Grundlagen und Entwicklung des LM1 in EN 1991-2:2004;
2. Überblick über die Verarbeitung und Klassifizierung von WIM-Daten aus der ASTRA-Datenbank, einschließlich neuerer Daten (ab 2022) in früheren Projekten nicht enthalten. Überblick über Algorithmen zur Durchführung von Verkehrssimulationen auf der Grundlage dieser Daten, um ein neues Lastmodell (NLM1) zur Beurteilung bestehender Brücken zu aktualisieren und zu kalibrieren.
3. Besseres Verständnis der kritischen Verkehrslastsituationen im Hinblick auf probabilistische Einwirkungen auf ein- und zweispurigen Fahrbahnen (gültig sowohl für bestehende als auch für neue Brücken) für typische Brückentypen aus der ASTRA-Datenbank für bestehende Brücken.
4. Definition eines neuen Lastmodells (NLM1) zur besseren Beschreibung der massgeblichen Lkw-Typen, einschliesslich Sonderfahrzeuge, und ihrer Einwirkungen für lokale Nachweise sowohl bei Brücken mit kurzen als auch mit langen Spannweiten (bis zu 80 m). Klärung, welche Unsicherheiten bei der Berechnung der Einwirkungen durch den Teilsicherheitsmodelfaktor γ_{Sd} abgedeckt werden, sowie die Behandlung dynamischer Einwirkungen.
5. Erweiterung des Modells auf zweispurigen Verkehr unter realistischen Annahmen, einschliesslich der Auswirkungen der Pannenstreifenumnutzung (PUN).
6. Vorschlag eines allgemeinen Verfahrens zur Quantifizierung der Sicherheitsreserven zwischen den Einwirkungen, die unter Verwendung des aktuellen LM1 oder anderer in der SIA 269/1:2011 vorgeschlagener Lastmodelle ermittelt wurden, und denen, die durch Simulationen unter Verwendung von WIM-Daten ermittelt wurden.
7. Vorstellung eines Ansatzes zur regelmässigen Aktualisierung der Annahmen des Verkehrsverhaltens, um deren Entwicklung zu berücksichtigen, im Hinblick auf eine entsprechende Überarbeitung der Bemessungs- und Bewertungsnormen alle 25 Jahre (in Kombination mit Ziel 2 und unter Berücksichtigung der Verwendung von „Lastzügen“ zur Simulation verschiedener Szenarien durch Auswahl der spezifischen Verkehrslasten).

Grundlegende Informationen

Hintergrundinformationen zu Lastmodellen

Das aktuelle Lastmodell 1 (LM1) gemäss SIA 261:2020 ist in Figure 5 (Hauptteil des Berichts) dargestellt, wobei die Anpassungsfaktoren α_{Qi} und α_{qi} die national definierten Parameter sind (NDP wie in EN 1991-2:2002 angegeben). Der Hauptunterschied zwischen LM1 gemäss EN 1991-2:2002 und gemäss SIA 261:2020 besteht darin, dass auf der dritten Fahrspur keine Achslastgruppe anzubringen sind. Zudem schlägt EN 1991-2:2002 drei weitere Lastmodelle vor, während die Schweizer Norm nur ein zweites Lastmodell (für Sonderfahrzeuge und Ausnahmefahrzeuge) vorsieht. Im weiteren Verlauf dieses Dokuments werden LM1 nach EN 1991-2:2002 und nach SIA 261:2020 als gleichwertig betrachtet und vereinfacht als LM1 bezeichnet.
Der aktuelle ASTRA-Forschungsbericht 82001 (Documentation ASTRA 82001, 2025) (Sjaarda et al., 2022) nutzt detaillierte Analysen sorgfältig aufbereiteter WIM-Messungen, um zu ermitteln, welche Lastkraftwagen und Lastfälle für die grössten Einwirkungen verantwortlich sind.
Das aktuelle LM1 kann zur Anpassung an massgebliche Verkehrslastfälle aktualisiert werden, wobei eine Kombination aus gleichmässig verteilten Lasten und konzentrierten Einzellasten beibehalten wird, insbesondere für die Beurteilung bestehender Tragwerke. Zu Beginn dieser Forschung wurden folgende Probleme bei der Tragwerksbemessung mittels LM1 identifiziert:

- Die Einzellast Q scheint zu gross zu sein und die Tandemachsen liegen zudem zu nahe beieinander (1,2 m);
- Die flächenverteilte Belastung q resultiert bei grossen Spannweiten in zu grossen Einwirkungen;
- Dynamischer Effekte werden zurzeit mithilfe eines einzelnen dynamischer Vergrösserungsfaktor bei der der Angabe der charakteristischen Lastwerte berücksichtigt. Dies entspricht nicht der Realität, da eine dynamische Erhöhung von der Art der Belastung abhängen sollte;
- Es ist unklar, wie γ_{Sd}, der Teilsicherheitsfaktor zur Berücksichtigung der Unsicherheiten bei der Berechnung von Einwirkungseffekten, berücksichtigt werden soll, bestimmt wird und welche weiteren Unsicherheiten er abdecken soll;
- Der standardisierte Sensitivitätsfaktor α_E = 0,7 ist ein oberer Grenzwert und führt somit zu einer zusätzlichen konservativen Schätzung, wie dies beispielsweise von fib (fib Model Code 2010) für eine Vielzahl von Szenarien gezeigt wurde;
- SIA 261 berücksichtigt keine Einwirkungen durch Sonderfahrzeuge, die derzeit im Strassennetz verkehren (SIA 261-10.3.4), SIA 269/1 berücksichtigt diese jedoch bei der Festlegung der Anpassungsfaktoren (siehe Anmerkungen zu Tabelle 1 in SIA 269/1:2011)
- Sowohl in der Praxis als auch in Forschungsarbeiten wurde ein uneinheitliches Niveau der Zuverlässigkeit bei verschiedenen Brückentypen beobachtet, siehe (A. Fürst, persönliche Mitteilung, April 2021) ;
- Die Aktualisierung der Anpassungsfaktoren $\alpha_{i,act}$ für LM1 gemäss SIA 269/1:2011 beschränken sich auf den gesetzlich zulässigen Verkehr und berücksichtigen nur die Steigerung des Verkehrs bis 2025;

- Die Einteilung in und Definition von bestimmten Brückentypen, z. B. kurze Brücken, ist unklar, und gewisse neuere Untersuchungen (wie beispielsweise diejenige von Meystre et al. (2014)) werden zurzeit nicht berücksichtigt.

Relevanz von WIM-Daten (Weigh-in-motion)

Moderne Ansätze nutzen probabilistische Methoden und WIM-Daten (Weigh-in-motion), um Streuungen und Extremszenarien zu berücksichtigen. Die WIM-Technologie ist für diese Forschung von entscheidender Bedeutung, da sie detaillierte Daten zu Achslasten, Fahrzeugkonfigurationen und Verkehrsflussmustern liefert. In über 25 Jahren hat die Schweiz eine robuste WIM-Datenbank aufgebaut, die hochwertige Daten für die Kalibrierung der Modelle mittels probabilistischer Methoden bereitstellt, welche Schwankungen und Extremszenarien berücksichtigen. Ausgewählte WIM-Daten erfüllen drei Hauptkriterien, darunter:

1. Repräsentativität des ASTRA-Strassennetzes, wodurch sichergestellt wird, dass die Daten die Vielfalt der Verkehrsbedingungen und Fahrzeugtypen im gesamten Netz widerspiegeln;
2. Messqualität, die genaue und zuverlässige Erfassungen von Gewichten und Anordnungen der Achsen garantiert;
3. Langfristige Stabilität, um über längere Zeiträume konsistente Daten für eine robuste Analyse bereitzustellen.

Methodik

Um die kritischen Verkehrskombinationen auf Brücken erfolgreich zu bewerten, ist es wichtig, das gleichzeitige Auftreten extremer Belastungen, das Auftreten verschiedener Verkehrstypen (d. h. fliessender, gestauter und stehender Verkehr) und den Einfluss der unterschiedlichen Konfigurationen der Tragwerke angemessen zu berücksichtigen. Solche Analysen werden zunächst für eine einzelne Fahrspur durchgeführt und dann auf den Fall von zwei Fahrspuren ausgeweitet. Zu diesem Zweck werden WIM-Daten aus der ASTRA-Datenbank analysiert und optimiert und anschliessend ein relevanter Verkehrssatz ausgewählt.
Zur Entwicklung des neuen Lastmodells werden Simulationen unter Verwendung von 3 Hauptlasttypen durchgeführt, siehe Abbildung 1. Unter Berücksichtigung einer einzelnen Fahrspur werden die folgenden Lastkombinationen betrachtet:

1. Eine Einzellast oder Achslast für lokale Nachweise;
2. Gruppen von Achsbelastungen für lokale und globale Nachweise typischer Plattenbrücken;
3. Eine Achsfolge, die eine Fahrzeugkolonne repräsentiert, für globale Nachweise von Mehrfeldbrücken oder Brücken mit größeren Spannweiten. Diese idealisierte Konfiguration wird dann auf die zusätzlichen Fahrspuren ausgeweitet; das gemeinsame Auftreten von Achsen und Lastkraftwagen sowie mehrere Fahrspuren werden bei verschiedenen Brückentypen berücksichtigt.

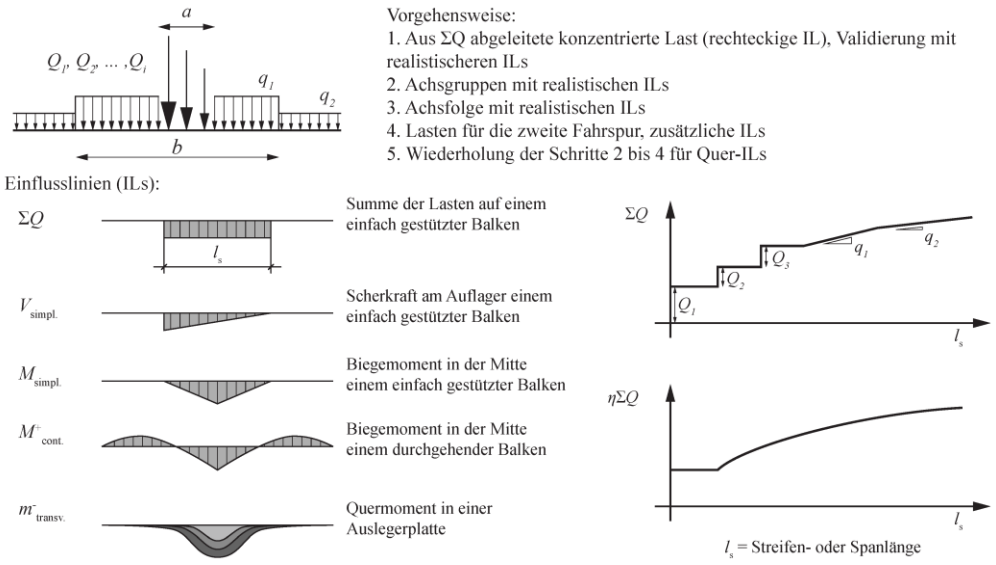

Abbildung 1: Vorgehensweise zur Erstellung eines neuen Lastmodells (Anmerkung: ILs steht für Einflusslinien)

Die Kalibrierung des neuen Lastmodells für die oben genannten drei Hauptlastarten, einschließlich ihrer Wechselwirkungen und Korrelationen, wird durchgeführt und kann eine Kombination aus semiprobabilistischer oder vollprobabilistischer Modellierung sein. Das Kalibrierungsverfahren wird in folgenden Punkten zusammengefasst:

- Auswahl relevanter Fahrspurkonfigurationen aus den WIM-Daten und Definition der Brückenpopulation (Systeme, Spannweiten, ...);
- Berechnung der verschiedenen Verteilung der Einwirkungseffekte (E_{sim}) und, bei vollständig probabilistischer Modellierung, Berechnung der entsprechenden Widerstandsverteilungen;
- Definition einer Konfiguration für das neue Lastmodell und Berechnung der entsprechenden Einwirkungen ($E_{d,mod}$);
- Durchführung von Zuverlässigkeitsanalysen (für die semiprobabilistische Analyse wird ein fester Wichtigkeitsfaktor α_E = 0,7 angenommen, wie in (EN 1990:2021 Eurocode – Projektbasis für die statische Berechnung von Tragwerken und Geotechnik, 2021) und in Anhang C von (SIA 269/1, 2011) definiert;
- Vergleich der Einwirkungseffekte ($E_{d,mod}$ und $E_{d,sim}$) für die Population der Brücken bei semiprobabilistische Analysen;
- Vergleich der Zuverlässigkeitsindizes (β und β_{tgt}) für die Brückenpopulation entsprechend der durchgeführten vollprobabilistischen Analysen;
- Optimierung des Lastfaktoren und Lastkonfigurationen des neuen Lastmodells, um eine für die ausgewählte Population der Brücken zu erzielende optimierte Konfiguration zu erzielen; $E_{d,mod}/E_{d,sim}$ muss auf der sicheren Seite liegen ($E_{d,mod}/E_{d,sim} > 1{,}0$), so nah wie möglich an der Einheit, so gleichmässig wie möglich und mit minimaler Variabilität;
- Das optimierte neue Lastmodell ist unter praktischen Gesichtspunkten kritisch zu prüfen, wobei der Schwerpunkt auf einfacher Umsetzung, Benutzerfreundlichkeit und Integration in aktuelle Regelwerke sowie auf Anpassungsfähigkeit unter Berücksichtigung potenzieller zusätzlicher Fahrspuren mit Schwerlastverkehr liegen sollte.

Das allgemeine Verfahren zur Quantifizierung der Sicherheitsreserven zwischen dem normativen LM1 oder einer Aktualisierung des Lastmodells für die Norm SIA 269/1 und Simulationen der tatsächlichen Belastungen und Lasteinwirkungen wird durch detaillierte Leitlinien erreicht:

- Einhaltung des in SIA 269:2011 beschriebenen Prüfverfahrens;
- Berücksichtigung der verschiedenen Arten von ASTRA-Brückentragwerken, bei denen sich LM1 als zu konservativ erweisen würde;
- Befolgung des schrittweisen Ansatzes für deterministische und probabilistische Nachweise, um die praktische Anwendbarkeit sicherzustellen. Dabei wird der Ansatz von Annäherungsstufen (LoA) eingeführt und angewendet.

Der Vorteil dieses Ansatzes besteht darin, dass er einen allgemeinen Anwendungsrahmen darstellt und für die Aktualisierung auf Grundlage neuer Erkenntnisse zur aktuellen und zukünftigen Verkehrsentwicklung angewendet werden kann. Aufgrund seiner allgemeinen Gültigkeit können niedrigere Annäherungsstufen (LoA) definiert werden, indem konservative Annahmen zu höheren LoAs getroffen werden. Diese Annahmen können auch auf deterministischen Analysen basieren, die in der Praxis häufig verwendet werden.

Ergebnisse

Die Ergebnisse zeigen, dass das vorgeschlagene *New Load Model 1*, das im Folgenden als NLM1 bezeichnet wird, einen bedeutenden Fortschritt gegenüber dem aktuellen LM1 darstellt und einen genaueren, zuverlässigeren und praktischeren Ansatz für die Belastung von Strassenbrücken bietet. Abbildung 2 zeigt die NLM1-Konfiguration, wobei die relative Position von $Q_{k,1}$ innerhalb von $q_{1k,1}$ so gewählt werden sollte, dass die maximale Wirkungsentfaltung erzielt wird, und die Position von $Q_{k,2}$ frei wählbar ist. Weitere Informationen finden Sie in Abschnitt 5.2. Die Optimierung von NLM1 erfolgt in mehreren Schritten, zunächst anhand von Simulationen ohne Berücksichtigung eines dynamischen Vergrösserungsfaktors (DAF) φ_{dyn} oder der Teilsicherheitsfaktor zur Berücksichtigung der Unsicherheiten bei der Berechnung von Einwirkungseffekten γ_{sd}. Diese werden separat untersucht und anschliessend explizit hinzugefügt (siehe § 5.1.4), sodass diese Faktoren für spezifische Fälle angepasst werden können oder im Falle, dass neue Erkenntnisse darauf hindeuten, leichter überarbeitet werden können. Die Kennwerte in Abbildung 2 werden jedoch der Einfachheit halber als $E_{di,act}/\gamma_F$ angegeben.

Zwar wurde NLM1 vor dem Hintergrund einer Ressourcenschonung und Verbesserung der Nachhaltigkeit bestehender Brücken entwickelt, jedoch könnte das NLM1 aber nach zusätzlicher Validierung und Kalibrierung auch für die Bemessung neuer Brücken eingesetzt werden.

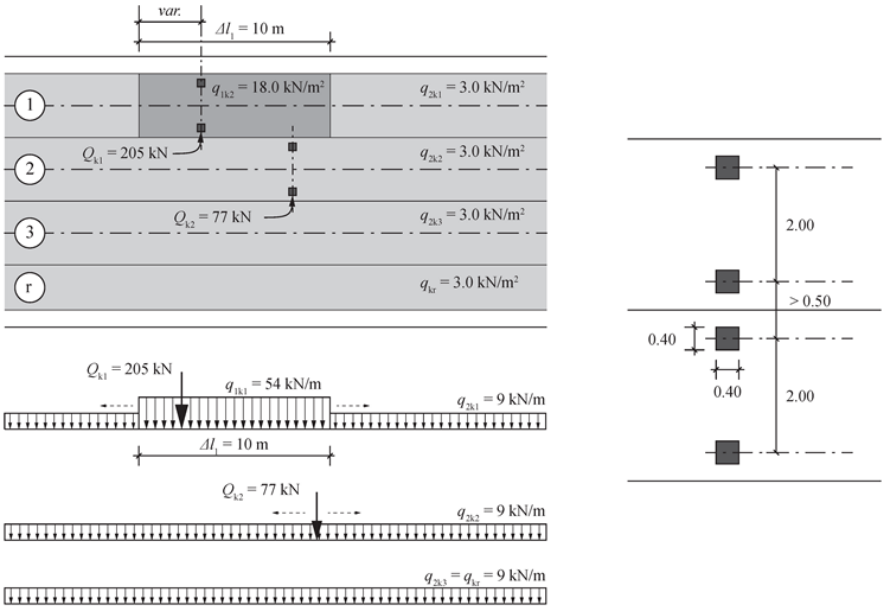

① $Q_{k,1}$ = 205 kN $q_{1k,1}$ = 18 kN/m² $q_{2k,1}$ = 3,00 kN/m²

wobei die relative Position von $Q_{k,1}$ (*var*) innerhalb von $q_{1k,1}$ so gewählt werden sollte, dass die maximale

Wirkungsentfaltung erzielt wird

② $Q_{k,2}$ = 77 kN $q_{2k,2}$ = 3,00 kN/m²

③ $q_{2k,3}$ = 3,00 kN/m²

q_{kr} = 3,00 kN/m²

Abbildung 2: Das neue Lastmodell 1 (NLM1) zur Bewertung bestehender Brücken, dargestellt im Code-Format mit den charakteristischen Norm Werten der Belastungen (die Bemessungswerte werden ermittelt unter Verwendung von: $\alpha_{i,act}$ = 1,00, γ_F = 1,50)

Folgende Punkte sind hinsichtlich der Entwicklung des NLM1 hervorzuheben:

- **Kalibrierungsprozess**: Schlüsselparameter wie die Grössen der verteilten Lasten und die Achslastgruppenkonfigurationen werden iterativ unter Verwendung der oben beschriebenen Methodik kalibriert. Dieser Prozess ist dank der Verfügbarkeit von WIM-Daten möglich, die eine solide Grundlage für die Kalibrierung der Modellparameter bildeten und die tatsächlichen Verkehrsbedingungen widerspiegeln.
- **Zukünftige Verkehrsüberlegungen**: Trotz vieler Ähnlichkeiten wurde in der Studie für ASTRA 82001 (Papastergiou et al., 2025), das Vorhandensein von PUN zwar untersucht, jedoch nur, um einen einzigen aktualisierten Faktor festzulegen (Schritt 0). In dieser Untersuchung wurde verfolgt, um ein allgemein gültiges neues Lastmodell vorzuschlagen, ein anderer Ansatz, nämlich die verschiedenen Autobahnspurkonfigurationen mit zwei Schwerlastverkehr_Spuren gut abzudecken, wobei die ungünstigste Konfiguration tatsächlich eine mit PUN ist. Zukünftiger Verkehrsanstieg wird berücksichtigt:
  - Wenn zwei Schwerlastverkehr Spuren simuliert werden, mit einem Anstieg der Anzahl schwerer Fahrzeuge um 67 % im Vergleich zu heute und unter Berücksichtigung ihrer Verteilung auf die Spuren;
  - Für weitere Fahrspuren (3., 4. ...) durch Erhöhung der flächenverteilte Belastung (UDL) von 2,25 auf 3,00 kN/m²im Vergleich zum aktuellen LM1.

Diese berücksichtigen Unsicherheiten hinsichtlich der zukünftigen Entwicklung des Schwerverkehrs, wie z. B. die Zunahme des Schwerverkehrs auf verschiedenen Fahrspuren, Verkehrsstaus sowie die Notwendigkeiteinbeziehung von Brücken mit bidirektionalem Verkehr auf mehreren Fahrspuren. Der Zeithorizont 2050 wurde festgelegt, da eine regelmäßige Überprüfung der Verkehrsentwicklung erforderlich ist. Dies kann jedoch in bestimmten Fällen dazu führen, dass NLM1 ungünstiger ausfällt als ASTRA 82001. Daher können die Konformitätsfaktoren aus der Überprüfung mit NLM1 niedriger sein als diejenigen, die mit ASTRA 82001 ermittelt wurden. Wenn ein Vergleich zwischen beiden vorgenommen werden soll, sollte dieser zwischen den Ergebnissen aus Schritt 0 mit PUN ($\alpha_{act,unique}$ = 0,60) und denen aus NLM1 erfolgen. Dennoch war es nicht das Ziel von NLM1, wirtschaftlicher (d. h. weniger konservativ) zu sein, sondern ein einheitlicheres Sicherheitsniveau zu erreichen, vielseitiger zu sein und somit eine Extrapolation zu ermöglichen, während ASTRA 82001 nicht außerhalb seiner Anwendungsgrenzen angewendet werden kann.

- **Ergebnisse für einspuriges Lastmodell**: Bei einspurigem Verkehr erzielt das NLM1 eine gleichmässigere Sicherheitsmarge bei den Einwirkungen als das aktuelle Lastmodell LM1. Tatsächlich resultiert das NLM1 in einer gleichmässigen Sicherheitsmarge unabhängig von der Spannweite, während das LM1 bei kurzen und großen Spannweiten (<15 m und >30 m) tendenziell zu konservativ ist, während sich die Sicherheitsmarge bei mittleren Spannweiten (15–30 m) deutlich verringert.
- **Ergebnisse für mehrspuriges Lastmodell***:* Im Falle von zweispurigem Verkehr zeigt sich die höhere Genauigkeit des NLM1 zusätzlich, da es das gleichzeitige Vorhandensein von Lastkraftwagen auf beiden Spuren berücksichtigt. Der probabilistische Ansatz stellt jedoch sicher, dass die Zielzuverlässigkeit ohne übermässige Sicherheitsmarge erreicht werden. Wichtige Leistungsindikatoren wie gleichmässige Zuverlässigkeitsindizes und eine verringerte Streuung bei den Einwirkungseffekten unterstreichen die Wirksamkeit des Modells. NLM1 deckt alle Extremszenarien des zweispurigen Verkehrs ab, bei denen ein hoher Anteil an Schwerlastfahrzeugen auf der 2. Spur verkehrt. Das Modell ist so kalibriert, dass es Fälle mit PUN (d. h. die Umwandlung von zwei in drei Fahrspuren) sowie Baustellenbedingungen (d. h. bei 2+2-spurigem Gegenverkehr auf einer Brücke, wobei der Schwerlastverkehr auf zwei Fahrspuren beschränkt ist) abdeckt;
- **Szenarien mit Sonderfahrzeugen**: NLM1 deckt Szenarien mit Sonderfahrzeugen, wie Mobilkranen oder überladenen Lkws[2] besser ab, welche in traditionellen Lastmodellen nicht ausreichend berücksichtigt werden. Die Flexibilität von NLM1 ermöglicht Anpassungen auf der Grundlage realer Verkehrsmuster, bei denen sich auf der ersten Spur die grösste Last über 10 m verteilt.
- **Konsistenz zwischen den Annäherungsstufen (LoAs)**: Sowohl bei semiprobabilistischen als auch bei vollprobabilistischen Analysen werden die gleichen Niveaus der Zuverlässigkeit erreicht, die über verschiedene Spannweiten und Brückentypen hinweg konsistent sind. Der Hauptfaktor für die Verkehrskalibrierung im Falle von semiprobabilistischen Analysen ist der Sensitivitätsfaktor der Einwirkungseffekte des Verkehrs. Die Untersuchungen zeigen, dass ein Wert von $\alpha_{E,Traffic}$

[2] Überlastete Achsen oder Gesamtgewichte, wobei die Autoren empfehlen, die Zahl der Verstösse durch vermehrte Kontrollen (durch die Polizei oder technische Geräte) auf ein Minimum zu beschränken

gemäss aktuellen Normen konservativ, für Strassenbrücken und den motorisierten Verkehr jedoch akzeptabel ist.

- **Vollprobabilistische Analyse der Zuverlässigkeit**: Es wird ein Algorithmus vorgeschlagen, der die Kalibrierung des Lastmodells mittels vollprobabilistischer Analysen ermöglicht. Diese Analysen zeigen, dass das NLM1 im Vergleich zu früheren Lastmodellen eine einheitlichere Sicherheitsmarge bietet. Zudem ermöglicht es weitere Verbesserungen des Lastmodells durch die Untersuchung einer Verringerung der Streuung der Modellunsicherheiten auf der Einwirkungsseite. Schliesslich ermöglicht es die Kalibrierung des Lastmodells für spezifische Fallstudien mit unterschiedlichen or speziellen Brückentypen.
- **Dynamische Faktoren und Mehrspur-Effekte**: Dynamische Vergrösserungsfaktoren und Mehrspur-Effekte werden explizit berücksichtigt, was die Genauigkeit der Vorhersagen der Einwirkungseffekte erheblich verbessert und es ermöglicht, diese im Falle zusätzlicher und neuer Erkenntnisse zu aktualisieren.
- **Verbesserung von Mängeln aktueller Lastmodelle**: Einschränkungen des LM1 bei der Erhaltung, wie beispielsweise die Unfähigkeit, komplexe Verkehrsszenarien oder unterschiedliche Brückengeometrien zu erfassen, werden durch das NLM1 wirksam behoben, wodurch sichergestellt wird, dass es sich gut für die Bewertung bestehender Brücken eignet und für die Bemessung neuer Brücken geeignet ist.

Empfehlungen für zukünftige Forschung

Im Laufe des Projekts wurden mehrere Themen angesprochen, die außerhalb des Forschungsrahmens lagen; diese sind im Folgenden aufgeführt:

- Weiterentwicklung des NLM1 zur Erweiterung seiner Anwendbarkeit und Ausarbeitung von Anwendungsregeln für andere Lasteinwirkungen, u. A. zur Bemessung von Ermüdung, Beschleunigung, Abbremsen, Zentrifugal- und Querkräften;
- Es sollten zusätzliche Untersuchungen durchgeführt werden, um den Einsatz von NLM1 für Stützmauern gemäss Schweizer Normen (SIA 261, 2020) und(SIA 269/1, 2011, p. 269) zu ermöglichen. Tatsächlich könnte das derzeitige LM1 zu übermässig konservativen Einwirkungen führen, die kostspielige Erhaltungsmassnahmen erfordern;
- Erweiterung der WIM-Datenbank um zusätzliche Verkehrsszenarien, unterrepräsentierte Brückentypen und geografische Regionen. Es wird empfohlen, das derzeitige Netz von WIM-Stationen und die Datenerfassung beizubehalten, um die Verkehrsentwicklung an bestimmten Standorten im Zeitverlauf untersuchen zu können;
- Prognose der zukünftigen Verkehrslasten unter Berücksichtigung der Auswirkungen neuer Technologien wie elektrischer Lastkraftwagen, autonomer Fahrzeuge und Veränderungen in den Verkehrsmustern. Die Verkehrsentwicklung wird sich sowohl auf die Projektierung neuer Brücken als auch auf die Beurteilung bestehender Brücken auswirken. Tatsächlich berücksichtigen aktuelle Modelle in erster Linie die aktuellen Verkehrsbedingungen. Es sei daran erinnert, dass das NLM1 die Nutzung der PUN berücksichtigt;
- Dynamische Effekte und die damit verbundenen Unsicherheiten müssen mithilfe verfeinerter Methoden genauer untersucht und modelliert werden, um ihren Einfluss auf die Einwirkungseffekte genau zu erfassen, insbesondere bei spezifischen

Szenarien mit Sonderfahrzeugen, die zu überhöhtem Konservatismus führen könnten;

- Der Sensitivitätsfaktor für Verkehrseinwirkungen in semi-probabilistischen Ansätzen, der derzeit bei 0,7 liegt ($\alpha_{E,Traffic}$), sollte genauer untersucht und es sollten alternative Werte vorgeschlagen werden, um den Konservativismus vor allem bei bestehenden Brücken zu verringern;
- Vollständige probabilistische Beurteilungen der Zuverlässigkeit sollten auf ein breiteres Spektrum von Brückentypen, die nichtlineare Kombination korrelierter Einwirkungen und auf Brückeneinstürze ausgeweitet werden. Zudem würde eine Unterscheidung zwischen Versagensarten die Beurteilungen der Zuverlässigkeit verbessern;
- Bei probabilistischen Zuverlässigkeitsanalysen wurde das in dieser Arbeit vorgeschlagene NLM1 mit der aktuellen Norm EN 1992-1-1:2004 zur Berechnung der Widerstandsseite verglichen. Es sollten jedoch auch Vergleiche mit der neuen Generation der Norm EN 1992-1-1:2023 durchgeführt werden, die nachweislich eine geringere Streuung bei den Widerstandsformeln aufweist;
- Wechselwirkungen zwischen verschiedenen Einwirkungen, wie beispielsweise die Wechselwirkung zwischen Moment und Axialkraft in der Nähe der Auflager eines Trägers, sollten untersucht werden. In dieser Arbeit werden die maximalen Einwirkungen unabhängig voneinander betrachtet, da vorläufige Untersuchungen gezeigt haben, dass die separate Maximierung jeder Einwirkung im Allgemeinen den konservativsten Fall darstellt. Es kann jedoch nicht ohne Weiteres bestätigt werden, dass dies für alle geometrischen Konfigurationen und Brückentypen gilt. Zudem sollte die zusätzliche Sicherheitsmarge bestimmt werden, der sich aus der separaten Betrachtung der Einwirkungen ergibt;
- Entwicklung vereinfachter Hilfsmittel für Praktiker, wie z. B. Schulungsprogramme, benutzerfreundliche Tools und Arbeitsabläufe, um die Anwendung fortschrittlicher Techniken zur Berechnung der Belastung auf transparente Weise zu erleichtern. Die Ermöglichung semi-probabilistischer und voll-probabilistischer Bewertungen in der Praxis ist ebenfalls entscheidend, um eine schnelle Akzeptanz durch Ingenieure und politische Entscheidungsträger sicherzustellen.

Résumé

Introduction

Exposé du problème

Une utilisation plus efficace des ressources est exigée dans tous les domaines, ce qui impose de repérer et d'éliminer les marges de sécurité injustifiées dans la conception. Depuis 1892, les exigences suisses en matière de charges de trafic pour la conception de nouveaux ponts routiers ont été définies et mises à jour régulièrement afin de tenir compte de l'évolution du trafic et des véhicules lourds. Ce n'est qu'à partir de l'introduction de la norme SIA 160:1956 que les charges de trafic représentées par des véhicules réels ont été remplacées par une combinaison de charges uniformément réparties et concentrées qui reproduit le trafic réel et les effets d'action correspondants. Ce travail se concentre uniquement sur les effets des charges verticales.

Pour la conception de nouveaux ponts, le coût économique et écologique lié à la prise en compte de charges de trafic supérieures à celles actuellement présentes sur le réseau routier peut être considéré comme un choix durable à long terme, car une réserve de résistance permet de s'adapter aux changements d'utilisation et de faire face aux innovations potentielles en matière de technologie des transports.
Cependant, pour les ponts existants, dans une optique de prise de décision durable, les considérations suivantes doivent être prises en compte :

- En général, le niveau de sécurité induit par les normes actuelles de conception/évaluation n'est pas uniforme entre les différents systèmes structuraux. Cette incohérence conduit à une sécurité non uniforme au sein du parc de ponts existant ;
- Lors de l'évaluation des ponts existants, le conservatisme caché conduit à des rénovations, des renforcements ou d'autres interventions de maintenance inutiles, chronophages et coûteuses, qui ne sont pas dans l'intérêt de la société.

Les points exposés ci-dessus sont confirmés par les problèmes observés dans la pratique avec les normes actuelles d'évaluation de structures (série SIA 269: 2011), qui ont entraîné une augmentation du nombre de mandats pour des analyses de trafic spécifiques au site, liées aux évaluations de la sécurité structurale des ponts. Alors que des progrès significatifs ont été réalisés dans le calcul de la résistance des éléments structuraux des ponts, relativement peu d'efforts ont été consacrés à l'étude des charges de trafic afin d'en réduire le conservatisme. À cette fin, une analyse critique du modèle de charge 1 (LM1) des normes de conception actuelles doit être effectuée afin d'identifier les lacunes du LM1; des alternatives à la mise à jour des coefficients d'actualisation applicables au trafic routier $\alpha_{i,act}$, voir SIA 269/1:2011, devraient également être étudiées, ainsi que l'influence de la réaffectation de la bande d'arrêt d'urgence (R-BAU).
À cette fin, l'objectif principal de cette recherche est d'identifier les réserves en termes d'effets des actions dues aux charges de trafic sur les ponts routiers et de développer un nouveau modèle de charge (NLM) amélioré à intégrer dans les futurs normes. D'autres aspects, tels que le traitement des effets dynamiques, l'impact des véhicules surchargés et des véhicules spéciaux, sont également abordés.

Objectifs de la recherche

Les besoins et les objectifs de recherche de ce projet sont résumés ci-après :

1. Revue historique des bases et du développement du LM1 de la norme EN 1991-2:2004.
2. Résumé du traitement et de la classification des données WIM issues de la base de données OFROU, qui inclut des données plus récentes (de 2022) que celles utilisées lors de projets précédents. Aperçu des algorithmes permettant de réaliser des simulations de trafic sur la base de ces données afin de développer et de calibrer un nouveau modèle de charge (NLM1) pour l'évaluation des ponts routiers existants.
3. Meilleure compréhension des situations critiques dues aux charges de trafic en termes d'effets d'action probabilistes sur une et sur deux voies (valable pour les ponts existants et les nouveaux ponts) pour les types de ponts usuels de la base de données des ponts existants de l'OFROU.
4. Définition d'un nouveau modèle de charge (NLM1) afin de mieux décrire les types de véhicules lourds concernés, y compris les véhicules spéciaux, ainsi que leurs effets sur les structures, pour les vérifications locales et globales des ponts courts et à plus longues portées (jusqu'à 80 m). Clarification des incertitudes dans le calcul des effets d'action sur les structures qui sont couvertes par le facteur partiel de modèle γ_{Sd} et par le traitement des effets dynamiques.
5. Extension du modèle à la circulation à deux voies avec des hypothèses raisonnables, en incluant l'influence de la R-BAU.
6. Proposition d'une procédure générale pour quantifier les réserves de sécurité entre les effets d'action obtenus à l'aide du LM1 actuel, ou d'autres modèles de charge proposés par la norme SIA 269/1:2011, et ceux obtenus en effectuant des simulations à partir de données WIM.
7. Établissement d'un cadre permettant de mettre à jour régulièrement les hypothèses de trafic afin de tenir compte de son évolution, avec la révision correspondante des normes de conception et d'évaluation tous les 25 ans (en lien avec l'objectif 2 et en permettant l'utilisation de « trains de charges » pour simuler divers scénarios en sélectionnant les charges de trafic spécifiques).

Informations de base

Contexte des modèles de charge

Le modèle actuel de charge 1 (LM1) selon la norme SIA 261:2020 est présenté à la Figure 5, où les coefficients d'actualisation α_{Qi} et α_{qi} sont des paramètres définis au niveau national (NDP selon la norme EN 1991-2:2002). La principale différence entre le LM1 de la norme EN 1991-2:2002 et celui de la norme SIA 261:2020 réside dans l'absence d'un essieu tandem (groupe de deux axes) sur la 3ème voie. De plus, la norme EN propose trois modèles de charge supplémentaires, tandis que la norme suisse ne propose qu'un deuxième modèle de charge (pour les véhicules spéciaux et exceptionnels). Dans le présent document, le LM1 selon la norme EN 1991-2:2002 et selon la norme SIA 261:2020 seront considérés comme équivalents et ce modèle sera simplement appelé LM1.

Le récent rapport de recherche de l'OFROU (Documentation ASTRA 82001, 2025; Sjaarda et al., 2022) s'appuie sur des analyses détaillées de mesures WIM

soigneusement traitées afin d'identifier les véhicules lourds et les cas de charge responsables des effets d'action les plus importants.
Dans l'ASTRA 82001, l'actualisation du LM1 permet de couvrir les cas de charge de trafic déterminants en conservant une combinaison de charges uniformément réparties et de charges concentrées d'essieux, en particulier pour l'évaluation des structures existantes. À l'origine de la présente recherche, les problèmes suivants avec le LM1 ont été identifiés :

- La charge concentrée Q semble trop élevée et les axes des essieux tandem sont également trop proches (1,2 m) ;
- La charge répartie q conduit à des valeurs d'effets d'action excessives pour les longues portées ;
- Le traitement des effets dynamiques, directement inclus sous la forme d'un facteur d'amplification dynamique unique dans les valeurs des charges caractéristiques, ne reflète pas la réalité car il devrait dépendre du type de charge ;
- La manière dont γ_{Sd}, le facteur partiel prévu pour tenir compte des incertitudes dans le calcul des effets des actions, est déterminé n'est pas claire, pas plus que les autres incertitudes qu'il est censé couvrir ;
- Le facteur de sensibilité normalisé α_E = 0,7 constitue une limite supérieure et introduit donc un niveau supplémentaire de conservatisme, comme le montrent de nombreux scénarios, par exemple ceux du fib (fib Model Code 2010) ;
- La norme SIA 261 ne tient pas compte des actions dues aux véhicules spéciaux circulant actuellement sur le réseau routier (SIA 261-10.3.4) ; cependant, la norme SIA 269/1 en tient compte lors de la définition des facteurs d'actualisation (voir les notes du tableau 1 de la norme SIA 269/1:2011) ;
- Un niveau de fiabilité non uniforme entre les différents types de ponts a été observé tant dans la pratique que dans les travaux de recherche, voir (A. Fürst, communication personnelle, avril 2021) ;
- Les facteurs d'actualisation $\alpha_{i,act}$ pour le LM1 selon la norme SIA 269/1:2011 se limitent au trafic légalement autorisé et ne tiennent compte que de la croissance du trafic jusqu'en 2025 ;
- Les définitions de certains types de ponts, tels que les ponts courts, ne sont pas claires, et des études comme celles réalisées par Meystre et al. (2014) ne sont pas prises en compte.

Importance des données de pesage en mouvement (WIM)

Les approches modernes recourent à des méthodes probabilistes et à des données de pesage en mouvement (WIM) pour tenir compte de la variabilité et des scénarios extrêmes. La technologie WIM est essentielle à cette recherche, car elle permet de fournir des données détaillées sur les charges par axe/essieu, les configurations des véhicules lourds et les schémas de circulation. En plus de 25 ans, la Suisse a constitué une solide base de données WIM, offrant des données de haute qualité pour l'étalonnage de modèles avec des méthodes probabilistes qui prennent en compte la variabilité et les scénarios extrêmes. Les données WIM sélectionnées répondent à trois critères principaux, à savoir :

1. La représentativité du réseau routier des routes nationales OFROU, qui garantit que les données reflètent la diversité des conditions de circulation et des types de véhicules sur l'ensemble du réseau ;

2. La qualité des mesures, qui garantit des enregistrements précis et fiables des poids et des configurations d'essieux ;
3. La stabilité à long terme, afin de fournir des données cohérentes sur de longues périodes pour une analyse fiable.

Méthodologie

Afin d'évaluer avec succès les combinaisons de trafic critiques sur les ponts routiers, il est important de traiter correctement la survenue simultanée de charges extrêmes, la présence de différents types de trafic (c'est-à-dire fluide, congestionné, embouteillé à l'arrêt) et l'influence des différentes configurations des systèmes structuraux des ponts. Ces analyses sont d'abord effectuées sur une seule voie, puis étendues pour couvrir les cas avec deux voies comportant du trafic lourd. À cette fin, la base de données WIM de l'OFROU est analysée, triée et un ensemble pertinent de données de trafic est sélectionné.

Pour développer le nouveau modèle de charge, des simulations sont réalisées en utilisant trois types de charges principaux, voir Figure 1. En considérant une seule voie, les combinaisons des types de charges suivantes sont prises en compte :

1. Une charge concentrée ou d'essieu simple pour les vérifications locales ;
2. Des groupes de charges d'essieux pour les vérifications locales et globales de ponts-dalle types ;
3. Une séquence d'essieux représentant une file de véhicules lourds pour les vérifications globales de ponts à portées multiples ou avec des portées plus longues. Cette configuration idéalisée est ensuite étendue aux voies supplémentaires ; la présence conjointe d'essieux et de véhicules lourds ainsi que de voies multiples sur divers types de ponts est considérée.

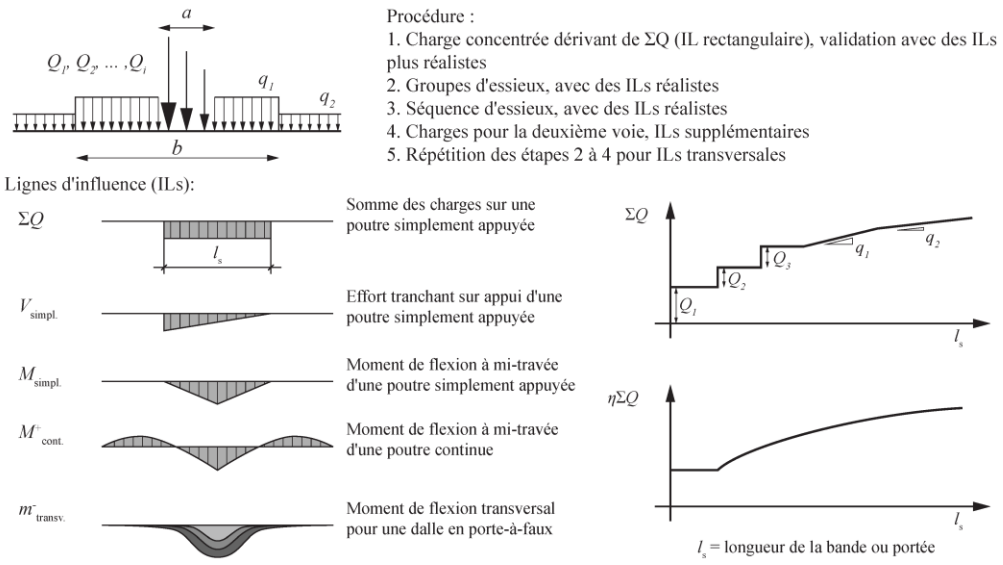

Figure 1: Méthodologie suivie pour établir un nouveau modèle de charge (remarque : ILs signifie « lignes d'influence »)

L'étalonnage du nouveau modèle de charge pour les trois types de charges principaux ci-dessus, y compris leurs interactions et corrélations, est effectué et peut provenir

d'une combinaison de modélisation semi-probabiliste ou entièrement probabiliste. La procédure d'étalonnage est résumée dans les points suivants :

- Choix des configurations de voies pertinentes parmi les données WIM et définition de la population de ponts (systèmes, travées, ...) ;
- Calcul des différentes distributions des effets des actions (E_{sim}) et, pour la modélisation entièrement probabiliste, calcul des distributions des résistances correspondantes ;
- Définition d'une configuration pour le nouveau modèle de charge et calcul des effets des actions correspondants ($E_{d,mod}$) ;
- Utilisation de méthodes d'analyse de fiabilité (pour la modélisation semi-probabiliste, un facteur de sensibilité fixé à $\alpha_E = 0{,}7$ est admis, tel que défini dans (EN 1990:2021 Eurocode - Bases de calcul des structures et de la géotechnique, 2021) et dans l'annexe C de (SIA 269/1, 2011) ;
- Comparaison des effets des actions ($E_{d,mod}$ et $E_{d,sim}$) pour la population de ponts pour les analyses semi-probabilistes ;
- Comparaison des indices de fiabilité (β et β_{tgt}) pour la population de ponts pour les analyses probabilistes ;
- Optimisation des valeurs pour la configuration du nouveau modèle de charge afin de l'optimiser pour la population de ponts sélectionnée ; le rapport $E_{d,mod}/E_{d,sim}$ doit être du côté de la sécurité ($E_{d,mod}/E_{d,sim} > 1{,}0$), aussi proche que possible de l'unité, aussi uniforme que possible, et minimisant la variance ;
- Examen critique du nouveau modèle de charge optimisé d'un point de vue pratique, en privilégiant la facilité d'implémentation, la facilité d'utilisation pratique et l'intégration dans les normes actuelles, ainsi que l'adaptabilité compte tenu de potentiels voies supplémentaires avec du trafic lourd.

La procédure générale de quantification des marges de sécurité entre le modèle de charge normatif LM1 ou un modèle de charge actualisé pour la norme SIA 269/1 et les simulations des charges réelles et de leurs effets est mise en œuvre en fournissant des instructions détaillées :

- Respecter la procédure d'examen décrite dans la norme SIA 269:2011 ;
- Prendre en compte les différents types de structures de l'OFROU pour lesquels le LM1 s'avérerait trop conservateur ;
- Suivre une approche par étapes pour des vérifications déterministes et probabilistes, en garantissant l'applicabilité pratique. Ainsi, l'approche par niveaux d'approximation (LoA) sera introduite et utilisée.

L'avantage de cette approche est qu'elle constitue un cadre général et qu'elle peut être mise à jour en tenant compte des nouvelles connaissances sur l'évolution actuelle et future du trafic. Compte tenu de sa validité générale, des niveaux d'approximation (LoA) inférieurs peuvent être définis en formulant des hypothèses prudentes par rapport à des LoA supérieurs. Ces hypothèses peuvent également s'appuyer sur des analyses déterministes, souvent utilisées dans la pratique.

Résultats

Les résultats montrent que le *nouveau modèle de charge* 1 proposé, qui sera désormais désigné par NLM1, représente une avancée significative par rapport à l'actuel LM1, offrant une approche plus précise, fiable et pratique de la modélisation des charges pour les ponts routiers. La Figure 2 montre la configuration du NLM1, où la position relative de $Q_{k,1}$ à l'intérieur de $q_{1k,1}$ doit être choisie de manière à obtenir un effet d'action maximal, tandis que la position de $Q_{k,2}$ est libre. Le lecteur est invité à se reporter au § 5.2 pour plus d'informations. L'optimisation du NLM1 s'effectue en plusieurs étapes, en commençant par des simulations sans inclure de facteur d'amplification dynamique (DAF) φ_{dyn}, ni de facteur d'incertitude de modèle relative aux effets d'action γ_{sd}. Ces éléments sont étudiés séparément et ajoutés explicitement (voir § 5.1.4), ce qui permet d'ajuster ces facteurs pour des cas spécifiques ou si de nouvelles connaissances indiquent que ces valeurs doivent être révisées. Les valeurs caractéristiques des normes dans la Figure 2 sont toutefois exprimées, pour plus de commodité, sous la forme $E_{di,act}/\gamma_F$.

Si le modèle NLM1 a été étalonné pour optimiser l'utilisation des ressources pour le domaine des ponts existants et contribuer au développement durable, il pourrait également être utilisé pour la conception de nouveaux ponts, moyennant une validation et un étalonnage additionnel.

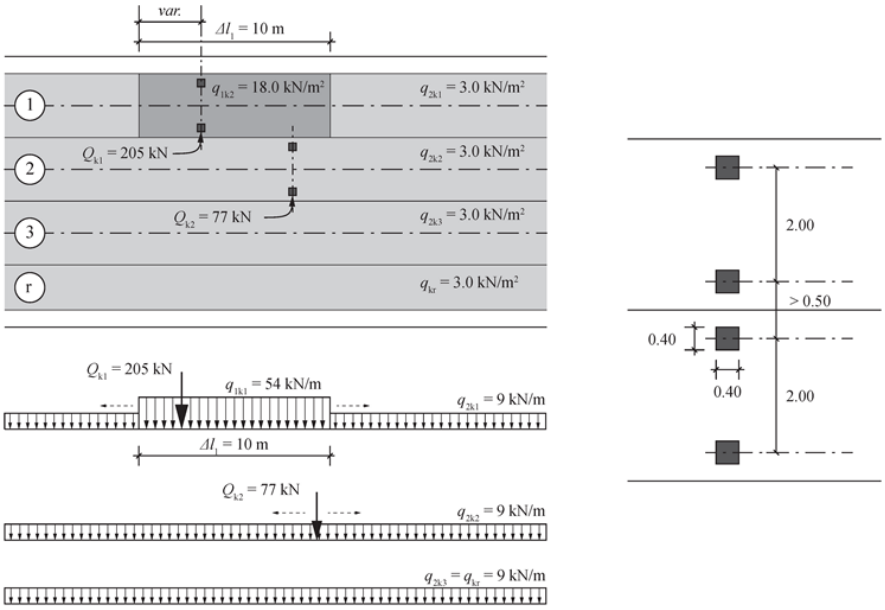

① $Q_{k,1}$ = 205 kN $q_{1k,1}$ = 18 kN/m² $q_{2k,1}$ = 3.00 kN/m²

où la position relative de $Q_{k,1}$ (*var*) à l'intérieur de $q_{1k,1}$ doit être choisie de manière à obtenir un effet d'action maximal

② $Q_{k,2}$ = 77 kN $q_{2k,2}$ = 3.00 kN/m²

③ $q_{2k,3}$ = 3.00 kN/m²

q_{kr} = 3.00 kN/m²

Figure 2: Le nouveau modèle de charge 1 (NLM1) pour l'évaluation des ponts existants, présenté sous forme normative avec les valeurs caractéristiques des charges (les valeurs d'examen sont obtenues en utilisant : $\alpha_{i,act}$ = 1,00 , γ_F = 1,50)

En ce qui concerne le développement du NLM1, les points suivants peuvent être soulignés :

- **Processus d'étalonnage** : les paramètres clés, tels que les valeurs des charges réparties et les configurations des groupes d'essieux, sont étalonnés de manière itérative à l'aide de la méthodologie décrite ci-dessus. Ce processus est rendu possible grâce à la disponibilité des données WIM, qui ont fourni une base solide pour étalonner les paramètres du modèle et refléter les conditions de circulation réelles.
- **Considérations relatives au trafic futur** : malgré de nombreuses similitudes, l'étude réalisée pour ASTRA 82001 (Papastergiou et al., 2025) a examiné la présence d'un R_BAU, mais uniquement dans le but de fixer un coefficient d'actualisation unique (étape 0). Dans cette recherche, afin de proposer un nouveau modèle de charge valable de manière générique, une approche différente a été adoptée, à savoir bien couvrir les différents schémas de voies autoroutières comportant deux voies avec des poids lourds, le pire scénario étant en effet celui avec R-BAU. L'augmentation future du trafic est prise en compte :
  - Lorsque deux voies avec du trafic lourd sont simulées, avec une augmentation du nombre de poids lourds de 67 % par rapport à aujourd'hui et leur répartition entre les voies ;
  - Pour un plus grand nombre de voies (3e, 4e...) en augmentant la charge uniformément répartie (UDL) de 2,25 à 3,00 kN/m²par rapport à l'actuel LM1.

  Ces hypothèses couvrent les incertitudes relatives à l'évolution future du trafic lourd, telles que l'augmentation du trafic lourd sur différentes voies, la congestion du trafic, ainsi que la nécessité d'inclure des ponts à circulation bidirectionnelle sur plusieurs voies. L'horizon 2050 a été fixé car une révision régulière de l'évolution du trafic doit être effectuée. Ces hypothèses de trafic peuvent toutefois conduire, dans certains cas, à ce que le NLM1 soit moins favorable que l'ASTRA 82001. Ainsi, les facteurs de conformité issus de la vérification utilisant le NLM1 peuvent être inférieurs à ceux obtenus avec l'ASTRA 82001. Si une comparaison devait être effectuée entre les deux, elle devrait être faite en entre les résultats de l'étape 0 avec R-BAU ($\alpha_{act,unique}$ = 0,60) et ceux du NLM1. Néanmoins, l'objectif du NLM1 n'était pas d'être plus économique (c'est-à-dire moins conservateur), mais d'atteindre un niveau de sécurité plus uniforme, d'être plus polyvalent et de permettre ainsi des extrapolations, alors que l'ASTRA 82001 ne peut pas être appliqué en dehors de ses limites d'applicabilité.
- **Résultats du modèle sur une seule voie** : dans le cas de scénarios de circulation sur une voie unique, le modèle NLM1 offre une marge de sécurité plus homogène au niveau des effets d'action que le modèle actuel LM1. En effet, le modèle NLM1 affiche des performances constantes quelle que soit la portée, tandis que le modèle LM1 a tendance à être trop en sécurité pour les portées courtes et longues (<15 m et >30 m), la marge de sécurité diminuant considérablement pour les portées moyennes (15-30 m).
- **Résultats du modèle à voies multiples** : les conditions de circulation à deux voies démontrent encore davantage la plus grande précision du NLM1, car il tient compte de la présence conjointe de véhicules lourds. Cependant, l'approche probabiliste garantit que le niveau de fiabilité requis est atteint sans marge de sécurité excessive. Les indicateurs de performance clés, tels que les indices de fiabilité uniformes et la variance réduite des effets d'action, soulignent l'efficacité du modèle. Le NLM1 prend en compte tous les scénarios extrêmes de circulation à deux voies, avec une forte proportion de poids lourds sur la deuxième voie. Il est calibré pour tenir compte des cas avec B-BAU (soit le passage de 2 à 3 voies) ainsi que des situations

de chantier (i.e. une circulation bidirectionnelle 2+2 sur un pont, avec 2 voies seulement autorisées au trafic lourd);

- **Scénarios impliquant des véhicules spéciaux** : le NLM1 couvre mieux les scénarios impliquant des véhicules spéciaux, tels que les grues mobiles ou les camions surchargés[3] , qui ne sont pas suffisamment pris en compte dans les modèles de charge des normes actuelles. La flexibilité du NLM1 permet des ajustements basés sur les schémas de trafic réels avec, sur la voie 1 et sur une longueur de 10 m, la charge répartie la plus élevée du modèle.
- **Cohérence entre les niveaux d'approximation (LoA)** : les mêmes niveaux de fiabilité sont atteints tant avec les analyses semi-probabilistes qu'avec les analyses probabilistes complètes, et sont cohérents pour différentes portées et différents types de ponts. Pour les analyses semi-probabilistes, le principal facteur dans le processus d'étalonnage est le facteur de sensibilité des effets de l'action du trafic. Cette étude démontre qu'une valeur de $\alpha_{E,Traffic}$ conforme aux normes actuelles est prudente mais acceptable pour les ponts routiers et le trafic motorisé.
- **Analyse de fiabilité entièrement probabiliste** : un algorithme est proposé pour permettre l'étalonnage du modèle de charge à l'aide d'analyses entièrement probabilistes. Ces analyses montrent que le NLM1 offre une marge de sécurité plus uniforme par rapport aux modèles de charge précédents. De plus, une analyse de fiabilité probabiliste permet d'améliorer encore le modèle de charge en étudiant la réduction de la dispersion des incertitudes du facteur de modèle d'effet d'action. Enfin, elle permet d'étalonner le modèle pour des études de cas spécifiques impliquant des types de ponts différents ou spéciaux.
- **Facteurs dynamiques et effets liés aux voies multiples** : les facteurs d'amplification dynamique et les effets liés aux voies multiples sont pris en compte de manière explicite, ce qui améliore considérablement la précision des prévisions des effets d'action et permet de les mettre à jour à mesure que de nouvelles connaissances sur ces facteurs deviennent disponibles.
- **Surmonter les limites des modèles actuels** : les limites du LM1 pour l'évaluation, telles que l'incapacité à modéliser des scénarios de trafic et de circulation complexes ou des géométries de pont qui varient, sont efficacement résolues par le NLM1, ce qui garantit qu'il est parfaitement adapté à l'évaluation des ponts existants et le rend apte aussi pour la conception de nouveaux ponts.

Recommandations pour les recherches futures

Au cours du projet, plusieurs thèmes ont été abordés qui ne relevaient pas du champ d'application de la recherche ; ils sont énumérés ci-dessous :

- Poursuivre le développement du NLM1 afin d'étendre son applicabilité et d'élaborer des règles d'application pour d'autres effets liés aux charges de trafic, à savoir la fatigue, l'accélération, le freinage, les forces centrifuges et transversales ;
- Des recherches supplémentaires devraient être menées pour permettre l'utilisation du NLM1 pour les murs de soutènement conformément aux normes suisses (SIA 261, 2020) et (SIA 269/1, 2011). En effet, le LM1 actuel pourrait entraîner des effets d'action trop conservateurs nécessitant des interventions coûteuses ;

[3] Surcharge des essieux ou du poids total : les auteurs recommandent de réduire au minimum le nombre d'infractions en renforçant les contrôles (effectués par la police ou à l'aide d'équipements techniques)

- Élargir la base de données WIM pour inclure des scénarios de trafic supplémentaires, des types de ponts sous-représentés et d'autres régions géographiques. Il est conseillé de maintenir le réseau actuel de stations WIM et la collecte de données afin de permettre d'étudier l'évolution du trafic dans le temps pour des sites spécifiques ;
- Prévision des charges de trafic futures en tenant compte de l'impact des technologies émergentes, telles que les poids lourds électriques, les véhicules autonomes et l'évolution des modes de transport de marchandises. L'évolution du trafic aura une incidence tant sur la conception des nouveaux ponts que sur l'évaluation des ponts existants. En effet, les modèles actuels ne tiennent principalement compte que des conditions de trafic actuelles. Rappelons que le NLM1 tient compte de l'utilisation de la R-BAU ;
- Les effets dynamiques et les incertitudes qui y sont liées doivent faire l'objet d'études plus approfondies et être modélisés à l'aide de techniques plus sophistiquées afin tenir compte avec plus de précision de leur influence sur les effets d'action, en particulier dans des scénarios spécifiques impliquant des véhicules spéciaux, qui peuvent conduire à un excès de conservatisme ;
- Le facteur de sensibilité des effets d'action du trafic dans les approches semi-probabilistes, $\alpha_{E,Traffic}$ actuellement égal à 0,7, devrait faire l'objet d'une étude plus approfondie et d'autres valeurs devraient être proposées afin de réduire le conservatisme, principalement pour les ponts existants ;
- Les analyses de fiabilité entièrement probabilistes devraient être étendues afin d'inclure un plus large éventail de types de ponts, la combinaison non linéaire des effets d'action corrélés et l'effondrement des ponts. De plus, une différenciation entre les modes de rupture améliorerait les évaluations de niveau de fiabilité ;
- Dans le cadre des analyses de fiabilité probabilistes, le modèle NLM1 proposé a été comparé à la norme EN 1992-1-1:2004 en vigueur pour le calcul des résistances. Toutefois, des comparaisons devraient également être effectuées à l'aide de la nouvelle génération de la norme EN 1992-1-1:2023, qui s'est avérée présenter une dispersion moindre dans les formules de résistances ;
- Les interactions entre divers effets d'action, telles que l'interaction moment-effort normal à proximité de l'appui d'une poutre, devraient être étudiées. Dans ce travail, les effets d'action maximaux sont considérés indépendamment les uns des autres, conformément à des études préliminaires indiquant que la maximisation séparée de chaque effet d'action constitue généralement le cas le plus prudent. Cependant, rien ne garantit que ce soit le cas pour toutes les configurations géométriques et tous les types de ponts. De plus, le niveau de sécurité supplémentaire résultant de la prise en compte séparée des effets d'action devrait être déterminé ;
- Développement d'outils simplifiés destinés aux praticiens, tels que des formation continues, des outils conviviaux et des procédures visant à faciliter l'application de techniques avancées de modélisation des charges de manière transparente. Permettre dans la pratique des évaluations utilisant des méthodes semi-probabiliste et probabiliste est également essentiel pour garantir une adoption rapide par les ingénieurs et les décideurs politiques.

1 Introduction

1.1 Problem statement

1.1.1 Normative bridge traffic load models: historical background

Before the late 19th century, traffic loads on bridges were not a major concern for bridge builders, since they could be neglected compared to the self-weight of the structure itself (Hanley et al., 2018; Henderson, 1954). With the introduction of traction engines, traffic loads became more relevant for bridge design and were generally considered by assigning actual vehicles with actual geometries and loads. These were regularly updated until the vehicles geometries and weights were replaced by fictitious models that incorporated both uniformly distributed and concentrated axle loads.

A large effort was made in the 1970's and 1980's to collect statistical data and, in combination with simulations, define the extreme values and models for traffic loads. On this basis, new models for traffic loads were developed in particular in the United States by the ASCE and AASHTO (ASCE, 1981; Kulicki & Mertz, 2006), in Belgium (Baus & Bruls, 1981), in Switzerland (Bez, 1989; *SIA 160*, 1989), in the UK (Dawe, 2003) (containing also a detailed historic overview of traffic load models for both UK and Europe), to cite only a few and in parallel within the framework of the Eurocode development in Europe (Sedlacek & al., 2008), first entitled ENV1991-3 and finally EN1991-2 (*EN 1991-2*, 2003). The fatigue limit state has followed in parallel similar developments (ASCE, 1981; Bruls et al., 1996).
Not surprisingly, the Swiss code published in 1989 (SIA 160: 1989) and the European Code (EN 1991-2:2002) have a very similar approach, since they have been developed in parallel in the 1980's and with cross-collaboration (Bez et al., 1987; (Sedlacek & al., 2008). The same applies to the current Swiss provisions (SIA 261:2020, and to the previous SIA 261:2003).

Focusing on gravitational loads and short spans, a simple manner to describe the code evolution is to compare the total load (Q_k) on a strip of length ΔL. This comparison is shown in Figure 3 and the following observations can be made:

- The axle load increased in time starting from the 1970s with newer editions of the SIA code;
- For new structures, the axle load group consisted of three axles in the editions from 1956 and 1970;
- For new structures, for very short strips (<3m), the tandem axle group of today's codes correspond to the highest values. For strips between 3m and 6m the highest values are obtained from SIA 160:1970;
- SIA 269/1:2011, used for existing structures, is calibrated based on WIM measurements and provides the lowest values, except for strips between 1.2 and 3 m; this indicates that local verifications of bridge slabs designed with SIA 160:1956 and SIA 160:1970, generally between 1956 and 1970, should be given particular attention.

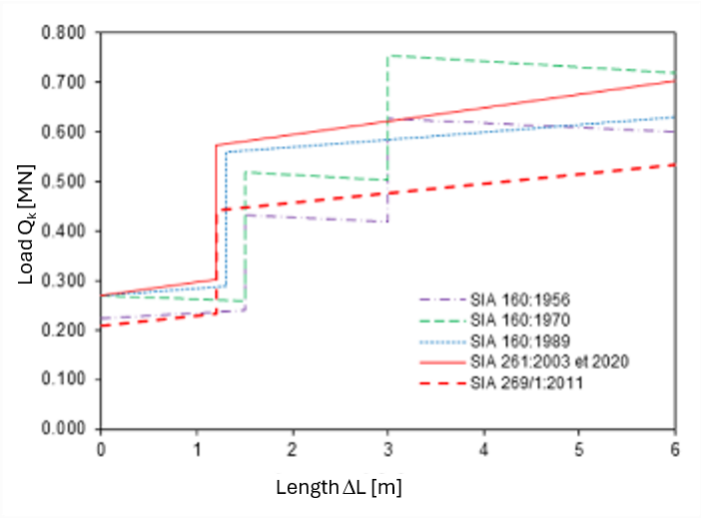

Figure 3: Comparison of the total load on lane 1 (slow lane) on a strip of length according to the different editions of the SIA code series

For longer spans, Figure 4 displays an extract from the VSS 623 (Vogel et al., 2009) presenting the total vertical road traffic loads (characteristic value) obtained from SIA 261:2003 and SIA 261:2020). For the design of new structures with SIA codes, the following observations can be made:

- The total load for spans smaller than 25m increased significantly after the code edition from 1935;
- The current code always leads to the highest values for roadway widths of 9m, corresponding to bridges with two lanes and an emergency lane;
- For roadways with a width of 12m, the current code leads to higher values except for spans above 50m designed according to SIA 160:1970;
- Previously, the 1970 edition was giving the highest total loads as compared to the editions from 1935, 1956 and 1989.

Since specific codes for assessing existing bridges were not available before the introduction of the SIA 269/1:2011, the model proposed by Meystre (Hirt & Meystre, 2006a) (gray line) can be used as a reference. While Meystre's model is always less conservative for bridges designed with SIA 160:1956 , SIA 160: 1970 and more recent SIA codes, for bridges up to 25m designed with the SIA 160:1935 this is not the case. Thus, particular attention should be paid to the latter.

For these reasons, and according to the above results, it can be concluded that particular attention should be paid to the local verifications of bridge slabs designed with SIA 160:1956 and SIA 160:1970, as well as to the verifications of bridges up to 25m designed with SIA 160:1935. It is also important to note that in the above the resistance calculation is not considered, i.e. the observations are only directly transferable to the load-bearing capacity if constant resistance is assumed.

The current main road traffic load model, denominated LM1, is based on a principle already used in former European codes which combines the uniformly distributed loads and axle loads on the same area, with values depending on the lane (i.e. lane 1 which corresponds to the slow lane carries the heavy traffic).

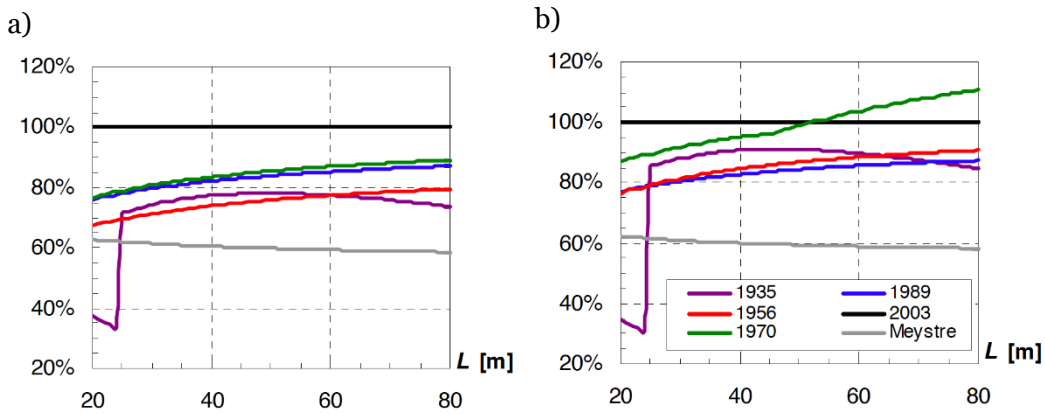

Figure 4: Comparison of the total load on bridges of lengths between 20 and 80 m according to the different editions of the SIA code series (Vogel et al., 2009), a) roadway width 9 m, b) roadway width 12 m

The current load models are derived mostly from data collected in France, Germany, Italy and Spain, since they had full records that also include all information about axle weights, spacing between axles, heavy vehicle lengths, distances between vehicles (Calgaro, 1997). Several traffic scenarios and influence lines have been used to fix characteristic loads of the load models, with reference to the Auxerre traffic, recorded on the motorway Paris-Lyon in France (Bruls et al., 1996). The reader is referred to Appendix A for more information on the historical developments of road traffic load models implemented in codes of practice.
The Load Model 1 (LM1) from SIA 261:2020 is shown in Figure 5, where the adjustment factors α_{Qi} and α_{qi} are the nationally defined parameters as in EN 1991-2:2002. The only difference between the EN and SIA is the lack of axle load group on the 3rd lane. In terms of number of models, the EN provisions have three more load models, whereas the SIA only has a second load model, to be used specifically for special and exceptional vehicles.

In current Swiss codes of practice, the adjustment factors α_{Qi} and α_{qi} have been calibrated to obtain the same magnitude of the loads Q_{ki} and q_{ki} as in the SIA 160:1989:

$$\alpha_Q = \frac{\gamma_{Q,SIA1989} \cdot DAF_{SIA1989} \cdot 4Q_{ki,SIA1989}}{\gamma_Q, SIA2003 \cdot 2Q_{ki,SIA2003}} = \frac{1.5 \cdot 1.8 \cdot 150}{1.5 \cdot 2 \cdot 300} = 0.90 \tag{1}$$

And $\alpha_Q = 0.90$ which is close to the average between the distributed loads on lanes 1 and 2:

$$\alpha_{q1} = \frac{\gamma_{Q,SIA1989} \cdot q_{k1,SIA1989}}{\gamma_{Q,SIA2003} \cdot q_{k1,SIA2003}} = \frac{1.5 \cdot 5}{1.5 \cdot 9} = 0.56 \tag{2}$$

$$\alpha_{q2} = \frac{\gamma_{Q,SIA1989} \cdot q_{k2,SIA1989}}{\gamma_{Q,SIA2003} \cdot q_{k2,SIA2003}} = \frac{1.5 \cdot 3.5}{1.5 \cdot 2.5} = 1.40 \tag{3}$$

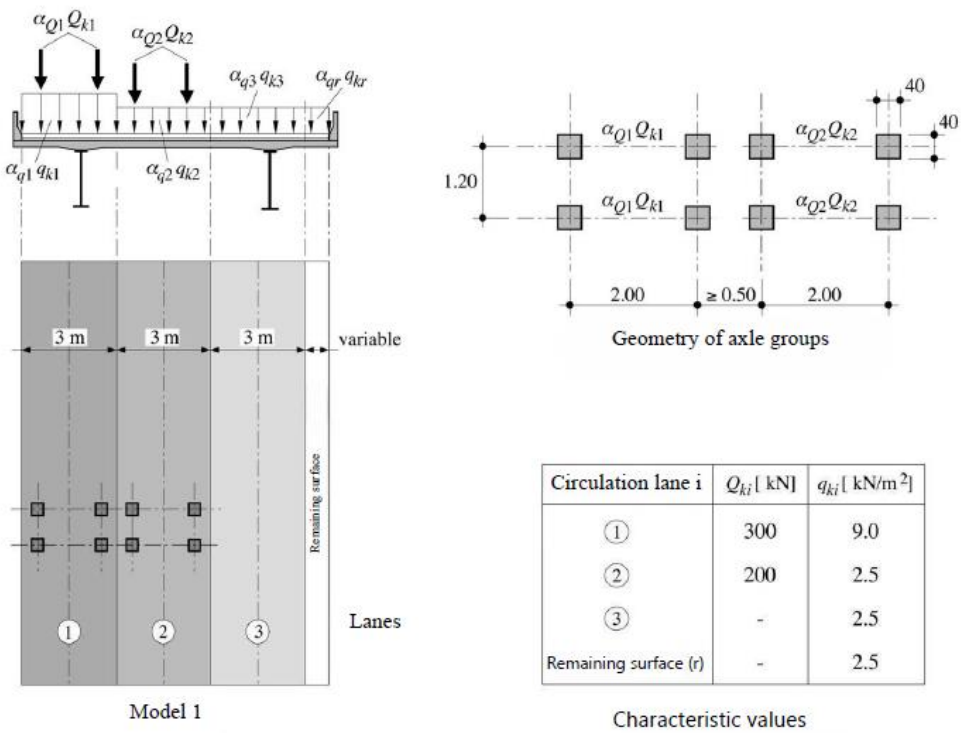

Circulation lane i	Q_{ki} [kN]	q_{ki} [kN/m²]
1	300	9.0
2	200	2.5
3	-	2.5
Remaining surface (r)	-	2.5

Figure 5: Load model 1 from SIA 261:2020

These values are also consistent with previous FEDRO research works by (Imhof et al., 2001) on the effect of increasing the allowed traffic loads from 28t to 40t. Finally, the design values correspond to the European ones, even though the Swiss provisions have kept the partial load factor value of 1.5 whereas the European provisions have lowered it to 1.35, keeping however α_Q = 1.00 (recommended value).

With respect to the examination of existing bridges, the Swiss Code SIA 269/1:2011 adopts the same approach as the code for new structures and the same Load Model 1 (LM1), however, updated adjustment factors $\alpha_{i,act}$ are provided depending on the type of bridge and the span. These values are based on the work performed by (Hirt & Meystre, 2006a; Imhof et al., 2001; Ludescher & Brühwiler, 2009).
These differences in terms of $\alpha_{i,act}$ clearly show that the LM1 for new structures is hindered by significant shortcomings: while a more conservative model may be justifiable for design, as mentioned above, the degree of conservatism appears to be inconsistent, since it depends on the type of bridge, the bridge span, the investigated action effect (bending, shear, ...) and the type of verification (global or local verification method).

It is important to note that also the $\alpha_{i,act}$ values proposed by SIA 269/1:2011 have several limitations:

a. They only cover "the road traffic permitted by law without load limits and take into account dynamic effects, and other wheel (axle) load increase as well as the foreseeable development of traffic up to the year 2025" (SIA 269/1:2011, clause 10.2.1.1);
b. The definition of bridge types lacks full clarity and does not always represent typical practical cases (e.g. short span bridges);

c. The work performed by (Meystre et al., 2014a) for deck slabs is not implemented;
d. Different values depending on the span, with stepwise changes at 5.3 and 10 m, are not suitable as they lead to differences in safety levels for similar bridges;
e. Various action effects, bending moment, shear, punching shear with different influence lines are not differentiated;
f. The treatment of special vehicles is not clarified.

The adjustment factors as given in SIA 269/1:2011 have recently been re-evaluated within the revision of the FEDRO documentation (Documentation ASTRA 82001, 2025). The re-evaluation of the adjustment factors allows to extend the applicability of the LM1 of SIA 269/1:2011 to the horizon 2050 while including traffic scenarios with wider roadways, up to a width of 15-18m. Specifically, on wider bridges, bidirectional traffic is accounted for with up to 4 lanes of heavy traffic with the possibility of adding a 3rd lane in each direction to the usual 2 lanes. This addition is denoted with the acronym REL which stands for Repurpose of Emergency Lane, which is widened to at least 3m and the usage limited to congested hours. The results show that, in most situations, in the general examination step, for approximate deterministic verifications (LoA I), a unique updated adjustment factor $\alpha_{act,unique}$ = 0.55 can be conservatively used. The report also provides specific rules and requirements for bridges with short and medium spans (< 20m), and suggests $\alpha_{act,unique}$ = 0.60 for the situations with REL on slab bridges.
Once again, as reported above, it is not possible to define a unique adjustment factor since the LM1 provides a non-uniform safety margin for various bridge types and spans.

1.1.2 Summary of critical review of LM1

No difference will be made herein between the LM1 from EN (European code) and from SIA (Swiss code). Recent FEDRO research works (Sjaarda et al., 2022)(Documentation ASTRA 82001, 2025) used detailed analyses of carefully processed WIM measurements to identify which heavy vehicles and load cases are responsible for the highest action effects. The optimization of the LM1 to cover all cases shows that by simplifying current traffic with a uniformly distributed load in combination with axles loads can be questioned, especially for assessing existing bridges. At the origin of this research, the following issues with the LM1 have been identified (see also appendix A):

- The concentrated load Q is considered to be too high with the tandem loads being too close (with 1.2 m);
- The distributed load q leads to excessively large action effect values for large spans;
- The dynamic amplification factor is included as a unique factor in the characteristic load values and does not represent reality, large concentrated loads generally are accompanied with larger dynamic amplification factors;
- It is unclear whether the partial factor γ_{Sd}, which covers the uncertainty in action effects calculation is considered and which uncertainties it covers;
- The additional conservatism due to the addition of a standardised sensitivity factor on the action side α_E = 0.7 is not clear;
- SIA261:2020 does not consider traffic loads due to special vehicles currently circulating on the road network (SIA261:2020-10.3.4), however, SIA 269/1:2011 considers loads due to such special vehicles when providing updated adjustment factors (see notes of Table 1 of SIA269/1:2011)

- A non-uniform reliability level for various bridge types has been observed both in practice and research.

1.2 Objectives of research

The research needs and objectives for this project are summarized as follows:

1. Historical review and bases of development of the LM1 in EN 1991-2:2004;
2. Overview of WIM data treatment and classification from the FEDRO database, including more recent data (from 2022) then previously. Algorithms overview for performing traffic simulations based on these data to update and calibrate a new load model (NLM1) assessing existing road bridges.
3. Better understanding of the critical traffic load situations in terms of probabilistic action effects on one and two lanes (valid for both existing and new bridges) for typical bridge types that are included in the FEDRO existing bridges database.
4. Definition of a new load model (NLM1) which better describes the governing truck(s), including special vehicles, and their action effects for local verifications both for short and long span bridges (up to 80 m). This will also clarify which uncertainties in action effects calculation are covered by the partial factor γ_{Sd} and the treatment of dynamic effects.
5. Extension of the above to model traffic on two lanes, with reasonable assumptions.
6. Proposal of a general procedure for quantifying the safety reserves between the action effects obtained using the current LM1, or other load models proposed by SIA 269/1:2011, and those obtained by performing simulations using WIM data.
7. Suggestions on how to approach FEDRO bridges for which the LM1 is too conservative.
8. Establishment of a framework for regularly updating traffic assumptions to allow accounting for its evolution, with the corresponding revision of design and examination structural codes every 25 years (in link with objective 2 and allowing for the use of "trains of loads" to simulate various scenarios by selecting the specific traffic loads).

1.3 Scope and limitation of research

This work addresses traffic loads on road bridges and proposes a new load model for the examination of existing bridges. However, general considerations concerning the applicability of the proposed load model to both new and existing bridges are made. The scope and limitations of this work are summarized below:

- Only a selected portion of WIM data from the national road network is considered; the selection is based on the representativity, quality and measurement duration of the WIM stations;
- No distinction is made for data within the national road network;
- According to the discussions with the accompanying committee, the proposed model accounts for the presence of special vehicles;
- Special vehicles are considered with their probability of occurrence at the WIM stations locations, even though some locations do not allow for the presence of mobile cranes;
- Assumptions regarding traffic development on the Swiss national road network include many uncertainties, the following points need to be clarified:

  - Regulatory changes are not considered, the characteristic values are determined using all stations and years;
  - When two lanes with heavy traffic are simulated, the increase in number of heavy vehicles and their distribution among lanes is considered;
  - When more lanes are simulated, the increase in heavy traffic in other lanes is also considered by increasing the UDL compared to the current LM1;
- These assumptions cover traffic development up to the horizon 2050 (to be consistent with (Documentation ASTRA 82001, 2025)). Anyway, updating of traffic evolution assumptions need to be regularly made. For unidirectional traffic bridges, the cases with two, two + REL and three lanes are covered; for bidirectional traffic, only bridges with two lanes are covered. Special circumstances such as proximity to construction sites (4-0 lanes, i.e. one bridge with all traffic as 2+2 bidirectional, with restriction only 2 lanes with heavy traffic) are also covered;
- For existing bridges, the characteristic values of the proposed load models are calibrated with a $\beta_{tgt,yearly} = 4.2$. However, these values can be adjusted for new bridges;
- Concerning the partial safety factor addressing the uncertainty in action effects calculation, no differentiation is made between various construction materials.

2 Methodology

The research methodology follows the same order as the research objectives, some highlights are presented below. To better evaluate the critical traffic configurations on road bridges, the problem of joint occurrence of extreme loads is investigated. Also, the various traffic forms (i.e. flowing, congested, jammed) are considered, combined with various structural systems.

Concerning WIM traffic measurements, the database made available from FEDRO was analysed and relevant sets of data were selected (Documentation ASTRA 82001, 2025). Initially, simulations for calibrating the new load model are divided into three levels for single-lane analysis as outlined below:

1. Single lane, single axle, generally for local verifications, typically punching shear;
2. Single lane, a group of axles, typically representing one or two heavy vehicles, for local and global verifications (slab bridges and transverse direction of girder bridges decks, generally for short to medium span bridges);
3. Single lane, a sequence of axles, representing a series of vehicles, for global verifications (multiple bridge types with generally longer spans);

Once defined, the load model is further refined and validated by extending the simulations to two-lane configurations, i.e. by adding the influence of the second lane and the possibility of the joint presence of axles and heavy vehicles. Considerations have also been made for other bridge types and a third lane.

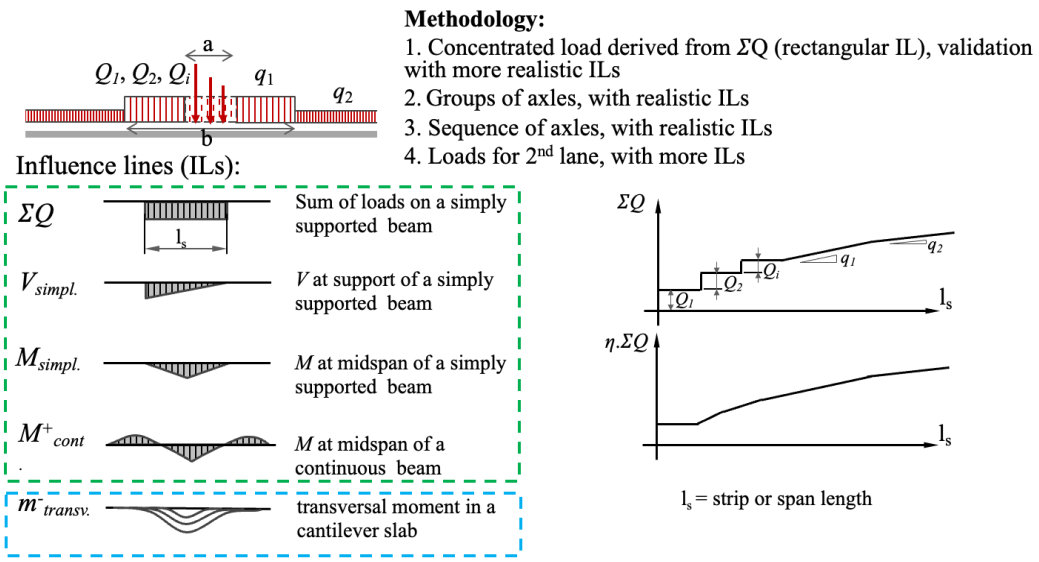

Figure 6: Methodology followed for establishing a new Load Model

Each of the levels above is calibrated using reliability analyses, that can be semi-probabilistic, full probabilistic or a combination of the two. The steps outlined below are followed:

- Definition of the axle-load sequences distributions;
- Definition of the typology of bridges under investigation (structural system, span, relevant action effect) and corresponding influence lines;
- For semi-probabilistic reliability analysis, computation of the distribution of the action effects (E_{sim}) and, for full-probabilistic, additional computation of the distribution of the resistance R;
- Definition of multiple load model configurations and computation of the corresponding action effects ($E_{d,mod}$);
- Reliability analysis (for semi-probabilistic by selecting a target reliability index β_{tgt} and a fixed importance factor $\alpha_E = 0.7$, as defined in EN 1990:2002, as well in SIA 269/1:2011, Appendix B);
- Comparison of the effectiveness of different load model configurations with respect to selected population of bridges:
  - for semi-probabilistic analyses, the ratio $E_{d,mod}/E_{d,sim}$
  - for full-probabilistic analyses, the obtained reliability index β and β_{tgt};
- Optimization problem: iterate on most promising load model configuration and parameters to find an optimized configuration with respect to selected population of bridges:
  - for semi-probabilistic analyses, mean $E_{d,mod}/E_{d,sim}$ above unity, as uniform as possible, and minimize variance;
  - for full-probabilistic analyses, a uniform distribution of the reliability index, meeting the condition $\beta_{tgt} = \min \sum w_i(\beta_i - \beta_{tgt})^2$;
  - Influence of the different failure modes and if differentiation between them is needed;
- Critical review of the optimized newly found load model configuration for the following constraints:
  - 1st, 2nd and other, supplementary, lanes;
  - practical applications;
- Adaptation and simplification of the new load model configuration and parameters and repetition of the analyses to reach the most practical and user-friendly model.

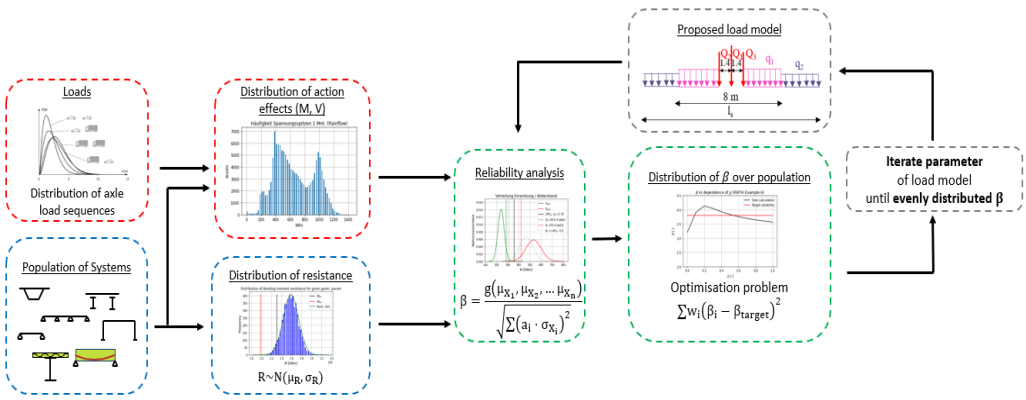

Figure 7: Workflow for calibration of load model (full-probabilistic illustrated)

3 From WIM data to traffic modelling

3.1 Selection of WIM data

Switzerland has been investing on the WIM station infrastructure for the past 25 years, an effort considerably more intense than other countries of comparable size. In addition to the sheer number of stations, throughout the year, the Confederation has collected a vast database of calibration data for each of them. The combination of these two types of information (WIM data and calibration data) is the fundamental source of data utilised in this study, as well as in previous ones (Documentation ASTRA 82001, 2025).

Figure 8 shows a map of Switzerland with the location of the available WIM stations, and * Average over all recorded years considering all vehicles above 3.5 t (trucks). Tends to decrease over time as numbers of cars and small trucks (up to 10 t) are observed to increase faster than numbers of heavy vehicles (above 10 t)

Table 1 summarizes the details of the 8 selected for this study. These WIM stations have been chosen for their representativeness of the Swiss network, the quantity, recording period and quality (from calibrations, stability over time) of the recorded data.

* Average over all recorded years considering all vehicles above 3.5 t (trucks). Tends to decrease over time as numbers of cars and small trucks (up to 10 t) are observed to increase faster than numbers of heavy vehicles (above 10 t)

Table 1 provides the following information:

- Station: name of the area corresponding to the station;
- Site: WIM station identification number;
- Highway: the highway section the site belongs to;
- State: the Swiss canton the site belongs to;
- Start and end year: beginning and end of the data collection periods; note that with respect to the WIM stations/years used previously (Documentation ASTRA 82001, 2025); data from stations available from 1.11.2021 to 31.12.2022 were added in this research;
- Truck rate: estimated ratio of heavy traffic over the total;
- Average Daily Truck Traffic (ADTT): average daily amount of heavy traffic (trucks);
- Layout: the layout of the traffic lanes. The first number represents the number of lanes and the second if the traffic is unidirectional (1) or bidirectional (2).

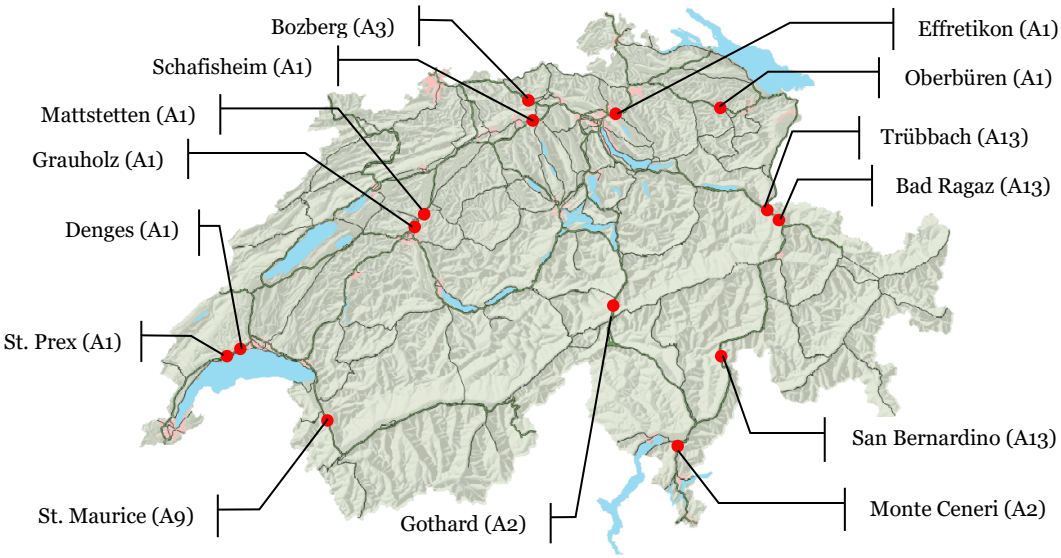

Figure 8: Map of Switzerland with location of WIM stations

Selected WIM stations/years in this research

Station	Site	High-way	State	Start year	End year	Truck rate*	ADTT	Layout
Ceneri	408	A2	TI	2006	2022	0.11	2682	11
Ceneri	409	A2	TI	2006	2022	0.09	2363	11
Schafisheim	411	A1	AG	2006	2009	0.12	4132	11
Schafisheim	412	A1	AG	2005	2009	0.09	3906	11
Mattstetten	413	A1	BE	2006	2010	0.10	3886	11
Mattstetten	414	A1	BE	2005	2010	0.10	4327	11
Oberburen	415	A1	SG	2006	2022	0.08	2200	11
Oberburen	416	A1	SG	2006	2022	0.08	2397	11
Trubbach	417	A13	SG	2006	2019	0.08	1526	11
Trubbach	418	A13	SG	2006	2019	0.08	1643	11
StMaurice	421	A9	VS	2009	2022	0.08	1390	11
StMaurice	422	A9	VS	2008	2022	0.05	1096	11
Gotthard	402	A2	UR	1999	2022	0.19	3408	12
SanBernar-dino	423	A13	GR	2011	2014	0.10	787	12

* Average over all recorded years considering all vehicles above 3.5 t (trucks). Tends to decrease over time as numbers of cars and small trucks (up to 10 t) are observed to increase faster than numbers of heavy vehicles (above 10 t)

Table 1: Selected WIM stations/years

It should be brought to attention that trucks with a weight lower than 6t have been excluded from the WIM data. The reason is that (Freundt, 2015; Sjaarda et al., 2022) have shown how they increase uncertainty in heavy vehicles percentages statistics and

that they are misclassified more often than the other classes, while, at the same time, they do not contribute significantly to the action effects.
For further details on the sampling, pruning and calibrating process of the WIM data, the reader is again referred to previously published (Documentation ASTRA 82001, 2025).

3.2 Modelling of traffic

3.2.1 Traffic modelling semi-probabilistic method

Two traffic conditions limits are used in all comparisons, flowing traffic (down to congested, with minimum speed of about 30 km/h) and jammed (standstill conditions). The traffic modelling is different for each scenario, as explained below.
For flowing traffic conditions:

- Given the large available amount of data (59 years considering all WIM station data adopted in this research), it is possible to calculate the design action effect corresponding to a yearly reliability target $\beta_{tgt,yearly} = 4.2$ and First Order Reliability Method (FORM) action side sensitivity factor $\alpha_E = 0.7$;
- Direct WIM analysis is possible. The traffic axles sequence based on WIM data is directly used to calculate the action effects. The design value of the action effects under the condition of flowing traffic $E_{d,WIM}$ for different types of influence lines is then calculated based on statistical analysis of these data;
- When using direct WIM, both the data from the different stations, combining unidirectional and bidirectional data were used. This last choice of combining unidirectional and bidirectional was illogical and would not be redone today. Cross-checks were made and showed that this choice did not affect the results in terms of design values of block maxima, i.e. they remain stable excluding or including bidirectional data.

For jammed traffic conditions:

- Since WIM station can only record traffic moving faster than a certain speed, (on average at least 20-30 km/h), jammed traffic data are not directly collected.
- To obtain the design action effect under jammed traffic, the simulation approach proposed in (Hirt & Meystre, 2006a; Sjaarda et al., 2022) is adopted. The JAM traffic is simulated based on the characteristic of traffic data recorded by WIM stations. For each relevant parameter per station and per year (recognized heavy vehicle type, total weight, inner-axle distances, weight distribution between axles, etc.), the probabilistic characteristics are represented as one or a combination of two beta laws, and include correlations between some parameters, see Appendix E for more information. In the simulated JAM traffic, the distances between vehicles are reduced from those in direct WIM analysis to represent the jammed traffic condition. Using the simulated jammed traffic sequences, the action effect data at different stations can be calculated. The design values $E_{d,JAM}$ for different types of influence lines are then calculated based on statistical analysis of these simulations. As above, a yearly reliability target $\beta_{tgt,yearly} = 4.2$ and First Order Reliability Method (FORM) action side sensitivity factor $\alpha_E = 0.7$ are used.

To determine a design value, the fitting technique developed during previous projects (Documentation ASTRA 82001, 2025) is used. First, different probability laws are fitted to the histogram, where each distribution best fit is determined by applying the Square Root Differences Theorem. The probability laws used are: Normal, Lognormal

(LN), GEV, GEVGumbel, and Lognormal tail fit (giving more weight to the top 5% of the data). Second, a goodness of fit of the tail part is performed to determine the distribution fitting the best the tail segment of the fitting curve; the following percentiles were used to test the fit of each distribution [0.90, 0.91, ..., 0.99993], as shown in Figure 9. Although one should typically favor a Weibull law for this tail fitting, different researchers – (Nowak & Hong, 1991), (Soriano et al., 2017), as cited by O'Brien and al. in their book (E. O'Brien et al., 2021) – have shown that fitting to a Normal distribution or Lognormal may work as well, even if they have, and also non-Weibull GEV laws, an unbounded tail.

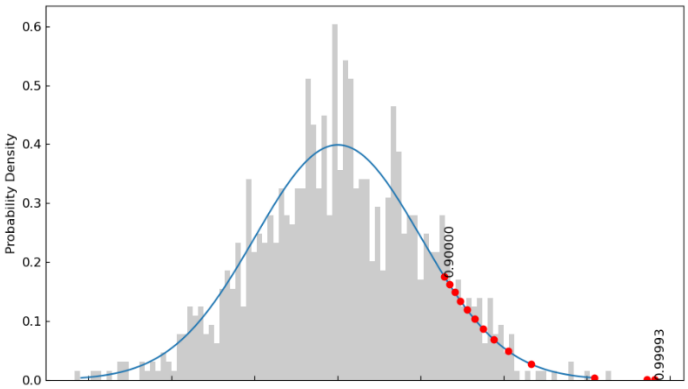

Figure 9: Qualitative fitting of a normal distribution using the assumed tail percentiles represented by the red dots.

For each scenario, the maximum value of the design action effect obtained from simulations with flowing and jammed traffic (refer to Eq. (4)) is then used as a reference value for the calibration of the new load model.

$$E_d = \max(E_{d,WIM}; E_{d,JAM}) \tag{4}$$

Where:

- $E_{d,WIM}$: direct simulation of traffic from flowing to congested (minimum speed of about 30 km/h) conditions on the influence lines.
- $E_{d,JAM}$: simulation of synthetic traffic based on WIM data in jammed conditions on the influence lines.

These two traffic scenarios and the different way they are simulated are assumed by the authors to sufficiently cover all cases as well as the complexity of traffic in terms of spatiality and temporality. For example, it can be shown that the HV bunching factor, i.e. HVs following each other, is function of the traffic state with higher HV bunching in jammed traffic, see chap. 3 of (Documentation ASTRA 82001, 2025). Simulating both scenarios led to the observation that, depending on the span, one or the other gives the maximum E_d. This connects also to EN1991 background (Sedlacek & al., 2008) and traffic simulations made back then, see Appendix A, Figs. 55 & 56, were flowing traffic is seen to lead to higher values for short spans whereas it is the opposite for long spans. By flowing it is meant free-flowing or congested but moving (at 30 km/h). The authors see two reasons that can explain this observation of higher values for free-flowing for short spans: a) there are many more vehicles travelling under these traffic conditions, therefore more statistical opportunities for maximum events with 1 or 2 trucks; b) in simulations, the breakdown and description of traffic with PDFs for, for ex. the total weight per truck type, per axle, distances between axles, incl. some

correlations coefficients does not reproduce the real complexity of the heavier individual HV's. But this influence on E_d is waived with longer spans, so only noticeable and relevant for shorter spans.

3.2.2 Traffic modelling probabilistic method

Concerning reliability analyses, the maximum traffic action effects are obtained as probability distribution functions of weekly maxima. As an example, Figure 10 shows the weekly maxima histogram of the positive moment at mid-span for a box-girder bridge with a span of 40m. The weekly maxima representation is found to be the best compromise between quality and amount of data for performing statistical analyses, see (Documentation ASTRA 82001, 2025) for more details on this subject. Histograms, as shown in Figure 10, are calculated for both traffic conditions, flowing and jammed, for each of the investigated influence lines and the respective action effect. In this case, fitting with only three probability laws is shown for figure clarity (among all laws tested, a lognormal distribution fitted best).

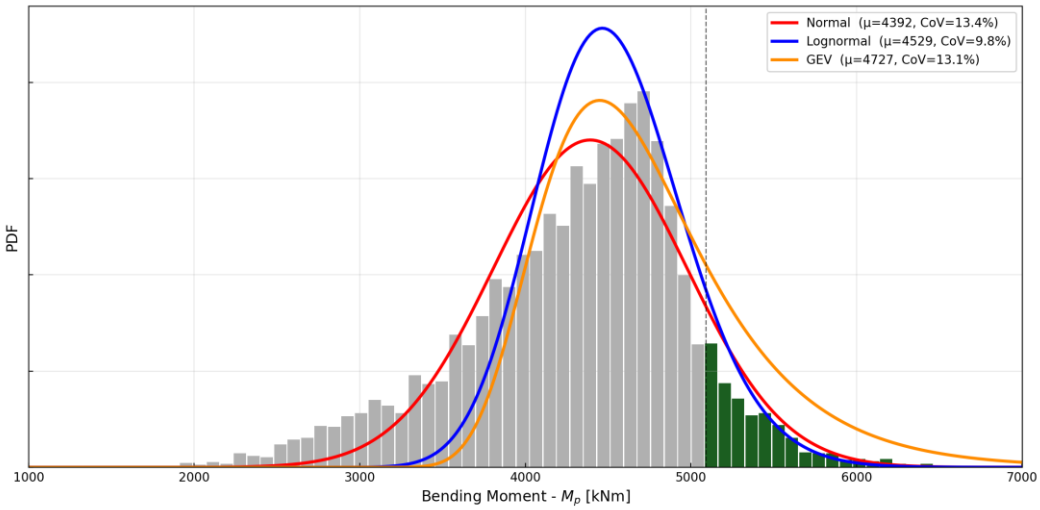

Figure 10: Example of a weekly maxima histogram: positive moment at mid-span for a simply supported box-girder bridge with a span of 30m (unidirectional traffic); Fitting and tail goodness of fit performed using a Normal, Lognormal and a GEV distribution.

3.2.3 Heavy vehicle lane distribution in JAM traffic simulation

Based on previous works (Documentation ASTRA 82001, 2025), two types of analysis are performed with respect to the distribution of heavy vehicles on a bridge:

- **Single lane analysis**: 100% of heavy vehicles are considered to be on the slow lane. The resulting design action effect E_d from single lane analysis is used as a reference for the calibration of the new load model for the first lane (slow lane). The shape (number of concentrated loads, number of distributed loads, distances between them, number of distributed loads, etc.) of the new load model is optimized and selected solely based on the single lane analysis results.
- **Double lane analysis**: heavy vehicles are considered to be distributed between two lanes (slow lane and REL lane, also representative of cases such as 3 lanes with two slow lanes, or a two-lane bidirectional road). The resulting design action effect for the two cases $E_{d,2la}$ and $E_{d,2lb}$ (their differences are explained in the following paragraph) are used to calibrate the new load model for the second lane.

Specifically, the heavy vehicle distributions for single lane and double lane jammed traffic simulations are the following:

- For single lane analysis: 100% - 0%. In single lane action effect analysis, 100% heavy vehicles are assumed to be located on the slow lane. Refer to Figure 11(a).
- For double lane analysis, with reference to Figure 11(b), two options are considered:
  1. 60% - 40% with total truck number unchanged but distributed among the two lanes;
  2. 100% - 67% with total truck number increased, such that the number and rate of trucks on the right lane (now the REL) remains unchanged and additional trucks are added on the 2nd slow lane respecting the 60-40 rule.

a) Truck distribution for single lane analysis

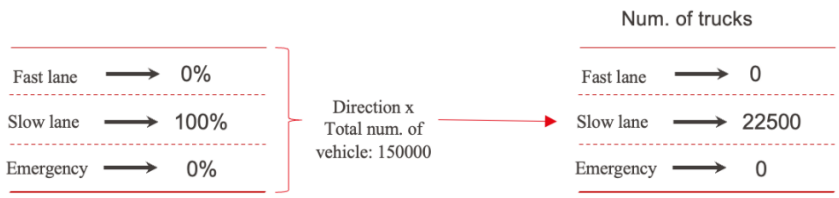

b) Truck distribution for double lane analysis

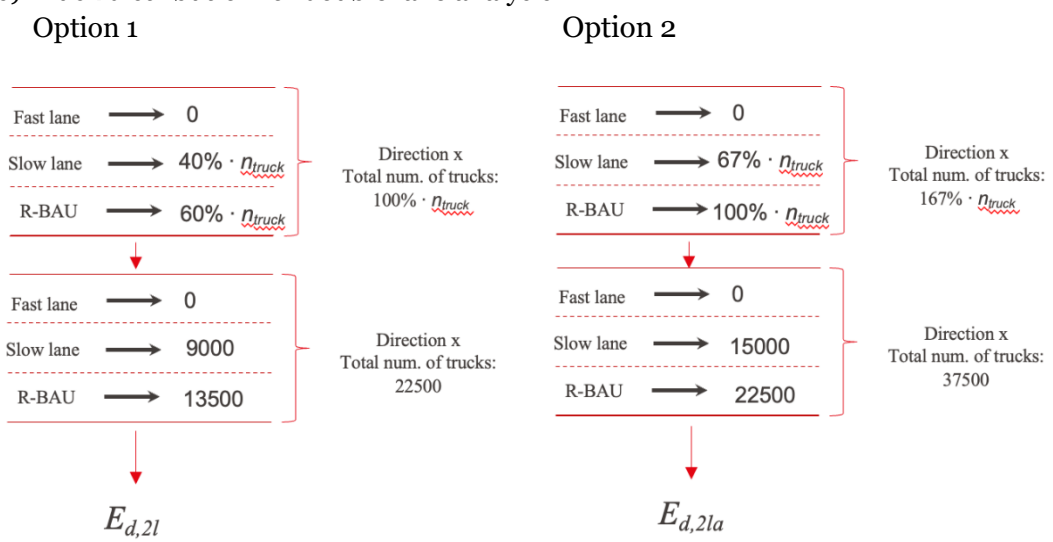

Figure 11: Heavy vehicle distribution in JAM analysis and resulting action effect E_d (a) for single lane and (b) for double lane for the cases 1 and 2 (note: R-BAU = REL).

To estimate the traffic distribution for the double lane configuration, the following aspects are considered:

- Traffic measurements during the experimental phase and opening of the REL in Denges (Fénart et al., 2016) (Fénart et al., 2017), show large variations depending on: the location (just after the start of the REL, in an intermediate section or just before its end), if it corresponds to an entrance, to junctions such as two highways merging or separating, and on the total traffic conditions (flowing, congested or jammed);
- With the REL active, a significant number of the vehicle drivers are not willing to change lane (especially when they need to cross a continuous line) so in general, it can be stated that all vehicles, including heavy ones, tend to stay in their lane;
- Based on the above two points, it appears that depending on the location, more heavy vehicles, corresponding to higher percentages, can travel in the REL lane. Since this situation is not conservative, it is the one used in the simulations. This

scenario corresponds realistically to congested traffic or jammed situations while being on the conservative side;

- With the assumed 60% - 40% distribution, the simulations are also representative of scenarios including bidirectional congested or jammed traffic, with one slow lane in each direction, since it is likely to have a different number and proportion of trucks in each direction;
- Comparisons of maximum traffic action effects on 12m wide bridges, such as unidirectional highway bridge with two lanes plus emergency lane, between normal use, situation of construction works (2+2 bidirectional traffic) and situation two lanes plus REL (Documentation ASTRA 82001, 2025; Sjaarda et al., 2022) showed the last one to be the controlling one. Thus, the scenario including construction works need not to be further studied to develop a new load model; it is implicitly covered.

Predicting future traffic is challenging as it depends on economic, sustainability and political decisions along with other unpredictable developments. Thus, a pragmatic approach is adopted, two options are considered:

- **Option 1**: Current maximum number of HV (heavy vehicles) on Swiss highways, distributed over two lanes, for comparison with the single lane analysis in terms of numbers;
- **Option 2**: Current maximum number of HV on the REL lane (the slowest), add supplementary 67% HV traffic on the middle lane, allowing for direct comparison of the influence of the second lane and of the probabilities of join presence of HV in both lanes;

For option 2, when increasing the total number of HV and distributing them more uniformly among two lanes (REL and middle), compared to the often used 90% and 10%, probabilities of joint occurrence of HV in both lanes increase, resulting to conservative estimations of extreme action effects.

Option 2 is also considered to cover vehicle upgrades, although in a simplistic way, such as the additional weight allowance in case of electric propulsion (a weight allowance of 1 to 2 tonnes more than diesel trucks of the same type), since both lanes are populated with HV having the same distributions instead of having lighter or not fully loaded trucks on the middle lane. This method of having additional weight allowance covered differs but performs as well as the simplified method used in the REAL-LAST project that was done through a constant bias on weights. To conclude, the proposed HV lane distribution in jammed traffic simulations is deemed to represent conservatively current and future heavy traffic (horizon 2050) while allowing for direct comparisons between single and double slow lane analyses.

(a)

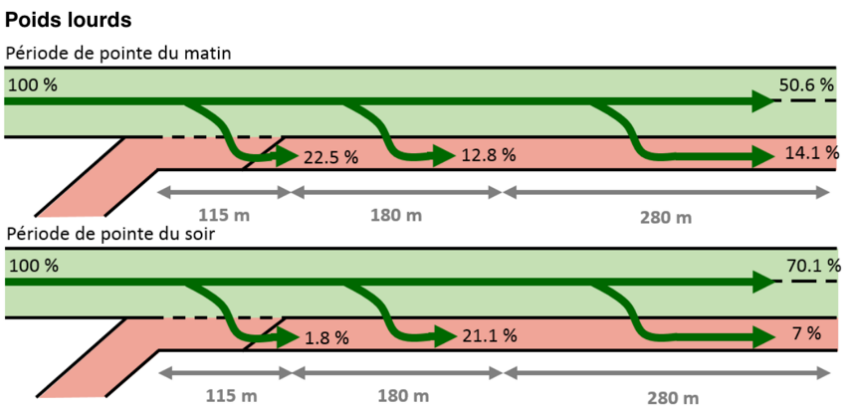

(b)

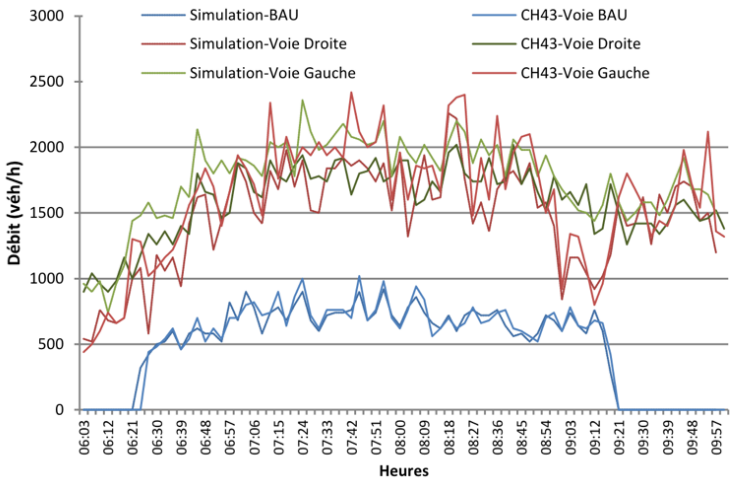

Figure 12: Vehicle distribution between lanes with REL at Denges (a) Heavy vehicle lane change, (b) all vehicles flow rates comparison. Extracts from (Fénart et al., 2016)

3.2.4 Modifications to the algorithms for JAM traffic simulation

With respect to previous work , several changes were made:

- An error was found in the measurement unit used in the code to indicate the distances between special vehicles such as mobile cranes. This has a significant impact on the results however does not significantly affect the outcome of Doc. ASTRA 82001 because of the other modifications listed below (partly compensating each other);
- The number of vehicles simulated in traffic jams was adjusted (together with the corresponding exceedance probability) from 1 million to 150000 for efficiency;
- A truck clustering factor, equal to 1.46, corresponding to the ratio between truck-truck transition probability and truck rate in a two-state Markov chain (Sjaarda et al., 2022), was incorporated to better reflect the likelihood of seeing trucks clustered together in traffic; but truck platooning was not considered;
- For double lane, a change towards a very aggressive heavy vehicles distribution between lanes in the final simulations with 60% in the REL lane and 40% in the middle one (previously some simulations were done with 50% and 45%);
- Implementation of other minor adjustments, with minimal impact on the results, like incorporating the rear distances of the trucks.

4 Design action effect on generic bridge types based on traffic simulation

4.1 Generic bridge types representative of FEDRO

First and foremost, bridges can be categorized from the structural point of view according to the structural scheme selected to carry the load.
An analysis of the KUBA database was carried out as part of the works related to the development of the SIA 269 series (Vogel et al., 2009), Table 2 summarizes the number and percentage of each type of bridge on the Swiss territory. Recently, a bachelor project created data sets that compiles much of the qualitative and quantitative information on existing Swiss bridges from different sources (Ammann et al., 2024); Figure 13 summarizes the number of bridges for each longitudinal structural type in function of year of construction as well as in function of span lengths. These data can be seen to be similar and should also be representative of the types of bridges that are expected to be constructed in the near future.

Bridge longitudinal structural types in Switzerland (Vogel et al., 2009)

Bridge type	Number	Percentage
Simple beam	274	9.4%
Continuous beam	1091	37.3%
Frame	1007	34.4%
Slab	255	8.7%
Inclined leg	212	7.2%
Arch	27	0.9%
Other (cable stayed, etc.)	62	2.1%

Table 2: Bridge longitudinal structural types in Switzerland (Vogel et al., 2009)

The last two entries of the table, representing the schemes with lowest percentage, have not been considered in this study. On the specific cases, practitioners should either be able to reason by extrapolation from the results of this research, where possible, or perform a specific detailed study during the preliminary design phase.
In addition to the structural scheme, bridges should be categorized according to their transversal and longitudinal system. In the following, the transversal and longitudinal structural systems considered in this study are listed and briefly described. A more detailed description can be found in (Mathevet et al., 2024).

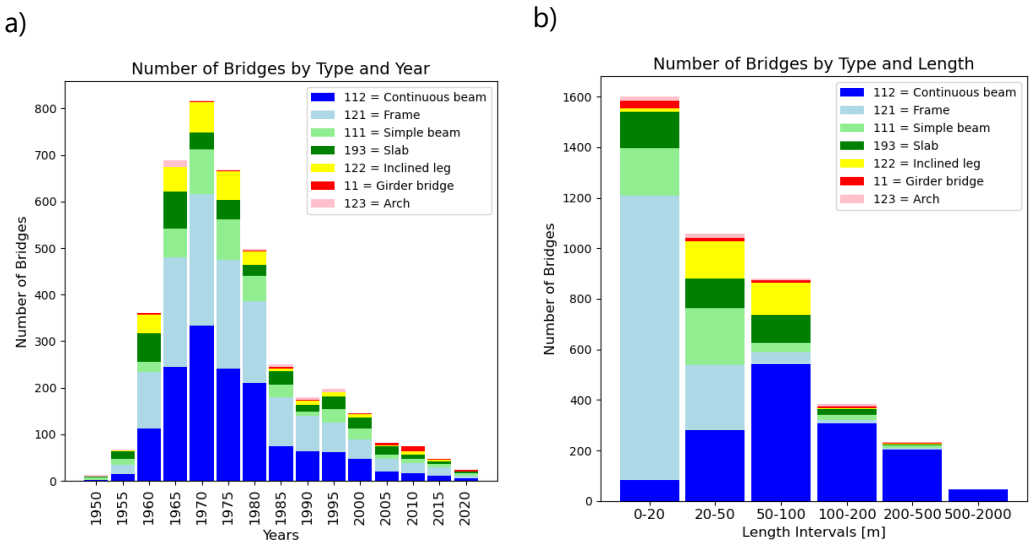

Figure 13: Bridge longitudinal structural types in Switzerland a) with year of construction b) with span length (Ammann et al., 2024)

4.1.1 Transversal systems (Figure 14)

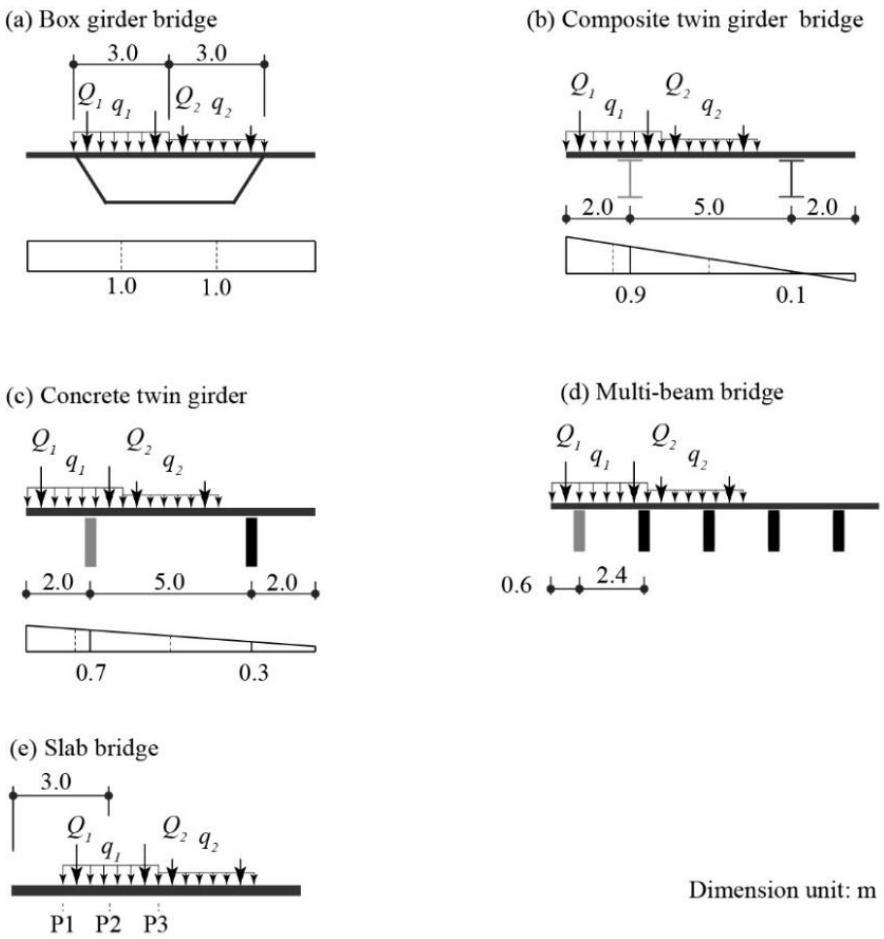

Figure 14: Transverse sections of investigated generic bridge types (units in meters)

a. Box girder bridges: characterized by a box shaped cross section that can be either reinforced concrete or composite. The traffic load is assumed to be positioned on the central portion of the section, while the external cantilevering portions of the top slab are left unloaded;
b. Composite twin girder bridges: the cross section is composed by a reinforced concrete top slab supported by two steel beams. The traffic loads are placed off centre to maximize the action effects on the supporting beams, with the assumption that traffic can be symmetrically placed and therefore both beams should be designed identical;
c. Concrete twin girder bridges: similar to the previous, with the difference that the supporting beams are also made of reinforced concrete, resulting in a different distribution of loads between the two. The traffic loads are placed identically as in the previous case; the design assumptions are also the same;
d. Multi-beam bridges: extension of the previous case to situations where the bridge is too wide to be supported by only two beams. The traffic loads are placed to maximize the action effects on one of the beams, with the assumption that all the beams should be designed according to the demand on the most solicited one;
e. Slab bridges: reinforced concrete slab cross section that resists the load with a true two-way action. The traffic load is positioned to maximize its effects on both the design directions.

Notice that all composite bridges are considered to have full composite action.

4.1.2 Longitudinal systems (Figure 15)

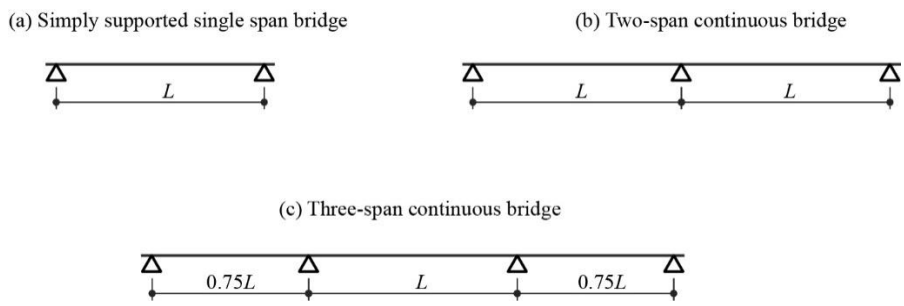

Figure 15: Longitudinal systems of investigated generic bridge types

a. Simply supported single span: a single longitudinal span with simple supports. No negative moment is present;
b. Two-span continuous bridge: two adjacent spans of equal length supported in three points. The central support is subject to equal negative moment on both sides and, in absolute value, to the highest moment;
c. Three-span continuous bridge: one long central span and two lateral spans that are only 75% the length of the central one, all supported in four points. This configuration has many locations that can be critical for both moment (positive and negative) and shear.

4.1.3 Cases investigated

Given the large number of available longitudinal and transversal schemes, many combinations are possible. The investigation carried out in this studied focused on the

combinations summarized in Table 3. The table summarizes not only the combinations of transversal and longitudinal schemes, but also the span lengths and internal forces that were considered and compared during this research.

Generic bridge types summary

Bridge type	Cross section	Longitudinal system	Main span* (m)	Inter-nal forces
Single span box girder bridge (**Box**)	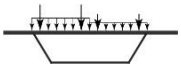		10:10:80 4:2:8	M_p, V
Two-span box girder bridge (**Box**)			10:10:80	M_n
Three-span box girder bridge (**Box**)			10:10:80	M_n2S
Single span standard composite twin girder bridge (**STw**)			10:10:80	M_p, V
Three-span standard composite twin girder bridge (**STw**)			10:10:80	M_n
Single span concrete twin girder bridge (**CTw**)	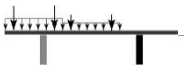		10:10:80	M_p, V
Three-span concrete twin girder bridge (**CTw**)			10:10:80	M_n
Single span multi-girder bridge (**MuP1**)			20:10:30	M_p, V
Three-span multi-girder bridge (**MuP1**)			20:10:30	M_n
Single span slab bridge (three locations in the slab P1, P2, P3) (**SlP1, SlP2, SlP3**)	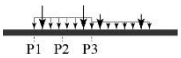		5:5:30	M_p

* ***gives the range of spans studied, hat is L_{inf}: ΔL: L_{sup}***
V: shear force near support point of simply supported bridge
M_p: positive bending moment at mid-span of simply supported bridge
M_n: negative bending moment over support of three-span continuous bridge
M_n2S: negative bending moment over support of two-span continuous bridge

Table 3: Summary of generic bridge types investigated

4.2 Global action effects: longitudinal shear and bending results

4.2.1 Single lane analysis results

The main results are presented herein in figures comparing the results for a load model with those from the traffic simulations over the bridges, expressed as $E_{d,SIA1l}/E_{d,1l}$ in function of the span length. The simulations use the information presented in §3.2 for the traffic modelling and in §4.1 for the longitudinal systems of investigated generic bridge types.

Recall that all calculations (code load model as well as simulations) are made with the traffic positions defined using 3-meter-wide notional lanes, which is a conservative assumption. The maximum traffic action effects between the two traffic conditions bounds, $E_{d,WIM}$ and $E_{d,JAM}$ as shown in Equation (1), are used in all comparisons herein. All simulations include the entirety of recognized vehicles, including mobile cranes up to 96 t circulating within normal traffic (see §3.2.1) to account for the presence of special vehicles.

In order to easily observe the performance differences of the possible traffic load models, a baseline comparison is made between the traffic action effects obtained from the current code load model 1 from SIA 261 and 269/1 (SIA, 2020; SIA 269/1, 2011) and the traffic simulations. For the current code load model, the adjustment factor value $\alpha_{\text{act,unique}} = 0.60$ from documentation ASTRA 82001, is used to obtain meaningful comparisons.

For single lane, Figure 16 presents the results of this comparison and shows that the single axle load gives a value 1.1 and, more important, that its performance varies with span length, which signifies it is the least conservative for spans in the range 10 to 30 m. However, using unique value $\alpha_{\text{act,unique}} = 0.60$ still allows to meet the minimum safety required for all cases.

Regarding the influence of the bridge section type and internal force, not all cases are considered relevant for each bridge section type; only the following are investigated (see also Table 3):

- *Mp* = sagging M, for all bridge section types;
- *V* = shear, for box girder and multi beam bridges;
- *Mn* = Hogging M, continuous beam (3 spans), for box girder and multi beam bridges;
- *Mn2S* = Hogging M, continuous beam (2 spans), only computed for box girder bridges.

This is justified by the outcome of previous studies, including the EN1991 background from (Sedlacek & al., 2008), see 10 Appendix A. Note that in Figure 16 the composite and concrete twin girder bridge results are not plotted because the loads are only on lane 1, thus they give exactly the same values as the box girder.

The most conservative results are obtained for the two cases of hogging moment (*Mn* and *Mn2S*) from spans of 30 m onwards, the reason being that the code load model corresponds to a long series of very heavy vehicles, on both spans, which obviously has a too low probability of occurrence to be realistic. On the other end, the least conservative results are obtained for the shear cases, which can indicate that the combination of the tandem axle with the UDL does not represent extreme cases that can occur in reality, as for example from overloaded mobile cranes.

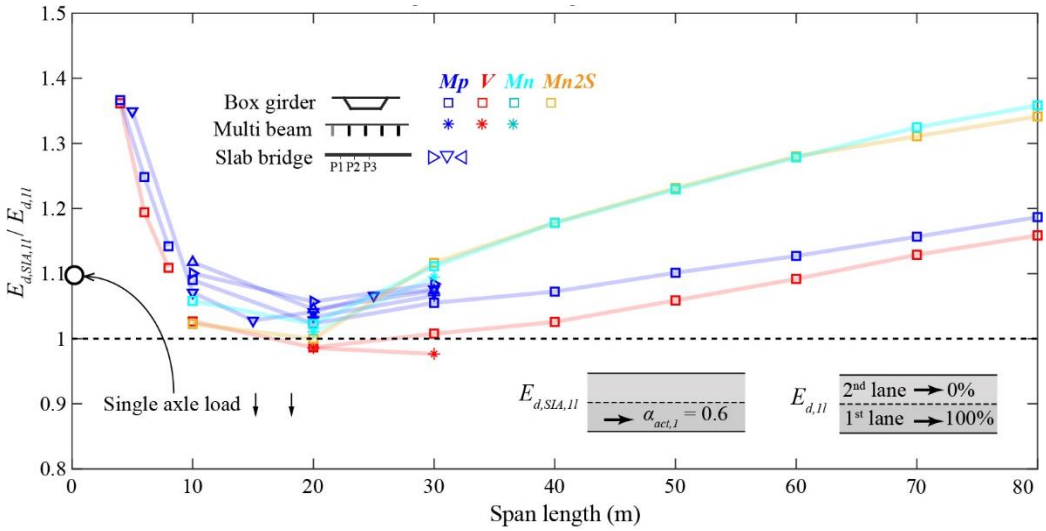

Figure 16: Ratio between single lane codified design action effect with $\alpha_{act,unique}$ = 0.6 and the design action effect from direct WIM and JAM analysis (refer to **Table 3** for more detailed explanation of definition of bridge types and internal forces)

4.2.2 Double lane analysis results

Similarly to the single lane analysis results, only the main results are presented herein, the reader is referred to Appendix B for more detailed information. The figures compare either the results from a double lane with traffic simulations on one lane, $E_{d,2l}/E_{d,1l}$, or the results between a load model and the traffic simulations on two lanes $E_{d,LM,2l}/E_{d,2l}$, as a function of the span length. The comparisons are first made for the double lane Option 1, where the total amount of traffic is maintained constant and distributed with the ratio 60% - 40% on the first (i.e. REL lane) and second lanes respectively. Figure 17 compares double lane and single lane WIM-JAM results, $E_{d,2l}/E_{d,1l}$. The effect of distributing the same heavy traffic over two lanes is shown to cause an increase of the extreme action effects of maximum 30% for the slab bridges and box girder bridges. The composite twin girder bridges are much less affected, which is predictable given their transverse distribution line.

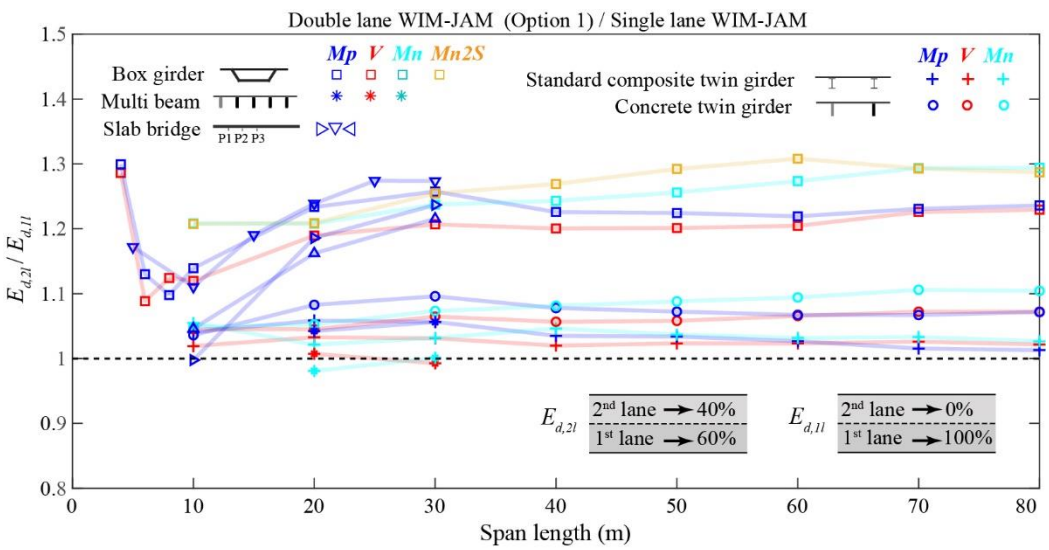

Figure 17: Ratio between double lane design action effect $E_{d,2l}$ (Option 1) and single lane design action effect E_d from direct WIM and JAM analysis

Figure 18 shows a comparison for double lane between the traffic action effects obtained from the current SIA code load model 1, updated (Documentation ASTRA 82001, 2025) and from the traffic simulations, $E_{d,SIA,2l}/E_{d,2l}$ (Case 1: 60%-40%). The updating uses the recent recommendation in Doc. ASTRA 82001 with $\alpha_{Q1,act} = \alpha_{q1,act} = 0.60$, $\alpha_{Q2,act} = \alpha_{q2,act} = 0.30$. It shows the very same shape as seen previously in Figure 16 for a single lane, the SIA updated values being always conservative (i.e. above unity). There are however slightly different ratios in function of the span in Figure 18 (note that this time the results for the twin girders need also to be plotted) compared to Figure 16.

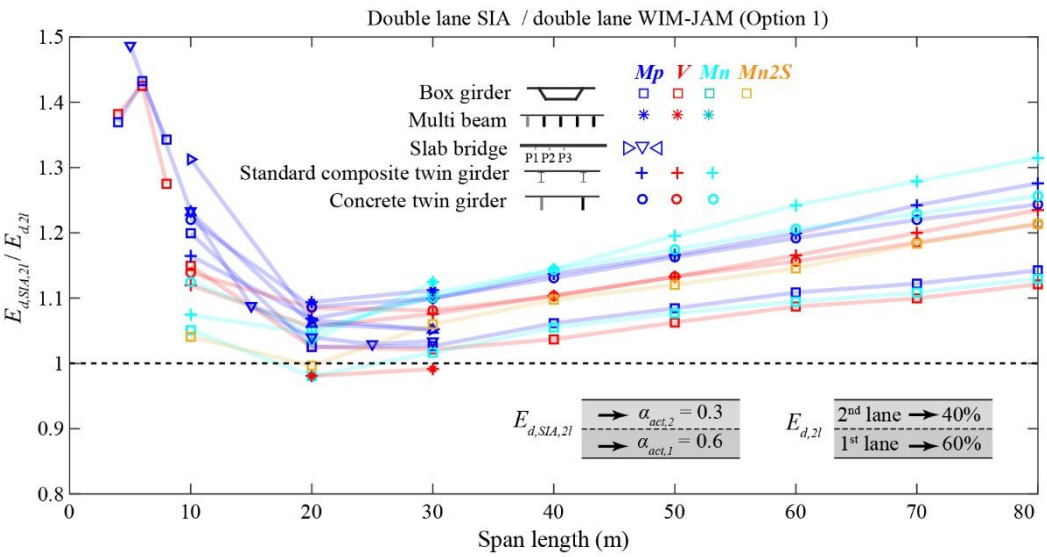

Figure 18: Ratio between double lane codified design action effect with $\alpha_{Q1,act} = \alpha_{q1,act} = 0.60$, $\alpha_{Q2,act} = \alpha_{q2,act} = 0.30$ and the double lane design action effect from direct WIM and JAM analysis (Option 1)

The case of Option 2, where the total load is maintained on the slow lane and an additional 67% is added to the second one, is discussed in the following. Figure 19 compares the double lane and single lane WIM-JAM result, $E_{d,2la}/E_{d,1l}$, and highlights the effect of increasing the heavy traffic by adding a second lane with an additional 67% of heavy trucks. One can notice that no increase in extreme action effects is noticeable for the shortest spans, while it was evident to a maximum of 30% for Option 1. As previously observed, composite twin girder bridges are less affected, although to a degree of 10 to 20%, higher than the case of Option 1.

Finally, Figure 20 shows the comparison for double lane between current SIA code load model 1, updated (Doc. ASTRA 82001:2025) and WIM-JAM results, $E_{d,SIA,2l}/E_{d,2la}$ (Option 2: 100%-67%). It displays again the very same shape as seen Figure 16 and Figure 18. However, this time and due to the increase in traffic, the SIA updated is not always conservative. In particular, the results are slightly unconservative for negative moment cases for box girder bridges with spans around 20 m, reaching the lowest value of 0.92. This is expected since the extreme combines the probability of heavy traffic both on the two lanes and on two adjacent spans. The shear cases also stay among the less conservative results.

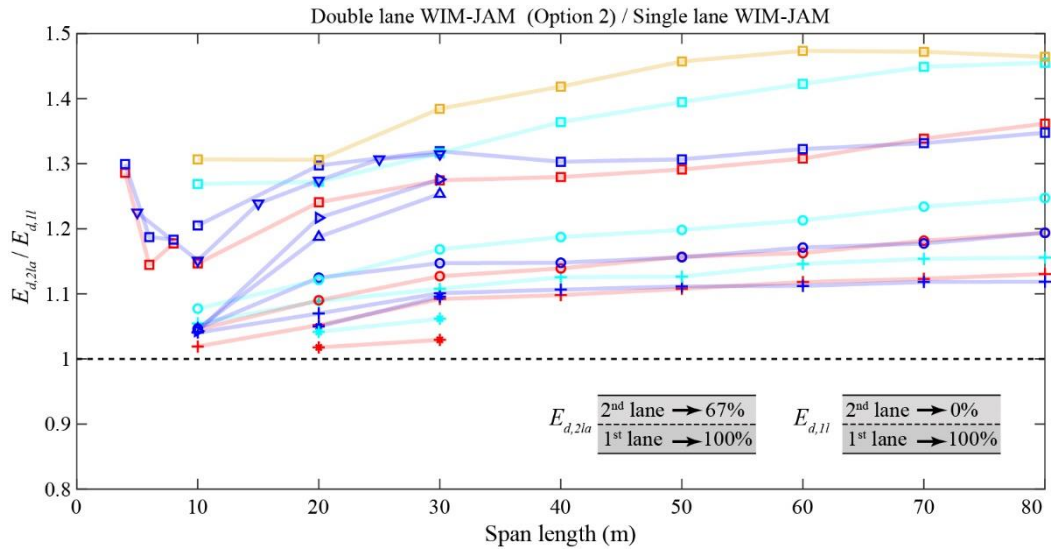

Figure 19: Ratio between double lane design action effect $E_{d,2la}$ (Option 2) and single lane design action effect E_d from direct WIM and JAM analysis (refer to Figure 20 for plot legend)

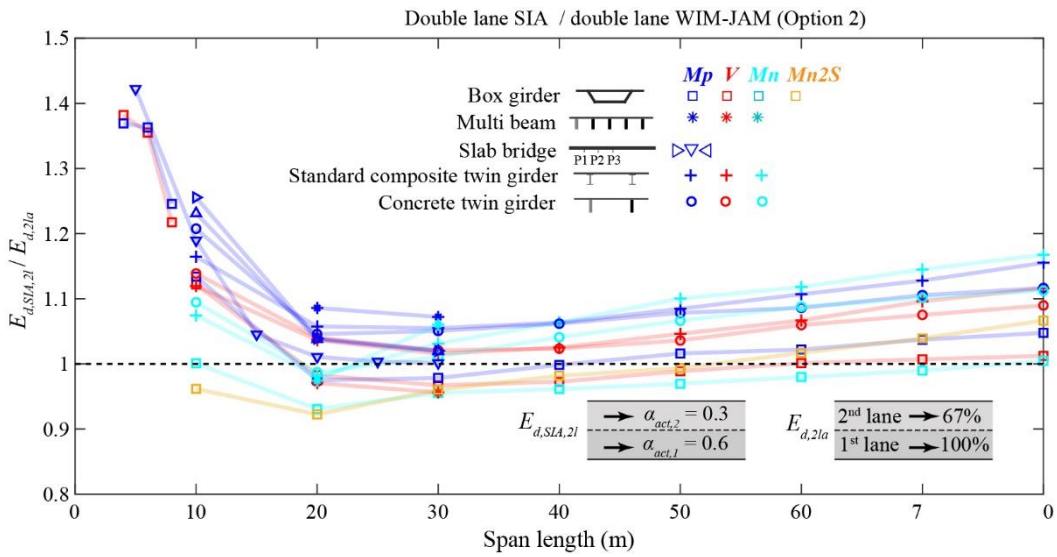

Figure 20: Ratio between double lane codified design action effect with $\alpha_{Q1,act} = \alpha_{q1,act} = 0.60$, $\alpha_{Q2,act} = \alpha_{q2,act} = 0.30$ and the double lane design action effect from direct WIM and JAM analysis (Option 2)

The results for two lanes, when compared to the ones obtained for a single lane, show that the largest increase in extreme action effect values comes for the two cases of hogging moment (*Mn* and *Mn2S*) for box girder bridges. Thus, the current load model is:

- For Option 1, still conservative for all action effects;
- For Option 2, due to the increase of traffic, it is mostly but not always conservative, in particular for spans around 20 m.

The fact that the code load model corresponds to a long series of very heavy vehicles, on both spans, but not necessarily on both lanes, results in realistic probability of occurrences for the negative moments and the shear cases. The current code load model is observed not to represent well the extreme action effects for the static systems and different internal forces with respect to span length. The indication for a single lane thus remains that the combination of the tandem axle with the UDL does not represent

well the extreme cases that can occur in reality. As already written in § 3.2.3 option 2 covers not only cases with REL (i.e. 2 lanes transformed into 3 lanes) but also construction works situations (i.e. 4-0 lanes, one bridge with all traffic as 2+2 bidirectional, with restriction only 2 lanes with heavy traffic).

4.2.3 Local action effects: transverse shear, bending and punching

WIM analyses on axle loads on a strip, represented as a rectangular influence line of varying length, are carried out with the purpose of studying the local action effects. Figure 21 shows the following cases, obtained combining data from all stations and years (see also Table 4 for the definition of each special vehicle):

- Single axle(s) include both single axles as well as each axle within a group of axles;
- Tandem axle(s) include single, tandem axles as well as two axles within a group of axles. Note that single axle loads will mostly be on the lower end of the PDF;
- Tridem axle(s) include tandem, tridem axles as well as three axles within a group of more axles (such as in mobile cranes with 4 or more axles of 12t closely spaced). Note that tandem axles will mostly be on the lower end of the PDF;
- In the legend, Class corresponds to the 40 t traffic data;
- Class+(All): Class data and all special vehicles from types 41 to 49;
- Class+(41 and 48): Class data and special vehicles type 41 (5 axle – 60t) and type 48 (6 axle – 72t).

Definition of the special vehicles representing the different types of mobile cranes

Class+ code	Axle Nb.	Total Weight [t]	Axle Group
41	5	60	code 14
42	6	60	code 33
43	7	72	code 34
44	8	84	code 44
45	9	96	code 45
46	8	96	code 332
47	6	72	code 132
48	6	72	code 15
49	7	84	code 25

Table 4: definition of the special vehicles representing the different types of mobile cranes

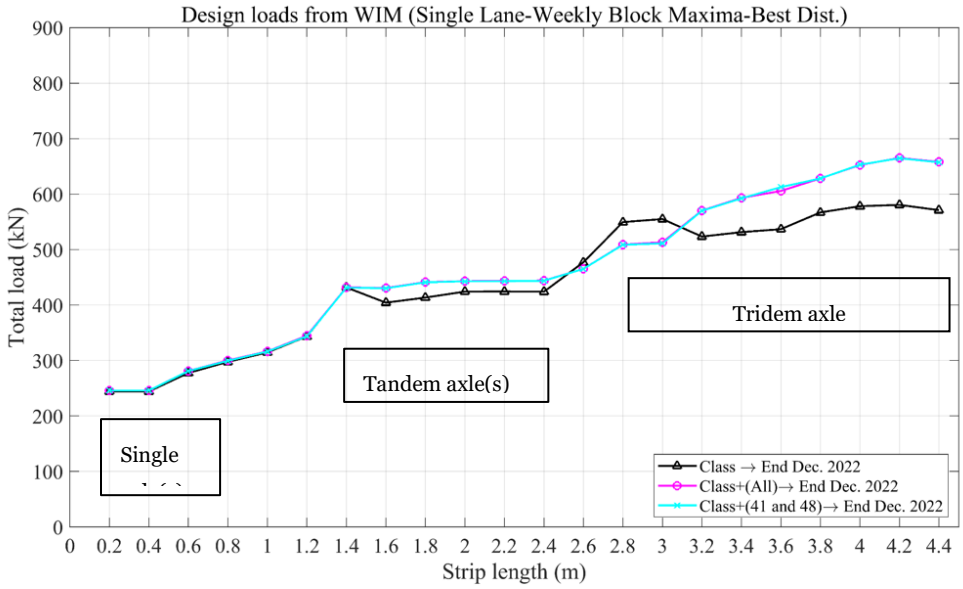

Figure 21: Design loads from WIM data strip analysis on a single lane, up to 4.4m

Less relevant for axles loads, but still interesting to observe is the increasing value of the total load extreme value on the slow lane of a bridge. Figure 22 gives the total design load on a strip up to 20 m long. One can observe the influence of the large special vehicles on the total load, which saturates logically from about 8 m for 60 and 72t (total wheel distance 7.2 to 9.2 m), and from 13 m for those up to 96t (total wheel distance 13.3 m). It is also interesting to note that the total design load for Class+ (41 and 48) equals 980 kN, which is 36% higher than the maximum authorised vehicle weight. Even if this value may be biased by the WIM measurement system, it is most likely representative of the fact that some mobile cranes circulate with counterweights, even though it is forbidden.

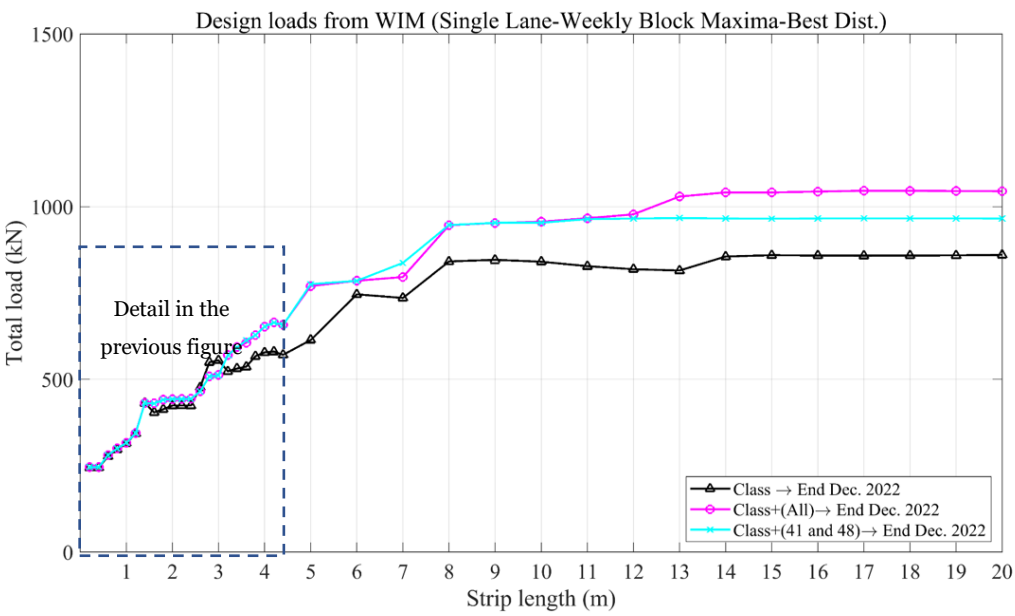

Figure 22: Design loads from WIM data strip analysis on a single lane, up to 20m

5 Proposition of a new load model

5.1.1 Investigated configurations of load models based on the analysis of WIM data

Following the historical and the critical review of LM1 from § 1.1, the design action effects on generic bridge types based on traffic simulation, which are presented in § 4, and the discussions within the research group, the load configurations shown in Figure 23 have been investigated. These models are mainly investigated for lane 1 and can possibly be used also for lane 2. For additional information on the investigated configurations see Appendix B.

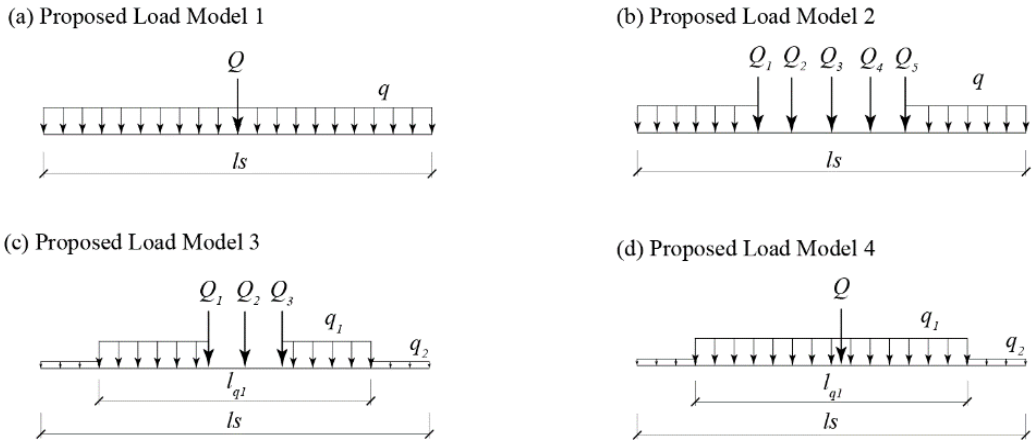

Figure 23: Investigated configurations of load models for the fist lane (*ls* is the bridge length, l_{q1} is the distribution length of the Uniformly Distributed Load 1 (UDL1)

The main characteristics of each model are resumed below:

(a) PM1 is the simplest model, defined by 2 parameters to be optimized: a Uniformly Distributed Load UDL *(q)* and a single axle load *(Q)*;

(b) PM2 is defined by 3 parameters: a UDL *(q)* and (5) axle loads *(Q)*. No distributed load is considered in between axle loads;

(c) PM3 is defined by 5 parameters: a UDL1 (q_1) over a fixed length (l_{q1}) with (3) centered axle loads (*Q*). As for PM2, no distributed load is considered between the concentrated loads. and a lower UDL2 (q_2) elsewhere;

(d) PM4 is defined by 4 parameters: A UDL1 (q_1) over a fixed length (l_{q1}), within it one axle load *(Q)* which has a relative location l_{q1}, and a lower UDL2 (q_2) elsewhere.

The above load model configurations are compared following the methodology described in § 2. As a result, the PM4 (defined by 4 parameters) showed the best potential, combining both flexibility and ease of use for engineers in practice while modelling traffic action effects accurately. Please note that modelling in this context does not refer to modelling heavy vehicles in a deterministic way, instead, it refers to the capability of capturing action effects of real traffic vehicles.

PM1 and PM2 show no significant improvement compared to the current Load Model 1 (LM1), not leading to a more uniform safety for different bridge types. On the contrary, PM3 with 5 parameters, adds complexity with respect to PM4 without leading to a more uniform level of safety. The results obtained with the investigated load configurations PM1-4 are compared in Appendix B. Please note that the selected load configuration (PM4) is investigated herein with an improved version of the algorithm which was used in Appendix B to perform the comparisons, thus, the results for PM4 given below might show some differences compared to those in appendix B.

The selected configuration (PM4) is optimized by variating the parameters as shown in Table 5. Specifically, 4 sets of parameters (PM4.1-PM4.4) are investigated in addition to the base PM4 parameters investigated in the previous step. Please note that the following investigation is performed considering only the first lane. Results from the new parameters investigation show the following key characteristics:

- PM4.1 – PM4.3 show generally less or comparable dispersion with respect to PM4 While the distributed loads are adequate for global verifications, the design axle loads are generally too low for local verifications;
- PM4.4 shows adequate design values for both local and global verifications and an overall good performance in terms of constant level of safety.
  Thus, the selected set of parameters is the PM4.4.

Variations of the new load model (c) on lane 1

New Load Model ID	Load model parameters (design* values)			
	Q_{Ed} [kN]	$q_{1,Ed}$ [kN/m]	$q_{2,Ed}$ [kN]	Δl_{q1} [m]
PM4	250	80	5	8.0
PM4.1	200	72	15	10.0
PM4.2	220	78	15	10.0
PM4.3	200	81	15	10.0
PM4.4	**245**	**70**	**14**	**10.0**

* Design values from simulations which do not include the dynamic amplification factor (DAF) and the model uncertainty in calculating action effects

Table 5: Parameters investigation for the load configuration PM4 for the first lane

5.1.2 Definition of the New Load Model 1 (NLM1) for the first lane

The PM4.4 which is the selected model from the previous investigation phase, is from now on denominated New Load Model 1 (NLM1) and is graphically represented in Figure 24(a) for lane 1. Figure 24(b) shows the action effect ratio between the NLM1 model for lane 1 and the simulations performed using the WIM-JAM traffic ($E_{d,NLM1,1l}/E_{d,1l}$). It can be observed that the single axle load is chosen to match the design value obtained from the strip analysis. Also, the most conservative results are obtained for the sagging moment (*Mp*) in short span bridges (up to 10 m), which represents the only drawback of deciding to use a single model for both local and global verifications. For spans above 10 m, the model reproduces traffic action effects very well with respect to the current LM1 (see Figure 16). In particular, NLM1 shows little influence with increasing span. However, a few cases fall between 0.95 and 1.00 (unsafe results), see hogging moment (*Mn2S*) for spans of 20 m, indicating that the single lane model slightly underestimates the total load on both spans.

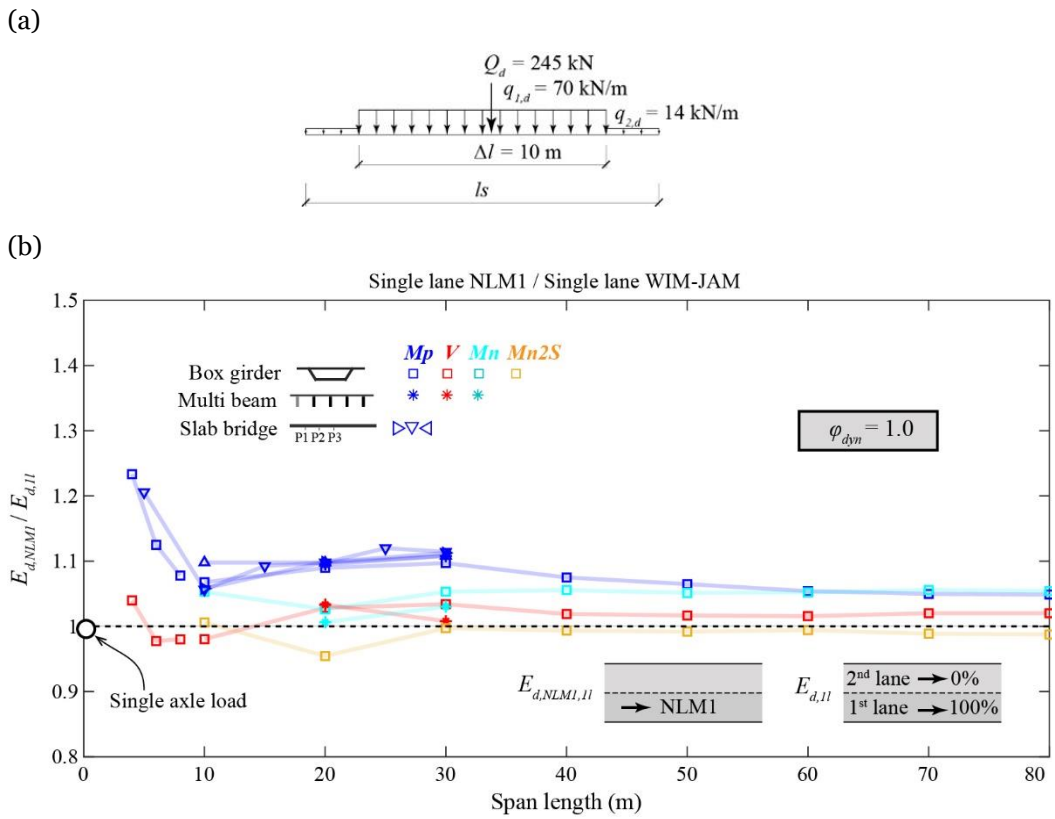

Figure 24: (a) Proposal of New Load Model 1 (NLM1) for first lane based on optimization of design action effects for generic bridge types, (b) Comparison as ratio between NLM1 design action effect and the design action effect from simulations (direct WIM and JAM analysis)

At this point, the model cannot be further optimized without considering the influence of other parameters, such as:

- The influence of the second lane;
- The Partial factor for calculating action effects, γ_{sd};
- The dynamic amplification factor φ_{dyn}, which depends on the span and the total traffic load.

Note that for Figure 24(b), the standard and concrete twin girder bridge results are not shown since they give exactly the same values as box girder.

The optimization of NLM1 is performed using the workflow which is graphically represented in Figure 25. The current phase is highlighted in red. Please note that until now, including this phase, the design traffic load values derive from the simulations; thus, these values **do not include the dynamic amplification factor (DAF) φ_{dyn} nor model uncertainty of action effects γ_{sd}** which are investigated in §5.1.4. Note that in this report the abbreviation DAF is used since it is commonly adopted in practice, however, a more suitable term describing the factor φ_{dyn} is Allowable Dynamic Ratio (ADR), see (E. J. O'Brien et al., 2010) for additional details.

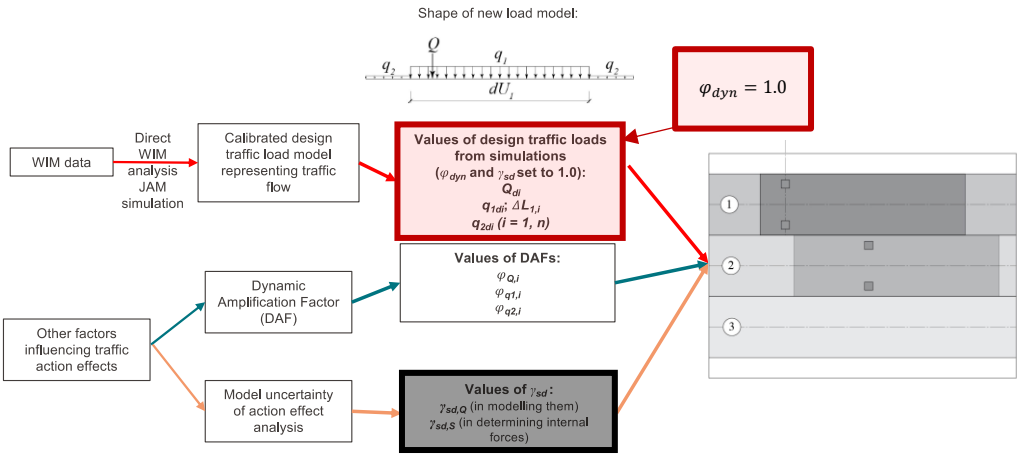

Figure 25: Workflow to determine the parameters of NLM1 (the dynamic amplification DAF and modelling γ_{sd} factors are dealt with in paragraph 5.1.4)

5.1.3 Optimization of NLM1 including traffic on the second lane

When heavy traffic is considered on two lanes, joint presence of several trucks must be studied with realistic yet conservative scenarios including future traffic development. The worst-case traffic scenario for highway bridges corresponds to the Reuse of the Emergency Lane for heavy traffic (REL), in fact this scenario is generally more aggressive than the bidirectional traffic on half of the bridge in case of construction sites on the other half, see (Documentation ASTRA 82001, 2025).

Two scenarios accounting for REL are investigated:

- Option 1 corresponds to moderate heavy traffic increase, with n_{truck} = 22500 trucks per year per direction. This assumes that the total number of trucks (n_{truck}) remains the same as for the single lane analysis, however, the distribution between lanes is 60% n_{truck} on the first lane and 40% n_{truck} on the second lane;
- Option 2 corresponds to a large increase in the number of trucks (1.67 n_{truck}). In fact, the number of trucks in the first lane remains the same as for the single lane analysis (n_{truck} = 22500) while the number of trucks in the second lane is 2/3 of the first lane, thus (67% n_{truck} = 15000);

After discussion of the results for Option 1 and 2 with the Advisory Commission, it was agreed to account for an increase in traffic as for Option 2 (n_{truck} = 1.67 n_{truck}) in the next optimization phase of NLM1. This case covers construction works situations (i.e. with 2+2 birectional traffic on one bridge, with restriction only 2 lanes with heavy traffic). Refer to §4.2.2 and Appendix B for additional details. It covers traffic increase up to the horizon 2050, when updating of traffic evolution assumptions need to be made. For the second lane, the load configuration is identical to the first lane, however, the load values are multiplied by a reduction factor (r), see Eq. 5-7, determined using a variance minimization optimization algorithm.

$$Q_{d2} = Q_{d1} \cdot r_{Lane2,Q} \tag{5}$$

$$q_{1d2} = q_{d1} \cdot r_{Lane2,q1} \tag{6}$$

$$q_{2d2} = q_{d2} \cdot r_{Lane2,q2} \tag{7}$$

The optimization with variance minimization led to the following values of *r:*

$$r_{Lane2,Q} = r_{Lane2,q1} = 0.20 \quad (8)$$
$$r_{Lane2,q2} = 0.70 \quad (9)$$

A critical review of the reduction factors concluded that the NLM1 would be largely simplified by setting $r_{Lane2,q1}$ = 0 since the contribution of q_1 is relatively low for the second lane. Accordingly, the following reduction factors are selected:

$$r_{Lane2,Q} = 0.25 \quad (10)$$
$$r_{Lane2,q1} = 0.00 \quad (11)$$
$$r_{Lane2,q2} = 1.00 \quad (12)$$

The resulting NLM1, including the second lane loads is presented in Figure 26. The location of $Q_{d,1}$ within $q_{1d,1}$ is variable and should be chosen to achieve maximum desired action effect and the location of $Q_{d,2}$ is free. Please note that the load values in Figure 26 for lane 1 and 2 are derived from traffic simulations and do not account for the model uncertainty in calculating action effects nor any dynamic effect.

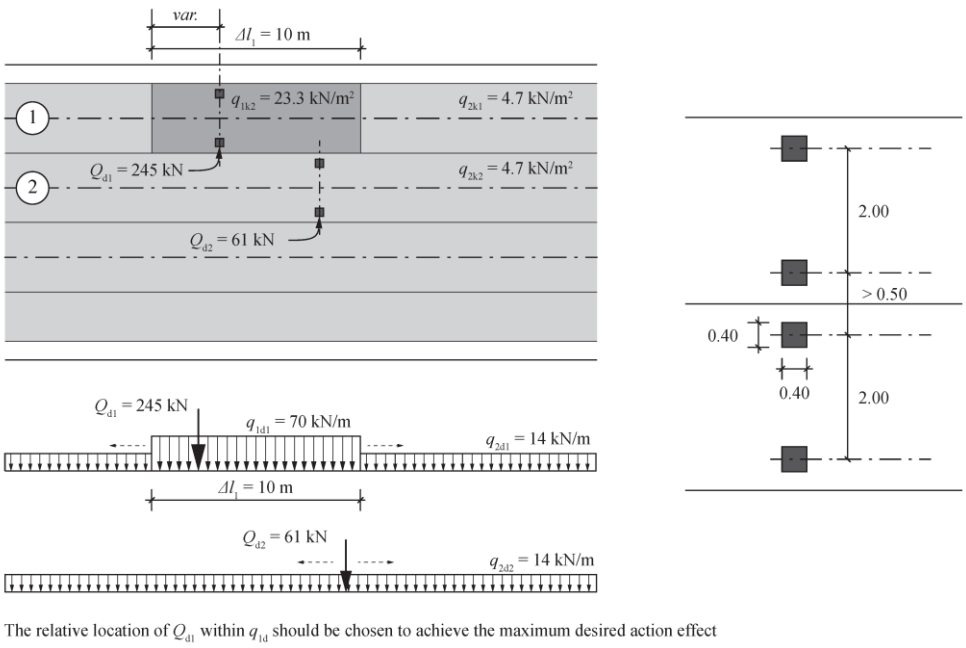

Figure 26: NLM1 for first and second lanes, design values of the loads (careful the load values are in kN and kN/m and are design action effect from simulations, the dynamic amplification DAF and modelling γ_{sd} factors are dealt with in paragraph 5.1.4)

Figure 27a-c show the ratio between the action effects obtained using the double lane design values of NLM1 (see Figure 26) and the simulations performed using the WIM-JAM traffic ($E_{d,NLM1,2l}$ / $E_{d,2l}$), with $E_{d,2l}$ obtained with increased number of trucks option 2). Compared to the performance of the current actualised load model (SIA 269/1 with $\alpha_{act,unique}$ = 0.60), presented in Figure 16, it can be observed that the NLM1 performs significantly better in every aspect: reduced variance, uniform behavior with respect to span, bridge system and action effect. While having a very good fit, the simplified version of NLM1 (for 2nd lane) remains also easy to use for designers.

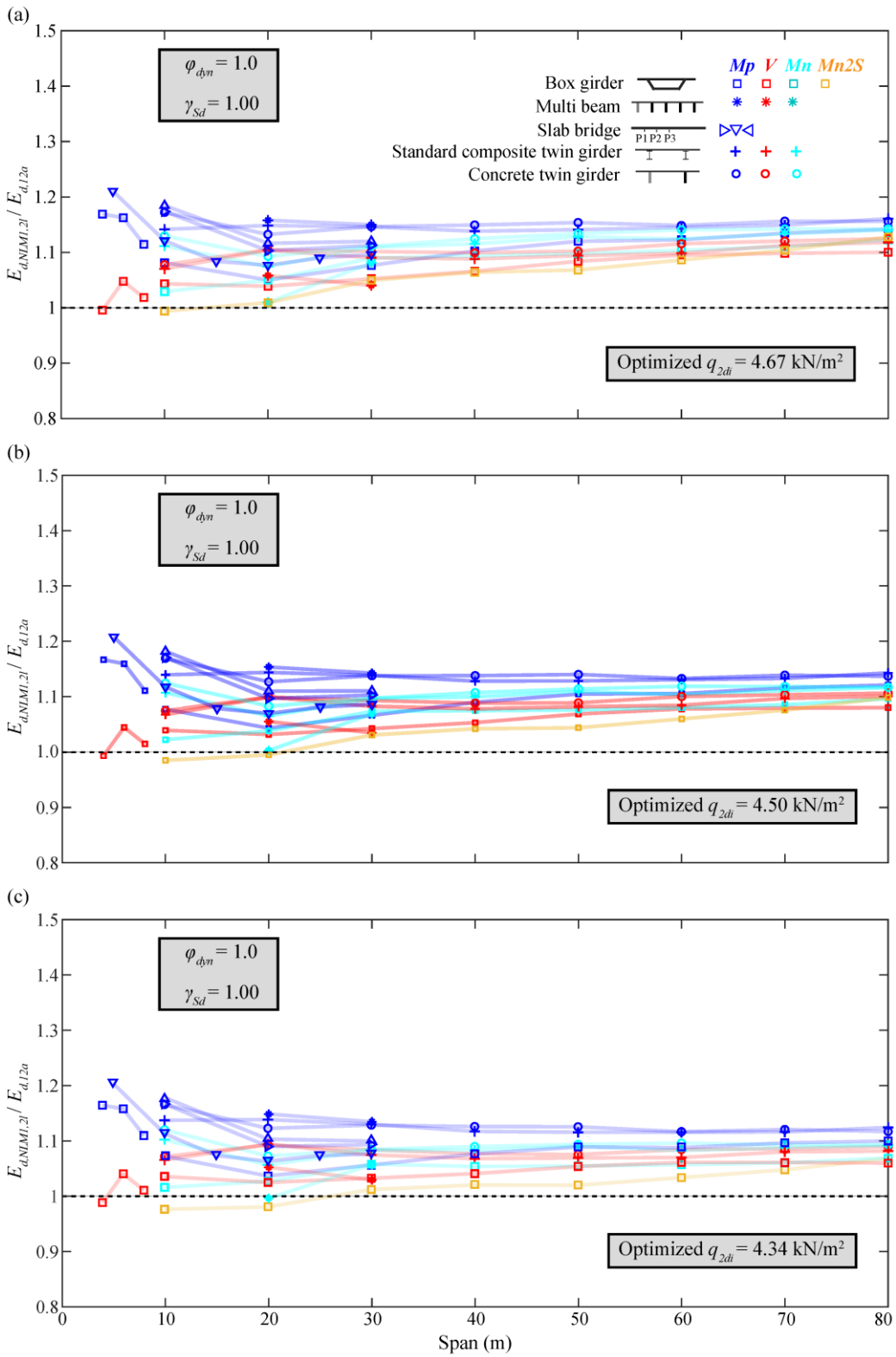

Figure 27: Ratio between action effects obtained using the double lane design values from NLM1 and from simulations, $E_{d,2l}$ (Option 2), for an optimised second distributed & second lane load (a) q_{2di} = 4.67 kN/m², (b) q_{2di} = 4.5 kN/m² and (c) q_{2di} = 4.34 kN/m²; please note that the dynamic amplification factor and the partial factor covering uncertainties in calculating action effects is not included yet.

The results displayed on Figure 27 also show that a distributed surface load q_{2di} = 4.34 kN/m² provides overall safe results without excessive safety margin. Three points fall slightly below unity but dynamic amplification factor and the partial factor covering uncertainties in calculating action effects are not included yet. Notice when optimizing q_{2di} to be 4.34 kN/m², then the value given in previous figures, especially Figure 26 are now incorrect (should be 13 kN/m).

For all the investigated spans and action effects, the NLM1 reproduces closely real traffic action effects, significantly better than the current LM1. Overall, within the investigated cases, it can be observed that the NLM1 leads to more conservative results for sagging moment (*Mp*) compared to shear force (*V*) and 2 span support moments (*Mn2S*). It is only for spans below 20 m that a few cases for shear force and support moment are close to unity.
Given that the axle load Q_{d1} is chosen to be representative of a single axle, NLM1 is adequate for both local (punching) and global verifications. With respect to the other local verifications, such as bending and shear as shown in Figure 28, the same considerations as with current code can be applied. The user has to consider both the concentrated loads, with a 45° repartition rule, as well as the UDL loads to compute the action effects in the critical sections.

It shall be emphasized that from the perspective of sustainability, any future attempt to increase truck axle load should be legally limited; and if any increase occurs, more axle weight controls, by means of law enforcement, must be put in place. Furthermore, the axle(s) load(s) cannot be allowed to drastically increase due to limitation requirements and control of pavement damage. A tentative to estimate the cost (as a result of adding overweight vehicles to the traffic stream) show that it ranges from small to big amounts (3600 times more) depending on overweighted vehicle class, bridge functional class, material type, and age (Agbelie et al., 2017).

a) Local failure modes (from (Fernández Ruiz et al., 2009)):punching (left), bending (middle) and shear (right)

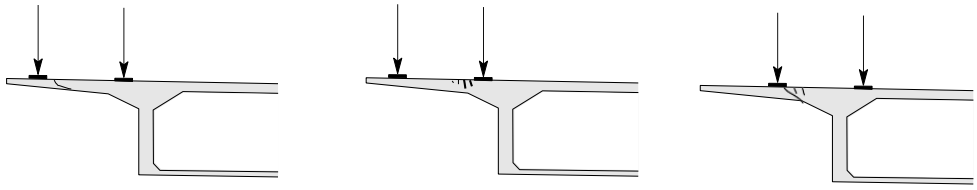

b) LM1 for local slab verifications (from (Fernández Ruiz et al., 2009)): one way and punching shear (left) and one way shear and flexure (right)

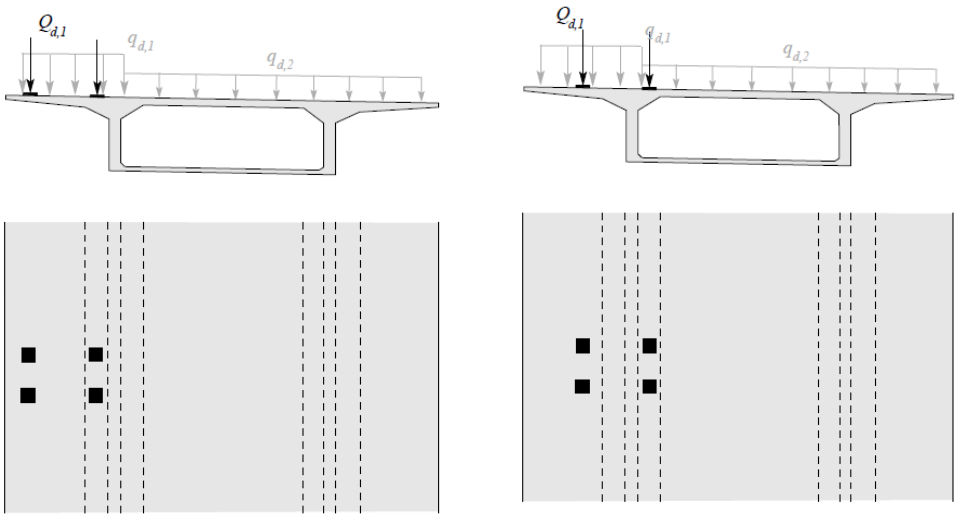

c) NLM1 for local slab verifications: one way and punching shear (left) and one way shear and flexure (right)

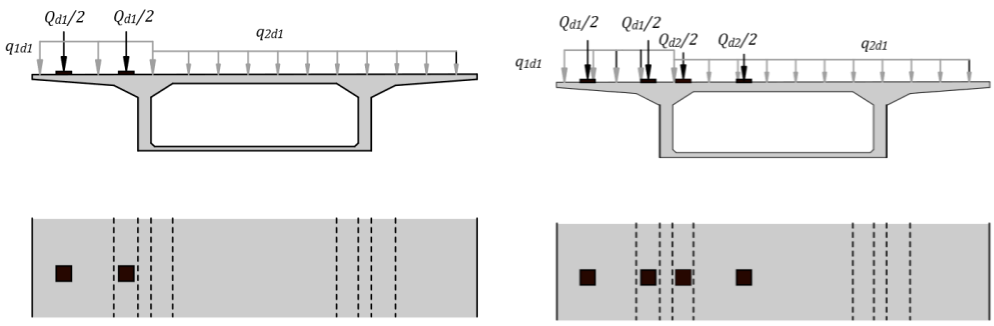

Figure 28: Example of local verifications (a) and comparison between LM1 (b) and NLM1(c)

Figure 28: shows a visual comparison of the critical location of the concentrated loads to perform local verifications on the slab portion of a box girder in the transversal direction among the different load models.

Figure 28: (a) shows the theoretical critical location where the concentrated loads should be placed to maximize the risk of triggering punching (left), bending (middle) and one way shear (right) failure modes, respectively.

Figure 28: (b) and (c) show where the concentrated loads should be placed for one way and punching shear (left) and one way shear and flexure (right) for the current LM1 and the proposed NLM1, respectively.

5.1.4 Other considerations in developing New Load Model 1 (NLM1)

These considerations refer to the framework presented in Figure 25. This paragraph discusses how to consider the uncertainties on the action side, that are condensed in the partial factor γ_{Sd}, and the dynamic effects.

Using the results presented in § 5.1.2, Figure 24 (b), and in § 5.1.3, a good estimation of the partial factor for uncertainty in modelling traffic actions, $\gamma_{sd,Q}$, can be obtained using the statistics from the ratio $E_{d,NLM1,2l}/E_{d,1l}$, which values are: μ_E = 1.05 and CoV_E = 4.1% and can be assumed to follow a lognormal distribution. This partial factor is then estimated as:

$$\gamma_{sd,Q} = exp\left(\alpha_{EQ} \cdot \beta_{tgt} \cdot CoV_E\right)/\mu_E = 1.00 \tag{13}$$

with a sensitivity factor related to modelling traffic actions effects equal to $\alpha_{EQ} = 0.4 \cdot 0.7 = 0.3$. The factor 0.4 is taken from Equation (C.9) in Annex C of EN1990: 2002 for an action effect of secondary importance.

To propose a partial factor value for uncertainties on the action effects side, γ_{sd}, the uncertainty in determining internal forces, $\gamma_{sd,S}$, needs to be considered. To this aim, the design value $X_d(\theta_E)$ from the full-probabilistic analysis was investigated and provided the value $\gamma_{sd,S}$ = 1.05, refer to § 6.3.1 for detailed information.

Finally, dynamic effects need to be considered. While few engineers dispute the fact that a vehicle can exert forces greater than its static weight when crossing a bridge, in particular the relevance of this factor at the ultimate limit state (ULS). For road bridges, there is an important difference between the code for new structures (SIA 261, 2020) and the one for existing structures (SIA 269/1, 2011). According to the latter, no dynamic factor needs to be added to the load model 1, even in the vicinity of expansion joints. This means that the dynamic amplification factors considered in the simulations of the relevant FEDRO projects (Hirt & Meystre, 2006a; Meystre et al., 2014a) are sufficient to cover these effects, meaning that the dynamic factors of the codes for the design of new structures are implicitly replaced by those of the simulations.

In Switzerland, the uniformity of the road surface is very good, which further reduces the dynamic effect in service conditions and near expansion joints. For these reasons, in this research it is assumed that the quality of pavements meets the highest requirements (OFROU, 2023), which corresponds to the qualification 'very good'. This will continue to be the case in the future because of the objective imposed by the Federal Roads Authority (FEDRO), who is also responsible for the resources to guarantee it. For the year 2022, the average pavement condition score is 1.32 on a scale from 1 to 5 where 1 is the best. This value corresponds to good overall condition.

However, in previous researches (Hirt & Meystre, 2006a; Meystre et al., 2014a), no pavement quality was specified and dynamic amplification factors ranging between 1.0 and 1.4 were used for all bridge types, with the exception of slabs, and independently from the traffic conditions, the action effect and the location on the bridge. For slabs and portal frame bridges, these values were differentiated between axle type and ranged from 1.1 to 1.4. Regarding the transversal direction analysis of the slab-like

upper part of box section and girder bridges, dynamic amplification factors between 1.4 and 1.2 were used for both the cantilevering portion and the portion between supporting beams.
For the examination of existing bridges with no particular dynamic problems, such as the cases (e.g. natural frequency far from a resonance frequency, whether or not linked to expansion joints), current knowledge suggests that these values are too high, as mentioned in (Documentation ASTRA 82001, 2025). Also, it should be noted that the concept of Assessment Dynamic Ratio (ADR) – probability of both maxima occurring simultaneously, i.e., dynamic interaction and static extreme – can be invoked to justify not increasing the static load values in simulations of the maximum action effects (E. J. O'Brien et al., 2010), in particular for bridges over 20 m for which the value of this systematic error is estimated at around 5% (Kalin et al., 2022). An appendix of ASTRA documentation 82001, revision 2025 (Documentation ASTRA 82001, 2025) provides more justification that for SLS, FLS and ULS verifications, the characteristic values of static traffic loads do not need to be increased by a DAF.
The only exception to the above applies to short bridges with spans of less than L = 20m, if a 'very good' pavement condition cannot be guaranteed. For these cases, ASTRA mandates that the following calibrated DAF, designated as φ_{cal}, be considered:

$$\begin{aligned} &L \leq 10\ m,\ \varphi_{cal} = 1.15 \\ &10 < L \leq 20\ m,\ \varphi_{cal} = 1.15 - 0.015 \cdot (L - 10) \\ &L > 20\ m,\ \varphi_{cal} = 1.00 \end{aligned} \tag{14}$$

The proposed values are based on the recent report from the REAL-LAST project, DACH Call 2021 (Vorwagner et al., 2024), that will be further used herein.
One should furthermore notice that issues relating to a 'dynamic' component in the WIM measurements has also been studied within (Documentation ASTRA 82001, 2025). WIM stations are being calibrated 'at speed' only, so the presence of a dynamic effect in the measurements cannot be stated with certainty, but there is calibration uncertainty due to speed and truck types, which was estimated to be ± 5%. Since it is essentially an epistemic uncertainty for properly calibrated WIM stations, it logically leads to larger axle loads extreme values and thus conservative action effects values.
In order to fix the DAF value(s) to apply to NLM1, one shall first properly reproduce the ADR decreasing value with respect to both increasing span and, logically, increasing total load on the bridge. The idea here is to use different $\varphi_{dyn,i}$ or to simplify the notation φ_i values for each component of the NLM1, with the rule of decreasing values, that is:

- For the axle load on lane 1, $Q_{k,1}$: $\varphi_{Q,1}$;
- For the UDL 1 on lane 1, $q_{1k,1}$: $\varphi_{q1,1}(\leq\ \varphi_{Q,1})$;
- For the UDL 2 on lane 1, $q_{2k,1}$: $\varphi_{q2,1}(\leq\ \varphi_{q1,1})$;

- For lane 2: $\varphi_{Q,2}$; $\varphi_{q1,2}$; $\varphi_{q2,2}$ ($\leq \varphi_{q1,2}$). Since heavy traffic is already present on lane 1, the total load on the bridge is larger and the DAF on the second lane should be very low; it could therefore be taken as unity.

In addition, the above DAF modelling in NLM1 considers *de facto* a decreasing influence of the dynamic effects with the span, representing a transition from flowing to jammed situation dominating the design action effects.
For these reasons, to find the value for each φ_i to be used in NLM1, the fitted DAF curves obtained from data from vehicles – bridge interaction simulations from REAL-LAST project (Vorwagner et al., 2024) are used. The resulting general DAF equation for $\varphi_{ULS,cap}$ is given below:

$$\varphi_{ULScap} = 1 + f_{95\%} \cdot \left(\frac{Q_{total}}{Q_{ref}}\right)^{-p} \cdot \left(\frac{L_{cap}}{L_{ref}}\right)^{-r} \tag{15}$$

Using equation (15), Figure 29 shows an example of the resulting capped DAF curves for bending moment of concrete bridges. For the example presented, the following values apply (see REAL-LAST report, section 3.4 for other cases): $f_{95\%} = 0.1162$, $Q_{ref} = 1580$kN, $L_{ref} = 30$m, $p = r = 0.4832$.

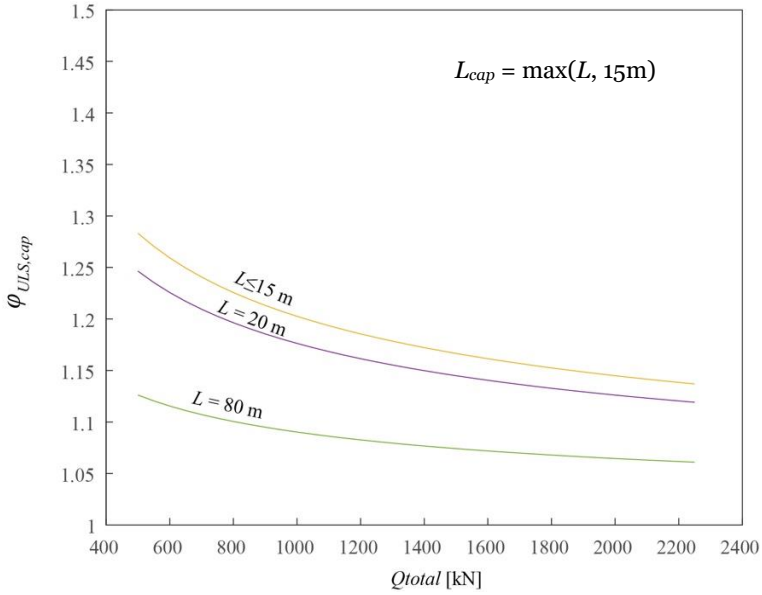

Figure 29: Example of resulting $\varphi_{ULS,cap}$ curves for bending moment of concrete bridges

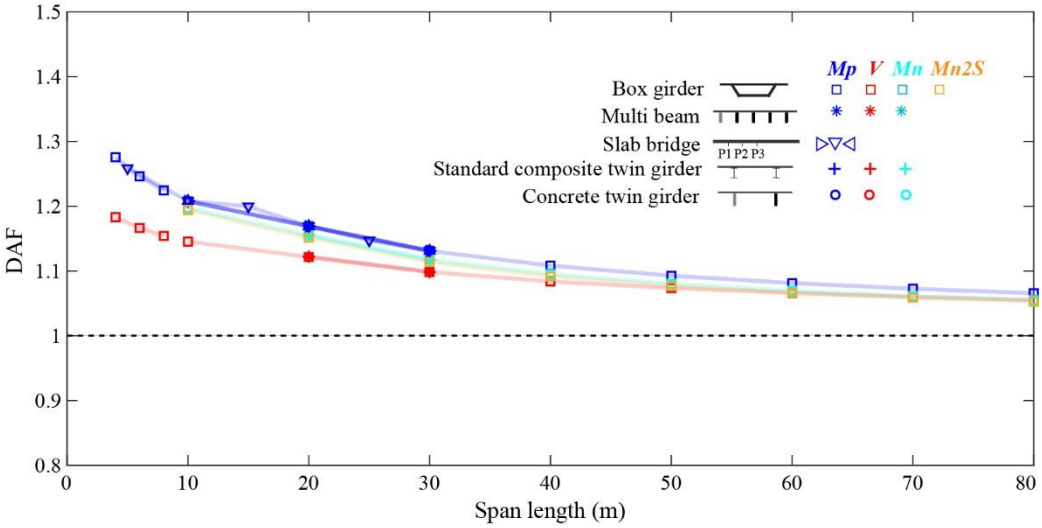

Figure 30: Resulting DAF found for the different cases of generic bridge types computed based on $\varphi_{ULS,cap}$ (capped DAF curves from REAL-LAST (Vorwagner et al., 2024))

The resulting DAFs computed using $\varphi_{ULS,cap}$ for the different cases of generic bridge types and internal forces are given in Figure 30. It can be observed that there are relatively small differences between the cases. Given these results, the following further assumptions are made:

- No differentiation between materials;
- No differentiation between Moment and Shear.

The following values are suggested after some trial and error for lane 1:

- $\varphi_{Q,1} = 1.2$
- $\varphi_{q1,1} = 1.1\ (\leq\ \varphi_{Q,1})$
- $\varphi_{q2,1} = 1.0\ (\leq\ \varphi_{q1,1})$

For lane 1 only, Figure 31 presents the results of the comparison between the NLM1 action effects (with $\varphi_{i,1}$, without γ_{sd}) and the design action effects found from the simulations and multiplied by the φ_{ULS} values found using REAL-LAST-capped DAF curves. On the one hand, the *Mn2S* case leads logically to the lowest values, since two spans must be loaded to get the design cases; on the other end, the *M*p case leads the higher values, never exceeding 1.15. Ideally, the results should be centered around unity, with a low variability. It can be stated that the values proposed give a very good overall approximation of the dynamic effects. Moreover, it is suggested to keep the φ_i values explicit in NLM1, thus allowing for a better understanding of what is covered in the load model and an easier adaptation of NLM1 in the future.

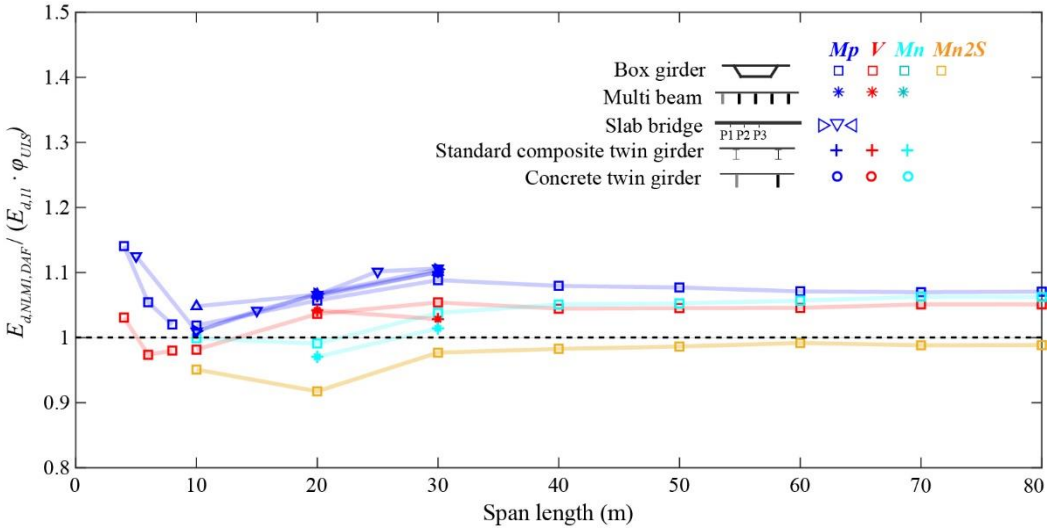

Figure 31: Comparison between the NLM1 action effects (with DAF $\varphi_{i,1}$, without γ_{sd}) and the design action effects from the simulations, multiplied by the capped $\varphi_{ULS,cap}$ curve values from REAL-LAST)

Finally, Figure 32 presents NLM1 in the code format. This means with the characteristic values when including γ_{sd} and dynamic effects, dividing the resulting design load values by $\gamma_{Q,act} = \gamma_Q = 1.50$ and giving the UDL per unit area (width of a notional lane being 3 m). The location of $Q_{k,1}$ within $q_{1k,1}$ should be chosen to achieve maximum action effect and the location of $Q_{k,2}$ is free. For the remainder of this report, the term **characteristic code value** is used to differentiate between results coming from simulations (called design values from simulations) and the latter, the conversion factor being:

$$E_{\mathrm{ki,code}} = E_{\mathrm{di,NLM1}} \cdot \gamma_{\mathrm{sd}} \cdot \varphi_{\mathrm{I}} / \gamma_{\mathrm{Q}} \tag{16}$$

For instance, for $q_{1\mathrm{k},1}$:

$q_{1\mathrm{k},1} = (70/3) \cdot 1.05 \cdot 1.1/1.5 = 18$ kN/m²

Then one needs to fix Q_{k2}, which together with the optimization above is chosen equal to 75 kN (instead of $Q_{\mathrm{d2}} \cdot \gamma_{\mathrm{sd}} \cdot \varphi_{\mathrm{I}} / \gamma_{\mathrm{Q}} = 43$kN). This choice is made because it corresponds to $7.5 \cdot 1.5 \cong 11.5$ tonnes, the load limit for a truck single axle according to OCR. If one looks at the ratios $Q_{\mathrm{di}} \cdot \gamma_{\mathrm{sd}} \cdot \varphi_{\mathrm{I}} / \gamma_{\mathrm{Q}}$ to Q_{di} for each lane, one sees that they differ somewhat because the dynamic coefficient value depends on the lane, but they stay close which validate further the choice for Q_{d2}:

- 1st lane: $Q_{\mathrm{d1}} \cdot \gamma_{\mathrm{sd}} \cdot \varphi_{1,1} / \gamma_{\mathrm{Q}}$ $\quad Q_{\mathrm{d1}} = 245 \cdot 1.05 \cdot 1.2 / (1.5 \cdot 245) = 0.84$
- 2nd lane: $Q_{\mathrm{d2}} \cdot \gamma_{\mathrm{sd}} \cdot \varphi_{2,1} / \gamma_{\mathrm{Q}}$ $\quad Q_{\mathrm{d2}} = 75 \cdot 1.05 \cdot 1.0 / (1.5 \cdot 75) =$ **0.86**

The last values to fix are the UDL on the remaining bridge accessible surfaces, third lane and remaining surface. Given the relative similarity of the characteristic code values between the current LM1 ($\alpha_{qi}\, q_{ki} = 2.25$ kN/m², $i = 2$ to n) and the proposed one for q_{2k2}, the reduced UDL for all lanes could be lowered to get closer to the LM1 value but still modelling properly the extreme action effect values on lane 1. The optimization process converges towards 3.00kN/m² as the characteristic code value for $q_{2\mathrm{k}1}$ and $q_{2\mathrm{k}2}$.

This value can conservatively be adopted for the other lanes as well (thus q_{2ki} = 3.00 kN/m², i = 1 to n) as the 3rd lane traffic affects mainly large bridges, where the self-weight is much higher than the 3rd lane heavy traffic load; it still needs to be multiplied by γ_{sd}.

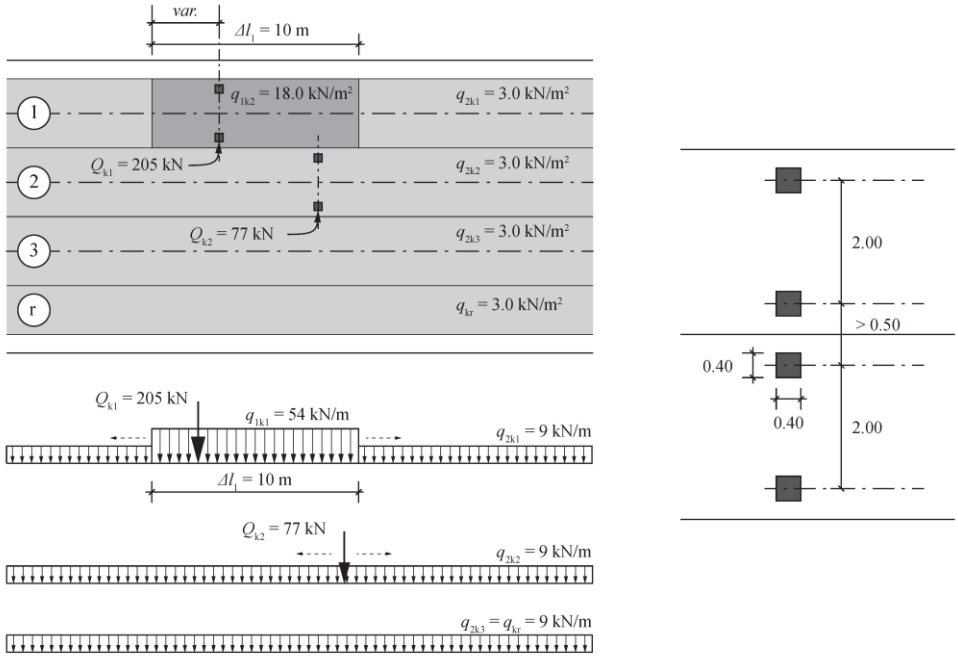

① $Q_{k,1}$ = 205 kN $q_{1k,1}$ = 18 kN/m² $q_{2k,1}$ = 3.00 kN/m²

where the relative location of $Q_{k,1}$ (var) within $q_{1k,1}$ should be chosen to achieve the maximum action effect

② $Q_{k,2}$ = 77 kN $q_{2k,2}$ = 3.00 kN/m²

③ $q_{2k,3}$ = 3.00 kN/m²

q_{kr} = 3.00 kN/m²

Figure 32: Proposition of new load model 1 (NLM1) for evaluation of existing bridges, presented in code format with the corresponding **characteristic code values** of the loads ($\alpha_{i,act} = 1.00, \gamma_{Sd} = 1.00, \gamma_F = 1.50$ and dynamic amplification factors included for ease of use)

This increase from 2.25 to 3.00kN/m² is also important to provide sufficient margin to cover uncertainties about future heavy traffic developments, such as an increase in heavy traffic in the other lanes (3rd , 4th lane), in traffic congestion, as well as the necessity to include bridges with bidirectional traffic on multiple lanes. They however may lead in certain cases to NLM1 being less favorable than ASTRA 82001. In this previous research, differences in lane configurations were either not differentiated but covered by a unique actualized coefficient (step 0), or differentiated (case specific αi,act values, step 1). The presence of REL was studied but only to fix a unique actualized coefficient (step 0). In this research, in order to propose a generically valid New Load Model a different philosophy was followed, namely to cover well the different highway lane patterns with two heavy traffic lanes, the worse being indeed with a REL. In addition, a heavy traffic of 167% the current maximum one was applied to calibrate NLM1. Thus the conformity factors from verification using NLM1 can be lower than those found using ASTRA 82001. If a "fair" comparison is to be made between both, it should be done between results from Step 0 with REL (α_{act} = 0.60) and those from the NLM1.

Nevertheless, it was not the goal of NLM1 to be more economical (i.e. less conservative) but to reach a more uniform safety level, to be more versatile and thus allow for extrapolation, whereas ASTRA 82001 cannot be applied outside its applicability limits. For additional information, the reader is also referred to Table 8, which summarizes the treatment of the uncertainty sources on action and action effects in function of the Level of Approximation (LoA), as well as the discussion with respect to full-probabilistic analyses in § 6.4.1 on the assumptions made on action effects model uncertainty.

5.2 Summary of the proposed New Load Model 1 (NLM1)

The workflow leading to the design values of the NLM1 for the evaluation of existing bridges is presented in Figure 33. The design values are given for national lanes 1 and 2 (3m wide each) and are obtained considering explicitly the dynamic amplification factor (φ) and the model uncertainty of action effects (γ_{Sd}).

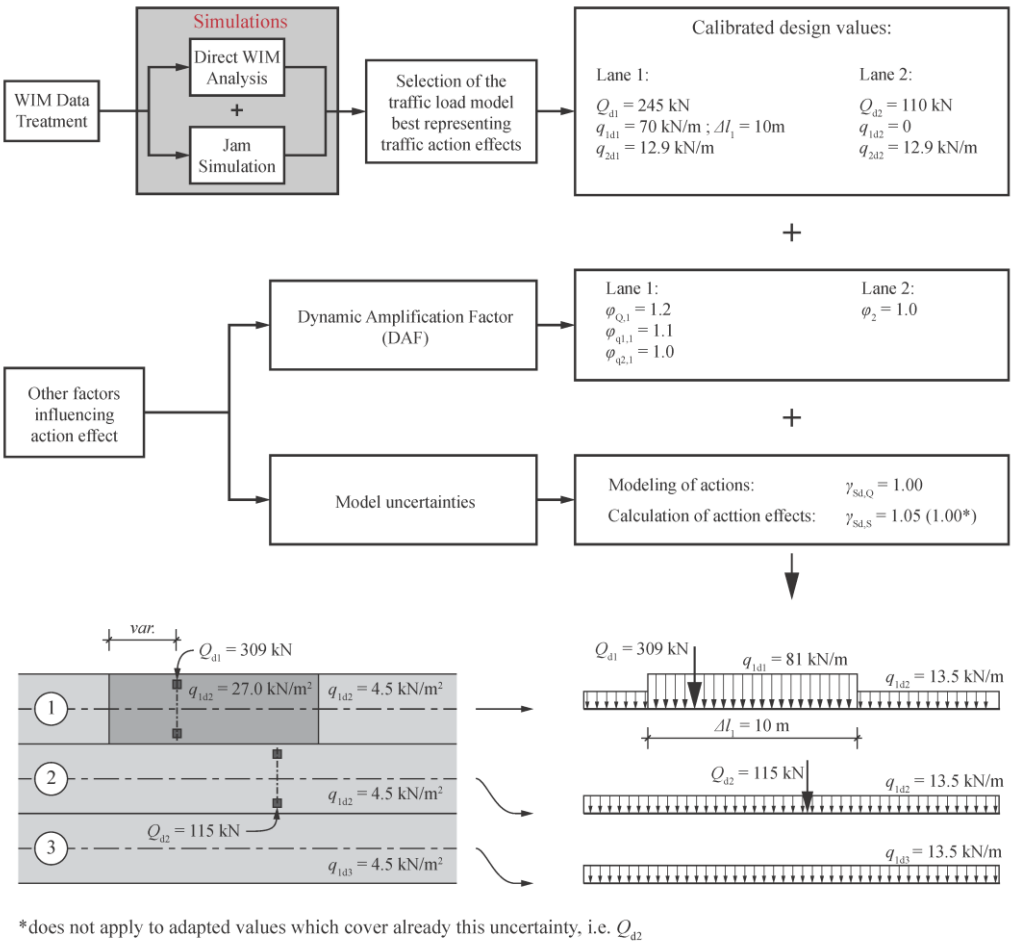

Figure 33: Workflow to determine the loads of the new load model 1 (NLM1) for evaluation of existing bridges, with the final examination values displayed

Finally, Figure 34 presents the NLM1 in the usual format with characteristic code values, i.e. dividing the design level values by $\gamma_F = 1.50$, with the values of the loads in kN and kN/m² (setting $\alpha_{i,act} = 1.00$).

Notice that the values for the third lane as well and for the remaining area are set to be equal to q_{2k2}, that is $q_{2k3} = q_{2kr} = 3.00$ kN/m². This value is not only consistent with the values on notional lanes 1 and 2, as in the current code, it also includes a margin for future traffic increase as well as compared to the current values in LM1 ($\alpha_{qi} \cdot q_{2ki} = 2.25$ kN/m²).
The concentrated loads shall be placed in the most unfavorable positions. In lane 1, the position of the axle load $Q_{k,1}, x_{loc}$, is variable within the length of UDL1. In lane 2, the axle load $Q_{k,2}$ can be placed anywhere on the influence line. Since the value of the axle load $Q_{k,1}$ is chosen to be representative of a single axle, NLM1 is adequate for both local (punching, bending, shear) and global verifications, following the same rules as the current code. Finally, it shall be emphasized that, from the perspective of sustainability, any future attempt to increase the truck axle weight should be legally limited.

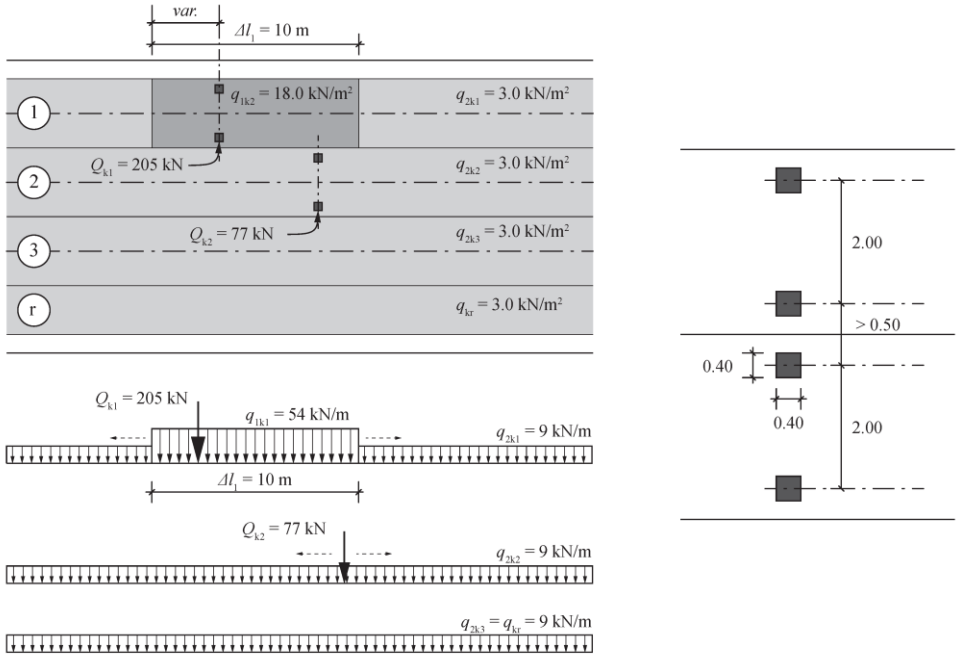

① $Q_{k,1} = 205$ kN $q_{1k,1} = 18$ kN/m² $q_{2k,1} = 3.00$ kN/m²

where the relative location of $Q_{k,1}$ (var) within $q_{1k,1}$ should be chosen to achieve the maximum action effect

② $Q_{k,2} = 77$ kN $q_{2k,2} = 3.00$ kN/m²

③ $q_{2k,3} = 3.00$ kN/m²

$q_{kr} = 3.00$ kN/m²

Figure 34: Proposition of new load model 1 (NLM1) for evaluation of existing bridges, presented in code format with the **characteristic code values** of the loads ($\alpha_{i,act} = 1.00, \gamma_F = 1.50, \gamma_{Sd}$ and dynamic amplification factors included for ease of use)

For examination, as already presented, one gets the examination values by multiplying the characteristic code values of the loads using $\gamma_F = 1.50$; the adjustment need not to be indicated in the figure since it equals unity, $\alpha_{i,act} = 1.00$.
Then, for new structures, a good first guess is to multiply the examination load values by the different factors as follows (such that $E_d = x \cdot E_{d,act}$):

Q_1: x = 1/(0.60·1.2) = 1.40
Q_2: x = 1/(0.60·1.1) = 1.52
q_i: x = 1/(0.60·1.0) = 1.67

Indeed, the adjustment factor value $\alpha_{act,unique} = 0.60$ from doc. ASTRA 82001 was used in comparisons and was found to be adequate to meet the minimum safety required, see for ex. Figure 16. This proposition however needs further validations. Note also that the resulting values also include our DAF proposition, with low values and differentiation in function of the load, which shall be discussed in case of new structures.

6 Full probabilistic analysis on generic and specific bridge types

6.1 Introduction

The calibration of the New Load Model 1 (NLM1) presented in the previous chapter is performed based on the design action effect due to traffic loads and the performance of the model is determined by comparing the action effect derived by the NLM1 with the one obtained running traffic simulations on a selected bridge database.
To this purpose, the following assumptions are made:
The design value of the traffic action effects was determined assuming a fixed sensitivity factor on the action side $\alpha_{E,Traffic} = 0.7$ long with a reliability index $\beta_{tgt,yr} = 4.2$, according to EN 1990:2002 (EN 1990:2021 Eurocode - Basis of Structural and Geotechnical Design, 2021). Fixing the sensitivity factor for action effects due to traffic loads implies a constant importance, independent on the influence of other loads such as the self-weight and independent on the uncertainties related to the resistance calculation. This choice can lead to an over-conservative assumption of the sensitivity factor for cases where the self-weight of the structure tends to be dominant compared to traffic loads or in cases where most of the uncertainty in determining the reliability index is related to the calculation of the resistance, which occurs mostly for brittle failure modes (Yu et al., 2021), (Malja, 2024).
That said, it is essential to investigate the impact of different uncertainties on the limit state function, which allows to calibrate the load model considering the actual importance of the other involved uncertainties. Also, this allows a more comprehensive investigation of the proposed load model when explicitly implementing the resistance calculation with the related uncertainties.

Thus, in this chapter, the aim is to investigate the influence of the involved uncertainties on the limit state function and assess the probability of failure by performing full-probabilistic reliability analyses in order to identify further hidden safety reserves for the New Load Model 1. In addition to the typical bridges presented in the previous chapters, additional case studies were investigated to assess structural safety considering more realistic influence lines. The following sections present the most significant assumptions regarding the statistical and deterministic input parameters for the full-probabilistic reliability analysis, followed by a discussion of the results for the typical bridges. Further background information concerning the input parameters required in order to perform the full-probabilistic analysis as well as extensive results can be found in Appendix C and D.

6.2 Input parameters for the full-probabilistic analysis

To perform a full-probabilistic reliability analysis, statistical parameters that describe the distributions of the basic variables involved are of main importance. This applies to both parameters on the action and the resistance side.
In the present study, the full-probabilistic limit state is assumed to take the following form:

$$g = \theta_{\mathrm{R}} \cdot R - \theta_{\mathrm{E}} \cdot \left(E_G + E_Q\right) \tag{17}$$

The limit state function is formulated as shown in Eq. (17) with the resistance R defined as the cross-sectional resistance and E_G and E_Q being the local action effect at the same cross-section for the permanent and the traffic load respectively. The variability of the resistance accounts for geometrical and materials uncertainty. The model uncertainty in resistance calculation, referred to generally as the resistance model uncertainty, is considered separately with the basic variable θ_{R}. This uncertainty covers the difference between the resistance calculated using a simplified model and the actual resistance without considering materials and geometrical uncertainties.

On the actions side, both action effects due to traffic loads Q and to permanent loads G are considered. The permanent load G consists of structural and non-structural permanent loads G_1 and G_2 respectively (Malja, 2024).
The uncertainty in the calculation of the action effects is considered explicitly by the basic variable θ_E. The parameter accounts for the difference between the calculated action effects resulting from the analysis of the structural model and the actual action effect in the considered section, see (Malja et al., 2024).
For a more detailed description, including the range of input parameters considered, the reader is directed to Appendix C.

6.2.1 Probabilistic representation of action effects

The traffic action effects for the typical bridges investigated were derived from the distributions and results presented in Appendix C. To fit the distribution of the traffic action effects E_{Q}, the probabilistic distribution of the station and the year which corresponds to either the highest or second highest (depending on which result leads to the smaller structural safety) resulting action effect was selected. This assumption differs slightly from the approach used for the semi-probabilistic calibration, which is explained in 3.2.2. A comparison between both procedures is presented later in Figure 37.
The station-assigned distribution of the traffic action effects is then used to obtain a 50-year extreme maxima distribution, allowing to perform a full-probabilistic reliability analysis on a 50-year time frame. Further details regarding the transformation procedure can be found in Appendix C.
Information regarding the probabilistic distributions of permanent actions as well as the considered model uncertainties are shown in Appendix C.

6.2.2 Probabilistic distribution of the sectional resistance

The probabilistic distribution of the resistance R, see Eq. (17), is determined considering the geometrical and materials distributions and is multiplied by the model

uncertainty in resistance calculation θ_R. Both probabilistic parameters depend on the section properties, structural system and the investigated failure mode. An in-depth investigation was performed to determine statistical parameters of the materials, geometry and model uncertainties. To account for a wide range of scenarios, involving various failure modes, the procedure explained in following paragraphs is followed.
Table 6 presents the failure modes investigated in this work. The investigated scenarios are based on the set of previously investigated generic bridges. A detailed description of the investigated failure modes can be found in Appendix C (Table 11 to Table 13).

Investigated failure modes

Material	Resistance function	
Reinforced concrete	Bending	M^+, M^-
	Shear	Without shear reinforcement
		With shear reinforcement
Prestressed concrete	Bending	M^+, M^-
	Shear	Without shear reinforcement
Composite girder section	Bending	M^+, M^-
	Shear	Neglection of concrete shear resistance

Table 6: investigated failure modes

The material and geometric input parameters for the resistance functions were randomly determined based on the probabilistic variables defined in Appendix C, and the probabilistic distribution of the resistance resulting from the Monte Carlo simulation was evaluated statistically. By fitting the results based on standardised probabilistic distributions (such as the normal or log-normal distribution), it is possible to determine the mean value $R_{\mathrm{m,SIM}}$, the standard deviation $\sigma_{\mathrm{R,SIM}}$ and the coefficient of variation $\nu_{\mathrm{R,SIM}}$, defined as the ratio between the standard deviation and the mean value, of the resistance functions.
In order to simplify the computation of the reliability analyses the statistical distribution of the resistance R is shifted by dividing the mean value $R_{\mathrm{m,SIM}}$ by the design resistance according to the Eurocode $R_{\mathrm{d,EC}}$. The new variable ζ is denoted as in (18). This relationship is illustrated in Figure 35.

$$\zeta = \frac{\mathrm{R_{m,SIM}}}{\mathrm{R_{d,EC}}} \tag{18}$$

This representation enables a more straightforward adaptation and comparison between different resistance functions. For further details, the reader is referred to the Appendix C.

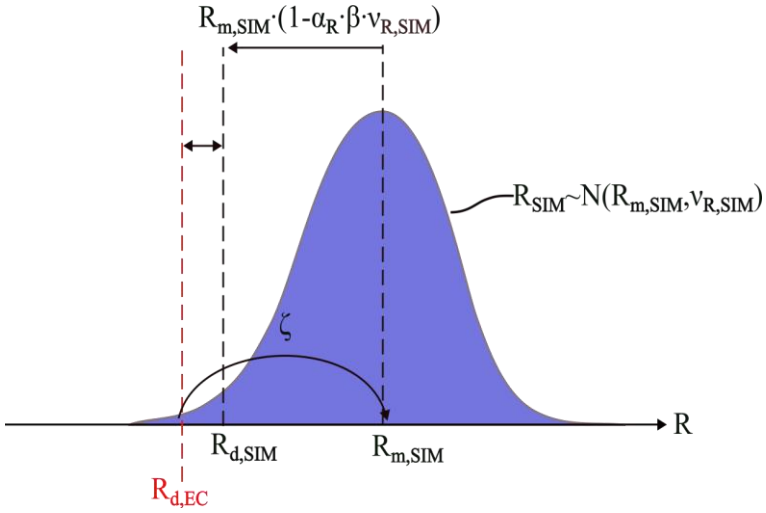

Figure 35: Description of probabilistic resistance function

The key findings from this evaluation are illustrated in Table 7. A detailed investigation in which also the influence of the uncertainty of the scatter of the resistance functions is highlighted can be found in Appendix C.

Selected probabilistic resistance parameters

Material	Resistance function		ζ	ν
Reinforced concrete	Bending	M^+, M^-	1.25	0.065
		M^+, M^-	1.38	0.065
	Shear	Without shear reinforcement	1.38	0.065
		With shear reinforcement	1.38	0.065
Prestressed concrete	Bending	M^+, M^-	1.30	0.04
	Shear		1.38	0.065
Composite girder section	Bending	M^+, M^-	1.26	0.057
	Shear	Steel resistance only	1.26	0.05

Table 7: selected probabilistic resistance parameters

6.3 Results from the load model calibration

According to the parameters presented in 6.2 and the bridges systems in Table 3, the corresponding design value is determined based on a full-probabilistic analysis. The algorithm for this calibration is presented in detail in Appendix C.
The analyses were performed excluding a dynamic amplification factor. As mentioned before, the dynamic amplification factor is considered as a deterministic parameter assumed according to findings from the REAL-LAST project (Vorwagner et al., 2024). The dynamic amplification factor was determined depending on the system (material and span length), but independent of traffic characteristics, such as the amount or type of traffic present on the bridge. The results presented previously (Figure 31) show a good agreement between the performance of the dynamic amplification factor of NLM1

and the propositions from (Vorwagner et al., 2024). Therefore, the dynamic amplification factor will not be considered probabilistically. In case that sophisticated probabilistic models for the dynamic amplification factor is developed in the future, this will allow to include those findings in this analysis as a further probabilistic parameter in Eq. (17).
The primary focus of the full-probabilistic analysis was to investigate the first lane of traffic. However, some investigations for the second lane were also conducted to better understand the influence of the transverse system and will be presented in 6.5.

6.3.1 Evaluation of action sided model uncertainty

The main output of the full-probabilistic analysis consists of the reliability index β and the sensitivity factor for each probabilistic variable α_i. Based on these two outcomes, the most likely failure point of the limit state function can be found by extrapolating each probabilistic variable to the probability of exceedance of $\Phi(\alpha_i \cdot \beta_{tgt})$. This failure point is referenced in literature as design value and can be expressed by the function $X_d(\cdot)$. However, this value does not necessarily coincide with the design values Ed or Rd characterised by partial safety factors used by structural engineers.
The design value for the uncertainty in the calculation of the action effects $\theta_{Ed} = X_d(\theta_E)$ is illustrated in Figure 36. For better visibility, the results are separated between reinforced concrete structures, including prestressed ones, and composite structures. The results demonstrate that the design value lies in a range between 1.05 and 1.13. The material and section-dependent results illustrated in Figure 36 originate from the different assumptions in the probabilistic distributions of the load and resistance sided parameters.
Since the mean value of θ_E was set to unity (see Appendix C), the partial safety factor for the uncertainty of computation of action effects γ_{sd} should be selected within the aforementioned range.

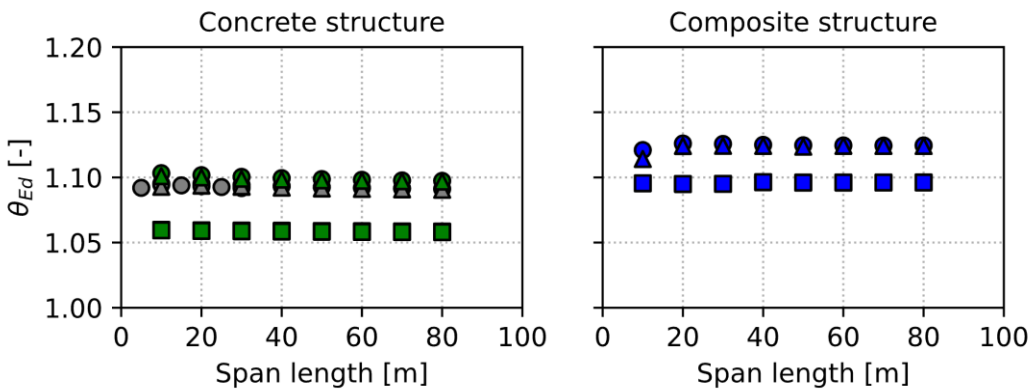

Figure 36: Design value of model uncertainty of action effects

As previously stated, the partial safety factor was selected to $\gamma_{sd,S} = 1.05$, which is compatible with the current Eurocode, which defines values of γ_{Sd} between 1.05 and 1.15 (see Table A1.2(B), note 4) (*EN 1990*, 2002; Yu et al., 2021), (Malja et al., 2024).
However, for simplicity, no differentiation for the partial safety factor between materials is made. The results discussed in 6.3.2 show that the lack of conservatism in the choice of $\gamma_{sd,S} = 1.05$ (where $X_d(\theta_E) \geq 1.05$ in Figure 36) is compensated by further hidden reserves identified in the full probabilistic analysis.

It should be noted that the full-probabilistic analysis does not include the uncertainty in the modelling of the action effects by a separate probabilistic parameter. Instead, this uncertainty was investigated prior in 5.1.4.

The semi-probabilistic calibration addresses this uncertainty by analysing the design traffic action effects resulting from each station and year. In this case, the extrapolated design values for each station and year are collected and stored in a probabilistic distribution. Selecting a relatively high quantile will probably cover the uncertainty in modelling the traffic actions. However, this procedure cannot be applied directly in the case of full-probabilistic analysis, as the traffic action effect E_Q must be represented as a probabilistic distribution evaluated based on a specific station and year. Therefore, the results derived in 5.1.4 were also assumed for the full-probabilistic analysis.
As for the semi-probabilistic analyses, the distributions of the traffic action effects from the different stations were analyzed by determining their corresponding design value (based on $\alpha_{\mathrm{E,Traffic}} = 0.7$ and $\beta_{\mathrm{syst}} = 4.2$). The distribution with the highest design value was selected as the input for the full-probabilistic analysis. However, this selection process does not guarantee that the most unfavorable traffic scenario in every instance is identified. Consequently, the full-probabilistic analysis was performed for the station corresponding to the highest and the second highest design value, allowing for the most critical case to be identified. The comparison between the design values evaluated based on the most critical station and based on the procedure described in 3.2.2 (denoted by $Q_{\mathrm{d,max}}$ and $Q_{\mathrm{d,repr}}$ respectively) is illustrated in Figure 37.

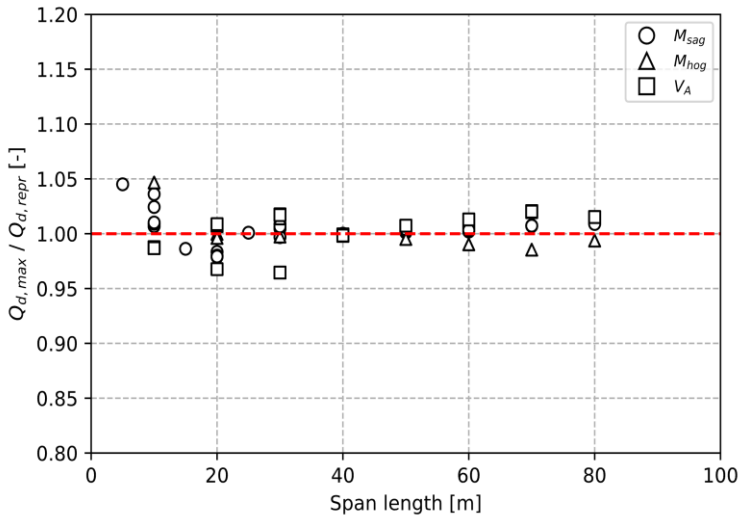

Figure 37: Comparison between global design value and station-wise design value

The results from Figure 37 demonstrate that the design values based on the station leading to the most critical response in the full-probabilistic analysis are situated in close vicinity to the values resulting from the approach utilised in the semi-probabilistic calibration. The values fall within the range of 0.95–1.05 for smaller bridges, with a notably decrease in scatter for longer span bridges. In conclusion, it can be stated that both procedures yield similar results.
It must be stated that this investigation permits only a qualitative statement, given the uncertainty surrounding the extent to which the semi-probabilistic approach adequately represents the uncertainty of representation of the traffic loads.

The results from the full-probabilistic analysis (see 6.3.2) highlight that the most decisive cases for the calibration of the load model can be found for small span girder bridges (10 and 20 m) especially evaluated in the hogging moment region. In such cases, the selection of the station for the full-probabilistic analysis results in a certain degree of over-conservatism.

In contrast to the discussions for the uncertainty in the modelling of the traffic actions, this can be omitted for the probabilistic representation of the self-weight. The Eurocode reliability background (European Commission. Joint Research Centre., 2024) which was the basis for the stochastic models of the permanent loads, states that the provided values already include the uncertainty of the load model.

6.3.2 Performance of proposed load model

Figure 38 illustrates the accuracy of the proposed new load model NLM1 with regards to the calibrated design values based on the full-probabilistic analysis for the bridge types presented in Table 3. The comparison is made through the ratio f_Q between the action effects derived for the NLM1 and the action effects resulting from the full-probabilistic analysis $E_{\mathrm{Qd,prob}}$. The probabilistic design value of the load model $E_{\mathrm{Qd,prob}}$ corresponds to the traffic action effects extrapolated to a probability of exceedance of $\Phi\left(\alpha_{E,Traffic} \cdot \beta_{tgt}\right)$, where the sensitivity factor is derived from the full-probabilistic analysis. This representation of $E_{\mathrm{Qd,prob}}$ already includes the design value of the model uncertainty θ_E as described in 6.3.1.

A value of $f_Q \geq 1.0$ indicates a conservative load model, while a value of $f_Q < 1.0$ suggests unconservative results with respect to the full-probabilistic calibration.

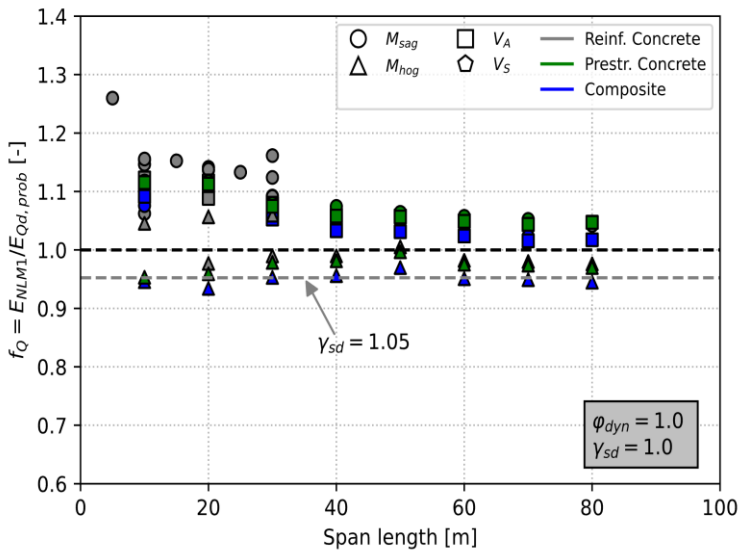

Figure 38: Difference between full-probabilistic results and semi-prob calibrated load model

The performance of the load model investigated in Figure 38 was conducted without considering a dynamic amplification factor on both the load model and the simulated traffic action effects nor an additional partial safety factor for the uncertainty of the action effects γ_{sd}. In order to consider γ_{sd}, the grey dashed line is introduced in Figure 38.

Based on the results from Figure 38, it seems reasonable to conclude that the NLM1 displays a certain degree of conservatism when comparing it to a full-probabilistic analysis. Despite the introduction of an additional factor of uncertainty in the full-probabilistic analysis, denoted by θ_E, the majority of systems still result in $f_Q \geq 1.0$. The introduction of $\gamma_{sd} = 1.05$ for NLM1 covers the largest part of the remaining un-conservative cases, leading to a generally safe-sided design. In order to better understand this over-conservatism, further investigations were conducted, whose results will be presented and discussed in the subsequent paragraphs.

Figure 39 depicts the sensitivity factors of the traffic action effect $\alpha_{E,Traffic}$ resulting from the full-probabilistic analysis. As the traffic action effects were extrapolated to a 50-year distribution, the index "50" has been added to the ordinate in Figure 39 in order to facilitate a differentiation from other results.

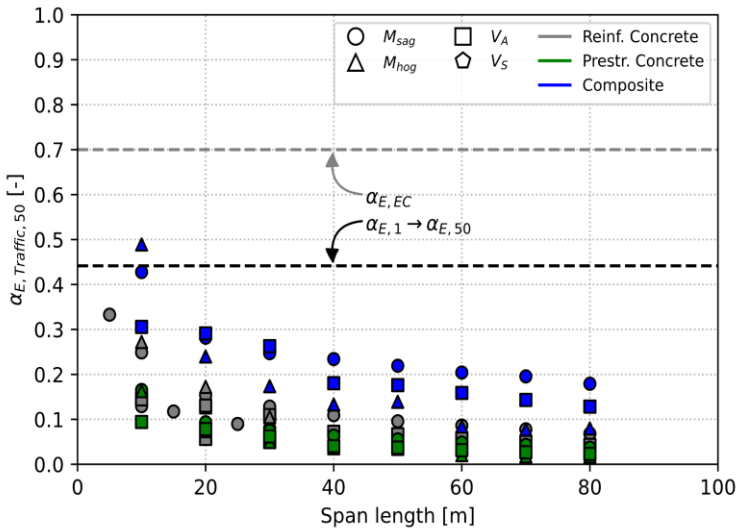

Figure 39: Traffic sensitivity factor based on full-probabilistic analysis

The results permit the following conclusions to be drawn:

- An increase in span length results in disproportionately higher permanent loads compared to the traffic loads. This is due to the imposition of permanent loads as a uniformed distributed load, which leads to a quadratic span-dependent increase in the action effects. This behaviour can only be observed to a limited extend for the traffic loads, as longer spans do not necessarily allow for the use of a high distributed load;
  An increase of the portion of permanent loads on the total loads on the bridge results in a shift in the load-sided sensitivity factors in favour of the permanent loads, thereby reducing $\alpha_{\mathrm{E,Traffic}}$;
- When focusing on a single span length, it becomes evident that composite bridge sections exhibit higher sensitivity factors than reinforced or prestressed concrete structures. One potential explanation for this phenomenon is the lower self-weight assigned to the composite bridges, which is already discussed in the preceding bullet point;
  A second explanation can be found in the description of the resistance side. The higher the scatter of the probabilistic resistance functions R and θ_R, the greater the importance of these parameters in a full-probabilistic analysis. By contrast this reduces the importance of other probabilistic variables depicted in the limit state function, among others $\alpha_{\mathrm{E,Traffic}}$. In cases where model uncertainties are high (e.g. concrete shear failure modes), the sensitivity factor for traffic action effects reaches values very close to zero.

Figure 39 provides a comparative analysis of the calculated values with those proposed by the Eurocode. The value of $\alpha_{\mathrm{E,EC}} = 0.7$ (in grey) is presented as a theoretical value, serving to illustrate the proposition from the Eurocode.
Furthermore, the equivalent sensitivity factor $\alpha_{\mathrm{E,50}}$ is presented, which yields the same design value when applied to the 50-year traffic distribution as a factor of $\alpha_{E,1} = 0.7$ for a reliability index $\beta_1 = 4.2$ for a yearly traffic distribution. This aligns with the assumption of the semi-probabilistic calibration presented earlier.

It can be noted that a significant degree of conservatism exists with respect to the description of the sensitivity factor for both a yearly and a 50-yearly description of the distribution of the traffic action effects. In only a limited number of cases, particularly in cases with unusually small spans, the calculated sensitivity factor exceeds the proposed values. This general underperformance of the sensitivity factor provides a deeper insight into the over-conservatism illustrated in Figure 38.

The sensitivity factors depicted in Figure 39 both give information about the importance of the traffic action effect on the limit state function as well as a metric, by which extent the action effects have to be extrapolated to reach the required design value. An interpretation of the results is however cumbersome, as this sensitivity factor is based on a 50-year traffic distribution, while the semi-probabilistic calibration was based on a yearly traffic action effect distribution. Therefore, the sensitivity factors depicted in Figure 39 are transformed into an equivalent sensitivity factor based on a yearly traffic distribution. The exact procedure required for this transformation is explained in Appendix C. The performance of the transformed yearly sensitivity factors is depicted in Figure 40.

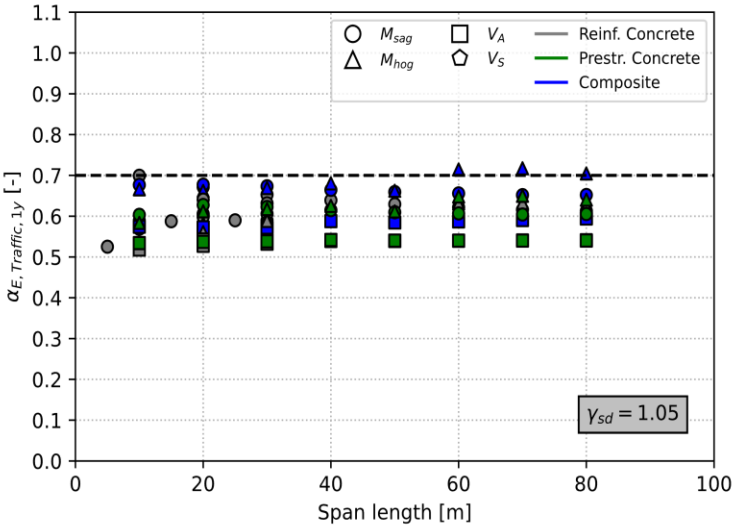

Figure 40: Sensitivity factors for 1-year traffic selecting $\gamma_{sd} = 1.05$

A comparison with the Eurocode proposition of $\alpha_{E,1} = 0.7$ still results in a certain degree of over-conservatism. However, the distribution of the results across the different structure types and failure modes is much more uniform compared to the results of Figure 39.
It should be noted, however, that the results depicted in Figure 40 have to be interpreted with some caution, given that certain inherent definitions of the sensitivity factors are no longer applicable. Therefore, $\alpha_{\mathrm{E,Traffic,1}}$ should only be used for a semi-probabilistic calibration of the load model.

Furthermore, the influence of the choice of γ_{sd} is particularly visible in the case of Figure 39 where the probabilistic distribution of the traffic actions is constituted by two factors: the distribution of the traffic action effects E_{Q} and the uncertainty in the calculation of the action effects θ_{E}. In the calibration of the required design value, the

product of both variables will first be computed. In a second step, the design value of the traffic action effects (separated from the uncertainty θ_{E}) is calculated dividing the previous result by γ_{sd}. The margin of over- or under-conservatism in the representation of the action effects model uncertainties is therefore transferred to the description of the traffic action effects. In other words, the selection of γ_{sd} affects the required design of action effects and, consequently, the sensitivity factor $\alpha_{\mathrm{E,Traffic}}$. Given the limited range within which $\alpha_{\mathrm{E,Traffic,1y}}$ operates, the results are highly sensitive to this choice. If, instead of applying $\gamma_{\mathrm{sd}} = 1.05$, a value of 1.10 is used (which remains within acceptable limits as illustrated in Figure 36), the calculated sensitivity factors tend to be smaller as can be seen in Figure 41.

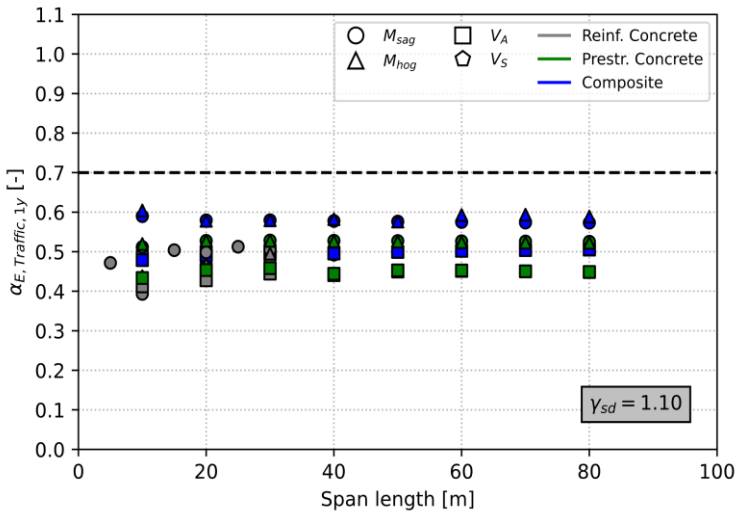

Figure 41: Sensitivity factors for 1-year traffic, selecting $\gamma_{sd} = 1.10$

6.4 Interpretation of the results

The preceding results concentrated on a comparison between the required design value according to the full-probabilistic analysis and the action effects from the proposed load model through the utilisation of the ratio f_Q. This comparison is consistent with the one presented for the semi-probabilistic calibration (see section 4). Nevertheless, in addition to this comparison, it is also possible to examine the systems' safety using the reliability index β_{syst}. The full-probabilistic analysis allows to quantify the discrepancy between the two design values by means of a reliability index. The design value resulting from the full-probabilistic calibration was determined by meeting a target reliability index of $\beta_{\mathrm{tgt,50}} \approx 3.2$. Altering the design value of the traffic action effects influences the admissible design resistance, which – since linked to the probabilistic distribution of the resistance function – also influences the reliability index (in case of interest, a more detailed explanation is provided in Appendix C). This relationship allows to investigate the influence of the design action effects of the NLM1 on the reliability index, which is illustrated in Figure 42 for the investigated systems and failure modes. This provides further insight into the influence of the traffic load model on the full limit state.

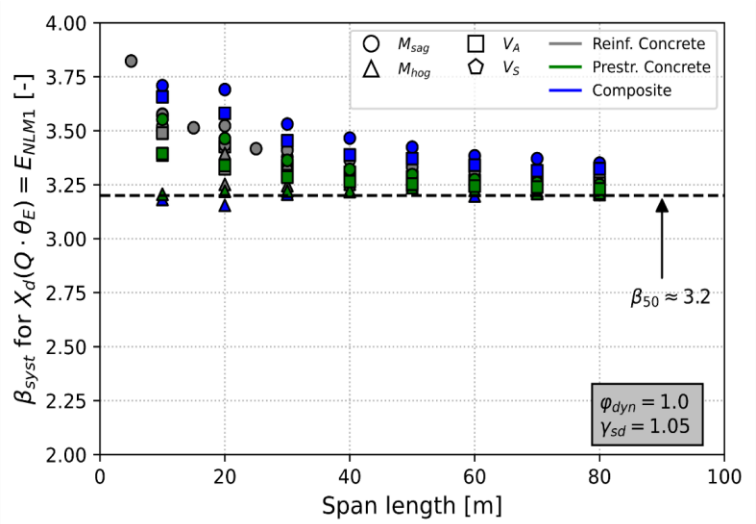

Figure 42: Reliability index based on calibrated NLM1

Figure 42 depicts a similar trend to the results illustrated in Figure 38, but with a notable reduction in the scatter band of the safety margin for longer span bridges. This representation allows to more accurately quantify the influence of discrepancies between the proposed load model and the results from the full-probabilistic calibration. To illustrate the influence on the system reliability further, the error between the target reliability (here $\beta_{tgt,50} \approx 3.2$) and the reliability from Figure 42 is determined with an error function. Minimizing Eqn. (19) would lead to an optimal load model.

$$\min\left\{\sum\left(\beta_{\mathrm{NLM1,i}} - \beta_{\mathrm{t}}\right)^2\right\} \tag{19}$$

Furthermore, incorporating of a weighting factor w_i is a potential addition to regulate the behaviour of the error function. In this instance, the sensitivity factor of the traffic action effects from the full probabilistic analysis is proposed as a weight factor:

$$\min\left\{\sum\left(\alpha_{\mathrm{E,Traffic,50,i}}\right)^2 \cdot \left(\beta_{\mathrm{NLM1,i}} - \beta_{\mathrm{t}}\right)^2\right\} \tag{20}$$

The reason for selecting the sensitivity factor based on the 50-year traffic distribution instead of the yearly traffic distribution is that $\alpha_{E,T,1}$ does not exhibit a linear relationship with an anchorage at 0. A more detailed explanation of this effect can be found in Appendix C. This effect can be illustrated better, when plotting the sensitivity factor in function of the load ratio χ (see Figure 43).

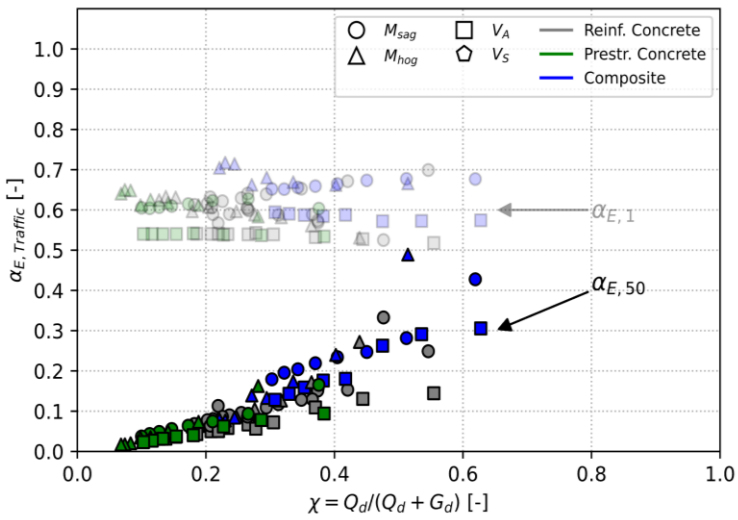

Figure 43: Influence of load ratio on sensitivity factors

The load ratio χ depicted on the abscissa of Figure 43 is calculated by extrapolating the probabilistic distributions of E_G and E_Q to a fixed quantile based on $\alpha_E = 0.7, \beta = 3.8$, showcasing that an increase in the load ratio results in higher sensitivity factors $\alpha_{E,Traffic}$. The results from the error-function both in the case without (Figure 44) and with (Figure 45) inclusion of a weight factor are presented below.

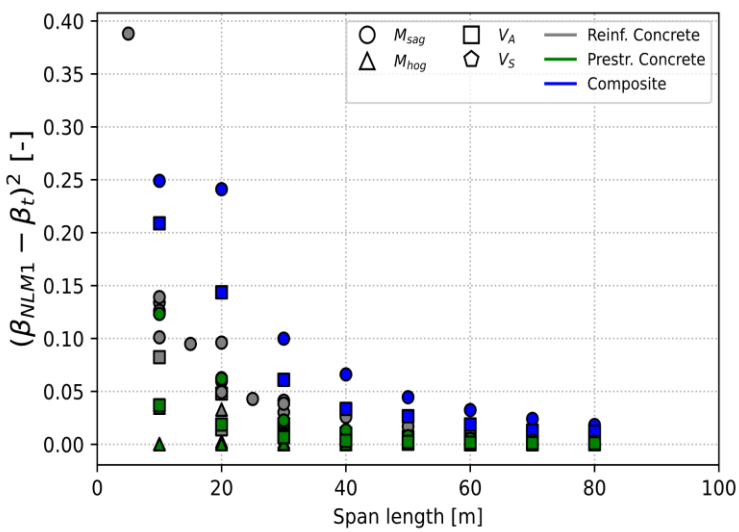

Figure 44: Error between NLM1 and target reliability

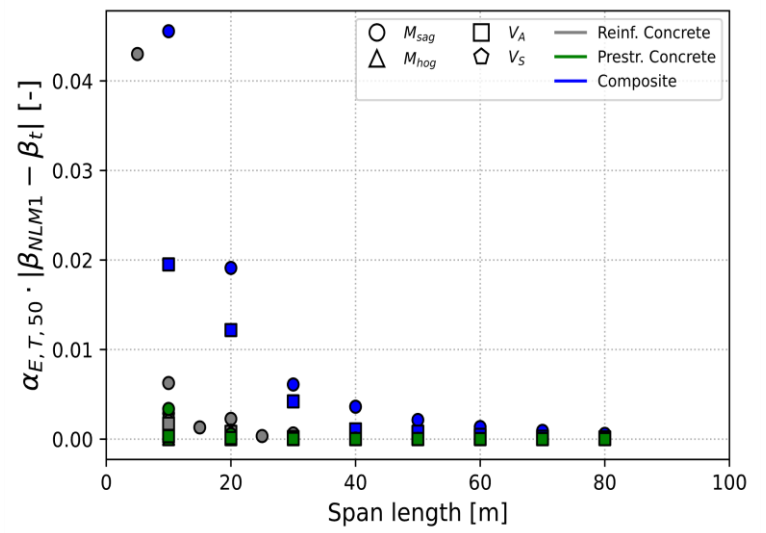

Figure 45: Relative error between NLM1 and target reliability – weighted by sensitivity factors

The trends between the results in Figure 44 and Figure 45 are very similar. However, Figure 45 allows to draw a more in-depth conclusion, as it also includes the significance of the load model with respect to the limit state function. While the error decreases with increasing span length in both cases, this effect is more drastic in the case of consideration of weight factors, identifying small span composite bridges as the most critical cases (besides the single 5 m span concrete bridge considered in the analysis).
A decrease of the deviation of the error function is particularly beneficial when considering small span bridges, as longer spans are almost not affected by changes in the load model. Further investigations on more realistic bridges and the Swiss bridge database demonstrate that small single span composite bridge systems – the critical cases depicted in Figure 42 and Figure 45 – are not present on the Swiss highway, in favour of longer, multi-span bridge systems, that possess additional hidden safeties.

It can be generally concluded that the proposed load model leads to a good general performance when comparing it with the results from the full-probabilistic calibration. The impact of the load model on the safety of the structures was further investigated, leading to a satisfying agreement between the target reliability level and the results from the analysis. To better understand the performance of the proposed load model in comparison to existing ones, a comparative analysis between the different load models will be presented in 6.4.1.

6.4.1 Accuracy of existing load models

This sub-chapter is dedicated to an investigation of the performance of existing load models, with the objective of providing a more contextualised analysis of the proposed load model. The methods presented and applied previously (see § 6.3.1 and 6.3.2) are used here to investigate the differences between the load models. The results presented here are only open to a qualitative interpretation, as certain backgrounds for the development of the load models are incomplete, thereby limiting the available knowledge for their assumptions.

The existing traffic load model of interest here is the load model LM1, which is based on EN 1991-2 (*CEN-TC250-SC1 N1569*, 2020) and its derivation depicted in SIA 261 (SIA, 2020).
As the existing load model already considers both the effect of uncertainty of action effects and a dynamic amplification factor implicitly, both of these factors should be included on NLM1 to allow for a persistent comparison. It is therefore necessary to incorporate the dynamic amplification factor into the calibration process of the action effects. For the sake of simplicity, the dynamic amplification factor derived in 5.1.4 was multiplied by the design value resulting from the full-probabilistic analysis. This design value is represented by the variable $E_{\mathrm{Qd,prob}}$ in Figure 46.
In addition to the performance of the NLM1, three distinct load model configurations are illustrated in Figure 46 which are based on LM1 but scaled by the factor α_Q. The load factor α_Q was selected as 0.90 (acc. to SIA 261), and 0.60. Additionally, the results according to the proposed values from SIA 269/1 Table 1 are illustrated in Figure 46 as well.

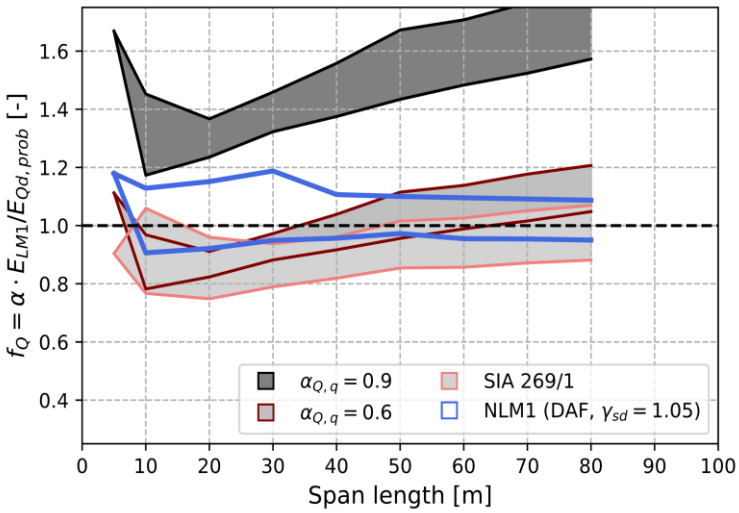

Figure 46: Accuracy of LM1 from EN 1991-2 based on full-probabilistic analysis

To facilitate a more transparent representation of the results, the performance of the load models is visualised using envelope curves, based on the maximal and minimal values for f_Q for each span length. As only a single bridge structure was examined with a span length of 5 m, the envelope is represented at L = 5 m by a single data point.
The results demonstrate that the NLM1 produces a more uniform envelope around a value of $f_Q = 1.0$. In contrast, the current existing load models exhibit a declining trend for span lengths between 10 and 30 meters, followed by an uptick for longer span. As a consequence, the conservatism of the load model increases with the span length of the bridges. The width of the envelope (which can be interpreted as the scatter of the results) exhibits a comparable behaviour across the different load models.
However, the graphic suggests that for $\alpha_Q = 0.60$ there is a significant degree of non-conservatism, particularly within the range of 10-30 m. It is challenging to make a definitive assessment, as the simulation algorithms of the traffic simulations used in these research projects is regularly updated to:

- Include more recent WIM station data sets;

- Remove the data sets of lower quality due to additional information that becomes available (recent calibration, weight controls by police, etc.)
- Improve the pruning algorithms to remove erroneous records, identification of special vehicles;
- For (Documentation ASTRA 82001, 2025) the algorithm included by default a partial factor of action effects model uncertainty equal to 1.0 for direct WIM simulations, and to 1.1 for simulation of jammed traffic (SIM) due to the assumptions in modelling jams.

The main reasons explaining the observed discrepancies are the assumptions made on action effects model uncertainty (in the current research the default partial safety factor of 1.1 on the SIM is removed) and on the dynamic amplification. Indeed, the choice for setting the dynamic amplification factor equal to unity for (Documentation ASTRA 82001, 2025) is bound to the use of an action effects model uncertainty; also it is waived in a simplified manner for short span bridges up to 20m in case the good pavement quality is not provided. Similarly, some under-conservatism exists in the description of NLM1 depicted in Figure 46. This shift can be explained by the dynamic amplification factor, which was applied subsequently.

This discussion is the point of view of the authors; it demonstrates anyway the difficulty of conducting a fully comprehensive analysis of the differences between the load models. However, the primary conclusion that can be drawn from Figure 46 is that the NLM1 results in a more uniform distribution of the accuracy when compared to the current descriptions provided in the codes. This uniformity is particularly evident for small span bridges, where the load model has a significant influence on the safety of the bridge structure.

6.5 Second Lane analysis

In order to investigate the influence of the second lane on the structural behaviour, a reduced number of full-probabilistic calculations were conducted for the NLM1 extended to the second lane. To investigate the most critical cases, the analysis was carried out on box girder sections due to their constant transverse influence line.

The traffic action effects were determined in accordance with the procedure previously outlined in 6.3. The results of the analysis are presented in Figure 47 to Figure 50. In order to facilitate an easier interpretation of the results, the full-probabilistic analysis was performed without the consideration of a dynamic amplification factor. The two previously discussed traffic scenarios, namely the distribution of the traffic on both lanes with a ratio of 60/40 and the increase in truck numbers resulting in a ratio of 100/67, were investigated. The most critical case is illustrated in Figure 47. These results are based on an increased traffic scenario, and the traffic action effects are based on the distribution resulting from the most critical station. In this case, the design of hogging moment regions for small span bridges does not fulfil the safety considerations.

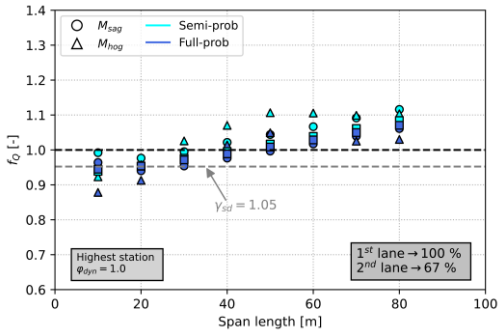

Figure 47: Second lane full-probabilistic analysis: increased traffic & highest stations

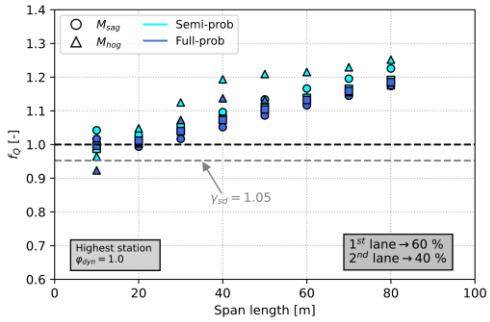

Figure 48: Second lane full-probabilistic analysis: distributed traffic & highest stations

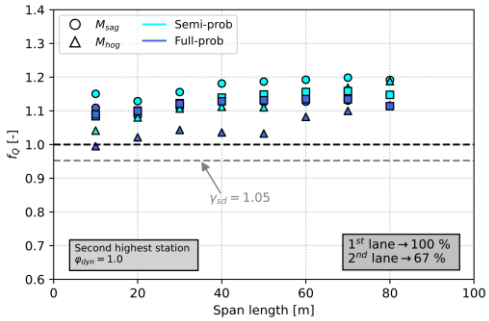

Figure 49: Second lane full-probabilistic analysis: increased traffic & second highest stations

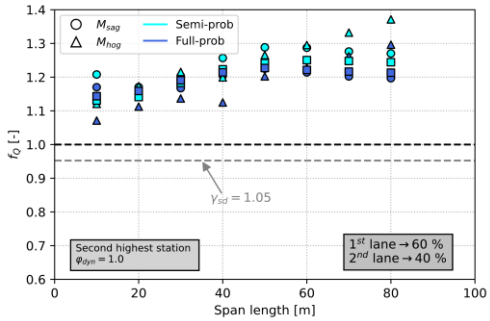

Figure 50: Second lane full-probabilistic analysis: distributed traffic & second highest stations

In particular, when both a traffic distribution of 60/40 and the second highest station are considered, the new load model ensures a safe and robust design. Given the crucial role of the small spans in the second lane analysis, further investigations were conducted, focusing on frame bridges, which allow to include a more realistic transverse influence line. These results are presented in Appendix D.

In conclusion, the following statements can be made:

- The calibration of the load model for the hogging moment region leads in general to the smallest amount of hidden reserves. This becomes evident in the second lane analysis, where no reserves can be activated to compensate for the second lane analysis. This is especially true in case of small span systems, where the selected transverse influence lines possibly overestimate the effect due to transverse distribution of the loads.
- In contrast to the semi-probabilistic calculation where the design traffic action effect is not linked directly to a specific traffic station, both the highest and second highest stations were investigated for the full-probabilistic analysis. The results demonstrate that the semi-probabilistic approach yields results between those of the first and second highest stations. This can explain why the full-probabilistic analysis produces in certain cases results which are not conservative.
- In the case of transverse influence lines with steep slopes (for example composite girder bridges), the existing conservatism in the description of the load model is

almost sufficient to compensate for the traffic action effects of the second lane, which itself has only a limited impact on the action effects of the first lane. This explains why the most critical cases are to be expected in the box girder bridges which are represented by constant transverse influence lines.

7 Implementation of a general procedure for updating traffic using the new load model (approach by Levels-of-Approximation)

7.1 Introduction

The different structural codes for design and examination have provisions, assessment steps, formulas, that are function of the structure complexity, load-bearing capacity check to be carried out and the time/information needed to perform such analyses. This can lead to confusion and inconsistencies. To avoid those and provide flexible and easy-to-use code provisions one can use the approach by levels-of-approximation (LoA), which is based on the use of rational theories grounded on physical models. For more detail see for example (fib CEB, MC2010) and (Muttoni & Ruiz, 2012). The behaviour and strength of structural members are characterized through a series of parameters (mechanical, geometrical and material properties) and a set of design equations. In the LoA approach, the accuracy of the estimate of the various physical parameters is refined in each new LoA by devoting more time to the analyses, so that the accuracy of the behaviour and strength is also improved. Furthermore, the model uncertainty of lower LoAs can be considered as a resultant of the uncertainty of higher LoAs and the additional epistemic model uncertainty introduced in the simplification procedure adopted for the derivation of the lower LoA formulae (Muttoni & Ruiz, 2012).
The main principles of such an approach can be extended to include the action effect side of safety checks, reusing the typical level range from LoA I, the lowest and least demanding, to LoA IV, the most demanding. They can be integrated in the 'Steps of the examination procedure' of SIA 269 Appendix A as given in Figure 51. It should be noted, however, that while moving to a higher LoA level does provide a greater confidence in specific results, it does not necessarily guarantee a higher level of structural checks compliance.
The advantage of such an approach is, by definition, that it contains the framework for regularly updating the partial factors or traffic assumptions and information using the higher LoA to define the lower LoAs, linked to deterministic examination and more often applied in practice. This is compatible with the constant traffic evolution and availability of new knowledge.

In the case involving traffic load models as studied here, each of the LoA corresponds to:

- LoA I: SIA 269 Chapter 4.2 procedure, deterministic examination (using values from the revised Documentation ASTRA 82001:2025, step 0, i.e., $\alpha_{act,unique}$).
- LoA II: deterministic examination, using analysis of traffic and of its action effects from simulations:
  - a) Doc ASTRA 82001, step 1, with specific $\alpha_{i,act}$ values (Documentation ASTRA 82001, 2025), implemented in a webtool: https://astra-82001.epfl.ch/#/;
  - b) Proposed new traffic load model (NLM1 from this research);
  - In case of combined use, if any inconsistencies, disregard the results from LoA IIa (they are obtained using a subset of generic bridge types and simulations, also of traffic increase scenarios);
  - Indeed, despite many similarities, in the study for ASTRA 82001 (Papastergiou et al., 2025), the presence of REL was studied but only to fix a unique actualized factor (step 0, LoA I). In this research, in order to propose a generically valid New Load Model a different philosophy was followed, namely to cover well the different highway lane patterns with two heavy traffic lanes, the worse being indeed with a REL. Future traffic increase is considered with the increase in number of heavy vehicles in lanes 1 and 2, and for more lanes (3rd, 4th ...) by increasing the Uniform Distributed Load (UDL) from 2.25 to 3.00kN/m² compared to the current LM1. These cover uncertainties about future heavy traffic developments, such as increase in heavy traffic in different lanes, in traffic congestion, as well as the necessity to include bridges with bidirectional traffic on multiple lanes. The horizon 2050 was set because regular review of traffic development need to be made. They however may lead in certain cases to NLM1 being less favorable than ASTRA 82001. Thus the conformity factors from verification using NLM1 can be lower than those found using ASTRA 82001. If a comparison is to be made between both, it should be done between results from Step 0 with REL ($\alpha_{act,unique}$ = 0.60) and those from the NLM1. Nevertheless, it was not the objective of NLM1 to be more economical (i.e. less conservative) but to reach a more uniform safety level, to be more versatile and thus allow for extrapolation, whereas ASTRA 82001 cannot be applied outside its applicability limits.
- LoA III: Semi-probabilistic examination using design traffic action effects analysis based on complete WIM-data, within the framework of SIA 269 § 5.2 and Appendix C:
  - Of traffic only with α_E = 0.7;
  - Of all action side effects, if sensitivity factors cannot be updated with the aid of FORM analyses (First Order Reliability Method), using the following factors α_E = 0.7 for the effects of leading actions, and α_E = 0.3 for the effects of accompanying actions;
  - The detailed procedure for updating actions due to traffic effects based on revised FEDRO WIM-data statistics reports to obtain the characteristic value of the variable action "$Q_{k,act}$" or of an action effect are given in a separate report (Miglietta & Nussbaumer, 2026a) (available soon).
- LoA IV: probabilistic examination. The only level where both action effects and resistance are both considered, using a full probabilistic reliability analysis, as presented in Chapter 6.

Notice that for LoA III and LoA IV, the REAL-LAST traffic sequences can be used instead of complete WIM data, guidance is given in (Miglietta & Nussbaumer, 2026a) (available soon). Depending on the bridge structural system and span, considerations on traffic evolution, such as lane placement, multi-lane distribution should be accounted for to simulate realistic load patterns.
The different procedures presented in §7.3 are consistent with the above LoAs and allow selecting sequences based on WIM data or from other sources (NLM1) accounting for criteria such as the bridge structural system and number of lanes to define most suitable procedure.

The authors find it useful to summarize below what the proposed NLM1 is applicable to:

- Update vertical traffic load effects;
- Existing bridges made of any construction materials (no differentiation between them has been made for the recommended values of action effects partial safety factors);
- $\beta_{tgt,yearly}$ = 4.2 (minimum calibration reliability level for using the NLM1 representative values with $\gamma_Q = 1.50$);
- All roads in Switzerland, same as with previous studies made to define traffic load models based on national road traffics for their representativity, with high heavy vehicle presence. No distinction is made within the network;
- Zones of pavement expansion joints;
- Two, two + REL and three lanes unidirectional, two to four lanes bidirectional as well as construction situation on 2 lane bridges (4-0 case);
- Traffic including special vehicles with their various probability of occurrence on the national roads where the WIM stations are located, considered as representative.

The road sections or highway entrance/exit with load limits, not allowing mobile cranes of all categories should be given special attention. This study can be used to reassess those using NLM1 and can result in removing some of these limits.

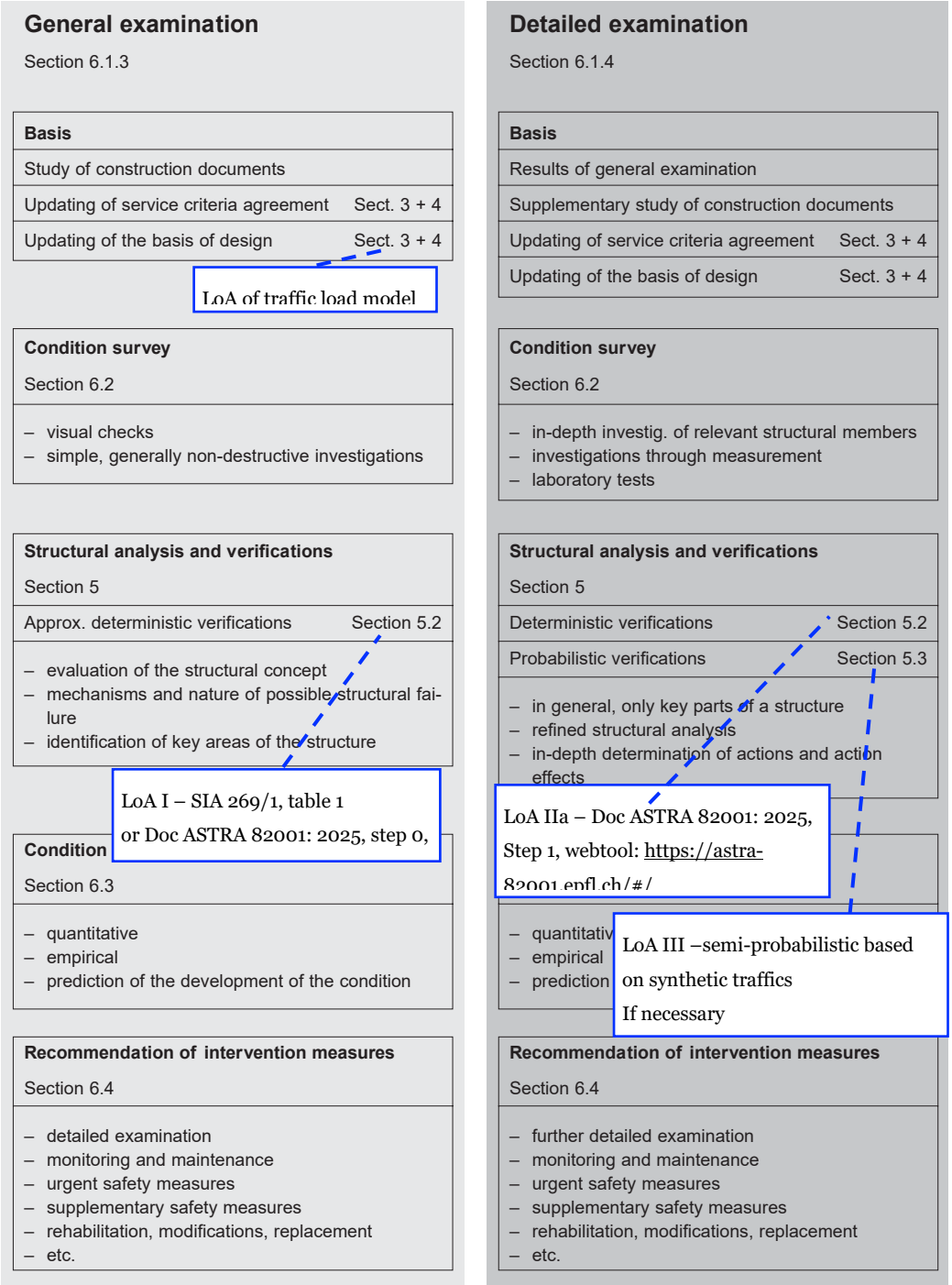

Figure 51: Integration of the LoAs of traffic load model in the examination procedure of SIA 269:2011

7.2 Limits of application

To fix the limits of application of the new normative traffic load model NLM1 proposed, the scope and limits of this research are restated:

- Can only be used to compute updated vertical load effects on existing road bridges. By default, corresponds to a $\beta_{\text{tgt,yearly}} = 4.2$ (min. target reliability level for calibrating, with $\gamma_Q = 1.50$, the NLM1 representative values);

- Does not cover roads with special traffic conditions, very different and/or higher in terms of heavy vehicle types, volumes or weights (e.g. with high frequency of special vehicles);
- Special vehicles are considered with their various probability of occurrence on the national roads where the WIM stations are located. Some roads may not be covered if more such special vehicles circulate, and some routes do not allow mobile cranes of all categories;
- With the exception of the electrification of the heavy vehicle fleets (1 or 2 additional ton allowed), no change in regulations are accounted for:
  - Pavement condition qualified as 'good to very good', FEDRO pavement quality goal. If it cannot be ensured, additional traffic induced dynamic amplification should be taken into account (it applies to short bridges with spans of less than 20m and a natural frequency close to a resonance frequency);
  - Traffic up to the horizon 2050 (corresponding with the updating of traffic evolution assumptions and the corresponding revision of design and examination structural codes)
  - Current legal limits according to the OCR: 11.5 t per axle for lorries and 12 t for special transport axles;
  - NLM1 cannot be used, was not designed nor checked, to determine the earth pressure acting on a retaining structure under the effect of road traffic loads.

7.3 LoA I and II, workflows for deterministic examination

As introduced above, deterministic examinations are based on semi-probabilistic analysis, such as the ones mainly used in Doc. ASTRA 82001 and in this research. This implies that there are limitations to the type of bridge it is applicable; also the road and traffic assumed are conservative.
Thus, Figure 52 presents the workflow for standard bridge cases, while Figure 53 presents the workflow for special bridge cases, where one can see that not all LoAs are available, i.e. the engineer will need to devote additional time to check elements of such bridges.

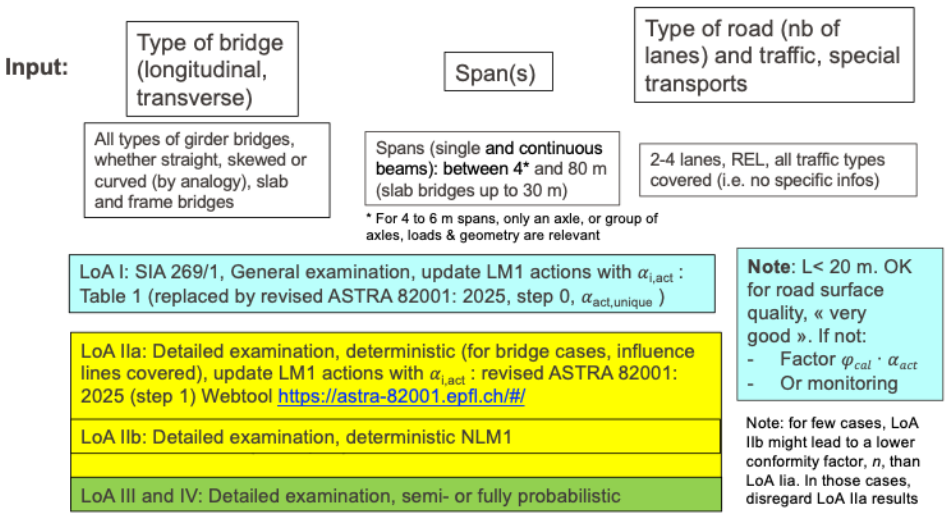

Figure 52: LoA I and II, workflow for standard bridge types

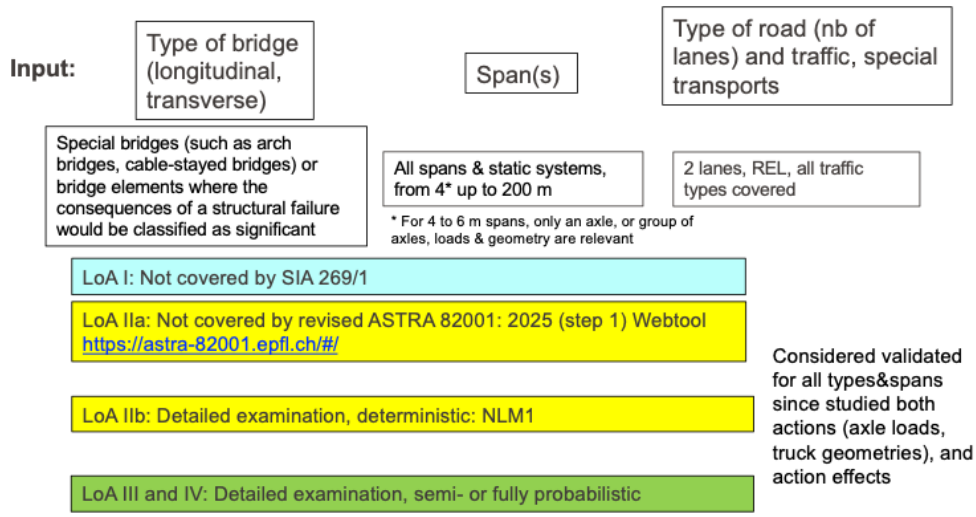

Figure 53: LoA I and II, workflow for special bridge types

7.4 LoA III and IV, workflow for probabilistic examination

The workflow is now valid for all bridge types since the engineer needs to devote more time to these analyses. Figure 54 shows the workflow for all bridge types for LoA III and IV. Note that LoA III, semi-probabilistic, only requires analyses of the action effects side, while LoA IV is the full probabilistic method. For LoA IV, information on both action effects and resistance is needed, thus limiting its application to very specific cases, performed with expert advice. Anyway, information regarding the traffics and proposed traffic sequences are available on the following repository: https://zenodo.org/records/11072646.

This report, see section 6.2.2, as well as the REAL-LAST report (Vorwagner et al., 2024) provide help about the modelling of the resistance side.

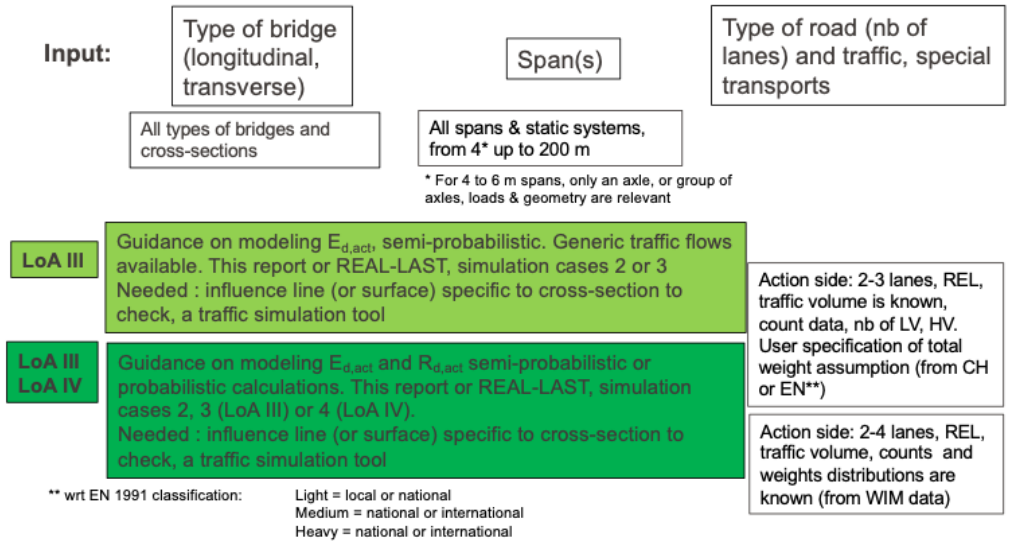

Figure 54: LoA III and IV, workflow for all bridge types

In order to complement the information given in this chapter, Table 8 contains a tentative list presenting the treatment of the uncertainty sources in function of the LoA, for LoA I to III.

Treatment of the uncertainty sources on actions and action effects in function of the LoA

Source	Type	Conservative?	v_{Ed} estimate (%) (+ means conservative)	Treatment							
					LoA I		LoA IIa		LoA IIb		LoA III
WIM data acquisition and processing (accuracy, vehicle classification. quality, timestamp rounded to 0.1s)	Epistemic	The different bias admitted balancing each other out	± 7 %	✓	Partly considered (improved processing)	✓	Partly considered (improved processing)	✓	Partly considered (improved processing)	✓	Synthetic traffic from pruned data [1]
Model and simulation parameters (multiple source)	To study	Unknown	From literature, $\gamma_{sd,Q}$ = 1.1	✓	Upper bound values $\alpha_{act,unique}$	✓	Concerns SIM only, load modelling factor, $\gamma_{sd,Q}$ = 1.1 $\alpha_{i,j,act}$ (i = Q_1,Q_2,q, j = global, local, V, M)	✓	$\gamma_{sd,Q}$ = 1.05 $E_{d,act}$ from NLM1	✓	User defined $E_{d,act}$
Dynamic amplification (DAF, ADR)	Syst. bias	No	-5 %		Ignored, but application limits [2]		Ignored, but application limits [2]	✓	Considered, differentiating between loads; and application limits [2]	✓	User defined
Lateral positioning of the SIA LM1	To study	Yes	Unknown		Ignored		Ignored		Ignored	✓	User defined
Target reliability index β_{annuel} (4.7 vs 4.2)	Syst. bias	Yes	First estimate +2.2 to +7% for 4.7 [3]	✓	Default β_{annuel} = 4.2 Choice [4]	✓	Default β_{annuel} = 4.2 Choice [4]	✓	β_{annuel} = 4.2 [4]	✓	User defined
Variation in target reliability index when permanent loads are taken into account	Systematic	Yes	0% for beam type bridges, L > 40m and all slabs, up to +10% for beam type bridges L ≤ 40m [3]		Ignored [3]		Ignored [3]		Ignored [3]	✓	User defined
Representativity of the WIM stations selected (14 in total)	Systematic	Unknown	Depends on road section: no WIM on cantonal roads, special vehicles weight limits on sections of highway	✓	Considered [5]	✓	Considered [5]	✓	Considered [5]	✓	Select synthetic traffic from pruned data [1]
Evolution of heavy-vehicle traffic trends (in % and volume, split between lanes, REL)	To study in more detail[5,6]	Unknown	Unknown	✓	VBSim. treated as a systematic error	✓	VBSim. syst. error	✓	VBSim, syst. error, option 2 for increase and set loads for lane 3[8]	✓	Select synthetic traffic from pruned data [1]
Evolution of traffic weights	To study	Unknown	Unknown	✓	VBSim. treated as a systematic error[5]	✓	VBSim. treated as a systematic error[5]	✓	VBSim. treated as a systematic error[5,8]	✓	Select synthetic traffic from pruned data [1]
Evolution of traffic control	To study	Yes	Unknown. From literature : more controls = fewer offenders		Partly accounted for via overloaded vehicles, systematic error, bias[5]		Partly accounted for via overloaded vehicles, systematic error, bias[5]		Partly accounted for via overloaded vehicles, systematic error, bias[5]		Partly accounted for via overloaded vehicles, syst. error, bias[5]
Modal evolution (e.g. truck convoys[7], electrification)	To study (with VBSim)	No	Unknown[7]		Application limits[5]		Application limits[5]		Application limits[5]		Partly accounted for in REAL-LAST via +1 or 2t (weight allowance for electric heavy vehicles)
Assumptions on the importance of uncertainties on E_i and R_i	Only action effect side considered	Unknown	Unknown		Fixed sensitivity factor $\alpha_{E,Tra}$ =0.7		Fixed sensitivity factor $\alpha_{E,Tra}$ =0.7	✓	$\alpha_{E,Tra}$ ≤0.7, checked using full probabilistic method [9]	✓	User defined

Notes :

✓ considered

[1] considered up to horizon 2050; for REAL-LAST synthetic traffic considers the evolution of heavy-vehicle traffic trends (in % and volume, weights, split between lanes); for Swiss WIM, see § 6.5, the full-probabilistic analysis results demonstrate that the semi-probabilistic approach yields results between those of the first and second highest WIM stations traffic

[2] For short bridges L< 20m, cases with natural frequency close to a resonance frequency are excluded. There, one needs to consider additional DAF if surface road quality is not "very good", for expansion joint effects, etc.

[3] See (Meystre et al., 2014b). In (Documentation ASTRA 82001, 2025), the semi-prob. approach was applied to traffic loads only. But the ratio of action effects from self-weights & permanent loads over traffic loads was studied in (Mathevet et al., 2024, p. 82001) as well as in Chap. 6, where it is concluded that the inclusion of the permanent loads tends to, logically, diminish the sensitivity factor α_E for the traffic action effect, the results being it indirectly increases structural reliability as this corresponds to a lower influence of traffic variations on safety level

[4] For special bridges (such as arch bridges, cable-stayed bridges) or bridge elements where the consequences of a structural failure would be classified as significant, use $\beta_{annuel} = 4.7$

[5] Processed by pooling data from 14 WIM stations over several years, which increases uncertainty and bias, accepted as representative also for the future, up to horizon 2050

[6] Doubling of heavy goods vehicles percentile was studied in (Documentation ASTRA 82001, 2006). This led to admitting that a margin of +5% was sufficient to consider the potential increase in the presence of heavy vehicles within traffic over 15-20 years (i.e. from 2005 to 2025). Such an increase did not happen, even if the numbers of heavy vehicles increased, their percentiles stayed constant or even decreased (Gotthard), see (Documentation ASTRA 82001, 2025)

[7] For the influence of heavy vehicles convoys, see report AGB 2017/004 (Sjaarda et al., 2022)

[8] Option 2, increased number of heavy vehicles with 100% in lane 1 and 67% in lane 2, as defined in § 4.2.2, which covers also cases with REL as well as construction works situations (i.e. with 2+2 bidirectional traffic on one bridge, with restriction only 2 lanes with heavy traffic). For lane 3, no simulations but distributed load set to same value as in lane 2, i.e. characteristic code value $q_{2k3} = q_{2kr} = 3.00$ kN/m²

[9] See § 6.3.2, NLM1 displays a certain degree of conservatism when comparing it to a full-probabilistic analysis, with yearly $\alpha_{E,Traffic} \leq 0.7$

Table 8: Treatment of the uncertainty sources on action and action effects in function of the LoA

8 Conclusions

The findings demonstrate that the New Load Model 1 (NLM1) represents a significant advancement over LM1, offering a more accurate, reliable, and adaptable approach to bridge traffic load modelling. This paves the way for more efficient resource utilization and improved sustainability in bridge evaluation; it can as well be suitable for design of new bridges while needing further validation and calibration.
More specifically, one can highlight the following:

1. **Calibration process**: key parameters, such as distributed load magnitudes and axle group configurations, are calibrated in an iterative manner starting with one lane and concentrated loads, then group loads, then longer sequences of loads and double-lane traffic simulations and analysis. WIM data provided a robust foundation for ensuring the calibrated model reflects actual traffic conditions. Reflections on practical application and ease of use led to the final proposed NLM1.
2. **Future traffic considerations** despite many similarities, in the study for ASTRA 82001 (Papastergiou et al., 2025), the presence of REL was studied but only to fix a unique actualized factor (step 0). In this research, a different philosophy was followed, namely to cover well the different highway lane patterns with two heavy traffic lanes, the worse being indeed with a REL. Future traffic increase is considered for lanes 1 and 2 with the increase in number of heavy vehicles, and for more lanes by increasing the Uniform Distributed Load (UDL) compared to the current LM1. These cover uncertainties about future heavy traffic developments, such as increase in heavy traffic in different lanes, in traffic congestion, as well as the necessity to include bridges with bidirectional traffic on multiple lanes. The horizon 2050 was set because regular review of traffic development need to be made. They however may lead in certain cases to NLM1 being less favorable than ASTRA 82001. Thus the conformity factors from verification using NLM1 can be lower than those found using ASTRA 82001. If a comparison is to be made between both, it should be done between results from Step 0 with REL ($\alpha_{act,unique}$ = 0.60) and those from the NLM1. Nevertheless, it was not the objective of NLM1 to be more economical (i.e. less conservative) but to reach a more uniform safety level, to be more versatile and thus allow for extrapolation, whereas ASTRA 82001 cannot be applied outside its applicability limits.
3. **Single-lane model results**: for single-lane traffic scenarios, the NLM1 achieves greater uniformity in action effects across different spans. In fact, the NLM1 shows a consistent performance independently of the span while the LM1 tends to be overly conservative for short and long spans (<15m and >30m) while the safety margin largely reduces for medium spans (15-30 m). From 80 m onwards, the LM1 could be considered overly conservative, however longer spans are out of the scope of this research. On the other hand, NLM1 maintains a consistent performance.
4. **Multi-lane model results**: double-lane traffic conditions further demonstrate the higher accuracy of NLM1, as it accounts for the joint presence of heavy vehicles. However, the probabilistic approach ensures that reliability targets are met without excessive overdesign. Key performance indicators, such as uniform reliability indices and reduced variance in action effects across a wide range of bridge types and

spans, underscore the model's effectiveness. NLM1 covers all extreme scenarios of double lane traffic with a large percentage of heavy vehicles on the 2nd lane. It covers cases with REL (i.e. 2 lanes transformed into 3 lanes) as well as construction works situations (i.e. with 2+2 bidirectional traffic on one bridge, with restriction only 2 lanes with heavy traffic). It covers traffic increase up to the horizon 2050, when updating of traffic evolution assumptions need to be made.

5. **Special vehicle scenarios**: the NLM1 better covers scenarios involving special vehicles, such as mobile cranes or overloaded trucks, which are often underrepresented in traditional load models. The flexibility of the NLM1 allows for adjustments based on real-world traffic patterns with, on the 1st lane, its large distributed load over 10 m. It must be emphasized that the distribution of overloaded trucks, having overloaded axles or being above authorized total weights, accounted for corresponds to those of the WIM data. Thus and has a general principle, the number of offenders must be kept to a minimum through more checks, performed by the police or technical equipment.
6. **Consistency between Levels of Approximation (LoA's)**: the same reliability levels are achieved with both semi-probabilistic and full probabilistic analyses, and are consistent across various spans and bridge types. For semi-probabilistic analyses, the main factor in the calibration process is the sensitivity factor of the traffic action effects $\alpha_{\mathrm{E,Traffic}}$. This project demonstrates that a value of $\alpha_{\mathrm{E,Traffic}}$ in accordance with current standards is conservative however acceptable for road bridges and heavy vehicle traffic. Note that the calibration of the load model for the hogging moment region leads in general to the smallest amount of hidden reserves. This becomes evident in the double-lane traffic conditions, where no further reserves can be activated to compensate for the heavy vehicles in the second lane and is especially true in case of small span systems possibly due to the standard way of accounting for transverse distribution of loads.
7. **Full-probabilistic reliability analysis**: an algorithm is proposed to allow calibrating the load model using full-probabilistic analyses. It provides insights into the safety performance of the proposed NLM1, showing that NLM1 results in a more uniformed safety description even when compared to previously developed code load models. Furthermore, it enables further improvements of the load model by investigating the reduction in the scatter of the action effect side model uncertainties. For most of the structures, the value of the sensitivity factor of the traffic action effects $\alpha_{\mathrm{E,Traffic}} = 0.7$ is demonstrated to be overly conservative. The inclusion of the permanent loads tends to, logically, diminish the sensitivity factor $\alpha_{\mathrm{E,Traffic}}$ the result being it indirectly increases structural reliability as this corresponds to a lower influence of traffic variations on safety level. This effect on reliability increases with span length (i.e. $\alpha_{\mathrm{E,Traffic}}$ diminishes with increasing span lengths). On the other hand, the load model has its highest influence on small span bridges due to their high load ratio (traffic induced action effects divided by total action effects) and $\alpha_{\mathrm{E,Traffic}}$ takes higher values for composite bridges compared to the other materials because they are ligher. The over-conservatism in the description of the reliability index allows to propose a model uncertainty factor $\gamma_{sd} = 1.05$ which corresponds to a lower bound of the calculated values. In light of these considerations, there is still room for improvement in the traffic load model and full-probabilistic analyses allow to calibrate the model for specific case studies involving other or special bridge types.

8. **Dynamic and multi-lane effects:** dynamic amplification factors and multi-lane effects are implemented in an explicit manner, significantly improving the accuracy of action effect predictions. As these are included in an original and explicit manner, it is easy to update them as new knowledge becomes available.
9. **Overcoming limitations of current models:** limitations of the LM1 for evaluation, such as its inability to capture complex traffic scenarios or varying bridge geometries, which have shown to be difficult to address using updated adjustment factors, $\alpha_{\mathrm{i,act}}$, are effectively addressed by the NLM1. This ensures that the proposed model is well-suited for evaluations of existing structures and has also the potential to be suitable for the design of new structures.

9 Research needs

During the course of the project, several topics were raised that were outside the scope of research, they are listed below:

- **Further development of NLM1 (LoA IIb):** the goal would be to extend its applicability and draft application rules for other traffic load effects, namely: fatigue, acceleration and braking forces, centrifugal forces and forces acting transversely. A further research topic would be retraining walls with Swiss codes (SIA 261, 2020) and (SIA 269/1, 2011). In fact, the current LM1 might result in overly conservative action effects requiring costly interventions.
- **WIM data:** expand collection to include additional traffic scenarios, underrepresented bridge types, and geographic regions. It is advised to maintain and renew the current network of WIM stations, to adapt it to keep a representative set of stations in Switzerland to allow investigating traffic development in time for specific sites.
- **Future traffic loads and trends**: The impact of emerging technologies, such as electric heavy vehicles, autonomous vehicles and changes in freight patterns (truck sizes, platooning, etc.), requires further investigation since traffic evolution will impact both design of new bridges and examination of existing ones. In fact, current models primarily account for current traffic conditions. Recall that the NLM1 takes into account the use of the REL and an increase in heavy traffic.
- **Dynamic effects**: more refined modeling techniques to better account for dynamic effects and load uncertainties can be developed, especially for unique scenarios like special vehicles, thus reducing conservatism. Indeed, the dynamic amplification factor was based on the results presented by (Vorwagner et al., 2024), based on an extrapolation to a 95 %-quantile of the results. On the contrary, dynamic amplification could be regarded using the ADR concept, that is to consider the probability of both maxima occurring simultaneously, i.e., dynamic interaction and static extreme. This would presumably result in a lower required dynamic amplification factor, given that the 95 %-quantile is relatively high. Nevertheless, this would likely result in intensified computation time, as the traffic action effects need to be multiplied with the dynamic amplification factor in each time step during the overpassing of the axle load sequence.
- **Further development of LoA III and LoA IV:** develop risk-based design methodologies to enable their systematic use for exceptional load cases and structure-specific evaluations.
- **Probabilistic approaches**: The sensitivity factor for traffic action effects in semi-probabilistic approaches, $\alpha_{E,Traffic}$ currently equal to 0.7, should be better investigated and alternative values should be proposed to reduce conservatism mostly in existing bridges. While the proposed model incorporates probabilistic elements, these approaches should be expanded to include a wider range of bridge types, non-linear combination of correlated action effects and bridge collapse (see below). Similarly, incorporating a differentiation between failure modes would enhance reliability computations.
- **Interactions between different action effects:** for example, the Moment-Axial Load interaction in the vicinity of a support, should be investigated. In this work, the

maximal action effects are considered independently from each other, while the effect of the other action effect is neglected. Preliminary investigations indicated that a separation and maximisation of action effects may be the most conservative case. It remains to be scientifically proven it is the case for all geometric configurations and bridge types, and what is the conservatism level. Furthermore, the simplified representation using a resistance and an action part permits only a simplified representation of the limit state function. Accordingly, no interaction between action and resistance side – as considered in a non-linear combination of action effects and plastic bridge collapse – were considered. An approach as proposed in (Rozsas et al., 2014) could be adopted here as well. Similarly, the incorporation of a differentiation between brittle and ductile failure modes could be considered.

- **Code evolution**: In probabilistic reliability analyses, the NLM1 proposed by this work has been compared using the current EN 1992-1-1:2004 to compute the resistance side. However, comparisons should also be performed using the new generation EN 1992-1-1:2023, which was shown to have a lower scatter in the resistance formulas.
- **Simplified tools for practitioners**: developing training programs, user-friendly tools, and workflows to facilitate the application of advanced load modeling techniques in a transparent manner. Allowing semi-probabilistic and probabilistic evaluation in practice is also critical to ensure quick adoption by engineers and policymakers.

Bibliography

Agbelie, B. R. D. K., Labi, S., & Sinha, K. C. (2017). Estimating the marginal costs of bridge damage due to overweight vehicles using a modified equivalent-vehicle methodology and in-service data on life-cycle costs and usage. *Transportation Research Part A: Policy and Practice*, *95*, 275–288. https://doi.org/10.1016/j.tra.2016.11.008
Ammann, A., Lignos, D., & Nussbaumer, A. (2024). *Data set for Swiss bridges* (Rapport projet Bachelor). EPFL - RESSLab.
ASCE. (1981). Recommended Design Loads for Bridges. *ASCE Journal of the Structural Division*, *107*(ST7), 1161–1213.
Baus, R., & Bruls, A. (1981). *Etude du comportement des ponts en acier sous l'action du trafic routier* (MT 145). Centre de recherches scientifiques et techniques de l'industrie des fabrications métalliques.
Bergmeister, K., Fingerloos, F., & Wörner, J.-D. (Eds). (2010). *Beton-Kalender 2010. 2* (99. Jahrgang). Ernst & Sohn.
Bez, R. (1989). *Modélisation des charges dues au trafic routier*. EPFL n° 793.
Bez, R., Cantieni, R., & Jacquemoud, J. (1987). Modeling of highway traffic loads in Switzerland. *IABSE Proceedings*, *11*. https://doi.org/10.5169/SEALS-40377
Boros, V., Novák, B., & Decker, U. (2015). Modifiziertes Verkehrslastmodell für kommunale Brückenbauwerke. *Beton- Und Stahlbetonbau, Wiley / Ernst&Sohn, Berlin*, *110*, 620–627.
Bruls, A., Croce, P., Sanpaolesi, L., & Sedlacek, G. (1996). ENV 1991- Part 3: Traffic loads on bridges Calibration of road load models for road bridges. *IABSE Colloquium*, *74*, 439–453.
Calgaro, J.-A. (1997). *ENV 1991-3 Traffic Loads on Bridges—Road traffic loads—Calibration of the main loading system—Background studies* (ENV 1991-3 Traffic Loads on Bridges) [Final version].
da Silva, L. S., Marques, L., Tankova, T., Rebelo, C., Kuhlmann, U., Kleiner, A., Spiegler, J., Snijder, B., Dekker, R., Dehan, V., Haremza, C., Taras, A., Cajot, L.-G., Vassart, O., & Popa, N. (2016). *SAFEBRICTILE: Standardization of Safety Assessment Procedures across Brittle to Ductile Failure Modes*.
Dawe, P. (2003). *Research perspectives: Traffic loading on highway bridges*. Thomas Telford Ltd. https://trid.trb.org/view/754810
Documentation ASTRA 82001. (2006). *Evaluation de ponts routiers existants avec un modèle de charge de trafic actualisé* [Office fédéral des routes OFROU, Division réseaux routiers (N), Berne]. OFCL vente des publications fédérales, Berne, No d'article : 806.328.f. http://www.astra.admin.ch/dienstleistungen/00129/00183/00518
Documentation ASTRA 82001. (2025). *Évaluation de ponts routiers existants avec un modèle de charge de trafic actualisé* (No. 82001).
EN 1990:2021 Eurocode—Basis of structural and geotechnical design. (2021). CEN/TC 250.
Eurocode 0—Bases de calcul des structures. (2002). CEN/TC 250, Brussels.
Eurocode 1: Actions on structures—Part 2: Traffic loads on bridges. (2003). CEN, Brussels.

European Commission. Joint Research Centre. (2024). *Reliability background of the Eurocodes: Support to the implementation, harmonization and further development of the Eurocodes*.
Feldmann, M., Funke, A., Wolters, K., Taras, A., Steinmetz, R., Kuhlmann, U., & von Arnim. (n.d.). *Zuverlässigkeit von Stahlbauten in Deutschland auf Grundlage der neuen Eurocode-Generation an Beispielen—Evaluation, Bewertung und Empfehlungen* (P 52-5-16.148.1-2079.21).
Fénart, M.-A., Dumont, A.-G., D'Angelo, L., & Nussbaumer, A. (2017). *Simulations de trafic intégrant la détermination d'indices de performance structurale Partie 1: Trafic* (VSS No. 685; Association Suisse Des Professionnels de La Route et Des Transports (VSS), p. 157). https://www.mobilityplatform.ch/fr/research-data-shop/product/685
Fénart, M.-A., Samoili, S., Founta, A., Dumont, A.-G., Maillard, P., Chapoton, J., & Roudy, M. (2016). *Effets sur le trafic de l'utilisation des bandes d'arrêt d'urgence* (VSS FB 1580). ASTRA-AGB.
Fernández Ruiz, M., Vaz Rodrigues, R., & Muttoni, A. (2009). *Dimensionnement et vérification des dalles de roulement des ponts routiers* (Rapport VSS n° 636; p. 65). VSS.
fib CEB. (n.d.). *Model Code 2010 Volume 1 & 2*.
Freundt, U. (2015). *Ermittlung von Prognosefaktoren für Kennwerte der Verkehrsbeanspruchung zum Nachweis der statischen Tragfähigkeit*. Auftraggeber, Bundesanstalt für Wasserbau.
Freundt, U., Böning, S., & Kaschner, R. (2011). Straßenbrücken zwischen aktuellem und zukünftigem Verkehr – Straßenverkehrslasten nach DIN EN 1991-2/NA. *Beton-Und Stahlbetonbau, Wiley / Ersnt&Sohn, Berlin*, *106*(11), 736–746.
Hanley, C., Frangopol, D. M., Kelliher, D., & Pakrashi, V. (2018). Reliability index and parameter importance for bridge traffic loading definition changes. *Proceedings of the Institution of Civil Engineers - Bridge Engineering*, *171*(1), 13–24. https://doi.org/10.1680/jbren.15.00049
Henderson, W. (1954). British Highway Bridge Loading. *ICE Proceedings*, *3*(3), 325–350. https://doi.org/10.1680/ipeds.1954.11638
Hirt, M. A., & Meystre, T. (2006a). *Evaluation de ponts routiers existants avec un modèle de charge de trafic actualisé* (Rapport AGB 594). VSS. https://www.mobilityplatform.ch/fr/
Hirt, M. A., & Meystre, T. (2006b). *Evaluation de ponts routiers existants avec un modèle de charge de trafic actualisé* (Report n° 594). VSS.
Höglund, T. (1997). Shear buckling resistance of Steel and aluminium plate girders. *Thin-Walled Structures*, *29*(1–4), 13–30.
Holický, M., Retief, J. V., & Sýkora, M. (2016). Assessment of model uncertainties for structural resistance. *Probabilistic Engineering Mechanics*, *45*, 188–197. https://doi.org/10.1016/j.probengmech.2015.09.008
Imhof, D., Bailey, S. F., & Hirt, M. A. (2001). *Modèle de Charge (Trafic 40t) pour l'Evaluation des Ponts-routes à deux voies avec Trafic Bidirectionnel* (Mandat de Recherche 81/99 ICOM 444-4). ICOM - EPFL.
Jacinto, L., Pipa, M., Neves, L. A. C., & Santos, L. O. (2012). *SAFEBRICTILE: Standardization of Safety Assessment Procedures across Brittle to Ductile Failure Modes* (pp. 84–89). https://linkinghub.elsevier.com/retrieve/pii/S0950061812003236

JCSS Probabilistic Model Code—Part 3: Material Properties. (2000). Joint commitee on Structural Safety.
Kalin, J., Žnidarič, A., Anžlin, A., & Kreslin, M. (2022). Measurements of bridge dynamic amplification factor using bridge weigh-in-motion data. *Structure and Infrastructure Engineering*, *18*(8), 1164–1176. https://doi.org/10.1080/15732479.2021.1887291
Kulicki, J. M., & Mertz, D. R. (2006). Evolution of Vehicular Live Load Models During the Interstate Design Era and Beyond. In *50 Years of Interstate Structures: Past, Present, and Future* (p. 26). Transportation Research Board. https://www.trb.org
Ludescher, H., & Brühwiler, E. (2009). Dynamic Amplification of Traffic Loads on Road Bridges. *Structural Engineering International*, *19*(2), 190–197. https://doi.org/10.2749/101686609788220231
Malja, X. (2024). *Influence of model uncertainty and long term deformations in action effects calculation in reinforced concrete structures*. EPFL.
Malja, X., Nussbaumer, A., & Muttoni, A. (2024). Model uncertainties in action effects and load bearing capacity calculation in statically indeterminate reinforced concrete structures. *Structural Concrete*, *25*(6), 4219–4239.
Mathevet, L., Vaccari, C., & Nussbaumer, A. (2024). *Annexes à la Documentation ASTRA 82001* (Annexes ASTRA 82001). EPFL - RESSLab.
Meystre, T., Stucki, D., & Lebet, J.-P. (2014a). *Charges de trafic actualisées pour les dalles de roulement en béton des ponts existants* (AGB 664 (VSS 21531 ?); VSS). OFROU.
Meystre, T., Stucki, D., & Lebet, J.-P. (2014b). *Charges de trafic actualisées pour les dalles de roulement en béton des ponts existants* (AGB 664; VSS). OFROU. https://www.mobilityplatform.ch/fr/
Miglietta, P., & Nussbaumer, A. (2026a). *Benchmark cases of WIM data for traffic simulations—Appendix to OFROU report 6*. INFOSCIENCE.
Miglietta, P., & Nussbaumer, A. (2026b). *Benchmark cases of WIM data for traffic simulations—Appendix to OFROU report 6*.
Muttoni, A., & Ruiz, M. F. (2012). Levels-of-Approximation Approach in Codes of Practice. *Structural Engineering International*, *22*(2), 190–194. https://doi.org/10.2749/101686612X13291382990688
Nadolski, V., & Sykora, M. (2014). Uncertainty in Resistance Models for Steel Members. *Transactions of the VŠB – Technical University of Ostrava, Civil Engineering Series.*, *14*(2), 26–37. https://doi.org/10.2478/tvsb-2014-0028
Nascimento, S., & Pedro, J. O. (2019). SHEAR STRENGTH OF STEEL-CONCRETE COMPOSITE PLATE GIRDERS – A REVIEW. *Ce/Papers*, *3*(5–6), 181–192. https://doi.org/10.1002/cepa.1193
Novak, B., & Lippert, P. (2015). Einwirkungen auf Brücken nach den Eurocodes. In *Betonkalender 2015* (pp. 585–678). Wiley / Ernst&Sohn.
Nowak, A. S., & Hong, Y. (1991). Bridge Live-Load Models. *Journal of Structural Engineering*, *117*(9), 2757–2767. https://doi.org/10.1061/(ASCE)0733-9445(1991)117:9(2757)
Nowak, A. S., & Szerszen, M. M. (1998). *Bridge load and resistance models*. *Vol. 20*(No. 11), 985–990.
O'Brien, E. J., Cantero, D., Enright, B., & González, A. (2010). Characteristic Dynamic Increment for extreme traffic loading events on short and medium span highway

bridges. *Engineering Structures*, *32*(12), 3827–3835. https://doi.org/10.1016/j.engstruct.2010.08.018
O'Brien, E., Nowak, A., & Caprani, C. (2021). *Bridge Traffic Loading: From Research to Practice* (1st edn). CRC Press. https://doi.org/10.1201/9780429318849
O'Connor, A., Jacob, B., O'Brien, E., & Prat, M. (2001). Report of Current Studies Performed on Normal Load Model of EC1: Part 2. Traffic Loads on Bridges. *Revue Française de Génie Civil*, *5*(4), 411–433. https://doi.org/10.1080/12795119.2001.9692315
OFROU. (2023). *Rapport sur l'état du réseau des routes nationales. Etat au 31.12.2022*. Office fédéral des routes (OFROU) Pulverstrasse 13, Ittigen CH-3003 Berne. https://www.astra.admin.ch/astra/fr/home/themes/routes-nationales/reseau/rapport-d-etat-des-routes-nationales.html
Papastergiou, D., Nussbaumer, A., Sjaarda, M. J., Mathevet, L., Miglietta, P., Brühwiler, E., & Bertola, N. (2025). *Documentation. Évaluation de ponts routiers existants avec un modèle de charge de trafic actualisé* (ASTRA 82001. Édition 2025 V2.01). Office fédéral des routes OFROU. https://www.astra.admin.ch/astra/fr/home/services/dokumente-nationalstrassen/standards-pour-les-routes-nationales/2--ouvrages-d-art0.html
prEN_1991-2: Traffic loads on bridges and other civil engineering works. (2020, August 12). CEN-TC250-SC1.
Rozsas, A., Kovacs, N., & Badari, B. (2014, September). *On the reliability of steel-concrete composite bridges—Investigation of Post-elastic Ultimate Limit States*. Eurosteel 2014.
Rymsza, J. (2016). Proposal to Change the Design Load in the Eurocode 1 Based on Loads from Vehicles with a Mass of 60 Tonnes. *Transportation Research Procedia, Transport Research Arena TRA2016*, *14*, 4020–4029. https://doi.org/10.1016/j.trpro.2016.05.499
Sedlacek, G., & et al. (2008). *Background document to EN 1991—Part 2—Traffic loads for road bridges—And consequences for the design*. JRC scientific reports.
Sedlacek, G., Merzenich, G., Paschen, M., Bruls, A., Sanpaolesi, L., Croce, P., Calgaro, J. A., Pratt, M., Jacob, B., Leendertz, M., de Boer, V., Vrouwenfelder, A., & Hanswille, G. (2008). *Background document to EN 1991- Part 2—Traffic loads for road bridges—And consequences for the design* [EN 1991-2]. JRC.
SIA. (1994). *Tragwerksnormen 1892-1956. Sammelband*. SIA, Zurich.
SIA. (2020, March). *SIA 261/1: 2020 Einwirkungen auf Tragwerke—Ergänzende Festlegungen*. SIA, Zurich.
SIA 160—Actions sur les structures porteuses. (1989). SIA, Zurich.
SIA 261. (2020). *SIA 261: 2020 Actions sur les structures porteuses*. SIA, Zurich.
SIA 269/1. (2011). *SIA 269/1: 2011 Existing structures—Actions*. SIA, Zurich.
Sjaarda, M., Nussbaumer, A., Breveglieri, M., & Feltrin, G. (2022). *Impact of heavy vehicle platooning on Swiss bridges* (VSS FB 713; p. 157). ASTRA-AGB.
Skokandić, D., & et al. (2020). Modelling of traffic load effects in the assessment of existing road bridges. *Journal of the Croatian Association of Civil Engineers*, *71*(12), 1153–1165. https://doi.org/10.14256/JCE.2609.2019
SOFiSTiK AG. (2023). *SOFiSTiK Manual*.
Soriano, M., Casas, J. R., & Ghosn, M. (2017). Simplified probabilistic model for maximum traffic load from weigh-in-motion data. *Structure and Infrastructure Engineering*, *13*(4), 454–467. https://doi.org/10.1080/15732479.2016.1164728

Sykora, M., Krejsa, J., Mlcoch, J., Prieto, M., & Tanner, P. (2018). Uncertainty in shear resistance models of reinforced concrete beams according to *fib* MC2010. *Structural Concrete*, *19*(1), 284–295. https://doi.org/10.1002/suco.201700169
Vogel, T., Zwicky, D., Joray, D., Diggelmann, M., & Høj, N. P. (2009). *Tragsicherheit der bestehenden Kunstbauten (Sécurité structurale des ouvrages d'art existants)* (AGB 2005/107 No. 623; p. 279). ASTRA - Bundesamt für Strassen, Bern, Schweiz.
Vorwagner, A., Ralbovsky, M., Freundt, U., Kaschner, R., Castillo Chang, O. B., Taras, A., Martinolli, S., Vill, M., Nussbaumer, A., & Sjaarda, M. (2024). *Reale Verkehrslastmodelle von Brückenbauwerken REAL-LAST* [DACH]. D-A-CH Kooperation. Bundesministerium für Digitales und Verkehr, Deutschland; Bundesministerium für Klimaschutz, Österreich; Bundesamt für Straßen, Schweiz. OneDrive-epfl.ch/REAL-LAST_partiel/Final report (de and en)
Waag, M. (1994). *Beanspruchung von Brückenbauten infolge Strassenlasten—Vergleich der Normen SIA 160 von 1956, 1970 und 1989*. Bundesamt für Strassenbau.
Wisniewski, D., Casas, J. R., Henriques, A. A., & Cruz, P. J. S. (2009). Probability-Based Assessment of Existing Concrete Bridges—Stochastic Resistance Models and Applications. *Structural Engineering International*, *19*(2), 203–210. https://doi.org/10.2749/101686609788220268
Yu, Q., Valeri, P., Fernández Ruiz, M., & Muttoni, A. (2021). A consistent safety format and design approach for brittle systems and application to Textile Reinforced Concrete structures. *Engineering Structures*, *249*, 113306. https://doi.org/10.1016/j.engstruct.2021.113306
Zingoni, A. (with International conference on structural engineering, mechanics and computation). (2013). *Research and applications in structural engineering, mechanics and computation: Proceedings of the Fifth international conference on structural engineering, mechanics and computation (SEMC 2013), September 2-4, 2013, Cape Town, South Africa*. CRC press.

10 Appendix A: load model code development

10.1 Introduction

The bases of development of the LM1 of EN 1991-2 (incl. the development of the 2nd generation, (*CEN-TC250-SC1 N1569*, 2020)) and SIA 261 (SIA, 2020) will be reviewed from the 1970s to today. The evolution in the concept of traffic load modelling, focusing on vertical loads and ULS verifications, will point out the main changes and background. Specific issues, such as the treatment of dynamic effects, will be given specific attention.

10.2 Design of new structures

10.2.1 Traffic load models on road bridges in the Eurocode

To begin this section, the four separate traffic load models (LM's) on bridges introduced by the Eurocodes in 2003 are listed herein. Each of the LM is dedicated to model certain action effects which result from the vertical load being applied to bridges. These models are valid for spans up to 200 m. For the derivation of these load models, data from traffic measured on several European highways were used. They are listed below:

a) Load Model 1 (LM1), presented in § 1.1.1, corresponds to what has been referred to as routes with "normal loading", for all spans and a carriageway width of up to 42 m (Hanley et al., 2018), but may not be predominant for short spans less than 7 m. LM1 departed from previous representations of normal traffic loading by eliminating country-specific features such as the uniform distributed load (UDL) as a function of span and invariant knife-edge load (across the lane width, thus in kN/m, to produce the worst shear force effect), and replacing them with a series of constant UDL, invariant with span length, in adjacent lanes and a tandem axle system of point loads.
b) LM2 represents the application of a single axle load applied on specific tyre contact areas which covers the dynamic effects of the normal traffic on short structural members. It may be predominant in the span range 3 to 7 m.
c) LM3 is a set of assemblies of axle loads representing special vehicles (e.g. for industrial transport) which can travel on routes permitted for abnormal loads. It is intended for general and local verifications.
d) LM4 represents a crowd loading, intended only for general verifications, to be used only for some transient design situations.

Differences in traffic in terms of composition, density and conditions should be taken into account through the use of adapted load models thru the proper choice of the adjustment factors α (for LM1) and β (for LM2).

These models define both design and representative values, associated with road traffic, which include dynamic effects, centrifugal, braking and acceleration actions to be

used for the design of new bridges or, by modifying adjustment factors, to be employed for the examination of existing bridges. Due to the fact that these traffic records are more than 30 years old, several authors reassessed these load models based on updated traffic monitoring data, and they concluded that these models comply with requirements of modern traffic (O'Connor et al., 2001; Rymsza, 2016).

For finding the extreme values of traffic load effects, in particular for LM1, the following points can be highlighted:

- For the axle load, it was based on the frequency distribution of the measurements of axle loads (basis Rheden) of axle n° 2 of articulated vehicles type 112 (symbolic: o--o----oo);
- The observed loads were applied to various theoretical influence lines and surfaces, varying internal force, span (ranging from 5 to 200 m), that is:
  - longitudinal and transverse bending moment,
  - the torsion in beams,
  - the normal and shear forces in beams,
  - the concentrated efforts in transverse or cross beams;
- The simulations include dynamic effects (discussed in more detail herein, see 10.2.3): for global effects and also a complementary amplification factor related to the local effects (expansion joints). This affects the value of the axle load. The results varied across different locations: 245 kN, 279 kN, 276 kN, 302 kN. They were multiplied with dynamic amplification factor (DAF) due to road roughness between 1.0 and 1.14 to get "**average characteristic axle load**", with a return period of 1000 years, from dynamic simulations of the flowing traffic at the points of measurements. This led to fixing the characteristic axle load to 300 kN in LM1. Since the characteristic value of the axle load in LM1 is about 2.5 times higher than the legally permitted load, it is a result of systematic overloading (Sedlacek & al., 2008);
- For short spans, as LM1 gives too low load effects. Therefore, LM2, comprising single axle with a load of 400 kN, was introduced. It corresponds to the heaviest extrapolated axle load (250 kN) multiplied by a dynamic factor 1.6 = 1.7/1.1 according to (Bruls et al., 1996). To prevent the formation of local weak points, LM2 is considered alone everywhere on the carriageway;
- Statistically, the combination of both factors (return period R and probability p) can be replaced by a single one which is the mean return period of a certain value, i.e. T = R/p = 50 years/ 0.05 = 1000 years. As noticed by (Calgaro, 1997), this notion has no physical meaning for a variable action: it is only an invariant and helpful factor to relate a probability to a reference period. Note also that, in terms of load effect, the difference between the return period values of 1000 years and of 200 years is small because the distribution of the traffic utmost effects is weakly scattered;
- The calibration outcomes were:
  - 2 optimal solutions found, the 1st had one concentrated axle load P_1 = 400kN for a loaded length L > 3 m, and UDL function of the span length, it was disregarded because the definition of the verification rules concerning local effects with one single concentrated load was not realistic,
  - The 2nd optimal solution had a uniform distributed load (UDL) in function of span length and a tandem load with axle spacing 1 m; this model was simplified/adapted to the LM1 known today,

- Out of all the influence lines computed, two are determining: M_0, the bending moment at mid span of a simple supported beam and M_2, the bending moment on the central support of a beam with two spans.

The calibration of the LM1 followed the principle that it includes dynamic amplification, with simultaneous concentrated and distributed loads (to have a model suitable simultaneously for the general verifications and the local verifications). The model found this way has a UDL which is function of the loaded length. For the final load model and to make it independent upon loaded length, the precision of "target" reliability values for the actions has been slightly decreased to get very simple model. This was done by comparing the proposed target values on graphs giving a fictitious load Q' in function of the span length L: $Q' = k.M/L$ or $Q' = k.V$, where M is a bending moment, V is a shear force, and k is a factor depending on the type of load effect. On such a graph, a load effect produced by a constant load is represented by a horizontal straight line (i.e. the value at the origin) and a load effect produced by a constant uniform distributed load is represented by a sloping straight line. Figure 55 is an adapted reproduction of the figure from the background document published by (Sedlacek & al., 2008) (fig. 3-25 from (Sedlacek & al., 2008)) for the case with two lanes of traffic, while Figure 56 reproduces the case the case with one traffic lane.

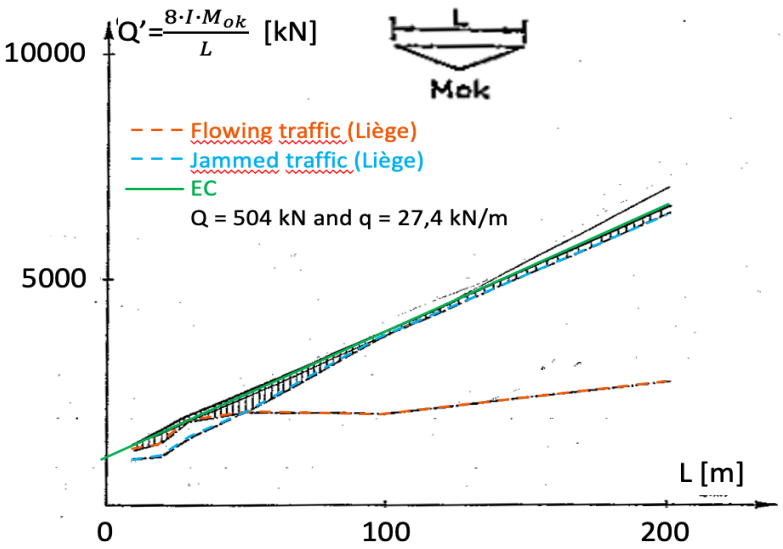

Figure 55: Target values for moment M0 - 2 lanes, adapted from (Sedlacek & al., 2008)

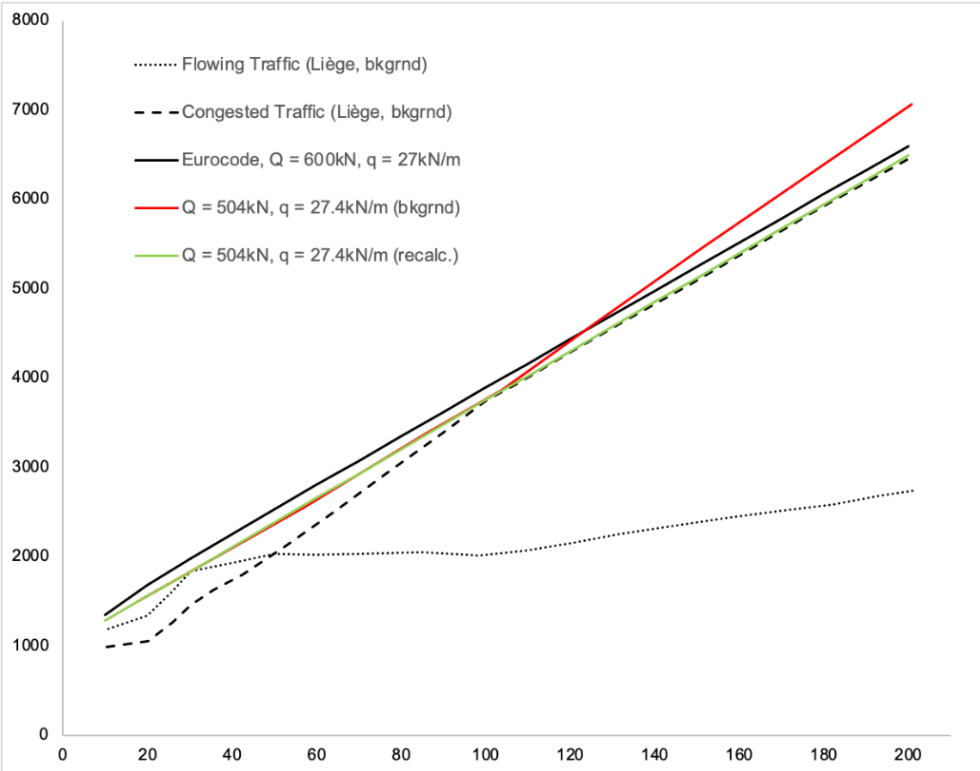

Figure 56: Target values for moment M0 - 1 lane, adapted from (Sedlacek & al., 2008)

The resulting model is the following (characteristic values for ULS):

- Lane 1, q = 27 kN/m, Q1 & Q2 = 300 kN ;
- Lane 2, q = 9 kN/m, Q1 & Q2 = 150 kN ;
- Lane 3 & 4, q = 7.5 kN/m, Q1 & Q2 = 100 kN.

The min. intensity of UDL = 2.5 kN/m² (i.e. 7.5 kN/m on a 3 m wide lane) stems out from existing national codes. One should mention that the second lane did not change much the results of the model calibration on the main lane.

Notice that the (Sedlacek & al., 2008) background also defines fatigue load models, but this is outside of the scope of this study.

The definition of representative values of loads is summarized as, considering a good pavement roughness:

- Characteristic values for ULS, as detailed before;
- The infrequent values, with a return period of one year, considering reduced dynamic effects and only a 1 % of the total traffic volume assumed to run in jam;
- The frequent values, return period of one week and free flowing traffic;
- The quasi-permanent values = 0 for traffic.

Up to this point, the partial load factors or adjustment factors have not been mentioned. The link between the representative values, the target reliability index, the partial factors and adjustment factors allow each country to achieve a level of safety similar to previous national codes. As for the load factor value, γ_F = 1.35, its value was recommended following reliability studies that led to fixing the annual target reliability index

for ULS to β_{tgt} = 6.00 as it corresponded to the minimum index found when recomputing existing bridges (Bruls et al., 1996). Notice that in the table C.3 of the current EN1990:2023, Annex C, the default value ranges between 4.2 and 5.2, depending on the consequence class.

Notice that, even if outside the scope of this study, an "impact factor" for fatigue design φ_{fat} has also been derived, see (Sedlacek & al., 2008) and (Bruls et al., 1996). It is defined as the ratio between the fatigue damage induced by the dynamic stress history and the fatigue damage induced by the static stress history and has more significance for railway bridges.

In European countries, the adjustment factors α_i for 2 or more lanes were adapted upward, when compared to the base values of EN 1991-2, see e.g. (Freundt et al., 2011) (Novak & Lippert, 2015) and Adjustment factors for design of new bridges in some EU countries, adapted from (Skokandić & et al., 2020). Adaptations were also proposed to account for the specific situation encountered in communal roads (Boros et al., 2015). Common to these studies is the inclusion of current data and models for traffic development as well as, once again, the lack of differentiation made with respect to static systems (with only single and symmetric double span longitudinal systems considered) and structural types used for calibrating the adjustment factors. The adjustments between SIA and EN are also shown Figure 57.

Adjustment factors for design of new bridges in some EU countries, adapted from (Skokandić & et al., 2020)

EU member country	Adjustment factor				
	α_{Qi}	α_{Qi}	α_{qi}	α_{qi}	α_{qi}
	$i = 1$	$i > 1$	$i = 1$	$i = 2$	$i > 2$
Austria	1.00	1.00	1.00	1.00	1.00
Croatia (and most EU countries)	1.00	1.00	1.00	1.00	1.00
Denmark	1.00	1.00	0.67	1.00	1.00
France	1.00	1.00	1.00	1.20	1.20
Germany	1.00	1.00	1.33	2.40	1.20
Netherlands	1.00	1.00	1.15	1.40	1.40
Switzerland*	0.90	0.90	0.90	0.90	0.90
UK	1.00	1.00	0.61	2.20	2.20

* load factor value γ_F = 1.50 (instead of γ_F = 1.35)

Table 9: Adjustment factors for design of new bridges in some EU countries, adapted from (Skokandić & et al., 2020)

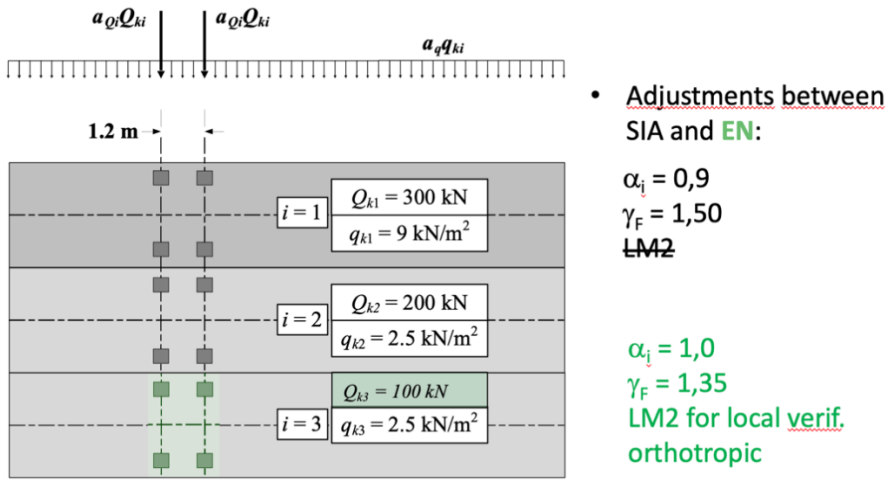

Figure 57: Load model 1, highlighting the differences between EN and SIA (from EN 1991-2: 2004)

10.2.2 Traffic loads on bridges, Switzerland

In Switzerland, the traffic loads to be assumed for designing new road bridges have been defined in ordinances and standards since 1892 (SIA, 1994) and were updated regularly to account for the evolution of traffic and vehicles. In the first provisions, the loads were defined to describe actual vehicles as for instance heavily loaded wagons (1892 and 1913), a steamroller (1913 and 1935) or a combination of trucks (1935). In the latter case, the effect of two trucks were defined with realistic weights and locations, whereas before and after the two trucks, the traffic actions of other vehicles were simplified with a uniformly distributed load with a magnitude decreasing with the span (q = 500 kg/m² - 2·ℓ , accounting for the fact that the probability of having high loads diminishes with the loaded area).

It is only with the code SIA 160:1956 that the loads of actual vehicles have been simplified and replaced by the combination of a uniformly distributed load and the effect of a single axle, with the aim of accounting for the influence of the size of the loaded area on the load magnitude. To verify local effects, an additional loading model consisting of three axles without concurrent traffic loads had to be verified. This new approach was introduced in 1956 to simplify the calculations and to account for the increased variety of heavy vehicles. The same principle (combination of a uniformly distributed load and axles acting on the same area) has been adopted for SIA 160:1968.

For the revision of the SIA in the 1980's, the original research leading to the traffic load model of SIA 160 (SIA 160, 1989) was (Bez et al., 1987); the proposed model combines three load types (see Figure 58):

1. Concentrated effect of an isolated truck located anywhere on the roadway or sidewalk;
2. A lane load placed at the most critical location on the roadway (determined using a stationary lane load but representing a line of slowly moving trucks);
3. A surface load assumed to be uniform over the entire remaining width of the roadway (representing a stationary lane load consisting of a mixture of trucks

and cars, or the so-called accompanying loads). Its value was determined in function of the number of lanes, for a length of 100 m.

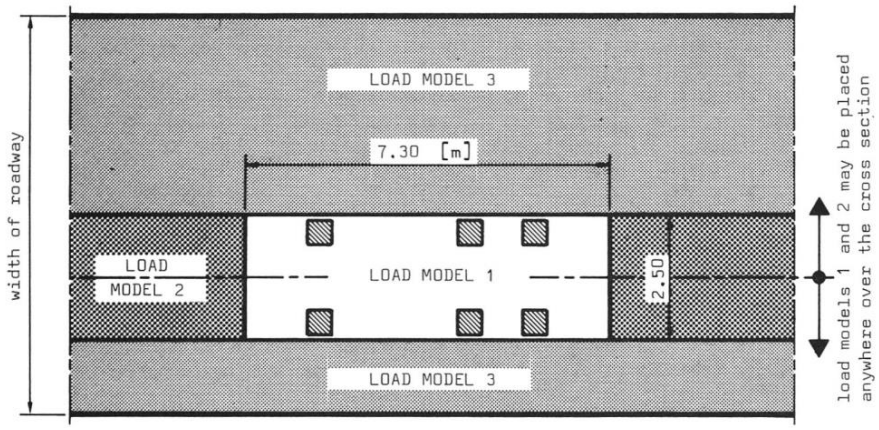

Figure 58: Load model 1, highlighting the differences between EN and SIA (Bez et al., 1987)

As one can notice, this load model differs from the one, more generic and slightly simpler for calculations adopted by the standard: it has a 3-axle truck instead of tandem axles, there is no distributed load where the truck is placed, the unique lane is 2.50 m wide instead of multiple lanes 3 m wide (with tandem axles as well). The final version of the SIA code used only the first loading model (distributed load + two axles per lane).

Current provisions (SIA 261:2020, and previously SIA 262:2003) are directly derived from the Eurocode provisions (EN 1991-2:2002). In current Swiss provisions, the adjustment factors a_{Qi} and a_{qi} (which are nationally determined parameters in EN 1991-2:2002) have been calibrated in order to obtain the same magnitude of loads as in SIA 160:1989 ($\alpha_Q = 0.9 = 1.5{\cdot}1.8{\cdot}4{\cdot}75/(1.5{\cdot}2{\cdot}300)$ and $\alpha_q = 0.9$ which is a compromise between $\alpha_{q1}=0.56=1.5{\cdot}5/(1.5{\cdot}9)$ and $\alpha_{q2}= 1.40 = 1.5{\cdot}3.5/(1.5{\cdot}2.5)$). These values are also in agreement with the result of the work by (Imhof, D., S. F. Bailey, and M. A. Hirt. 2001. *Modèle de Charge (Trafic 40t) pour l'Evaluation des Ponts-routes à deux voies avec Trafic Bidirectionnel*. Mandat de recherche 81/99. Lausanne: ICOM – EPFL) conducted to account for the increase of the allowed traffic loads (28t → 40t). The fact that the European Standard of 2003 and the Swiss code of 1989 have a very similar approach is not surprising, since they have been developed in parallel with cross-collaboration.

10.2.3 Dynamic factors

In the former Swiss codes, the dynamic effect of road traffic on bridges has been accounted for explicitly (SIA codes from 1935, 1956, 1968 and 1989) with a dynamic factor to be applied to the traffic loads. This dynamic factor was varying between 1.30 and 1.11 for spans between 10 and 80 m for all traffic loads in older versions, with a fixed value of 1.80 to be applied only on the concentrated loads in the code of 1989. Since 2003, the dynamic factor is considered implicitly in the characteristic values of the traffic loads.

Regarding the Eurocodes, the basis for the assumed factors is described in the background published by (Sedlacek & al., 2008). Note that the values implicitly used in the SIA are justified also by the equivalence made between the SIA and Eurocode load

levels. Within the Eurocode development, two types of simulations of action effects were made: a static modelling (with dynamic amplification factor, DAF) and dynamic simulations, with vehicle-bridge interaction considered. Different simulations were made, with one lorry or several on one lane, then with more realistic flowing and congested traffic conditions and more lanes as well. Of course, DAF > 1 (or φ_{cal}) is purely conventional because the static and dynamic x-fractiles don't correspond necessarily to the same load case. DAF up to 1.7 were found for very short spans (up to 5 m) and flowing traffic on one slow lane (i.e. highway with 2 lanes, with only one with heavy traffic, which can be considered the usual case). The DAF was, logically found to be larger. It was also found that the DAF is larger for moments compared to shear, see for example Figure 59. In case of congested traffic, the DAF found were always lower in comparison and below 1.15, with little influence of the pavement quality. Logically, the DAF decreased in the case of a four lanes roadway as compared to the two lanes. In those cases, it is equal to 1.10 independently from span. The effects of the above on the design value of the vertical axle load, which governs when verifying for local effects remains an open question. Today, the above values are considered to be too high (Documentation ASTRA 82001, 2025)(REAL-LAST, 2024). One shall notice that most investigations on the dynamic effects on bridges have been conducted assuming a linear behaviour of the structure or based on measurements under service conditions. For non-linear behaviour (and particularly for ductile failure modes), this assumption is potentially too conservative. This issue deserves to be investigated more in detail to remove unnecessary conservativeness.

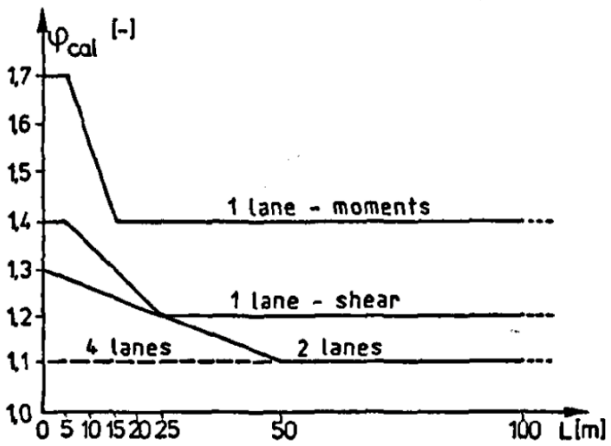

Figure 59: Dynamic amplification factors, from Eurocode background (Sedlacek & al., 2008)

For the examination of existing structures, an explicit consideration of the dynamic actions would be probably more consistent with an attempt to describe more realistic load models. Currently, with respect to the loads to be used for the examination of existing bridges (SIA 269/1:2011), the calibration has been conducted on the basis of the work by (Ludescher & Brühwiler, 2009) and leads to lower amplified action effect values. The recent Documentation ASTRA 82001 (Documentation ASTRA 82001, 2025) justifies even lower values.

In this project, the recent results obtained within the REAL-LAST project (Vorwagner et al., 2024) are used to define the dynamic factor at ULS, φ_{ULS}.

The equation describing the results has been used, with a capped value at 15m, that is:

$$\varphi_{ULS.cap} = 1 + f_{95\%} \cdot \left(\frac{Q_{total}}{Q_{ref}} \right)^{-p} \cdot \left(\frac{L_{cap}}{L_{ref}} \right)^{-r} \qquad L_{cap} = \max(L, 15\text{m}) \qquad (21)$$

Where the values for $f_{95\%}$, Q_{ref} , L_{ref} , p and r are function of the internal force considered and which values be found in the REAL-LAST report, section 3.4 (Vorwagner et al., 2024).

11 Appendix B: Comparative study on the possible configurations for new load model

11.1 Action effect data analysis of selected cases (single lane), leading to possible configurations of normative load model

When studying the axles loads, their local action effects, one can either use:

- The strip analysis, the WIM data circulating on a rectangular influence line of varying length, see § 4.2.3 and Figure 21;
- Or a direct representation of, for example, the type of vehicles with the tandem axles responsible for the block maxima, as shown in Figure 60, or the histograms of shear weekly block maxima data in Figure 61.

Each figure leads to different observations. From Figure 21, it is seen that tandem axles (more precisely, 2 axles out of a group) control the maximum total load when their spacing ranges typically between 1.4 and 2.4 m; also Class+ lead to higher values (approx. 5% higher than Class).

This is confirmed by the pie charts from Figure 60, where one sees that the dominating trucks are type 22 (belonging to Class), which are construction works trucks and then, for Class+, crane trucks, 60 and 72 t. This also validates once more the choice of using weekly block maxima as the best compromise to have enough blocks and properly include the heaviest action effects in the statistical analysis. All the same, the longer the observation block, the more types 22 and crane trucks are dominating. Finally, in Figure 61, the order of magnitude of the upper quantiles (tail) are seen to be indeed coherent, shear values above a) 350 kN and b) 600 kN, to those given for the total load for tandem and tridem axles in Figure 21. However, for the percentages of trucks in the tail for Class+, the determining types are a bit different, they are of the types 60t crane, 113, and 23, for two or may be three axles (for 4m), and essentially 60t and 72t cranes for 10m. Similar conclusions were reached, on older and less complete WIM datasets, in the previous studies (Hirt & Meystre, 2006b).

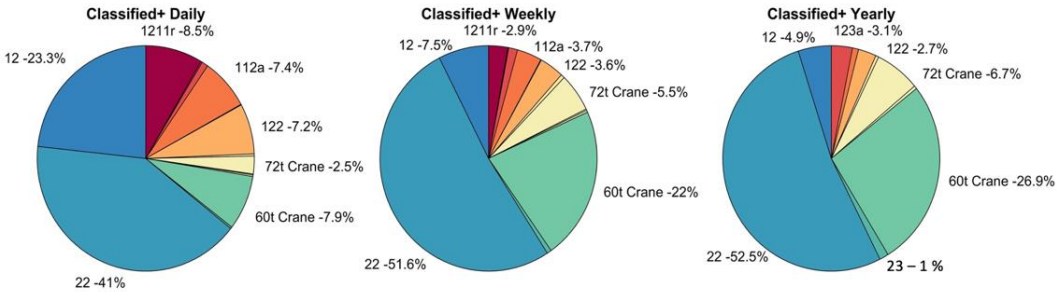

Figure 60: Pie charts showing the truck types responsible for the tandem axles block maxima and the influence of the observation time for each block (single lane analysis)

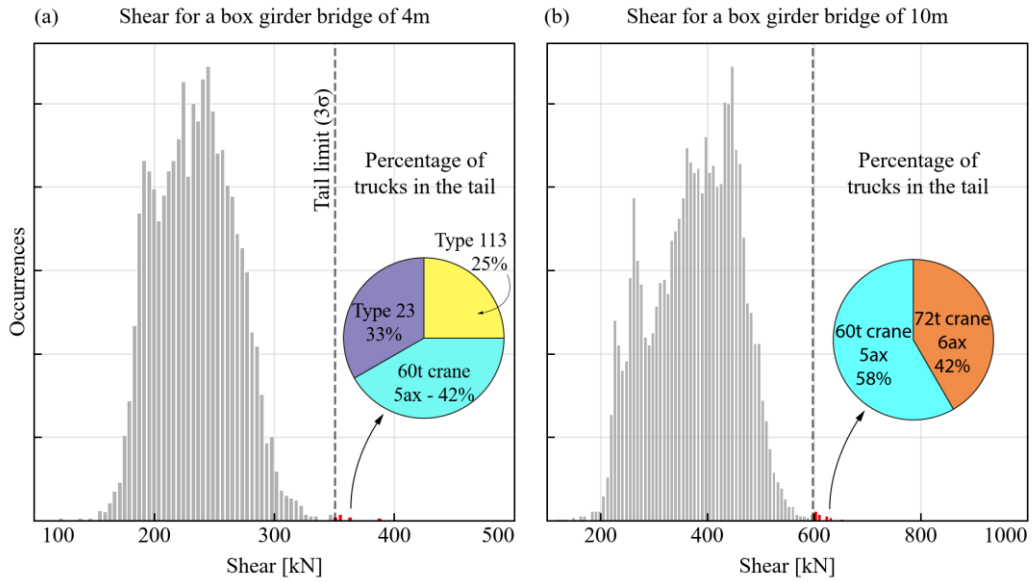

Figure 61: Histograms of shear weekly bloc maxima for a box-girder bridge of (a) 4m and (b) 10m considering a single lane; pie charts showing vehicles distribution in the tail values further than 3 standard deviations (3σ)

Figure 63 and Figure 64 help understanding the link between actions (axle loads) and action effects (shear and bending moment). Indeed one can notice that the maximum axle load is above 200kN and, on the overlapping plots of all cases, that apart from the dominating axle, there is a concentration of several axles over a length of around 8m. This gives an indication that the load model should contain:

- one or more axles loads,
- a UDL with a high value over a limited length.

To this, one shall most likely add a second UDL for longer influence lines. This led to the load model variations 2 to 4 presented in Figure 62 (same as Figure 23 in the main document).

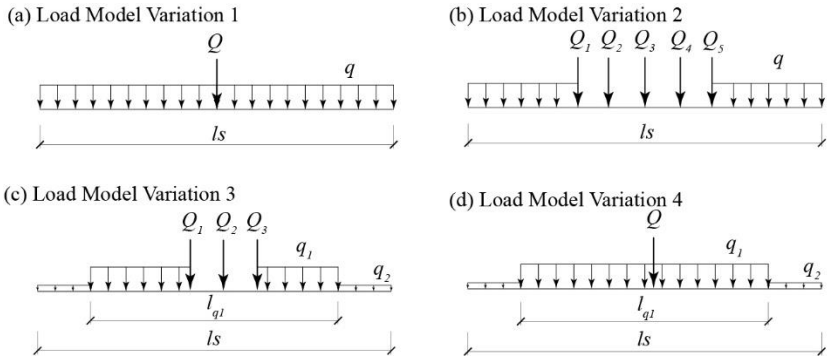

Figure 62: Different variations of load models for fist lane (ls is the bridge length, l_{q1} is the length of UDL 1)

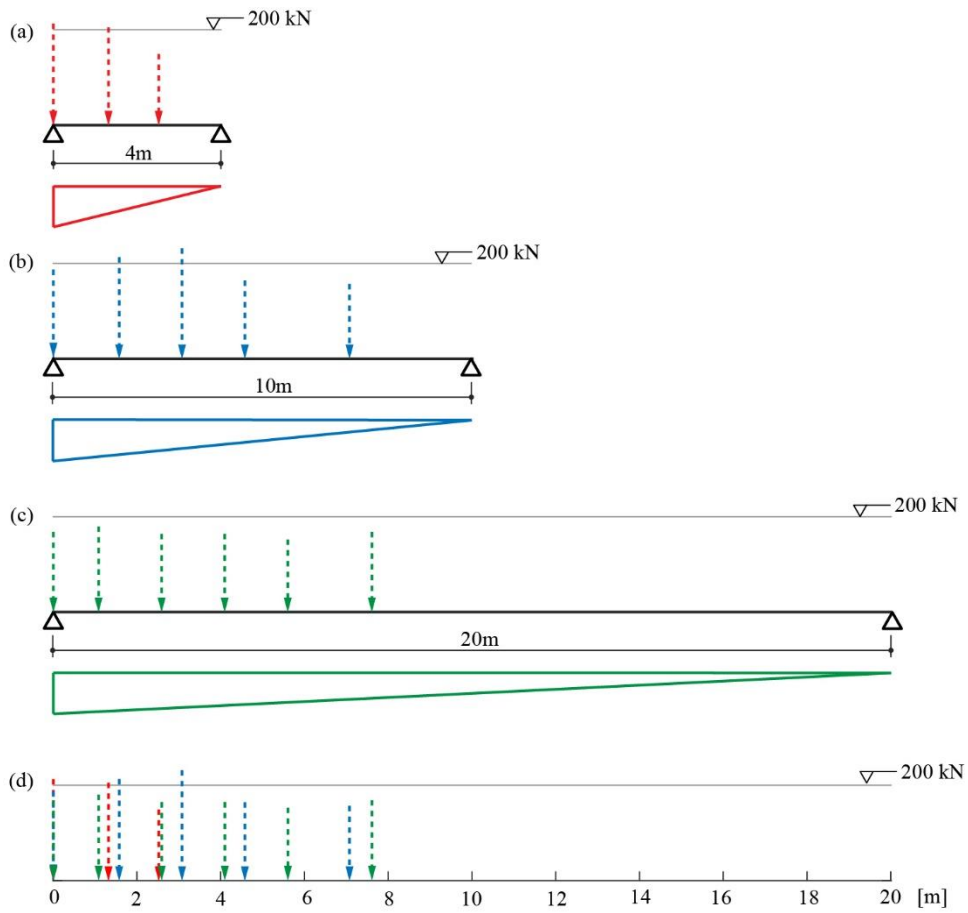

Figure 63: Axle loads for maximum shear cases in WIM analysis of box girder bridges with spans of (a) 4m, (b) 10m, (c) 20m and (d) overlapping plots of all cases

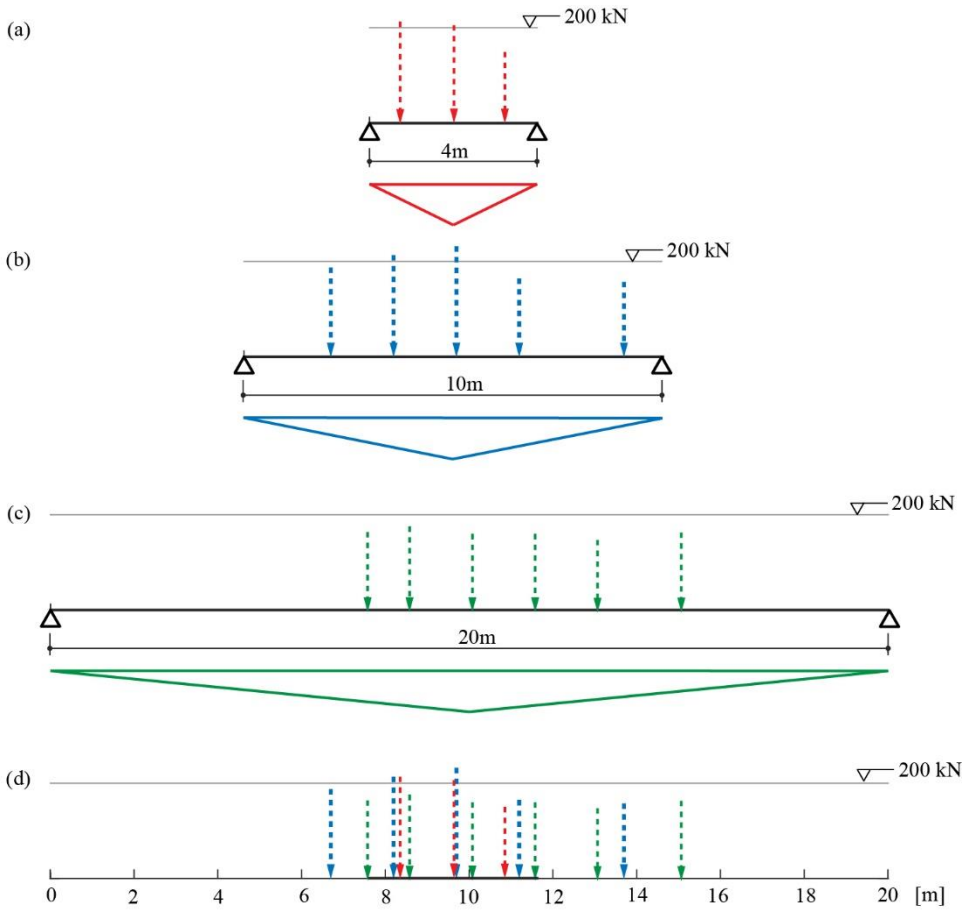

Figure 64: Axle loads for maximum bending in WIM analysis of box girder bridges with spans of (a) 4m, (b) 10m, (c) 20m and (d) overlapping plots of all cases

11.2 Action effect data analysis of selected cases (double lane)

First, Figure 65 shows the results of an earlier strip analysis (Hirt & Meystre, 2006b) which is useful to illustrate, in the case of bidirectional traffic, the multiple axle presence in function of axle spacing and simultaneous presence of other axle(s) in the other lane. It can be observed that for small strip widths, between 0.5 and 1 m, a diffuse group is present and correspond to the simultaneous presence of one axle in each lane. Also, one sees that both Class and Class+ show very similar plots; in other words, special transports (12t per axle) presence only affects slightly the values and distribution of the maxima. Tandem axles distance is most often close to 1.4m or to 1.8m (the second group includes pairs of axles of special vehicles). Finally, one can observe a small bias towards heavier axles having larger inter-axle spacings.

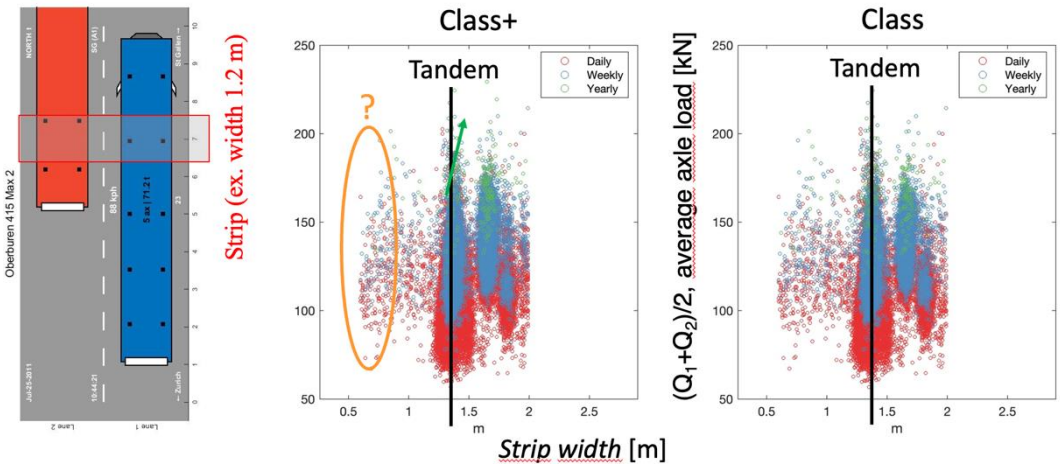

Figure 65: Strip analysis of the average axle group load (axles can be located on one or both lanes)

Then, in this project, an initial analysis to identify the traffic situations leading to maximum action effects on two lanes was carried out using a reduced set of WIM stations:

- For bidirectional (12): Gotthard and St-Bernardino;
- For unidirectional (11): Mattstetten, Oberbüren, Trubach, Mte Ceneri.

and a reduced set of influence as well as transverse distribution lines:

- Local effect, slab cantilever subjected to axle, or axle group,
- Global effect, slab frame bridge, span 10 m (single span but fixed in side walls, degree of fixity 50%) see (Hirt & Meystre, 2006b),
- Global effect, single span or 2-spans beams subjected to heavy vehicle (HV) traffic, with spans 20, 40 and 80 m. The values used are those corresponding to the worst case, which is the box girder with no transverse distribution line.
- Internal forces M_p, V, and M_n;

The main results were as follows:

- The maximum load effects, M_p, V, and M_n, for all spans, involve most often the same trucks;
- For the box girder, for Class, 4 truck combinations are responsible for 25 out of the 36 critical cases;
- For Class, the truck combinations most often found are: **2x123a** or **2x23** ;
- Class+ often leads to different critical cases than Class, that is involving as well 60 and 72 t crane trucks;
- One exception, for Class+, for M_n and 80m span, the critical cases involve different truck combinations with either types 113a, 1211r and 122, or crane trucks.

To be complete, the trip analysis of axle loads for double lane, in complement to Figure 21 which is for only one lane (lane 1) is now presented. Figure 66 presents the graph of the total load for two lanes. Compared to a single lane, one can notice that the jointly present total loads on both lanes are higher, but not that much higher; for single axles it is 320 kN compared to 233 kN, i.e. the joint probability of axle presence do not lead to values corresponding anywhere to extreme combinations of axle loads on both the 1st and 2nd lane. Note that there are slight differences from the values in Figure 16 and Figure 21; they result from algorithm updating and inclusion of more WIM station*years data in the course of this research. Anyway, the value remains similar to the

NLM1 sum of optimised values of the axle loads from simulations, that is 245 + 61 = 306 kN (refer to § 5.1.3).
In conclusion, the load model needs to account for a second axle or set of axles, with a significantly lower weight, the question of differentiating the UDL into a regional UDL and a remaining UDL on the second lane will result from the simulations.

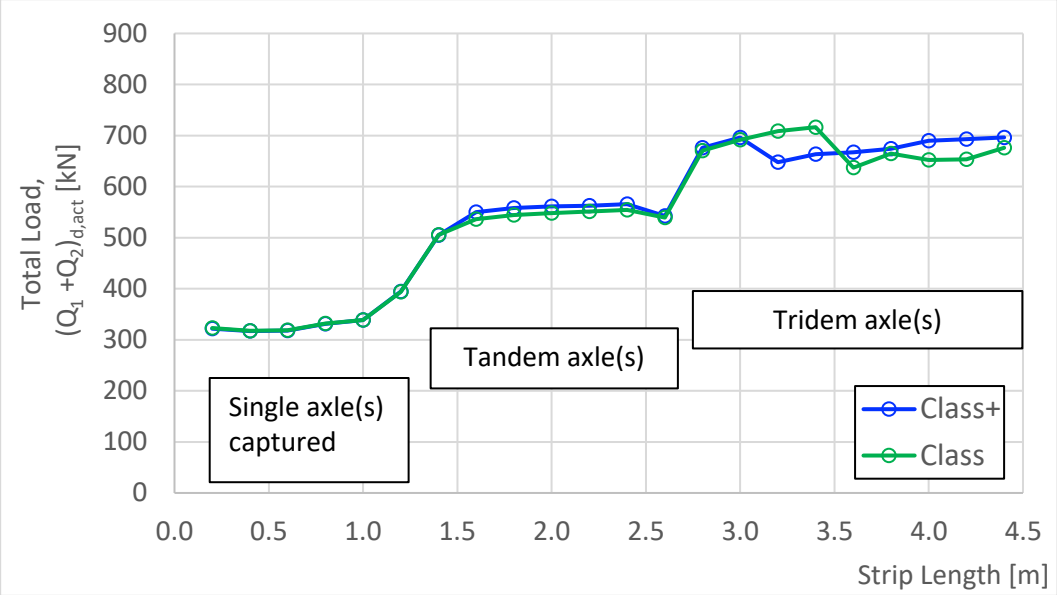

	Single	Tandem	Tridem
Q1d	233	215	171
Q2d	87	66	54
Q1d+Q2d	320	562	675

Figure 66: Design loads from WIM data strip analysis on two lanes, up to 4.4 m

11.3 Application of the single lane load models

This paragraph only contains additional information related to the positioning of the different loads for each load model to get the maximum load effects.
Figure 67 shows the positions for the single span cases and Figure 68 those for the hogging moment on an intermediate support.

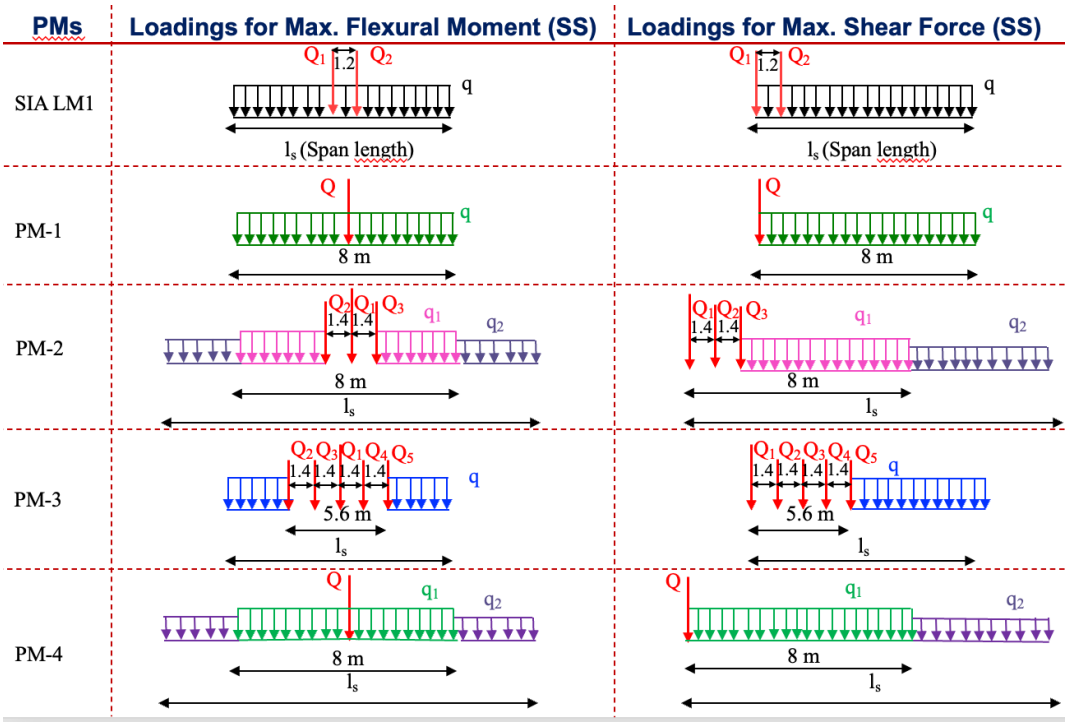

Figure 67: Single span cases, positions of the concentrated and UDL corresponding to the maximum load effects for the four candidate load models (PM in the figures) and the SIA LM1

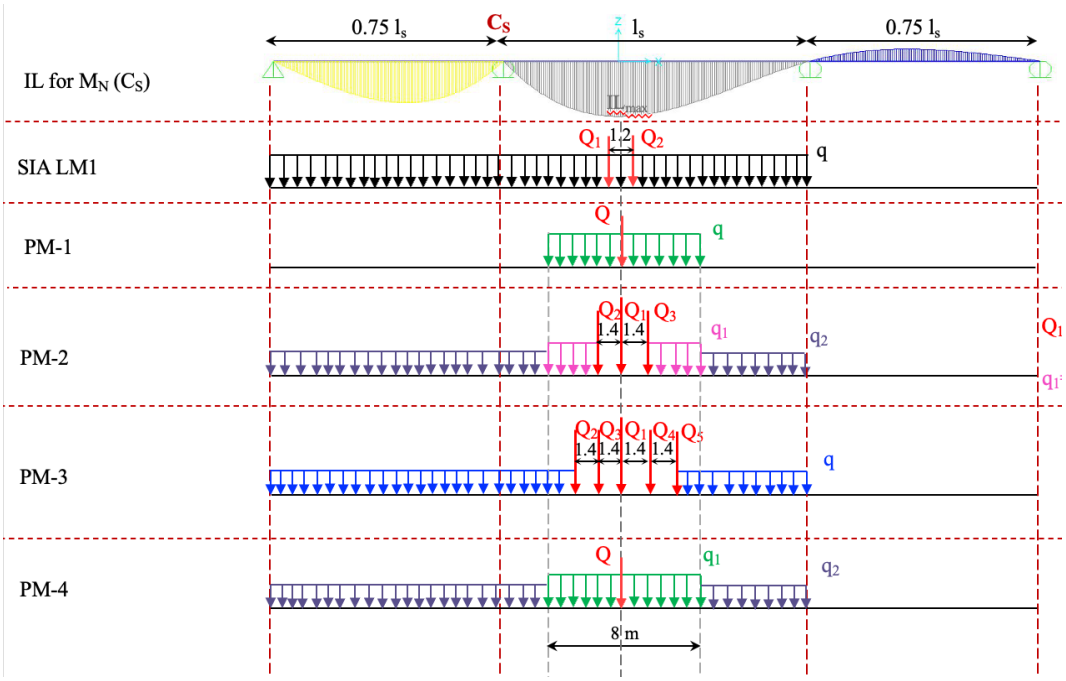

Figure 68: Three span case, positions of the concentrated and UDL corresponding to the maximum load effects (hogging moment) for the four candidate load models and the SIA LM1

11.4 Comparisons between load models (double lane)

As presented in the main document, § 5.1.3, the following two options are studied:

- Option 1: corresponds to a scenario of moderate heavy traffic increase, with 22500 trucks/per year/direction, the total number of trucks remains the same as in single lane analysis, distribution between lanes (first and second): 60% n_{truck} - 40% n_{truck};
- Option 2: high demand (37500 trucks/per year/direction), the number of trucks on the 1st lane remains the same as in single lane analysis: 100% n_{truck} - 67% n_{truck}.

When modelling the traffic flow for double lane JAM analysis accounting for the REL, with the 60% - 40% distribution of trucks, one assumes the total number of vehicle ($n_{JAM,yearly}$) for JAM traffic unchanged. Also, the number of trucks on the slow lane ($n_{truck,slow,JAM,yearly}$) remain the same as in single lane analysis. Thus:

- Total number of vehicle $n_{JAM,yearly}$ = 150000
- Number of trucks on the slow lane: $n_{truck,slow,JAM,yearly}$ = 22500 (for r_{truck} = 0.15)
- Number of trucks on R-BAU = ($n_{truck,R\text{-}BAU,JAM,yearly}$ / 60%) · 40% = 15000
- Increased truck ratio $r_{\text{truck,R-BAU}}$ = ($n_{truck,slow,JAM,yearly}$ + $n_{truck,R\text{-}BAU,JAM,yearly}$)/ $n_{JAM,yearly}$ = r_{truck} · 5/3= 0.25.

With these settings, the simulations can be carried out. The results are first presented in a way that the loads on the second lane are all reduced proportionally by a factor r_{Lane2} with respect to those in the first lane. Note that all results presented are with NLM1 as shown in Figure 26, that is before final optimisation, i.e. with for example q_{2ki} = 3.11 kN/m² (or 14 kN/m).

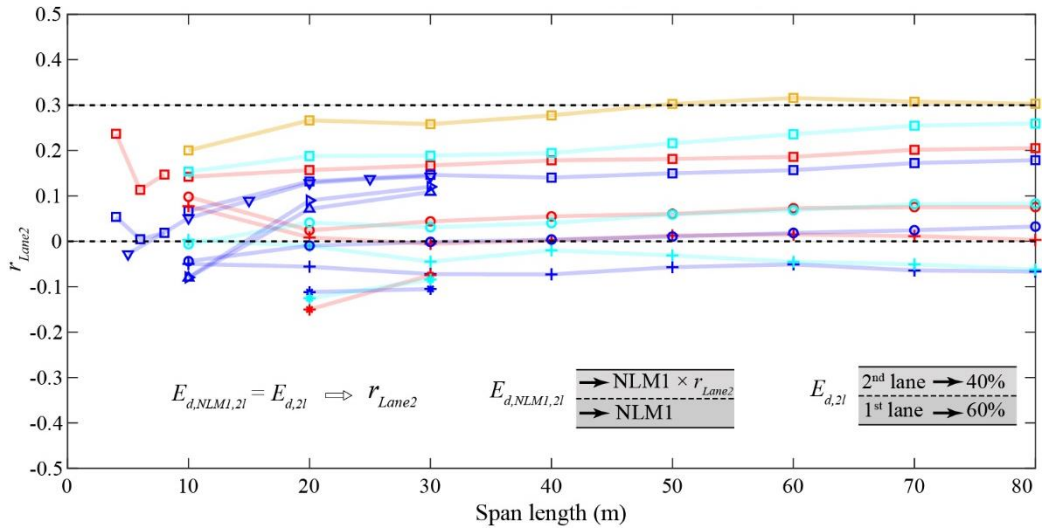

Figure 69: Required second lane load ratio r_{Lane2} for NLM1 to achieve exactly the double lane action effect *Ed,2l* (Option 1), (refer to Figure 71 for legends of plot)

Figure 69 presents the required NLM1 double lane ratio r_{Lane2} to achieve the exact design action effect $E_{d,2l}$ (for double lane Option 1: 60% - 40%). Figure 70 presents the same but for option 2 to achieve exact design action effect $E_{d,2la}$ (Double Lane Option 2: 100%-67%). This way of reducing for the 2nd lane suits better Option 1 whereas for Option 2, there is bias with increasing span and also the value r_{Lane2} = 0.3 leads to some non-conservatism, i.e. it is too low. An adjustment to r_{Lane2} = 0.5 resolves the non-conservatism but not the bias as shown in Figure 72 which now refer to unit value by

showing the ratio $E_{d,NLM1,2l}/E_{d,2l}$; and presented similarly, Figure 71 confirms that r_{Lane2} =0.3 works well for option 1.

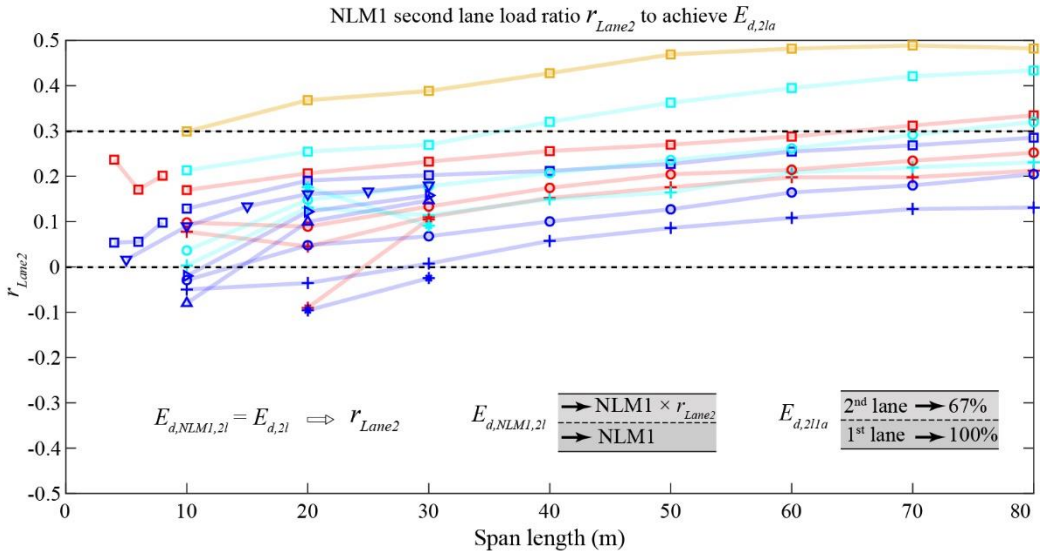

Figure 70: Required second lane load ratio r_{Lane2} for NLM1 to achieve exactly the double lane action effect *Ed,2la* (Option 2) (refer to Figure 71 for legends of plot)

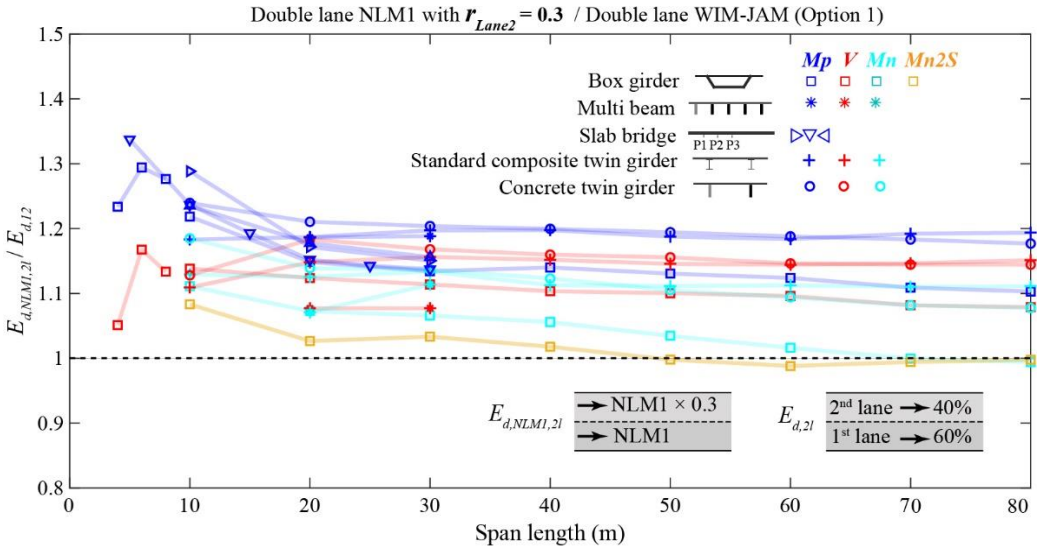

Figure 71: Ratio between double lane design action effect with NLM1, r_{Lane2} = 0.3 and the double lane action effect *Ed,2l* (Option 1)

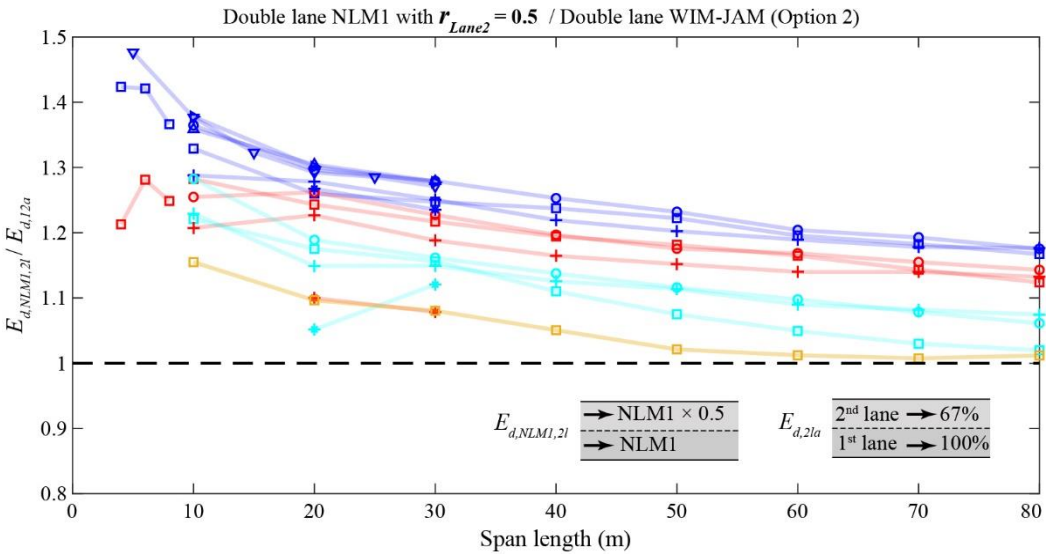

Figure 72: Ratio between double lane design action effect with NLM1, r_{Lane2} = 0.5 and the double lane action effect *Ed,2la* (Option 2) (refer to Figure 71 for legends of plot)

After discussion with the advisory commission, it was decided to continue the optimisation with the more conservative option, that is Option 2. This choice was made because it allows also to cover better potential future increase in heavy traffic and as well peculiar cases (not studied in detail here) such as the bridges in highway junctions (which are locations with more traffic jam hours) as well as the bidirectional traffic (2 lanes, one in each direction), since from the experience of the authors it is more aggressive than the case 4-0. Indeed, Option 1 does not cover it because the probability of occurrence with 22500 trucks in one direction can be below a heavily loaded bidirectional road section. The proximity to construction sites (4-0 lanes) is also covered as it implies 2+2 birectional traffic on one bridge, which means with the restriction of having only 2 lanes with heavy traffic due to the available pavement width.
The bias observed can be corrected during the optimisation process as the different components of NLM1 can be differentiated, and also the comparisons shown above correspond with the NLM1 as shown in Figure 26, thus do not yet take into account nor the system uncertainty, neither any dynamic amplification (DAF).

12 Appendix C: full-probabilistic analyses and input variables

12.1 Introduction to full-probabilistic analysis

In order to facilitate a better understanding of the background to the performed full-probabilistic analysis presented in the preceding chapters (mainly Chap. 6), this appendix will provide the necessary information to enable understanding of the calculations presented in the previous chapters as well as to facilitate a more nuanced understanding of the conclusions that resulted from the analysis.
First, some important terms will be defined. The subsequent two sub-chapters will address the interpretation of the full-probabilistic analysis and present the developed algorithm.

12.1.1 Basic definitions

Limit state function
The limit state function designated as $g(X)$, is an analytical (or even numerically) defined function that establishes a relationship between different probabilistic parameters. Failure of the structure is indicated if $g(X) \leq 0$, whereas safety is reached in the case that $g(X) > 0$. The vector X comprises all probabilistic variables that are necessary for the description of the limit state function.
Typically, the limit state function used in problems encountered by structural engineering can be expressed with

$$g = R - E \tag{22}$$

where the variables R and E represent the resistance and the action side of a structure, respectively. However, these variables may themselves comprise of multiple probabilistic parameters. For instance, the resistance term investigated in this study is represented by two parameters R and θ_R, rather than a single variable, as illustrated in the general description above.

Reliability index
The reliability index corresponding to a given limit state function is directly correlated with the failure probability of the structure under investigation. The failure probability

$$p_f = P(g(X) < 0) \tag{23}$$

can be described as well with the value on a standard normal distribution found for the probability of p_f:

$$\beta = \Phi^{-1}(p_f) \tag{24}$$

This transformation allows for a much more straightforward comparison between the safety of different limit state functions, as a comparison with failure probabilities would lead to much smaller differences, thus making them much more difficult to interpret. Nevertheless, this also demonstrates, that the relationship between the reliability index and the failure probability is not linear. Consequently, a quantitative comparison between reliability indices must be approached with caution.
EN 1990 Annex C gives the following equation for the calculation of the reliability index:

$$\beta = \frac{\mu_R - \mu_E}{\sqrt{\sigma_R^2 + \sigma_E^2}} \tag{25}$$

Where μ_i corresponds to the mean value of the resistance (or action) and σ_i to the standard deviation. Nevertheless, this simplified equation is only valid under the condition that the limit state function is linear (i.e. $g(X) = R - E$) and that both R and E are independent and undergo a normal distribution. However, this is not typically the case, necessitating a more sophisticated formulation to determine the reliability index for the limit state function depicted in this study. In this study, the probabilistic variables are not only not necessarily normal distributed, but the function is also not linear, as the model uncertainty is multiplied with the base variables R and E. To evaluate the reliability index, the so-called Hasofer-Lind algorithm is applied (Hasofer & Lind, 1974). The main aspects of the algorithm will be explained next.

<u>Hasofer-Lind algorithm</u>
The Hasofer-Lind algorithm is designed to identify the design point for which the most probable failure occurs, meaning the point closest to the failure surface. The design point $\overline{X_d}$ is situated on the failure surface, thus $g(\overline{X_d}) = 0$. This is also the case for the reduced design points $\overline{Z_d}$ which are located within the standard normal space. This transformation is beneficial as the reduced design points can be calculated directly from the sensitivity factors α_i and the reliability index β_{syst}, i.e. $\overline{Z_d} = \Phi(\alpha_i \cdot \beta_{syst})$.
The sensitivity factors α_i can be calculated as the relative derivative for the variable X_i based on all variables:

$$\alpha_i = -\frac{\frac{\partial g}{\partial Z_i}}{\sqrt{\sum\left(\frac{\partial g}{\partial Z_i}\right)^2}} \tag{26}$$

Based on the previously introduced boundary conditions, an equilibrium between the reliability index and the sensitivity factors can be established. This allows to determine the reliability index β_{syst}. Various algorithms are available for solving these equations, with the aim of determining the reliability index of the investigated limit state function. The accuracy and computation time of these algorithms may vary depending on the application and complexity of the problem.

12.1.2 Consideration regarding the sensitivity factors

The sensitivity factors α_i can be calculated as given in equation (26). They highlight the importance of a specific probabilistic variable in relation to the limit state function. In accordance with the definition of the sensitivity factor, the following relation apply:

$$\sum \sqrt{\alpha_i^2} = 1.0 \tag{27}$$

Where, for a constant variable, a sensitivity factor of $\alpha_i = 0$ results.
The Eurocode EN 1990 provides proposed values for the sensitivity factors on both the action and the resistance side. For dominant actions and resistances, the proposition is

$$\alpha_E = 0.7,\ \alpha_R = 0.8 \tag{28}$$

However, this is only applicable within the range of $0.16 \leq \sigma_E/\sigma_R < 7.6$. In the case of a non-dominant variable (which does not fulfil the aforementioned criterion), the proposed sensitivity factor is given as $\alpha_{non-dom} = 0.4$, while the dominant variable should be assumed to be $\alpha_{dom} = 1.0$.In the case of multiple variables (in contrast to the simplified representation of EN 1990), however, it is not explicitly said how the sensitivity factors should be adapted, if at all. Consequently, the typical approach is to apply the aforementioned propositions during the calibration process.
Figure 73 and Figure 74 provide a visual representation of the range of applications for the ratio σ_E/σ_R. The graphs demonstrate that a notable deviation from the values for both the sensitivity factors and the reliability index exist within this range. In particular, the sensitivity factors exhibit a significant alteration, demonstrating their dependency on the underlying assumption of the scatter of the probabilistic variables.
In the present study, a limit state function comprising of a normal distributed action and resistance side, based on the calculation of the reliability in accordance with equation (25) was used. Meanwhile, the design values E_d and R_d were based on the definition provided in EN 1990.

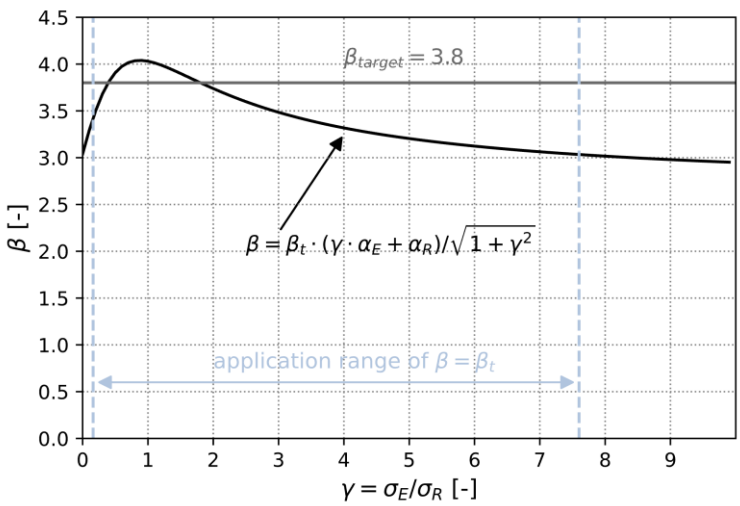

Figure 73: Influence of ratio of scatter on reliability index

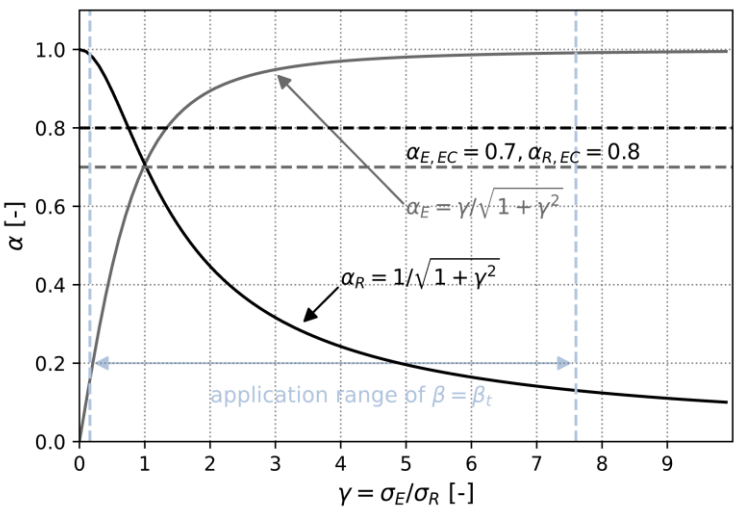

Figure 74: Influence of ratio of scatter on sensitivity factors

A further insight should be given on the time-dependency of the sensitivity factors. The following formulation from EN 1990 allows for a transformation of reliability indices between different time frames. This enables the evaluation of the reliability index required to target when the actions are considered for a different time frame.

$$\beta_n = \Phi^{-1}[[\Phi(\beta_1)]^n] \tag{29}$$

Where a transformation between the time T_1 for β_1 and the timeframe T_n (or T_2) results in β_n. n is the ratio between T_2 and T_1. In the case of a semi-probabilistic calibration, the Eurocode demands that the reliability index should be adjusted in accordance with equation (29). The issue is that the sensitivity factor α_E, which is required for the analysis, remains constant at 0.7. There is no mention of the influence of the considered time frame on the sensitivity factor. This however results in different levels of safety, which should also be considered in the transformation. Instead of applying the reliability index only in the transformation, it would be more appropriate to apply the product of the sensitivity factor and the reliability index:

$$\beta_{E,n} = \beta_n \cdot \alpha_{E,n} = \Phi^{-1}\left(\Phi\left(\beta_0 \cdot \alpha_{E,0}\right)^n\right) \tag{30}$$

An investigation of different time frames, with the objective of calculating the required $\alpha_{E,i}$ to achieve the same combined reliability index for another time frame, is illustrated in Figure 75. The analysis is based on a reliability index of $\beta = 3.8$ for a time frame of 50 years.

It becomes evident that the application of fixed sensitivity factors for shorter time frames results in a significantly reduced sensitivity factor requirement for longer time frames. This implies in reverse, that if $\alpha_E = 0.7$ was defined for shorter time frames, the safety would not be sufficient for larger time frames. In other words, if the safety needs to be reached for larger time frames, a higher value for the sensitivity factor $\alpha_E = 0.8 \div 0.9$ is required. The mere transformation of the reliability index (without consideration of the sensitivity factor) is inadequate and fails to account for the divergence in

the safety considerations. However, it should be noted that this effect is relatively minor when applying it to typical cases investigated in structural engineering. For example, in order to fulfil the safety-requirements of a 50-year or 100-year distribution, the sensitivity factor of the yearly distribution needs to be increased from 0.7 to approximately 0.8. Nevertheless, this effect leads to a certain inconsistency in the calibration processes.

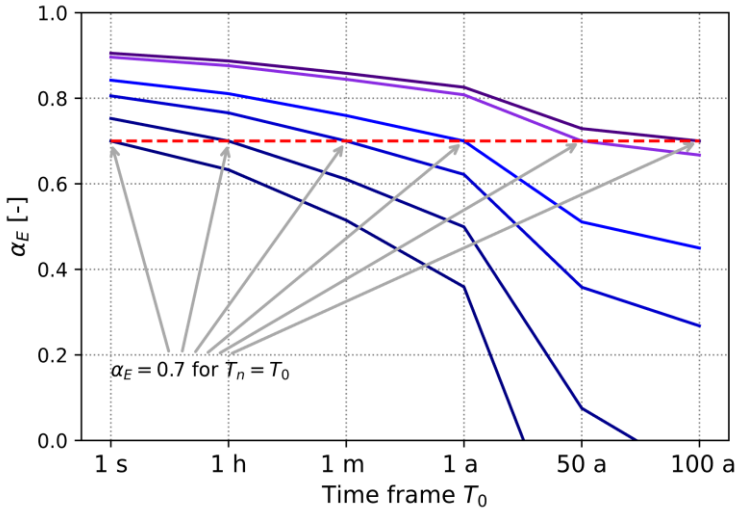

Figure 75: Required sensitivity factor dependent on observed time frame (for $\beta = 3.8$)

12.1.3 Application of full-probabilistic analysis for calibration of load model

The previous sub-chapter presented the necessary background to perform full-probabilistic analysis and demonstrated the possible drawbacks in a semi-probabilistic calibration of the load model. Unfortunately, existing literature does not provide direct information on how a full-probabilistic analysis can be used for the calibration of a load model, which itself represents only one part of a full-probabilistic limit state. Consequently, a number of different solutions were investigated and will be presented next. This will especially assist the reader in understanding the solution that was ultimately implemented.

<u>Calibration based on the sensitivity factor</u>

As a first proposal, the sensitivity factors of the traffic action effects $\alpha_{\mathrm{E,Traffic}}$ derived from the reliability analysis could be applied as a primary parameter for the calibration of the load model. Certain primary assumptions must be made regarding the resistance of the investigated section. The design resistance of the section could for example be based on the design of the permanent loads and the current LM1, or alternatively, on the reduced load model with the adjustment factor $\alpha_Q = 0.60$. Subsequently, the sensitivity factor $\alpha_{\mathrm{E,Traffic}}$ is then derived from the full-probabilistic analysis, with the probabilistic distributions of the action effects and the resistance side being inserted. Rather than utilising the sensitivity factor $\alpha_E = 0.7$ for the calibration of the load model, the factor derived from the full-probabilistic analysis could be applied.

Although this approach generally considers the influence of the different probabilistic variables of the limit state function (as for example the load ratio), it has certain limitations: Firstly, this procedure fails to take into account the current state of safety of

the structure under investigation. In contrast to the sensitivity factor, the structural safety – described by β – is not only significantly influenced by the coefficient of variation of the parameters, but also by its first mode (e.g. the mean value). Consequently, if only $\alpha_{\mathrm{E,Traffic}}$ is taken into account, the calibrated load model remains unchanged, irrespective of the actual safety status of the structure. A second issue arises from the general encouragement of more accurate representation of both action and resistance functions. A lower scatter of the resistance function (for the same mean value) results in a lower scatter of the resistance and thus a larger sensitivity factor $\alpha_{\mathrm{E,Traffic}}$. This indicates that a better representation of the model uncertainties would here not be encouraged; rather, it would result in a larger calibrated load model being required. Based on these findings, a different approach is selected for the use of information from the full-probabilistic limit state function.

<u>Full-probabilistic calibration of partial safety factors</u>

The existing literature, and particularly the Eurocode, does not adequately address the question, how one component of the limit state function should be modified for the calibration of a design value in case of a full-probabilistic analysis. There exist however general rules for a calibration based on partial safety factors. They are presented not only in the new EN1990, but explained more in-depth in the reliability background of the Eurocodes (European Commission. Joint Research Centre., 2024). Different working projects (e.g. (Feldmann et al., n.d.)) have been performed, and a simplified program from the Joint Committee on Structural Safety (JCSS) is also available, allowing users to utilise this procedure for a calibration of partial safety factors (link to the free download: https://www.jcss-lc.org/codecaljcss/).

The general procedure requires first of all a design equation of the following form:

$$z = \frac{\gamma_m}{R_k} \cdot \left((1-\chi) \cdot \gamma_G \cdot G_k + \chi \cdot \gamma_Q \cdot Q_k \right) \tag{31}$$

Where:

$$\chi = \frac{Q}{Q+G} \rightarrow R \cdot z = (1-\chi) \cdot G + \chi \cdot Q_k \tag{32}$$

This then results in a limit state function which looks like this:

$$g(X) = z \cdot R \cdot \xi - (1-\chi) \cdot G - \chi \cdot Q \leq 0 \tag{33}$$

The objective is to identify a pair of partial safety factors $(\gamma_{\mathrm{M}}, \gamma_{\mathrm{G}}, \gamma_{\mathrm{Q}})$ that provides an optimal approximation for $\beta_{\mathrm{syst}} = \beta_{\mathrm{target}}$ for the investigated systems. In the case of considering multiple structures and load types, this usually gives different pairs of partial safety factors that do not satisfy the requirement of $\beta_{\mathrm{syst}} = \beta_{\mathrm{target}}$ in every case. To address this, an optimisation procedure is applied, allowing for the weighting of different parameters to achieve a more uniform reliability across the different structures, materials and failure modes. Consequently, the following error function must be minimised to identify the optimal pair of partial safety factors:

$$\min\left\{\sum w_i \cdot (\beta_i - \beta_t)^2\right\} \tag{34}$$

Furthermore, the optimisation function of equation (34) enables the incorporation of weight factors $w_i w_i$, which can be based on different factors as number of types of structure i or further safety considerations. This value can be applied to adjust the significance for certain structures in the optimisation process. Additionally, the procedure allows for the definition of a minimum reliability threshold that must be met.

<u>Proposed calibration algorithm</u>

Given that the objective of this project was to focus on the calibration of the load model, it was necessary to adapt only one part of the design parameters. Consequently, the aforementioned procedure is not directly applicable. Some adaptations are therefore required. The general procedure used for the calibration can be seen in Figure 76.

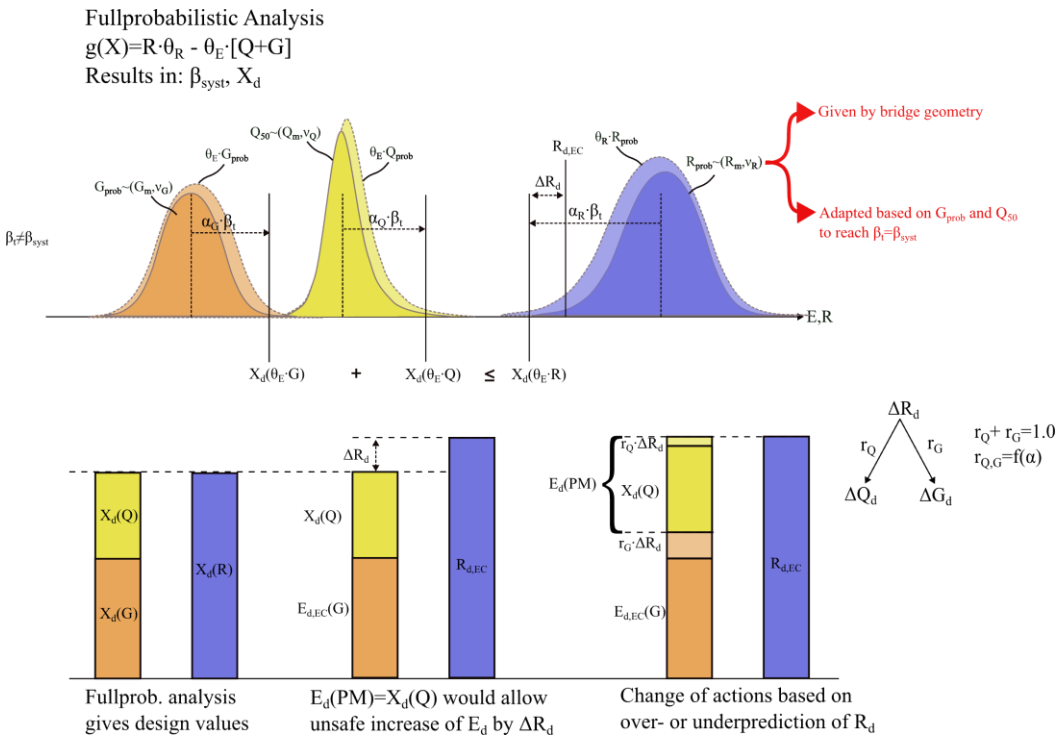

Figure 76: Proposed approach for the calibration of the load model

First (upper half of Figure 76), the reliability index, the sensitivity factors and the probabilistic design values are calibrated for the investigated limit state function. Although the probabilistic distribution of the action side is typically known for the investigated bridge type based on prior analysis, this is not necessarily the case for the resistance side. In the event that the bridge characteristics in question are known, it is possible to utilise these in the representation of the resistance. In a more general case, the proposal is to adapt the mean value (or design value from the code) in order to achieve $\beta_{syst} = \beta_{target}$.

Following this initial investigation, further adaptations are necessary for the calibration of the load model (see bottom half of Figure 76). Given that the probabilistic design values are in equilibrium, reaching $g(\bar{X}) = 0$, a potential approach would be to propose them directly as the design values. The direct implementation of the full-probabilistic design values necessitates the calibration of all design values. This would result in a discrepancy between the implied design value of the resistance side $X_d(R)$ (based on the full-probabilistic analysis) and the design resistance $R_{d,EC}$ currently in use. In the event that the design resistance currently specified by the code $R_{d,EC}$ exceeds the value of $X_d(R)$, the calibration would be deemed unsafe. In contrast, if $X_d(R)$ is greater than $R_{d,EC}$, the opposite is true.
In order to incorporate this influence, the difference in the resistance $\Delta R_d = R_{d,EC} - X_d(R)$ is incorporated in the calibration of the traffic action side. The calibrated design traffic action effects are increased (or decreased respectively) by a portion of ΔR_d. In contrast to the procedure presented in the research project REAL-LAST (Vorwagner et al., 2024), where this difference was applied as a simplified, conservative assumption entirely to the calibration of the load model, this portion is determined in function of the sensitivity factors. Therefore, ΔR_d is applied partially to the traffic action effects and partially to the other considered permanent loads.

$$\Delta X_d = r_X \cdot \Delta R_d \tag{35}$$

Therefore, the calibrated load model can be computed with:

$$E_d = Q(X_d) + \Delta X_d \tag{36}$$

The factor r_x takes into account the importance of the action effects by means of the sensitivity factors:

$$r_X = \left(\frac{\alpha_{Q,\theta_E}}{\alpha_E}\right)^2 \tag{37}$$

Depending how the uncertainty of the action effect θ_E is treated, α_{Q,θ_E} needs first to be calculated:

$$\alpha_{Q,\theta_E} = \alpha_Q \cdot \sqrt{1 + \frac{\alpha_{\theta_E}^2}{\alpha_G^2 + \alpha_Q^2}} \tag{38}$$

The sensitivity factor of the total action effects α_E can be derived based on the assumption that:

$$\alpha_E = \sqrt{\alpha_{\theta_E}^2 + \alpha_G^2 + \alpha_Q^2} = \sqrt{\alpha_{G,\theta_E}^2 + \alpha_{Q,\theta_E}^2} \tag{39}$$

As a consequence of the incorporation of ΔR_d, the design value of the calibrated load model is modified, thereby influencing as well the sensitivity factor that is linked to the calibrated design value. In order to ensure consistency, the sensitivity factor $\alpha_{\mathrm{E,Traffic}}$ is re − evaluated on the basis of the design value $X_{\mathrm{d}}(\mathrm{R}) + \Delta X_{\mathrm{d}}$. The results demonstrate that this influence is typically negligible and does not affect the overall outcome of the results.

This calibration method addresses the aforementioned shortcomings associated with calibration based on sensitivity factors. In instances where the calculated reliability differs from the target reliability, the design values should be adjusted accordingly. Rather than utilising the design values derived from the full-probabilistic analysis, they should be determined based on $\alpha_{\mathrm{i}} \cdot \beta_{\mathrm{target}}$. An example for the application of overdesign for the calibration process can be found in appendix D.

<u>Further considerations for the full-probabilistic analysis</u>
Given the general information provided for the full-probabilistic calibration of the load model, a series of further considerations are presented that are necessary for a consistent calibration of the load model.
In general, the load model can be calibrated using the semi-probabilistic method with a traffic distribution from any reference timeframe. In such a case, an adaptation of β (and, as mentioned demonstrated, of α_E) is required, which would be leading to the same results. In contrast, for a full probabilistic analysis, this is not the case. The time frame under consideration is of importance for the calibration of the load model, as it influences the safety and the sensitivity factors of the analysis.
While the permanent loads and the resistance are largely independent of the observed timeframe, only the traffic action effects require extrapolation. In order to correctly consider the traffic action effects for the full-probabilistic calibration, they are extrapolated to a 50-year block maxima distribution. By applying equation (29) for $\beta_1 = 4.2$ and $T_2/T_1 = 50$, this gives $\beta_2 = 3.2$.
The general procedure is shown in Figure 77.

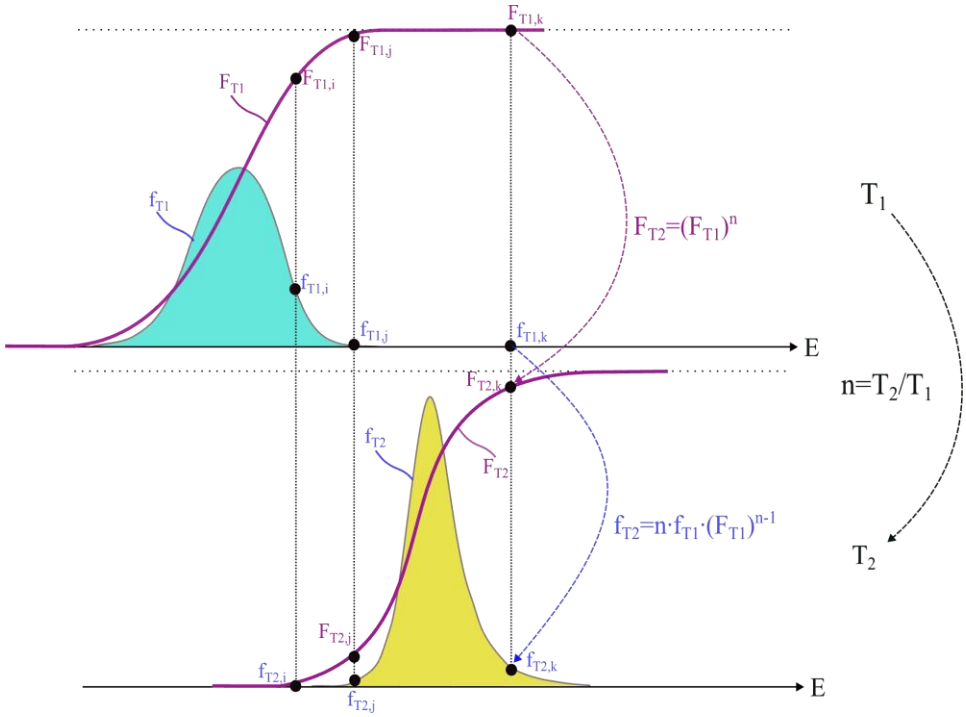

Figure 77: Applied procedure for extrapolation of probabilistic distribution of traffic action effects

The transformation between the time frame T_1 and the time frame T_2 is achieved by transformation of the cumulative distribution function $F(\cdot)$:

$$F\left(X_{max,T_2} \leq x\right) = F\left(X_{max,T_1} \leq x\right)^n \tag{40}$$

Derivation of both sides, allows to determine the probabilistic distribution function $f(\cdot)$ of the time frame T_2:

$$f_{T_2} = n \cdot f_{T_1} \cdot \left(F_{T_1}\right)^{n-1} \tag{41}$$

Where F_{T_1} corresponds to the cumulative distribution function of the time frame T_1. In general, the probabilistic variables of f_{T_2} are determined through the application of a best-fit algorithm. However, in certain instances, it is possible to directly determine the values of the extrapolated distribution. One such instance is when f_{T_2} follows a Gumbel distribution. In this case, the probabilistic variables of the specified time frame T_2 can be determined through analytical means:

$$\beta_{G,2} = \beta_{G,1}, \mu_{G,2} = \mu_{G,1} + \beta_{G,1} \cdot \ln\left(\frac{T_2}{T_1}\right) \tag{42}$$

In order to compare the sensitivity factors derived from the full-probabilistic analysis with the assumptions of the semi-probabilistic calibration, the sensitivity factor $\alpha_{E,Traffic}$ is transformed to a yearly traffic distribution, by applying equation (30).
It should be noted however, that this reliability $\alpha_{E,0}$ does not provide direct information about the impact of the traffic action effects on the limit state function. This sensitivity

factor only permits a qualitative statement about the position of the calibrated load model in relation to the yearly traffic distribution. This, however, leads to the general observation, that the boundaries for $\alpha_{E,0}$ are shifted in comparison to $\alpha_{E,n}$ and are not anchored at zero.

For example, transforming the sensitivity factor by n=50, results in values for the sensitivity factor not being lower than $\alpha_E = 0.5$. This can be explained by the fact that the transformed distribution of action effects leads to a considerably higher mean value, which in turn results in a much higher design value. If this design value is now expressed in probabilistic terms using the probabilistic distribution based on T_1, a certain sensitivity factor is required even when $\alpha_{E,n} \to 0$. The general behaviour between $\beta_n, \alpha_{E,n}$ and the corresponding values for $\alpha_{E,1}$ based on a time ratio of n=50, is illustrated in Figure 78.

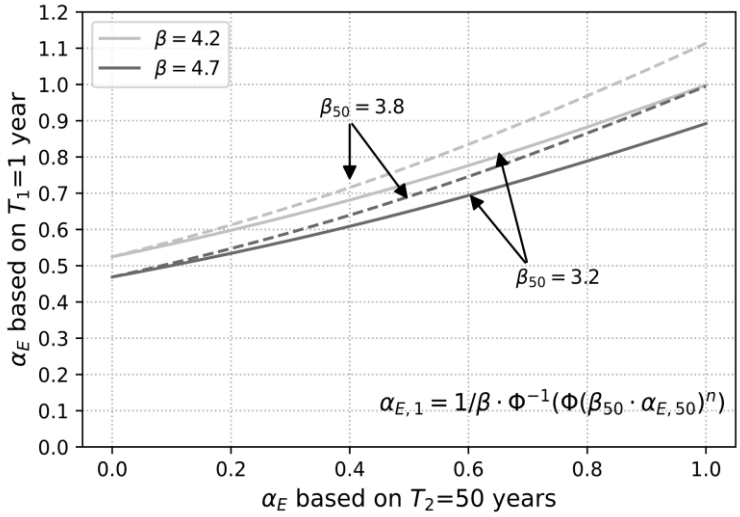

Figure 78: Transformation of sensitivity factor between time frames (n=50)

12.2 Probabilistic description of input variables

The previous sections presented the procedure and terminology used for the full-probabilistic analysis and the calibration of the load model. In consequence, this section offers guidance for the derivation of the input parameters required for the probabilistic analysis as well as providing tables with values that could be used. The majority of these values are based on a previously performed literature study.

12.2.1 Permanent loads

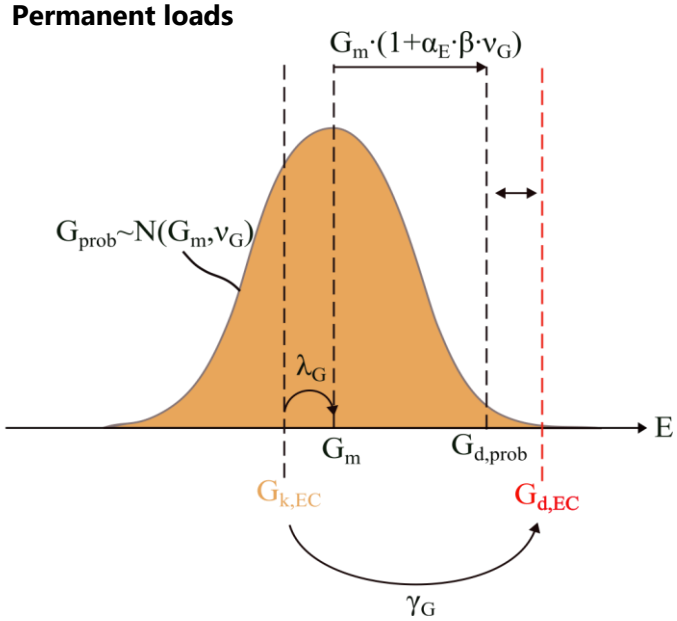

Figure 79: Probabilistic representation of permanent loads

The considered permanent actions can be separated into a portion of self-weight and further permanent loads. As additional permanent actions, an asphalt layer was considered.
In general, for the description of permanent loads is based on two key parameters: a bias λ_G and a coefficient of variation ν_G. This approach allows for a probabilistic representation of the loads based on their characteristic value. This relationship is also illustrated in Figure 79.

Self-weight
In the case of the more generic bridges investigated in this study, the self-weight is considered using an analytical expression for a uniformed distributed load according to (Waag, 1994) with:
For concrete bridges:

$$g = \left(0.35 + 0.45 \cdot \frac{L}{100}\right) \cdot \gamma_c \tag{43}$$

For steel-concrete composite bridges:

$$g = (0.16 + 0.008 \cdot B) \cdot \gamma_c + 0.10 \cdot \left(1 + \frac{0.2 \cdot L}{0.6 + 0.035 \cdot B}\right) \tag{44}$$

The unit for g is in $[kN/m^2]$ and B and L are in $[m]$, while $\gamma_c = 25.5\ kN/m^3$.
In the analysis for the composite bridges it is assumed that the load consists of a concrete layer with a thickness of around 20 to 30 cm and a steel girder, described by the right side of equation (44). As in the scope of the project a range of bridges were analysed – from idealised to more realistic structures – a comparison can be made between the simplified analytical values and those based on an in-depth analysis.

For the specific bridges investigated in this study (see Table 16:), the accuracy of the simplified representations of the self-weight can be investigated. Figure 80 illustrates the ratio between the action effects resulting from equations (43) and (44) and the values directly resulting from the structural analysis software SOFiSTiK.

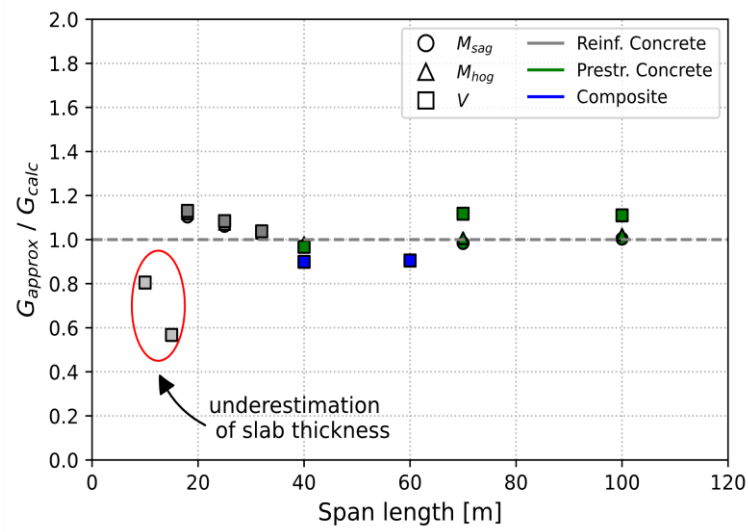

Figure 80: Ratio between approximated and calculated self-weight

The investigation demonstrates that the simplified formulations are particularly precise in the case of longer span girder bridges, with accuracy levels between -10 % and 15 % depending on the span length and the considered reaction force. Given the assumed slenderness of the concrete slab of $L/20$ for portal frame bridges (see Figure 97), this results in higher slab thicknesses compared to the values resulting from the analytical approximative formulations. It may therefore be that the self-weight due to the concrete slab for the generic frame bridges investigated in this study may be underestimated. This is, however, not a significant issue, as it would result in a slight increase in the importance attributed to traffic action effects, leading to a higher required design value for calibration and a more conservative approach.
The formulations of equations (43) and (44) permit the calculation of characteristic (or nominal) values for the action effects of the self-weight. Subsequently, a bias factor λ_G – defined as the ratio between the mean value and the characteristic value – and a coefficient of variation v_G are required, to allow a probabilistic description of the self-weight. Some proposed values from the literature are given in Table 10.

Probabilistic parameters for permanent loads

Description / Limitation	λ_G	v_G	Source
In-Situ concrete	1.05	0.1	(Nowak & Szerszen, 1998)
Steel	1.03	0.08	
Asphalt layer	0.75	0.25	

Concrete	1.00	0.05	(European Commission. Joint Research Centre., 2024)
Steel	1.00	0.025	

Table 10: Model uncertainties for the calculation of action effects

A sensitivity study highlighted that the choice of the probabilistic parameters of the action effects only play a marginal role and does not significantly influence the results. The absolute values of the permanent loads – expressed by the load ratio χ, defined as the traffic action effect / permanent loads effect – χ has a much higher influence, as will be illustrated herein with a parametric study.

Asphalt layer

Additionally, an asphalt layer was considered as probabilistic distributed load. Here, the values from (Malja, 2024) were selected. A very simplified formulation is given in (Rigendinger, 1994) covering a thickness of 10 cm with a self-weight of 24 kN/m³.
The investigation from (Malja, 2024) for different bridges in Switzerland showed that the nominal thickness between 50 mm and 75 mm with a bias of 1.1 up to 2.4 (and a scatter between 8.4 % and 21.6 %).
For the investigation of the bridges, a nominal value of 75 mm with a bias of 1.3 and a scatter of 15 % was assumed. This choice lies in between the results.

Prestressing forces

The effect of prestressing forces can either be interpreted as residual stresses acting on the entire structure (including the prestressing tendon) or as anchorage, deviation and friction forces (without the prestressing tendon). While in the first case the prestressing of the structure is treated as part of the resistance, in the latter case, the prestressing is treated as a load. Based on typical procedures in bridge design, the prestressing forces were interpreted as part of the resistance side. Therefore, a consideration on the action side can be omitted. The restraint actions should however be considered in static undetermined systems. The limited available data for probabilistic distributions of prestressing forces limited the consideration of the prestressing. Similar to the permanent loads presented before, the influence of the scatter was rather small. Therefore, this effect was only considered for certain parametric multi-span bridges.

12.2.2 Probabilistic representation of resistance functions

Probabilistic material and geometric parameters

Description	μ	σ	X_d	Source
	Concrete material properties			
Compressive strength	$f_{cd} \cdot \gamma_c + 8\ N/mm^2$	$\frac{8}{1.64}\ N/mm^2$	f_{cd}	EN 1992-1-1, SIA 262
		$f(f_{cm}, \text{Production})$		(Spaethe, 1992)
	$f_{c,ij} = \alpha(t,\tau) \cdot (f_{co,ij})^{\lambda} \cdot Y_{i,j}$			(JCSS Probabilistic Model Code - Part 3: Material Properties, 2000)
	$f_{ck} \cdot \exp(1.645 \cdot V_{fc}) \cong 1.179 \cdot f_{ck}$	$0.1 \cdot f_{cm}$		EN 1992-1-1:2023
Elastic modulus				
Description	μ	σ	X_d	**Source**
	Reinforced steel material properties			
Yield strength			f_{sd}	SIA 262
	$f_{sk} + 2 \cdot \sigma$	$30\ N/mm^2$		(JCSS Probabilistic Model Code - Part 3: Material Properties, 2000)
	$\exp(1.645 \cdot V_{fs}) = 1.077$	$0.045 \cdot f_{sd} \cdot \gamma_c$	f_{sd}	EN 1992-1-1:2023
	Structural steel material properties			
	$(1.10 \div 1.25) \cdot f_{yk}$	$(3.5\ \% \div 5.5\ \%) \cdot f_{ym}$	f_{yd}	(EN 1993-1-1:2022)
	$f_{y,k} \cdot \alpha \cdot \exp(-u \cdot v) - C$			(JCSS Probabilistic Model Code - Part 3: Material Properties, 2000)
	$f\left(\frac{h}{b}, f_{yk}, t_f\right)$	$f\left(\frac{h}{b}, f_{yk}, t_f\right)$	-	(da Silva et al., 2016)
	Prestressing material properties			
Yield strength	$f_{pk} + 1.645 \cdot 40$	$40\ N/mm^2$		(JCSS Probabilistic Model Code - Part 3: Material Properties, 2000)
0.1% proof strength	$0.90 \cdot f_{pk}$	$50\ N/mm^2$		(Jacinto et al., 2012)
E-modulus	$195\ N/mm^2$	$5\ N/mm^2$		(Jacinto et al., 2012)

Table 11: Probabilistic material and geometric parameters

Based on the investigated resistance functions, the main focus on the selected probabilistic parameters was on concrete and steel material properties. For this, a literature study was conducted to determine ranges or select specific values for the further investigation. The values found in the literature are depicted in Table 11. As not all studies align with the simplified categorisation of Table 11, certain cells are left empty.

12.2.3 Propositions for resistance model and action effects determination uncertainties

The following section presents the findings of a literature review listing proposed values for the description of resistance function model uncertainties as well as model uncertainties in the determination of the action effects are presented next.

Model uncertainty for the determination of the resistance functions
Table 12 provides a general overview of the model uncertainties associated with the investigated resistance functions, as depicted in Table 6.
Due to the number of different propositions provided for the concrete shear and bending failure modes, they are depicted in separate tables (Table 13 and Table 14).

Overview resistance model uncertainties

Description		μ	v	Resistance function	Source
Steel bending		1.0	0.05	-	Steel bending
		1.0 ÷ 1.1	0.05 ÷ 0.07		(Nadolski & Sykora, 2014)
Steel shear		1.0	0.05		Steel shear
		1.17	0.11		(Höglund, 1997)
Concrete shear, no shear reinforcement.	$\rho_l \leq 1$ %	1.28; 0.82	0.17; 0.16	fib MC: LoA I; LoA II	Concrete shear, no shear reinforcement.
	$1 < \rho_l \leq 2$ %	1.83, 0.92	0.12, 0.12		
	2 % $< \rho_l$	2.08, 0.94	0.12, 0.13		
	-	0.98	0.18	EN 1992-1-1	(Holický et al., 2016)
		1.20	0.1		
		1.10	0.107		
Concrete shear, with shear reinforcement.		1.07 ÷ 2.5	0.12 ÷ 0.27	See Table 14	

Table 12: Overview resistance model uncertainties

In the case of model uncertainties of composite sections, the values for the resistance of a steel section are given, since no literature values were found. This then implies a failure of the steel section, while the influence of the concrete slab is neglected in this consideration.

Model uncertainty for concrete bending moment resistance

Description	μ	v	Source
-	1.072	0.052	(Cervanka, Cervanka, & Kadlec, 2018)
Including effects due to normal and shear forces	1.2	0.15	(JCSS Probabilistic Model Code - Part 3: Material Properties, 2000)
-	1.17 / 1.02	0.065 / 0.06	(Wisniewski et al., 2009)
-	1.15	0.13	(Zingoni, 2013)
-	1.09	0.045	EN 1992-1-1:2023

Table 13: Model uncertainty for concrete bending moment resistance

Model uncertainty for concrete shear resistance with reinforcement

Description / limitation		μ	v	Resistance function	Source
Light reinforcement		1.8	0.25	EN 1992-1-1	(Zingoni, 2013)
Moderate reinforcement		1.25	0.25		
Heavy reinforcement		0.8	0.2		
$a_v/d < 2.25$	Rectangular CS	1.68	0.35	EN 1992-1-1	(Pejatovic, Fernandez Ruiz, & Muttoni, 2022)
	Flanged beams	1.17	0.12		
$a_v/d \geq 2.25$	Rectangular CS	1.54	0.23		
	Flanged beams	1.37	0.27		
"Concrete shear"		1.4	0.25	-	(JCSS Probabilistic Model Code - Part 3: Material Properties, 2000)
Lightly reinforced beam		2.5	0.26	fib, LoA 1	(Sykora et al., 2018)
Moderate reinforced beam		1.86	0.24		
Heavily reinforced beam		1.43	0.28		
Lightly reinforced beam		1.68	0.26	fib, LoA 1	
Moderate reinforced beam		1.47	0.21		
Heavily reinforced beam		1.17	0.24		
Lightly reinforced beam		1.13	0.24	fib, LoA 3	
Moderate reinforced beam		1.18	0.19		
Heavily reinforced beam		1.07	0.24		

Table 14: Model uncertainty for concrete shear resistance with reinforcement

In the case of highly reinforced beams, only limited results and data points were investigated in (Zingoni, 2013). Thus, this value has to be taken with caution.
In Table 14, the parameter α corresponds to the length of the shear stress field and d to the available static height of the beam.
The differentiation between lightly, moderately and heavily reinforced beams is made based on a distinction of the reinforcement ratio. Thereby, the maximal stress based on $\rho_w \cdot f_{y,w}$ is limited by 1 N/mm² for lightly and by 2 N/mm² for moderately reinforced beams.

Model uncertainty for the determination of the action effects
The proposed values for the model uncertainty of the calculation of the action effects are illustrated in Table 15. This value is then directly incorporated into the full-probabilistic analysis by the probabilistic variable θ_E. This variable considers the discrepancy between the action effects resulting from the calculation of the structural model and action effects acting on the actual structure.

Model uncertainties for the calculation of action effects

Description / Limitation	μ	v	Source
Bending moment in slabs	1.0	0.2	(Joint Committee on Structural Safety , 2000)
Shear force in slabs		0.1	
Traffic loads	1.0	0.1	(Steenbergen & Vrouwenvelder)
Permanent loads		0.07	
General	1.0	0.065	(Malja, 2024)

Table 15: Model uncertainties for the calculation of action effects

Based on the good documentation and thorough investigation of the results, the values from (Malja, 2024) where selected, thus resulting in $\theta_E \sim LN(1.0, 6.5\%)$.

12.2.4 Probabilistic distributions of resistance functions

In order to allow for a probabilistic representation of the resistance functions, a number of different resistance models were investigated using Monte Carlo simulations to gain a better insight into both the scatter of the material and geometric properties as well as uncertainty of the resistance model. The cross-sections were thereby based on the parametric bridge models shown in Figure 97 to Figure 100.

Concrete bending resistance
The scatter of the concrete bending resistance function was investigated in dependence of the reinforcement ratio. If the geometry of the bridge is given, the amount of reinforcement can influence as a major parameter the bending resistance, thus selecting this parameter as variable. Both the T-beam section as well as the slab section were investigated. The results will however be presented in detail only for the T-beam section, as they provide more diverse results and can be applied directly to the resistance scatter of the slab bridge.

The concrete bending resistance was evaluated based on the resistance function from EN 1992-1-1 with a variable reinforcement ratio ρ_s. Both the resistance function for a positive and a negative bending moment were investigated. Using a Monte Carlo simulation, the distribution of the resistance function was evaluated for the material and geometric distributions described above. This then allows to determine a mean resistance R_m as well as a scatter (here described using the coefficient of variation ν_R) of the resistance function. In order to compare the results for different reinforcement ratios (ranging from 0.1 to 1.5 %), the mean resistance was divided by the design resistance $\mathrm{M_{Rd,EC}}$ calculated according to EN 1992-1-1. This ratio corresponds to the variable ζ_R presented in the main part of this report.
To illustrate the value associated with a possible design of the section, the mean resistance is extrapolated using the coefficient of variation ν_R and $\alpha_R = 0.8$ and $\beta = 3.8$:

$$M_{Rd,SIM} = R_m \cdot \exp(-\alpha_R \cdot \beta \cdot \nu_R) \tag{45}$$

This value does not correspond directly to a design value, since the resistance sided model uncertainties are not considered here, but put into perspective the influence of the scatter on the resistance functions.
The results are illustrated in Figure 81. The results lead to the following observations:

- An increase of the reinforcement ratio leads to an increase of the mean resistance. A higher reinforcement ratio activates a larger amount of the concrete zone in compression to reach equilibrium. Since the ratio between mean resistance and nominal (or design) resistance is larger in case of concrete compression compared with the yield strength of reinforcements, this increase of ρ_s leads to a higher mean resistance. Contrary, the mean resistance of sections with small reinforcement ratios are very close to the mean resistance of the reinforcement. This is illustrated in Figure 81 with the point-dashed lines.
- The negative bending moment resistance is more sensitive to an increase in the reinforcement ratio than the positive bending resistance. For example, for material scatter according to JCSS, the mean resistance of the positive bending moment increases from approximately 1.25 to 1.27, whereas the increase for the negative bending moment is from 1.30 to 1.45. This discrepancy can be attributed to the geometric characteristics of the t-beam section. With its broader top flange, the leaver arm is only minimally affected in case of compression at the top. Contrary, the leaver arm undergoes a significant decrease when the required compression zone in the web is increased.
- Based on the previous findings, the probabilistic resistance parameters for slab bridges can be concluded to correspond to a t-beam section with a small reinforcement amount. Both positive and negative bending moment resistances behave similarly due to the symmetric geometry. The same can be said for increasing reinforcement ratios.
- The extrapolation of the results to a quantile corresponding to a design value illustrates that the difference between the assumptions of the material properties decrease, while the difference between positive and negative loaded sections remains. It is therefore sufficient to differentiate between a positive and negative bending failure mode. Since the model uncertainty is not introduced in this investigation, it is reasonable that the extrapolated design value lies above of $M_R/M_{Rd,EC} = 1.0$.

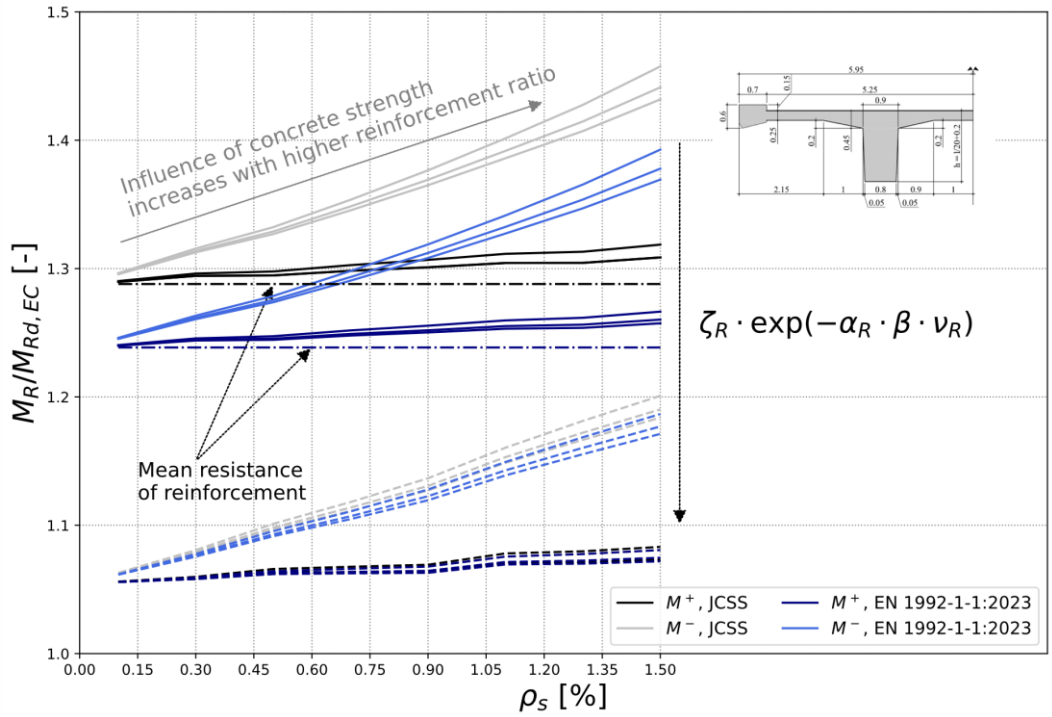

Figure 81: Probabilistic bending resistance of T-beam section

Composite steel-concrete section bending resistance

A similar analysis was performed for the positive and negative bending moment of the composite cross-section. The reinforcement ratio of the section was varied for typical cross-section configurations of composite bridges with spans between 40 and 60 m. Probabilistic input parameters based on (JCSS Probabilistic Model Code - Part 3: Material Properties, 2000) and EN 1992-1-1:2023 for the concrete and reinforcement bars were chosen. The results illustrated in Figure 82 highlight, that the overall results lie in the range of $\zeta_R = 1.25 \div 1.30$ and $\nu_R = 0.05 \div 0.06$.

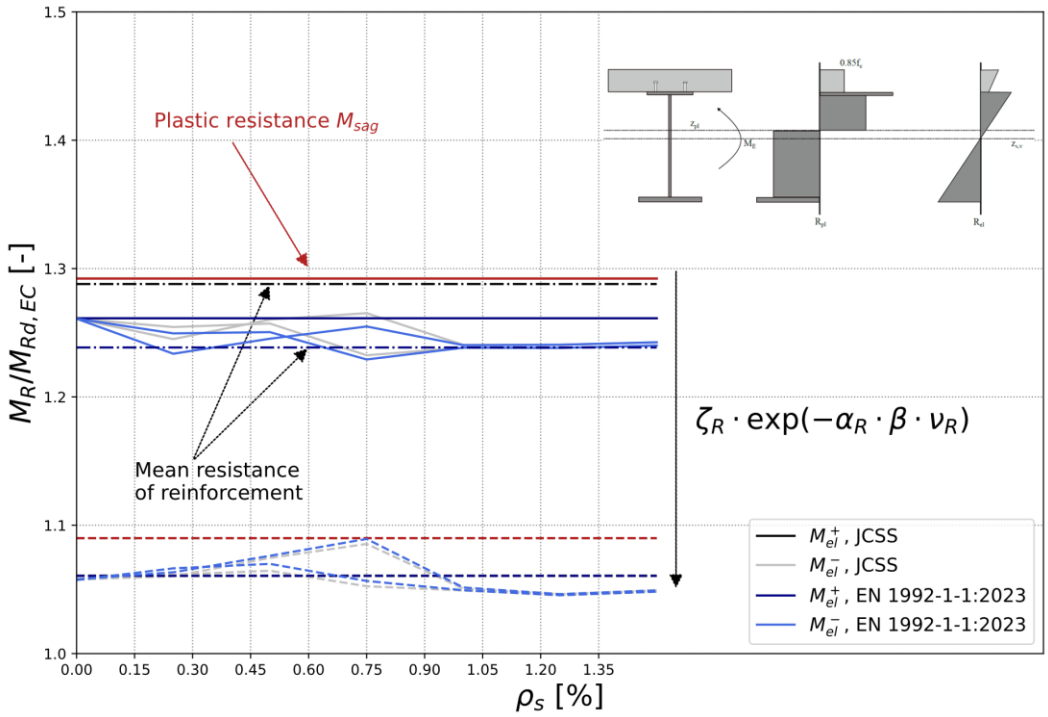

Figure 82: Probabilistic bending resistance composite girder

It can be noted that the reinforcement ratio ρ_S of the rebars inside of the concrete slab only have an influence on the negative cross-section resistance due to the cracking of the concrete. Based on the typical dimensions of the girder, only an elastic evaluation was conducted for the negative bending moment case. In contrast, in the case of positive bending moment both the elastic and plastic resistance are illustrated. The different values for the scatter of the material properties influence the results only marginally. Furthermore, the difference between the results from the positive and negative bending moment resistance is relatively minor. It is therefore appropriate to assume a fixed value for the probabilistic distribution of the resistance function.

Shear failure: concrete girder

In the case of shear failure, a number of different resistance functions based on different standards were considered, in order to gain a deeper insight into the variability of the concrete shear resistance failure mode. This reasoning can be attributed to the fact that the proposed model uncertainties for the various resistance functions and sources in question do not align. The analysis was conducted using the resistance function from both the first and second generation of Eurocodes (EN 1992-1-1:2004 and EN 1992-1-1:2023), as well as the three levels of approximations LoA from the fib Model code (fib CEB, n.d.).

The results are illustrated in Figure 83 by varying the amount of shear reinforcement ρ_w.

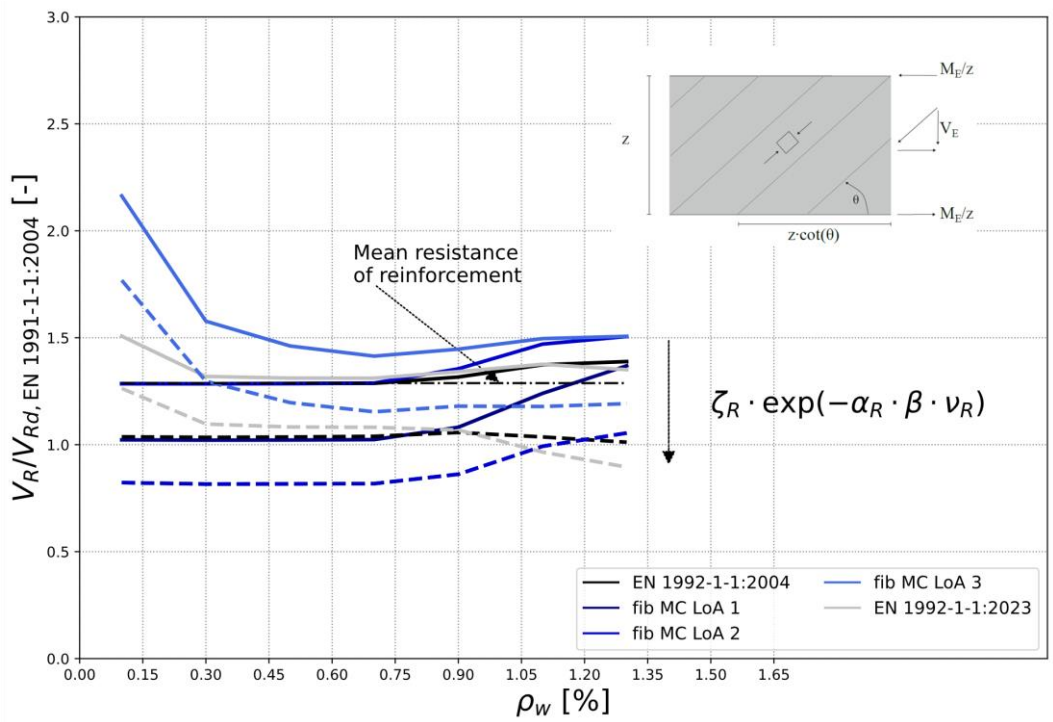

Figure 83: Probabilistic distribution of concrete shear resistance

The different investigated resistance functions do not allow for a conclusive picture for the choice of probabilistic parameters for the full-probabilistic analysis. Additionally, the results may question the applicability of the different resistance function approaches, as no clear trend is visible.
Therefore, the analysis is repeated by including the model uncertainties from Table 14. The mean value of the resistance was adapted by multiplication with the mean value of the model uncertainty:

$$\zeta = \zeta_R \cdot \mu_{\theta_R} \tag{46}$$

The scatter of the resistance function was determined by using the approach of propagation of uncertainty. Therefore, the coefficient of variation ν is computed with

$$\nu = \frac{\sqrt{\left(\mu_{\theta_R} \cdot \sigma_R\right)^2 + \left(\mu_R \cdot \sigma_{\theta_R}\right)^2}}{\mu_R \cdot \mu_{\theta_R}} \tag{47}$$

Therefore, the value associated with a possible design of the section can be computed as before:

$$R_{d,SIM} = \zeta \cdot \mu_{\theta_R} \cdot exp\{-\alpha_R \cdot \beta \cdot \nu(R, \theta_R)\} \tag{48}$$

The results are illustrated in Figure 84. While there is still a considerable scatter in the mean resistance ζ, the magnitude of the scatter for the values associated with a possible

design value is significantly smaller. This demonstrates the similarity between the approaches when referred to an extrapolated design value.

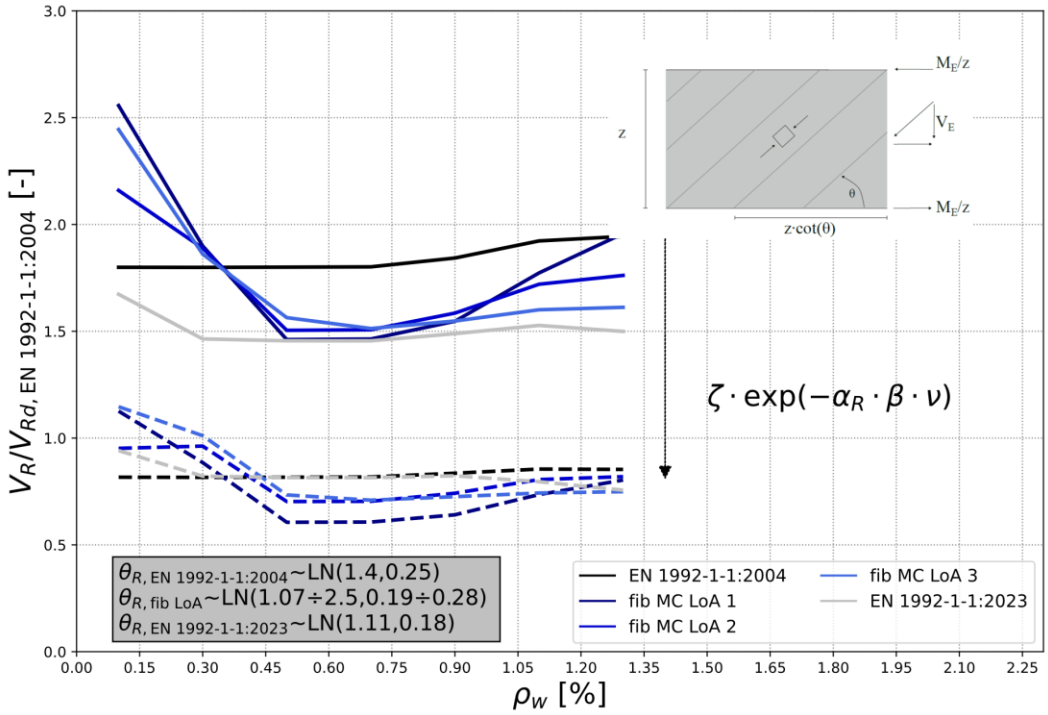

Figure 84: Distribution of concrete shear resistance, including the model uncertainty

It can be assumed that the selection of the resistance function and the associated model uncertainty will influence the results from the full-probabilistic analysis (as also illustrated in Figure 87). This influence can be attributed to the scatter of the resistance function, which is – as illustrated in Figure 84 – highest for the Eurocode resistance function first generation (EN 1992-1-1:2004) and lowest for 2nd generation EN 1992-1-1:2023.

Shear failure: composite girder

In accordance with the provisions from EN 1994-2, the concrete slab resistance is not included in the calculation of the shear resistance of a composite girder. Consequently, the resistance function is reduced to that of a pure steel girder. Recent studies (for an overview of the performed studies and resistance model propositions see (Nascimento & Pedro, 2019)) have demonstrated that in cases where the concrete can be assumed uncracked (e.g. in regions with pure shear loading or in case of positive bending moment), the concrete slab can account for an additional part of the shear resistance. It is important to note that this effect was not taken into account in the analysis, which leads to an underestimation of the resistance.

In the case of steel shear resistance, the resistance either corresponds to the cross-section resistance or a shear buckling failure occurs first. Which of the failure occurs depends on the slenderness ($\lambda = h_w/t_w$) of the section. In case of shear buckling failure, the cross-sectional resistance is multiplied by a reduction factor χ_w according to EN 1993-1-5. The shear reduction factor dependents from the geometry (or slenderness) of the web and the corresponding material parameters.

In the absence of shear buckling, the probabilistic distribution of the resistance function can be estimated directly from the distribution of the yield strength. However, this is not the case in the case of local buckling, as the shear resistance is no longer proportional to the yield strength (due to the reduction factor χ_w). Consequently, if the set of geometrical configurations results in a behaviour in the transition zone between cross-sectional and buckling failure mode, the probabilistic distribution of the resistance cannot be assigned to either of the two failure modes. This behavior is illustrated in Figure 85.

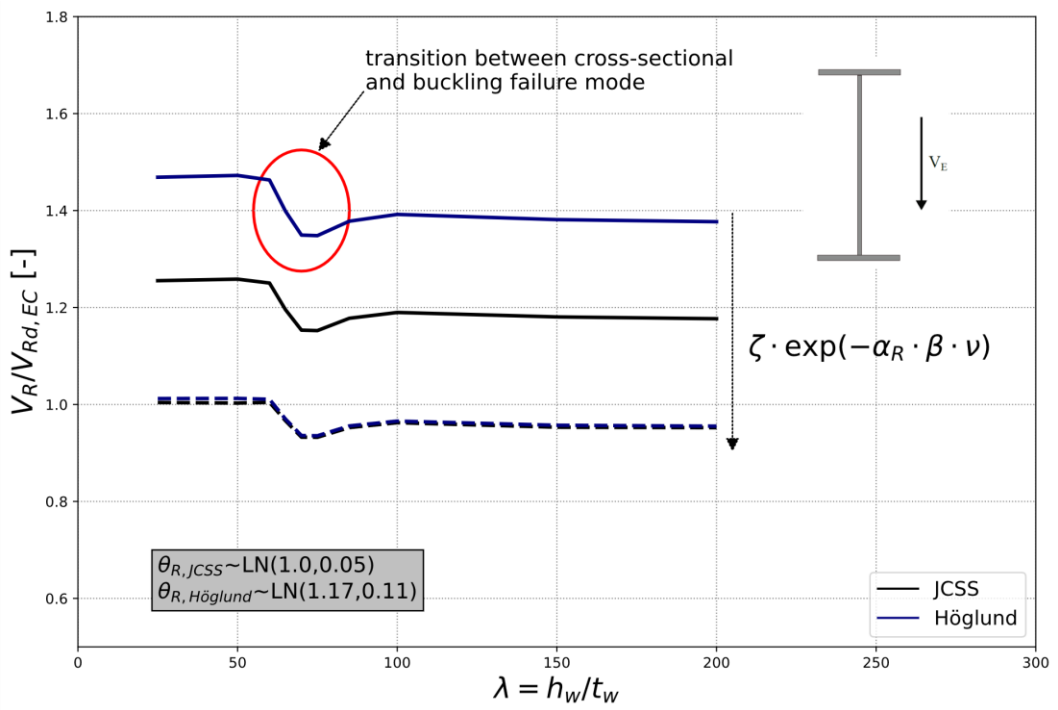

Figure 85: Probabilistic distribution of shear resistance: composite section

As with the case of concrete shear resistance, the influence of the model uncertainty is also considered here (and accounted for by the same analytical expressions ζ and ν). It can be observed that while the mean resistance $\zeta = \zeta_R \cdot \mu_{\theta_R}$ varies significantly in the two cases considered (either (JCSS Probabilistic Model Code - Part 3: Material Properties, 2000) or (Höglund)), the difference in the design values is very small. An influence in the results (as illustrated in Figure 89) can be observed due to the difference in scatter for both approaches, although this effect is much smaller in value compared to the case of concrete shear resistance. Consequently, the choice of model uncertainty has a relatively minor impact.

Summary

The preceding analysis underscores the challenge in selecting a single fixed value for the probabilistic parameters of different failure modes. It is important to note that these values depend on different assumptions from the scatter of material properties and model uncertainties. As shown for the different investigated resistance functions and failure modes, the probabilistic distribution of the resistance function is dependent on the geometrical configuration of the structure and the section. The study provides

demonstrates the influence on the probabilistic distribution of the resistance function based on the most significant properties (as reinforcement ratio and slenderness). Consequently, for the purpose of further analysis, specific values were selected as fundamental parameters for the full-probabilistic investigation, which were already presented in Table 7. Subsequent analysis will, nevertheless, demonstrate the influence of different selections of base values for the model uncertainty by means of envelope functions.

The impact of potential inaccuracies in the selection of the distribution parameters of the resistance functions on the outcome of the full-probabilistic calibration remains to be clarified. In order to illustrate schematically this influence, a parametric study was conducted. For a traffic action effect with $Q \sim G(1000, 5\%)$ and parameters for the self-weight assumed with $\lambda_G = 1.1$ and $\nu_G = 0.1$, the traffic action effects E_{calib} based on a full-probabilistic analysis were determined. To emphasise the influence of the probabilistic distribution of the resistance side, the resistance model uncertainty θ_R was maintained constant at unity, thereby excluding its influence on the analysis. The distribution of the self-weight was back-calculated by using selected values for the load ratio χ, defined as the traffic action effect / permanent loads effect.
The results for a range of values of $\zeta_R = 1.2 \div 1.8$ and the coefficient of variation $\nu_R = 0.05 \div 0.2$ are depicted in Figure 86. These results are expressed by the ratio between the calibration of the full-probabilistic analysis and the mean traffic action effects.
The results illustrate different effects:

- An increase in the mean resistance parameter ζ_R results in a reduction of E_{calib}. Consequently, the selection of lower values for ζ_R will result in a more conservative outcome. The opposite is true for the scatter of the resistance function. An increase in the coefficient of variation results in a higher value of E_{calib}. In the case of $\chi = 0.5$, this can result in a scatter between 0.75 and 1.75, which corresponds to a multiplication by a factor of 2.
- However, the influence is significantly reduced when the influence of the traffic action effect on the total loading is smaller. This is illustrated by the parameter χ, which was set at 0.5 initially and reduced to 0.25 in a subsequent calculation, thereby increasing the influence of the permanent loads. In the latter case, the results demonstrate a significantly lower scatter, with all values falling within the range of 1.0 to 1.20.
- A load factor of $\chi = 0.5$ is only attained for very small span bridges. Besides in frame bridges, this scatter effect has not been observed for the investigated parametric bridge cases.

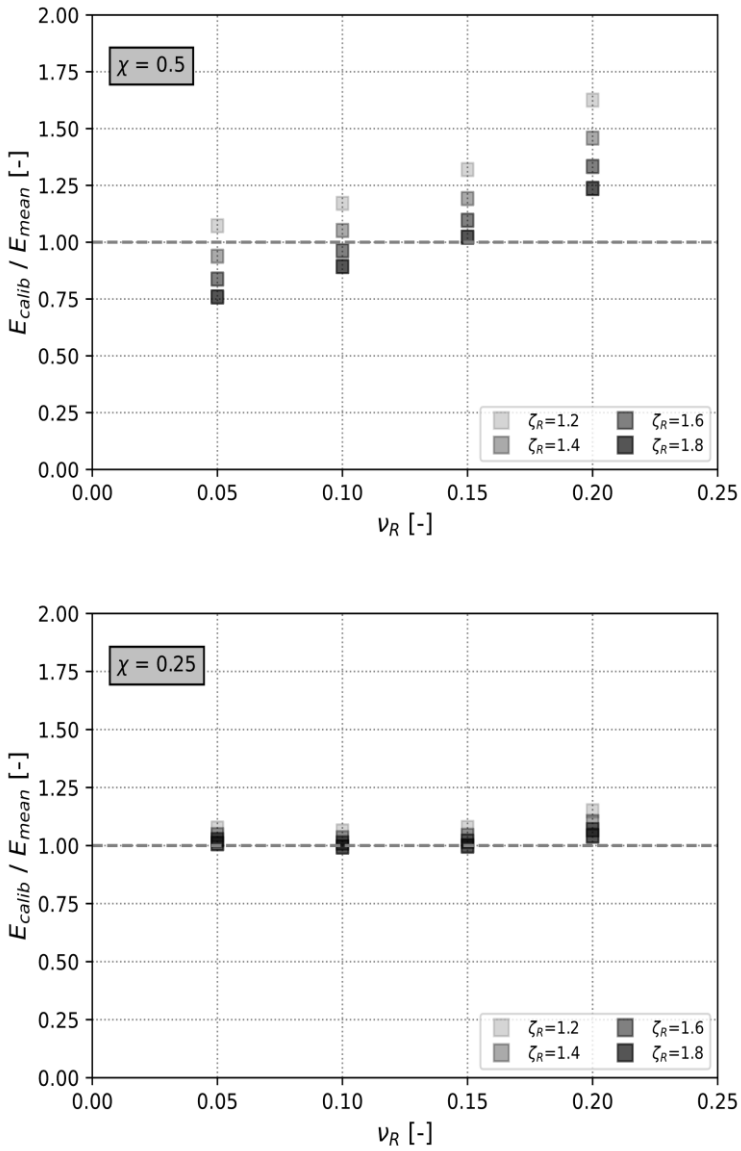

Figure 86: Influence of the choice of probabilistic resistance parameters on the traffic calibration for load ratios a) $\chi = 0.5$ and b)) $\chi = 0.25$

The influence of the scatter of the resistance function is reduced further when a resistance model uncertainty θ_R is additionally considered. Previous results indicate that the importance of both parameters (R and θ_R) on the limit state function is approximately equal, with their degree of importance varying depending on the scatter of both parameters. Furthermore, the parametric study presented above assumes for certain cases relatively high values for ν_R which were not observed in the analysis (where the values typically scatter between 5 % and a maximum of 10 %). It can thus be concluded that the maximum uncertainty resulting from the selection of an inappropriate scatter of the resistance model for the calibration of the action side is, in the majority of cases, contained within a relatively limited range.

13 Appendix D: Further bridge-specific full- and semi-probabilistic analyses

13.1 Introduction

The investigations highlighted until now give a good overview of the results and highlight the better representation using the newly proposed load model. In this chapter, the results for more specific investigations will be presented additionally. They focus on the influence of the choice of the resistance function and the effect on the load model calibration based on more representative structures.

13.2 Uncertainty in the scatter of the resistance functions

The probabilistic distributions used for the full-probabilistic analysis conducted in the main part of this study were based on the analysis presented in the previous chapter. The calculations were conducted using fixed pairs of distributions from the previous investigations. To gain a deeper insight into and highlight the impact of varying base values for the probabilistic distributions, this chapter will examine a few illustrative examples.

First, the various analytical functions and assumptions regarding material properties for the concrete shear failure mode will be investigated further. For the 5 different functions previously discussed (see Figure 84), the evaluation for a medium amount of reinforcement is presented. The envelope of the results (depicted with the variable f_Q) is illustrated in Figure 87 (for more detailed results, please consider Figure 88).

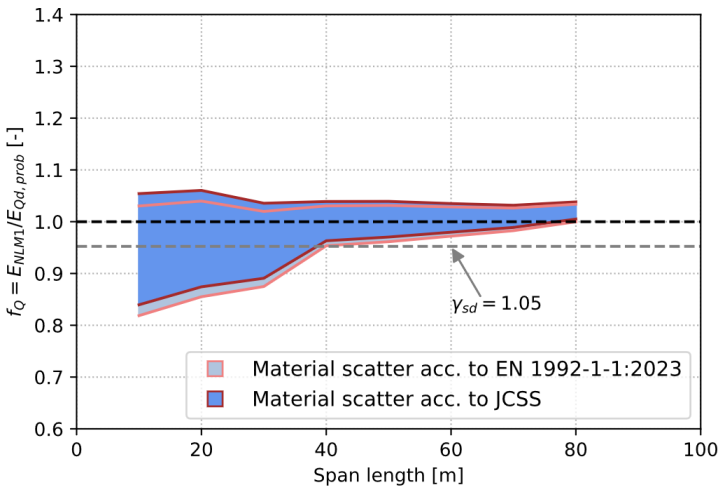

Figure 87: Envelope curve for concrete shear resistance functions

The general conclusion that can be drawn from the above investigation is that the difference in the choice of the scatter of the material parameters plays a subsidiary role as both envelope functions are very close to each other. The scatter between the results from the resistance functions results mainly from the difference in the sensitivity factors and ΔR_d from the full-probabilistic calibration. The primary cause of the discrepancies can be attributed to the scatter of the model uncertainty θ_R, influencing especially the required additional safety in the calibrated load model. It is evident that this scatter decreases with increasing span length, as the significance of the load model decreases in the limit state function. These findings also lead to the conclusion that particular caution is essential in the case of examination of small span bridges.

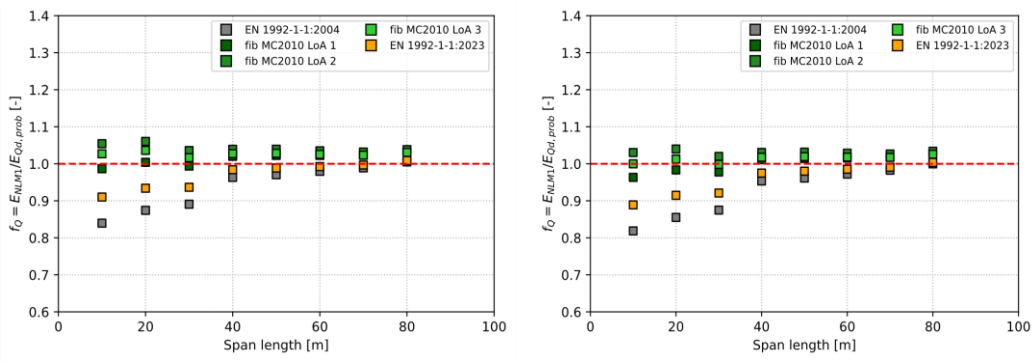

Figure 88: Accuracy of different concrete shear resistance failure modes (left: JCSS, right: EN 1992-1-1:2023)

Similar conclusions can be derived in the context of composite shear resistance (see Figure 89). However, the scatter is not as substantial as that observed in the case of concrete shear failure modes, which decreases rather moderately with increasing span length. This is primarily because the sensitivity factors of the resistance function (as well as of the resistance model uncertainty) are rather small and thus have a smaller influence. Moreover, the resistance function itself is already more consistent within the probabilistic framework, which results in a lower correction term ΔR_{d}.

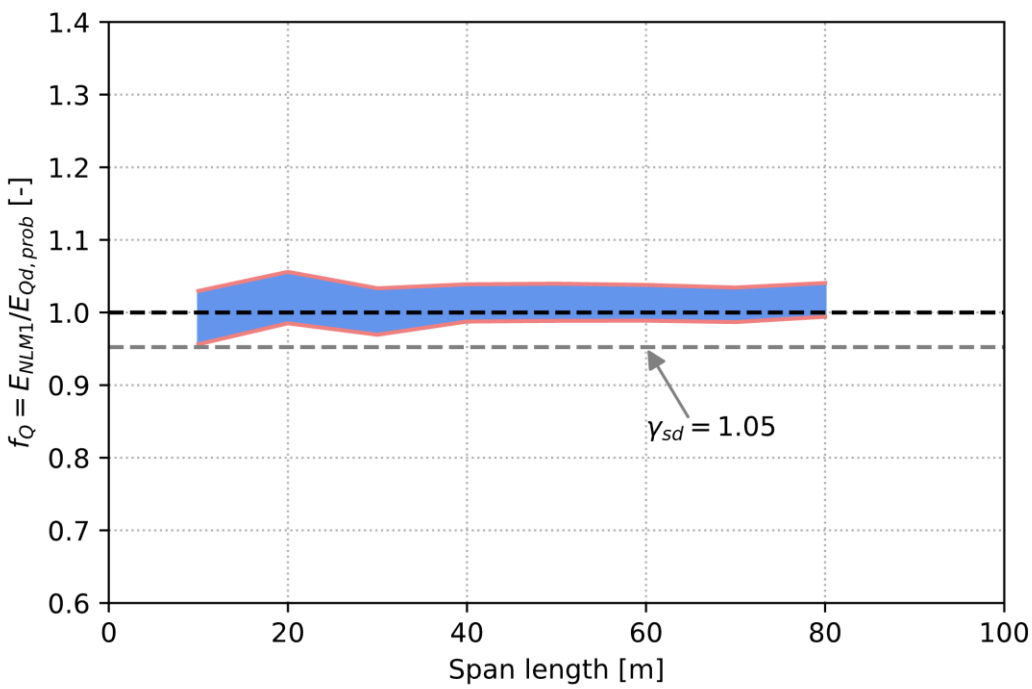

Figure 89: Envelope curve for composite shear resistance functions

13.3 Investigation of parametric bridges

13.3.1 Swiss bridge data base

To gain a better overview of the highway bridges present in Switzerland, the research team was provided by OFROU with a database comprising of information concerning bridges on the Swiss highway network. Some minor adaptions were made in response to identified inconsistencies in the database. This analysis enabled a more precise identification of relevant structures worthy of further investigation. The following section presents a selection of evaluations derived from the data.

Figure 90 depicts the erection year of the Swiss highway bridges, which highlights the fact that most of the bridges in the inventory are 50 years old or more.

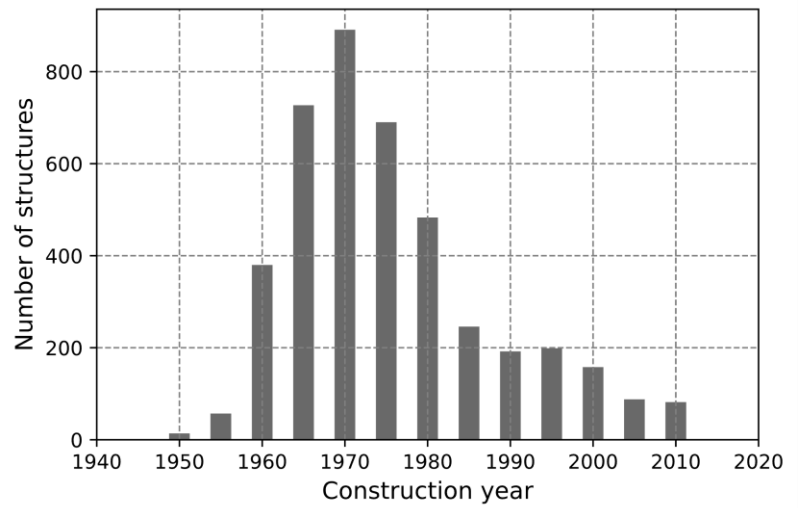

Figure 90: Distribution of erection of Swiss highway bridges

The provided database differentiates between girder bridges, frame bridges and slab bridges. The girder bridges are further divided into single and multi-span bridges, thereby indicating the number of spans of the bridges.
Of particular interest for the investigation was the span length, which was determined for the different types of bridges in the subsequent figures (see Figure 91 to Figure 94).

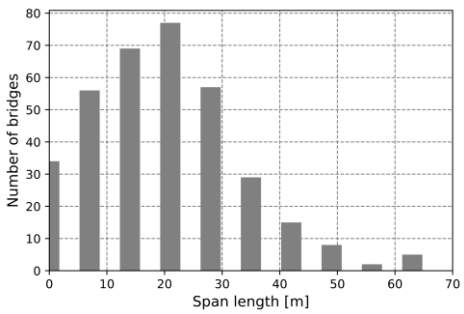

Figure 91: Distribution of span length for single span girder bridges

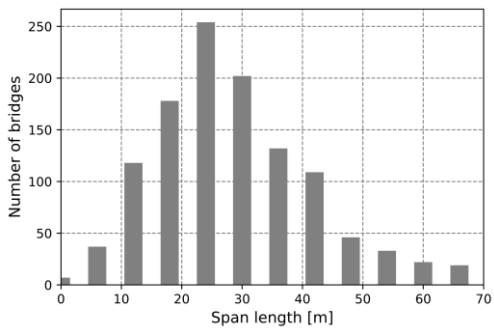

Figure 92: Distribution of span length for multi-span girder bridges

The differentiation between single and multi-span girder bridges demonstrates that there is an increase of span length for the multi-girder systems. This is to be expected, given that the interior supports act as a form of restraint, reducing the sagging bending moment and allowing for longer spans.
In the case of frame and slab bridges, much smaller span lengths are to be expected (Figure 93 and Figure 94).

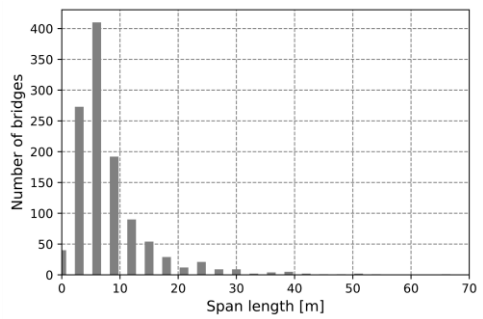

Figure 93: Distribution of span length for frame bridges

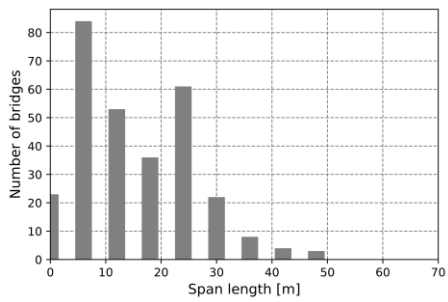

Figure 94: Distribution of span length for slab bridges

The data indicates that most slab bridges act as single span bridges. Based on the number of bridges, most of them are either multi-girder or frame bridges.
In addition, the database includes information to other types of bridges. These were not included in this study as the primary focus was to examine the characteristics of typical bridges in Switzerland. It should therefore be noted that special bridges (e.g. special constructions or bridges comprising of exceptionally long spans) fall outside the scope of this project and require a separate consideration.
Figure 95 and Figure 96 illustrate the distribution of the construction material in relation to the span length, with a distinction made between concrete and composite structures. The y-axis of the histograms indicates that most bridges are composed of concrete, while the minority are steel-concrete composite bridge structures.

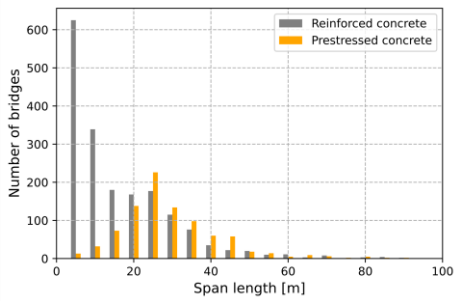

Figure 95: Distribution of span length for concrete and prestressed concrete bridges

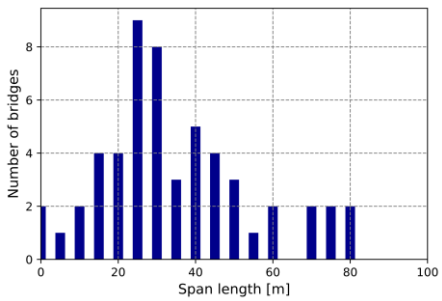

Figure 96: Distribution of span length for steel-concrete composite bridges

Not surprisingly, reinforced concrete structures are employed especially for small and medium span bridges, whereas prestressed concrete is used for longer span bridges. In a similar manner, steel-concrete composite bridges follow a comparable trend to that observed in prestressed concrete bridges. It is important to note, however, that the material alignment based on the database is not always consistent. In certain cases, bridges are classified as prestressed concrete bridges even when they are prestressed exclusively in the transverse direction.
One significant deficit in the database is the absence of cross-sectional properties. This was addressed by utilising typical values for the cross-section provided by literature in function of the longitudinal system (span length, number of spans, width of the bridges, etc.). Typical values for concrete bridges are tabulated for example in (Bergmeister et al., 2010).

13.3.2 Additional investigated parametric bridges

In addition to the bridges presented in chapter 4, which represent a diverse variety of bridges present on the highway, further bridges were selected to facilitate a more comprehensive understanding and investigation of specific behaviours.
In addition to three concrete bridge types, a composite bridge type was investigated as well. The general information is depicted in Table 16. The bridges are based on parametric models, which enable the modelling of bridges with varying spans.

Summary of parametric bridge models

Type number	Material	System	Cross-section	# Spans	Span length [m]
1	Reinf. Concrete	Frame bridge	Slab	1	10, 15
2	Reinf. Concrete	Girder bridge	Twin-Girder	4	18, 25, 32
3	Prestressed Concrete	Girder bridge	Box-girder	4	40, 50, 60
4	Steel-concrete composite	Girder bridge	Twin-Girder	3	40, 60

Table 16: Summary of parametric bridge models

In addition to straight frame bridges, investigations were conducted on bridges inclined by 30° and 45°. This demonstrated the influence of the skewness of bridges on the load model. Further data and images of the bridges are given in Figure 97 to Figure 100.

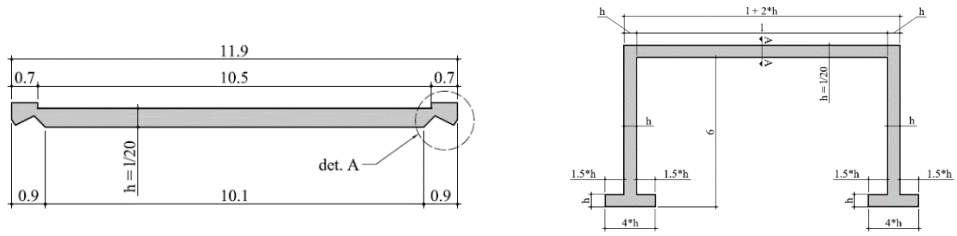

Figure 97: Parametric portal frame bridge

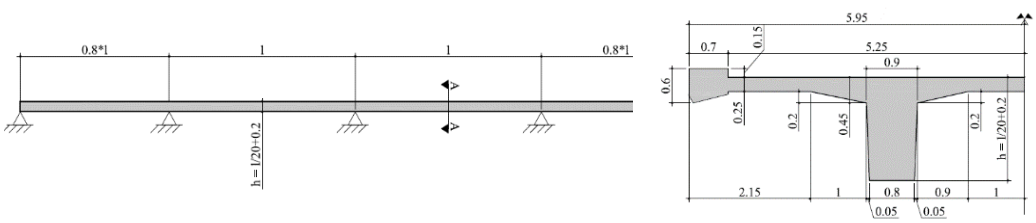

Figure 98: Parametric T-beam girder bridge

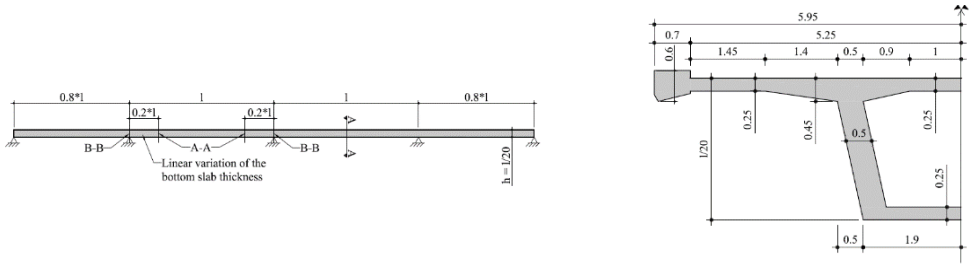

Figure 99: Parametric box girder bridge

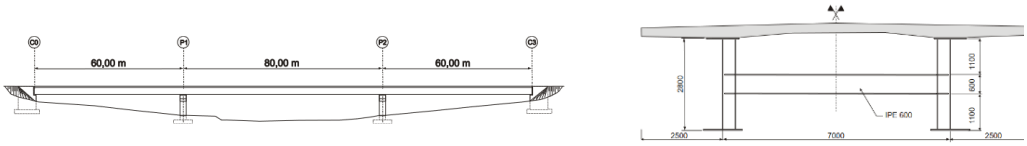

Figure 100: Parametric composite bridge

The investigations of the probabilistic distribution of the resistance functions (see chapter 12.2.4) were based on the cross-section properties of these parametric example bridges.

13.3.3 Structural models of bridges

The bridge models were represented using influence lines, as was the case for the generic models investigated previously. The bridges were based on shell and beam models represented in the software SOFiSTiK (see Figure 101). The software SOFiSTiK was selected for its parametric representation of the bridges using a text editor. Additionally, the software can be activated directly via the command prompt and has a link to python-scripting, which allows for more efficient and automated use of the software, especially for determining results for a multiple number of systems.

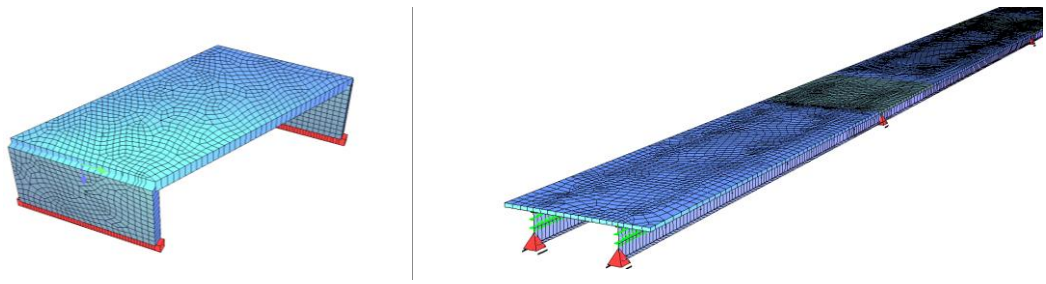

Figure 101: SOFiSTiK bridge models of frame bridge (left) and composite bridge (right)

The software SOFiSTiK includes an integrated tool that enables the direct evaluation of influence lines and surfaces. As demonstrated in (Vorwagner et al., 2024), it is feasible to generate influence lines and surfaces in a systematic way through the utilisation of this in-built function. To obtain a regular grid of data points, a second algorithm must be employed, allowing to interpolate the results at the required positions. This function presents a significant challenge when investigating influence surfaces based on shell element models. The manual explicitly states that this built-in function should not be used for such elements (SOFiSTiK AG, 2023). Accordingly, an alternative

approach was selected, whereby the influence line was determined by placing a point load at different positions on the bridge and evaluating the action effects at the points of interest. A built-in integration function of the software SOFiSTiK was then used to obtain reaction forces based on beam-like elements instead of shell elements. Although being less efficient than the in-build function, this approach allowed to eliminate some problems, leading to promising results.

The findings presented in the chapters above can thus explain the slightly different behaviour of the results, if the bridges from Table 16: are selected for the analysis. Here, an example traffic was selected which was based on the simulations from the station Oberbüren 2011. The overview of the results is depicted in Figure 102.

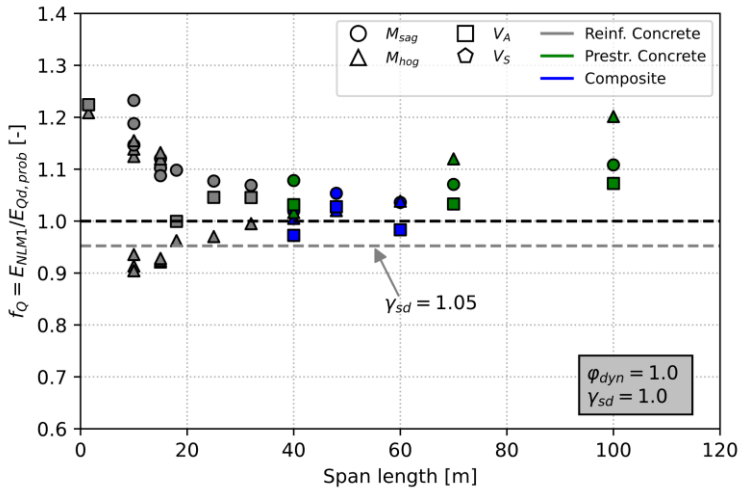

Figure 102: Difference between full-probabilistic results and semi-prob calibrated load model

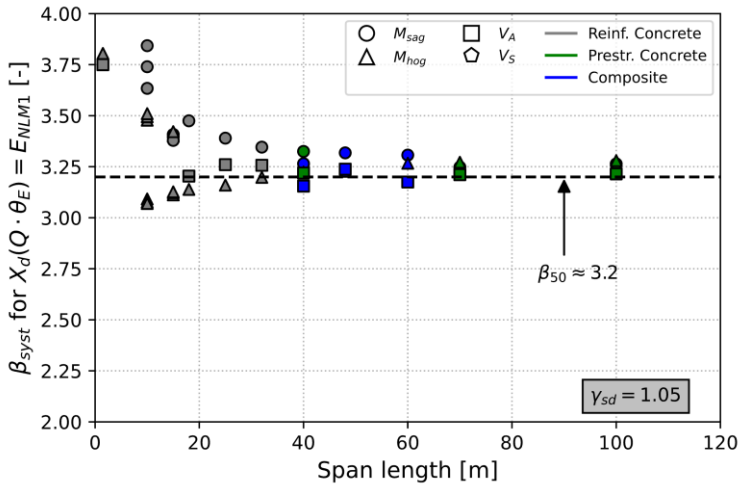

Figure 103: Reliability index based on calibrated NLM1 for further bridges

A comparison of the results with the more accurate representation of bridges from Table 16 reveals the following conclusions:

- An increase in the number of spans (especially for longer spans) results in an over-conservative representation of the load model. The objective of maximising the action effect of the load model implies that sections of the structure that would

otherwise have a reduction effect on the action effects, are not loaded. Nevertheless, this does not reflect the actual behaviour of the traffic. A potential solution to this problem is presented in chapter 13.5.

- Small span bridges (with L < 20 m) undergo a higher scatter than longer spans bridges. This phenomenon has previously been observed for the performance of the load model for generic bridges (see Figure 38). This effect can be explained partially by the impact of the transverse influence line. A more detailed examination of this problematic will be provided in chapter 13.4.
- Most of the results are situated above or in close proximity to the partial safety factor of γ_{Sd}, therefore reasoning this choice. The apparent unsafe design of certain portal frame structures will be discussed in greater detail in chapter 13.4.
- The investigated traffic is based on traffic simulations from the station Oberbüren, which represents one of the most critical instances. Consequently, the results can be applied to structures based on other sections, resulting in higher safety margins.
- Figure 103 illustrates that the overall safety of the systems is in good agreement with the target reliability. This also demonstrates that the relative error of the system is small. This can be attributed to the fact that the general bridge systems may include certain unrealistic combinations (e.g. very small composite bridges) with smaller safety margin, which are not considered in the parametric bridge analysis.

13.4 Skewed frame bridges

The analysis of generic bridges, as well as the investigation of further parametric bridges (chapter 13.3), reveals that particular attention should be devoted to short-span bridges. Consequently, portal frame structures were of greater interest, both for frame structures with straight and inclined bearings. The bending and shear influence lines situated for a lane positioned in half of the width of the bridge are illustrated in Figure 104. The influence lines were evaluated for structures with an inclination of 0°, 30° and 45°. The form of the influence line for positive bending moment and shear force resembles the shape of the influence line for single span structures. However, the influence line for the hogging moment – in this case evaluated at the bearing of the structure – resembles one half of the negative moment influence line of a two-span bridge. In general, the shape of the influence lines with inclined bearings is similar to that of the straight ones, but for longer spans. This is particularly evident in the positive bending region (top left of Figure 104).

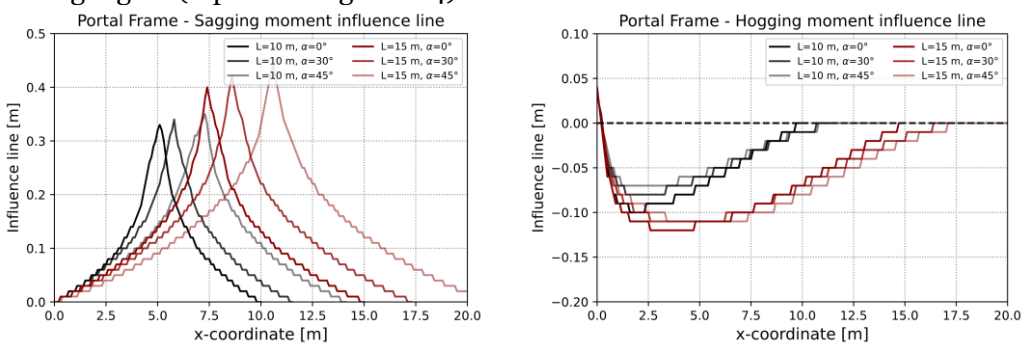

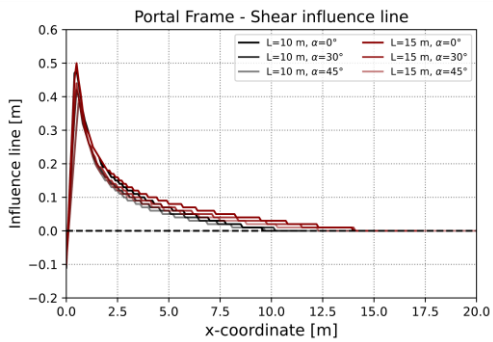

Figure 104: Influence lines of portal frames and the influence of inclined bridges

The incorporation of a second lane into the analytical framework leads to the consideration of specific effects within the analysis. In the preceding analysis, the lane configuration of the load model was based on the configuration of the traffic itself. This indicates that, in the case of a single lane configuration, the load model was positioned on the same influence line as the axle load sequence from the traffic simulation. This simplification ignores the fact that the engineer should place the load model on the bridge to reach the highest action effects. By neglecting this effect in the calibration process, the derived load model is calibrated on the safe side.
In the case of a two-lane analysis, the addressing of lane 1 and lane 2 can have an impact on the maximal action effects. This is illustrated in Figure 105, which depicts the influence lines for lane 1 and lane 2 for two portal frame bridge configurations. While the assignment of lane 1 and lane 2 is apparent in the case of the 10 m bridge, this is not so clear in the case of the 15 m bridge. It is recommended that both configurations should be assigned lane 1 correspondingly to investigate, which configuration leads to the highest action effects. It can be demonstrated that this effect is especially relevant in the case of negative bending moment for inclined frame bridges. This may provide an explanation for the apparent un-conservatism observed in the analysis of portal frame bridges (see Figure 102).

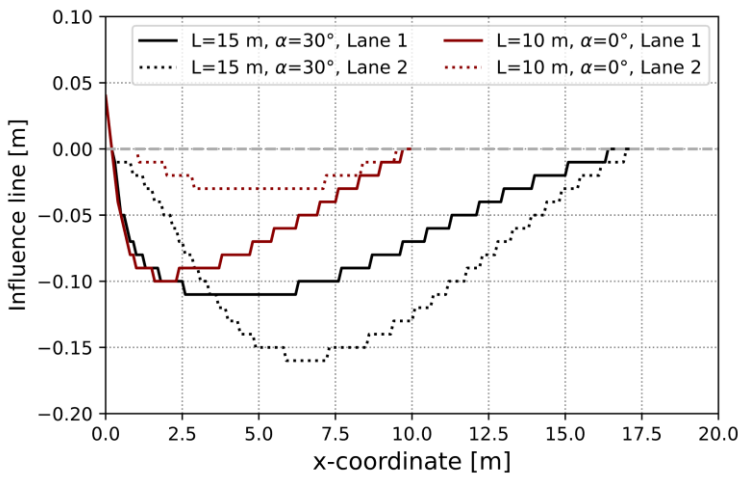

Figure 105: Influence line of second lane for frame bridges

A second lane analysis for those bridge structures for the same investigated traffic indicates that by considering the transverse effect of the frame bridges, this influence is sufficiently targeted (see Figure 106 and Figure 107).

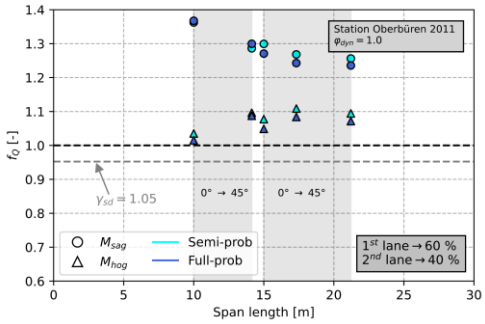

Figure 106: Second lane full-probabilistic analysis: Portal frame bridges, distributed traffic

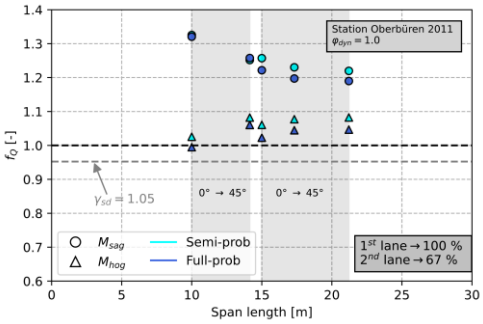

Figure 107: Second lane full-probabilistic analysis: Portal frame bridges, increased traffic

13.5 Influence of number of spans

In the general analysis presented in the main part of this report, only the most critical cases of span configurations were considered. Therefore, the selected bridge configurations consist of single span bridges in case of bending and shear as well as two-span systems for negative bending moment. In the event of considering more adjacent spans, a distinct amount of conservatism can be noted with increasing span (see the results for box girder bridges in Figure 102). The traffic load model is placed in the most unfavourable position on the influence line. Sections of the bridge that would lead to an unloading or reduction of the maximal action effects are not loaded. However, this limitation does not apply to the calculation of traffic action effects based on traffic simulations. As the total length of the bridge increases, the probability of axle loads occurring in unloading spans during maximal action effects rises. Consequently, the traffic load model for action effects for multi-span girder bridges tends to be conservative. This discrepancy in the influence lines and the appearance of unloading sections is demonstrated quantitatively for a box girder bridge in Figure 108.

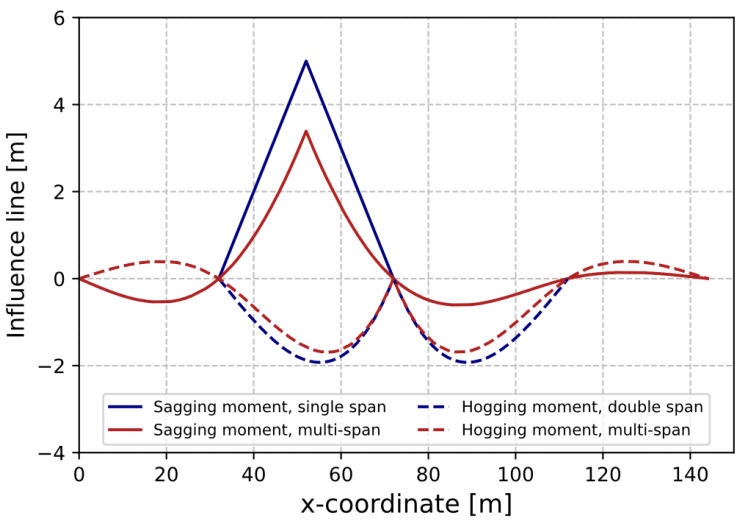

Figure 108: Comparison of bending moment influence line

The shape of the influence lines in Figure 108 demonstrates that, particularly in the case of positive bending moments, a lower maximal moment is reached when the unloading sections of the structure are loaded. This serves to confirm the presence of additional safety for the examination of more realistic bridges comprising of multiple spans when subjected to the new developed load model.
To investigate the behaviour of box girder bridges with varying spans (40, 70, 100 m), an exemplary axle load sequence derived from traffic simulations was used to derive the design values for the traffic, both for the single span bridges as well as for the multi-span systems.

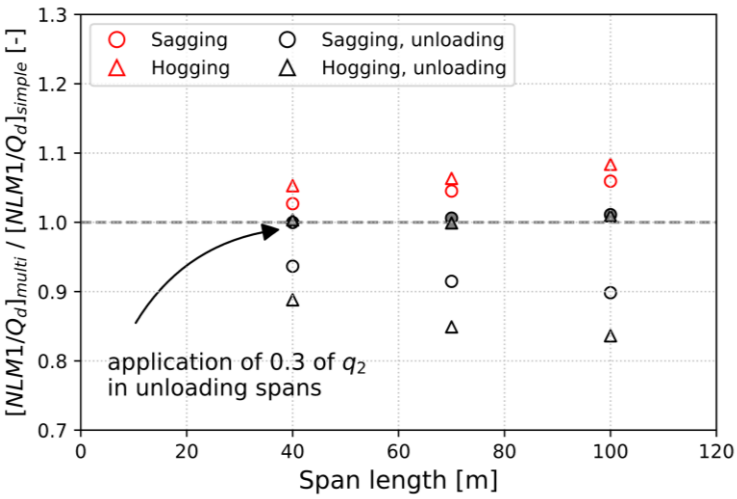

Figure 109: Comparison of simple vs. multi-span systems

Figure 109 illustrates the results of the investigation into the influence lines, expressed as a ratio of fulfilment between the multi-span bridge girders and the more simplified systems. In this context, the term “simplified” refers to the single span and two-span bridge structures that have been used for the representation of the most critical bridge cases, which have been applied for the general calibration of the load mode.
This comparison is illustrated by the red data points in Figure 109. The additional safety margin resulting from this representation is in the range of 5 to 10 %. In this instance, the unloading sections of the multi-span system are not subjected to loading by the traffic load model.
In contrast, the white data points marked with “unloading” represent the results in which the traffic load model is applied to the structure in both the loading and the unloading sections. It can be observed that this representation overestimates the traffic present in the unloading sections. The unloading of the structure is excessive, which would yield unconservative results (up to nearly 20 %).
A more appropriate representation would be one in which the distributed load in unloading spans is reduced, yet not entirely disregarded. For the bridges examined in Table 16: , a more accurate approximation of the traffic would be approximately 30 % of the distributed load q_2 in the unloading regions of the bridge, under both positive and negative bending moments.

14 Appendix E: Benchmark cases of WIM data for traffic simulations

14.1 Analysis of traffic and inputs of traffic

The truck databases used to construct the probabilistic traffic models are based on the Swiss WIM measurements. The WIM database includes axle weight and spacing data for each measured truck. To define the probabilistic traffic model, the trucks are categorized into 13 truck types.

Herein, a specific station and year is used as an example, namely **Ceneri 2018**. The heavy vehicles categories are the same as the ones defined by Meystre and Hirt (Hirt & Meystre, 2006a) except that, as in (Meystre et al., 2014b) and (Documentation ASTRA 82001, 2025), the Type-23 is added, giving a total of 13 heavy vehicles types. To these, one can add the different cranes types, i.e. 60, 72, 84 and 96 tons. The ranges for each axle weight and spacing are defined, so that each heavy vehicle could be slotted into one of these types. Given the enhanced treatment of the data, there are only few % of vehicles that remain unclassified and it was chosen to delete them.

Figure 110 shows samples of gross vehicle weight (GVW), axle weight and spacing data for truck Type 113a. The distance between axles or group of axles (the base point for an axles group is the location of the first axle) is defined with Beta distribution function.

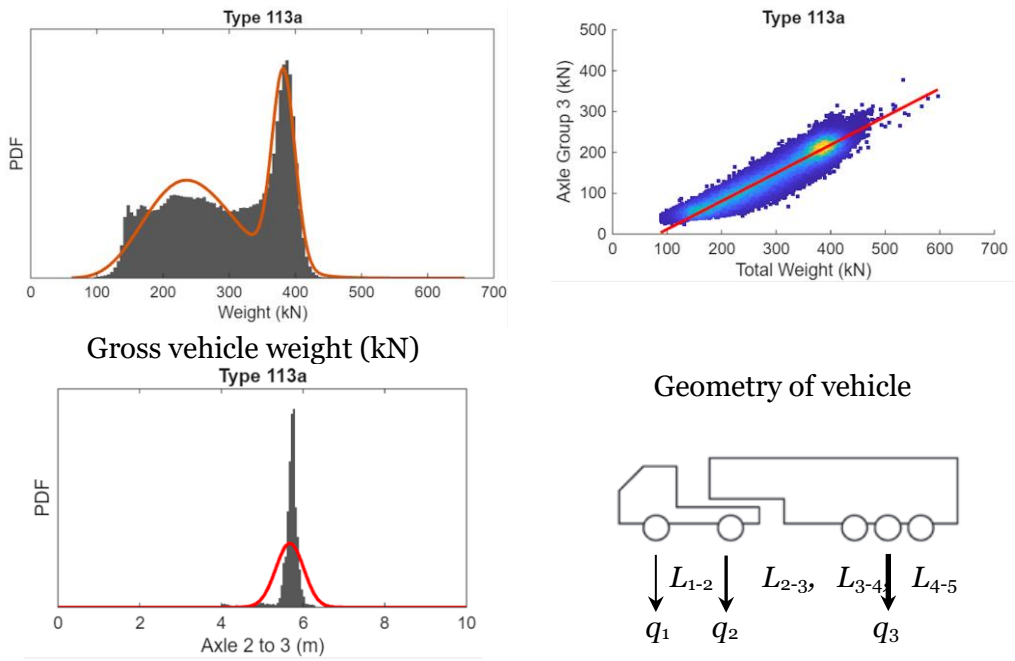

Figure 110: Sample of statistical analysis of data from the Ceneri traffic 2018, heavy vehicle type 113a

To define the trucks GVW, the bimodal Beta distribution is used and often has two peaks because of loaded and empty heavy vehicles, and bimodal Beta distribution allows modelling these two peaks. The GVW distribution of each heavy vehicle type is shown in Figure 111. Table 17 shows the parameters of the bimodal Beta distribution for the GVW for each heavy vehicle type (only parameters for 60t cranes are given). Two parameters of the Beta distributions are fixed, the minimum is set to zero (A_1, A_2) and the maximum to 100 t (B_1, B_2).
The axles load repartition for each vehicle type is defined as a linear function of GVW. For the case of heavy vehicle type 113a, as an example, axles load repartition of the most loaded axles group can be calculated as $q_3 = a_3 \times GVW + b_3$, then the second axle load q_2 can be determined as $a_2 \times (GVW - q_3) + b_2$, and the last axle can be obtained as $q_1 = GVW + q_2 - q_3$. For the group of axles (tandem or tridem), load ratio between two or three axles which compose the group is fixed.
In addition, other histograms and fitted beta laws are given: Figure 112 shows all the axle group axle spacings, Figure 113 shows the heavy vehicles axle or axle groups weights and Figure 114 the axle groups weights linear relationships.

GVW distribution parameters of heavy vehicles from the Ceneri traffic 2018

Type	Geometry	Contribution of 2nd beta distribution [%]	1st beta distrib.		2nd beta distrib	
			α_1	β_1	α_2	β_2
11		45,34	16,90	145,29	53,23	280,41
11		45,34	16,90	145,29	177,38	500,82
12		4,08	21,35	92,78	35,08	75,17
22	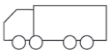	48,78	27,70	144,26	89,37	137,66
23		77,21	15,11	55,33	47,08	227,29
111		44,33	8,68	43,80	17,78	54,96
1111r		30,51	29,77	125,97	153,11	362,60
112r		55,09	15,99	57,05	85,91	138,42
1211r		36,53	19,24	54,35	646,59	1000,80
122		4,70	19,34	49,50	34,00	63,35
1112r		43,48	24,88	101,30	15,56	52,46
112a		68,62	51,86	282,25	301,74	487,58
113a		33,97	10,15	30,69	12,94	21,71
123a		61,84	27,95	93,20	297,26	108,83
14 (cranes)		79,89	30,23	22,58	53,23	280,41

Table 17: GVW distribution parameters of heavy vehicles from the Ceneri traffic 2018

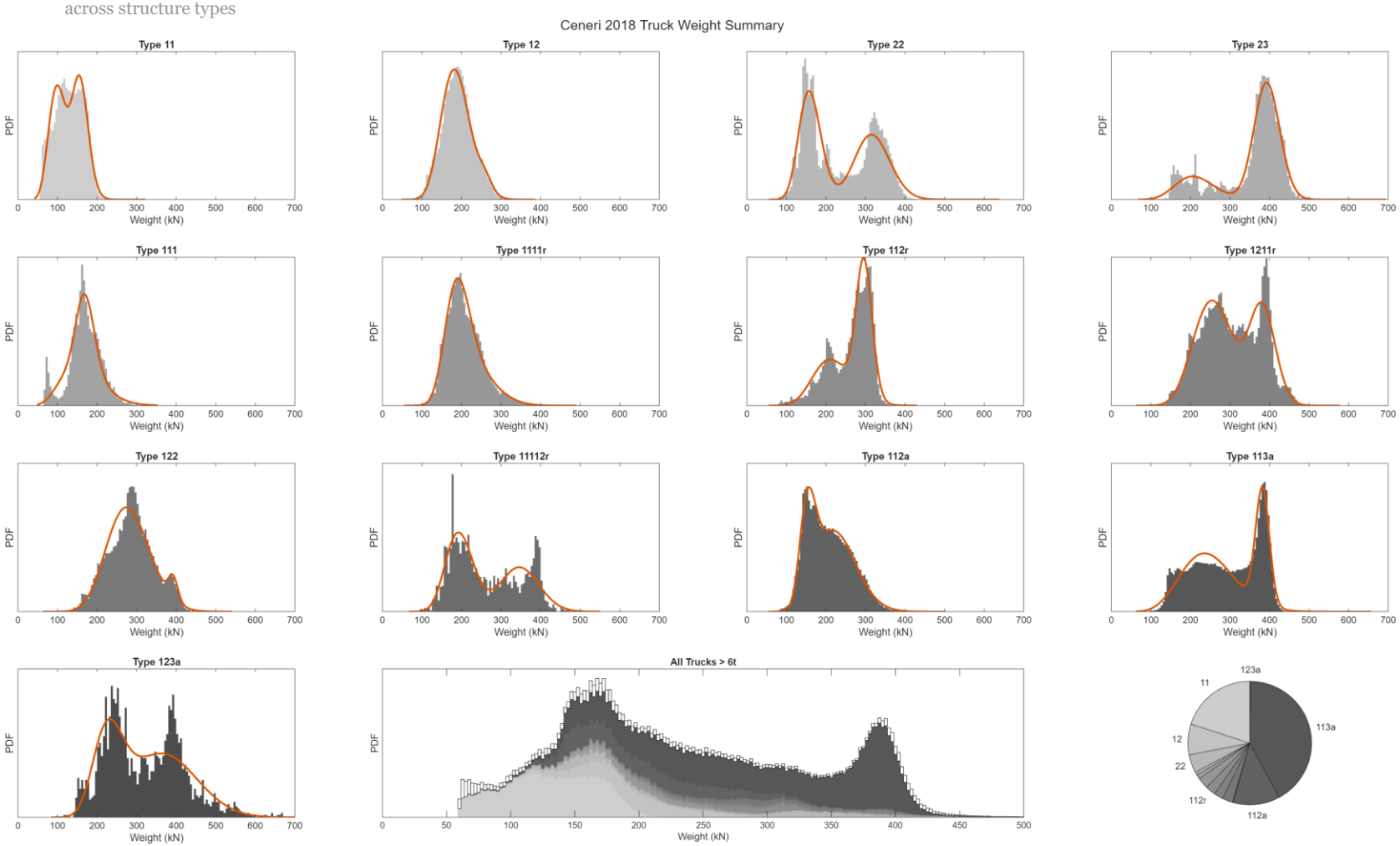

Figure 111: GVW distribution of each heavy vehicle type from the Ceneri traffic 2018

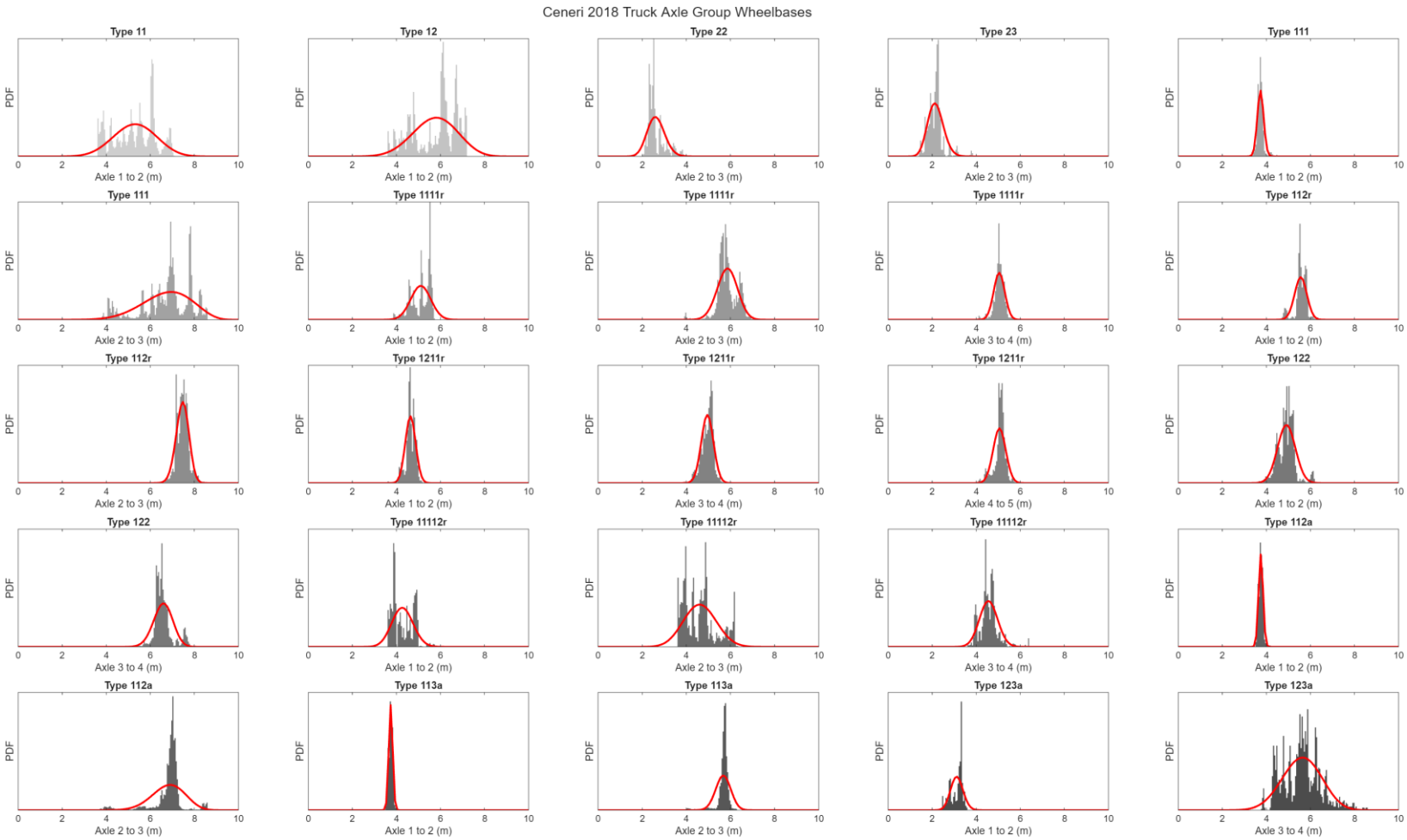

Figure 112: Heavy vehicles axle or axle groups spacings distributions for all types from the Ceneri traffic 2018

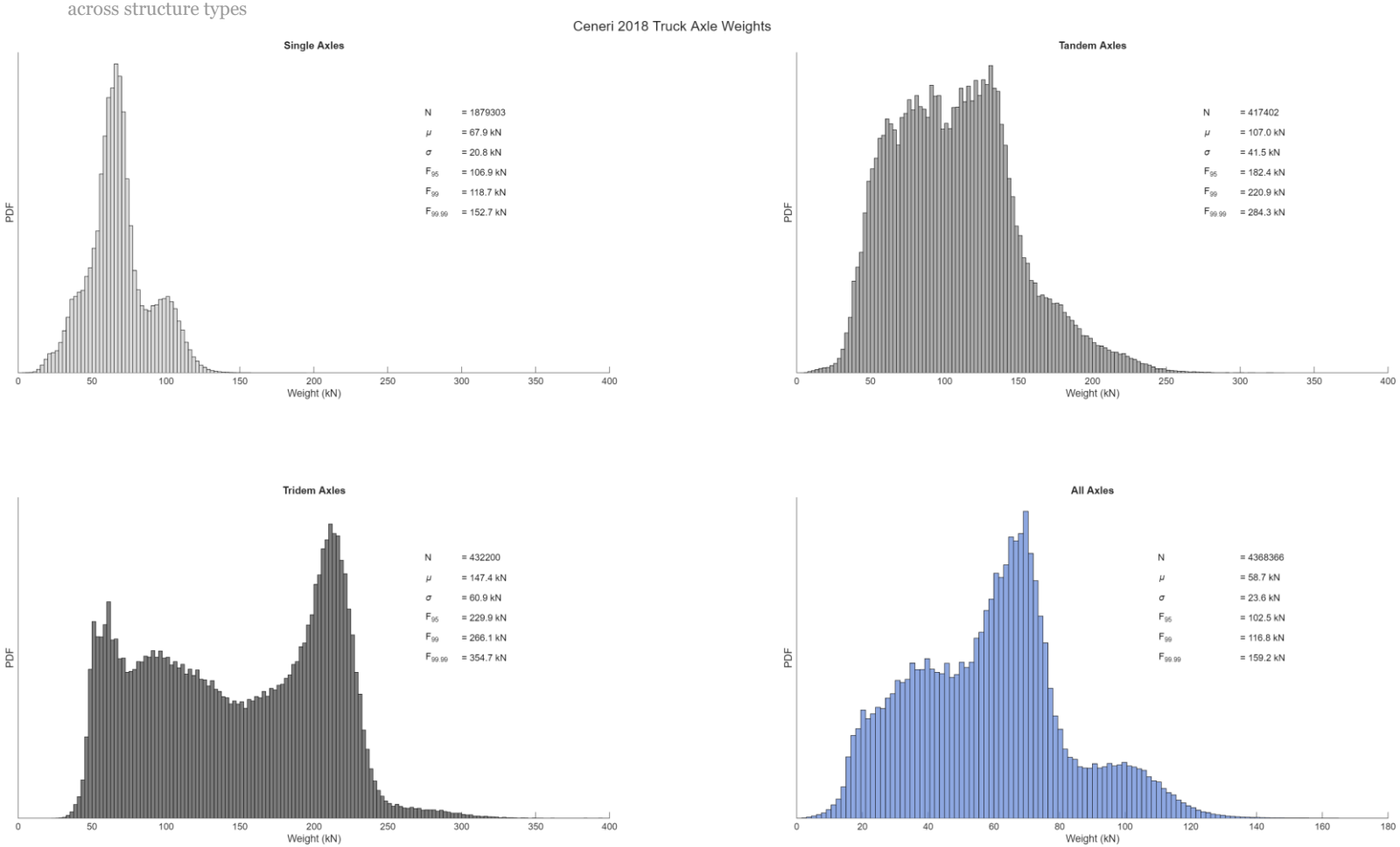

Figure 113: Heavy vehicles axle or axle groups weights distributions, all types combined, from the Ceneri traffic 2018

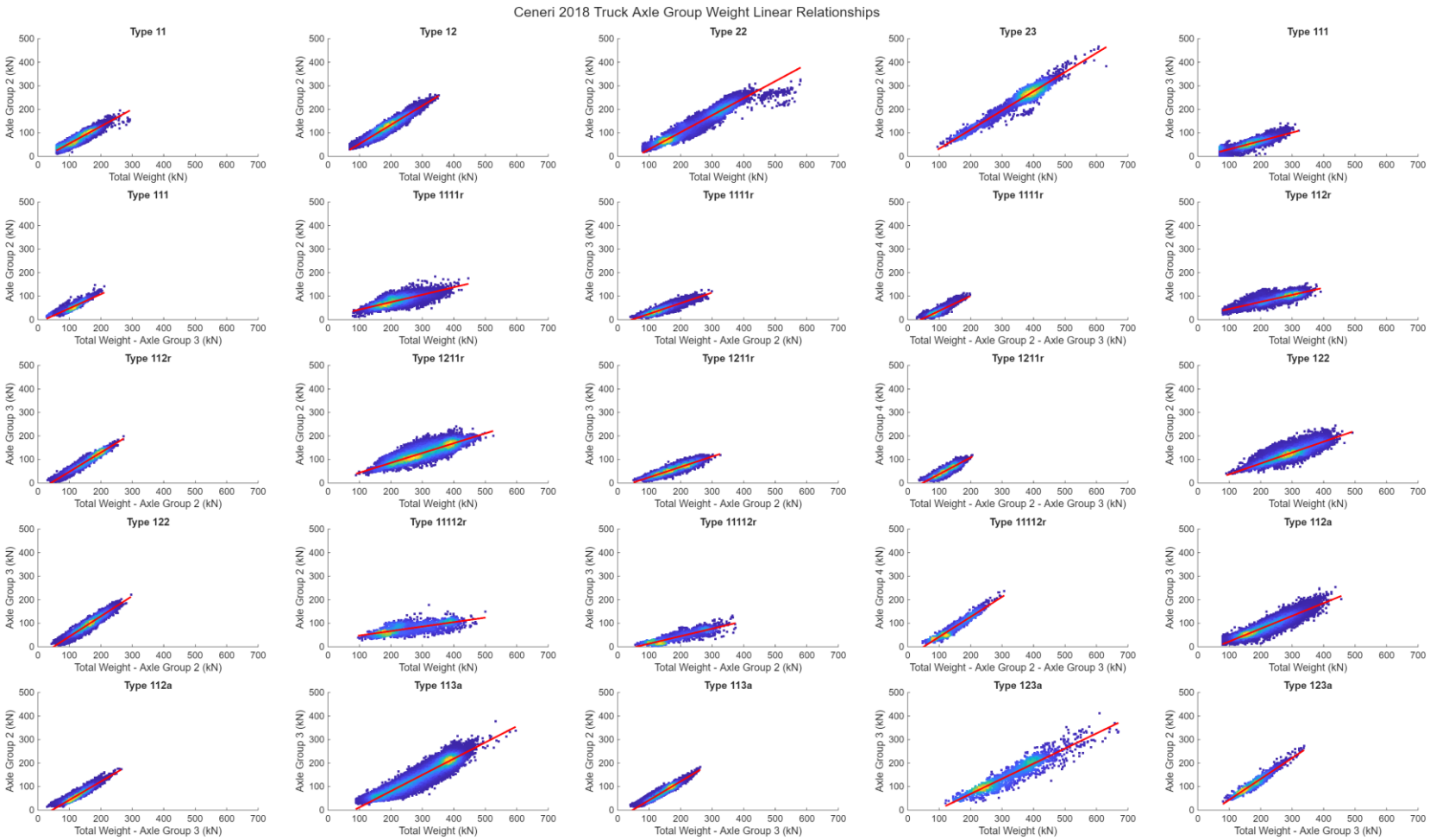

Figure 114: Axle groups weights linear relationships for all types from the Ceneri traffic 2018

14.2 Benchmark cases

The benchmark cases consist in the publication on repository Zenodo of WIM axle sequences data and of results obtained from traffic simulations using this data and allows to:

- Ensure perenity of the work carried out for future load model revisions;
- Provide a basis for using future FEDRO WIM-data statistics reports as they become available to obtain/compare characteristic values of the variable action "$Q_{k,act}$" or of an action effect
- Provide a basis for using different data, such as REAL-LAST axle loads sequences;
- To validate other developed codes for simulating traffic on a bridge to get actualized design action effect values, $E_{d,act}$.

The full description of the benchmark cases is available in a separate short EPFL research report (Mathevet, Miglietta & Nussbaumer, 2026b).

Use of Data

The data used in this project are the records from WIM stations owned by FEDRO as well as, for selecting the recording period and quality, the data of the calibrations regularly carried out at each of the station. This is the fundamental source of data utilised in this study, as well as in previous ones (Documentation ASTRA 82001, 2025). This is presented in Chapter 3 and in particular * Average over all recorded years considering all vehicles above 3.5 t (trucks). Tends to decrease over time as numbers of cars and small trucks (up to 10 t) are observed to increase faster than numbers of heavy vehicles (above 10 t)

Table 1 summarizes the details of the 8 stations selected for this study. These WIM stations have been chosen for their representativeness of the Swiss network, the quantity, recording period and quality (from calibrations, stability over time) of the recorded data. The raw data from each year and station has been screened (the terms sampling and pruning are used in the report) to compact information, eliminate errors and recognize heavy vehicles types and create files directly usable for traffic simulations.

The traffic modelling and simulations are made using an EPFL in-house developed software, programed in Matlab and stored in a Github repository. It is an open source software which access is currently restricted but can easily be made open at the request of FEDRO.

Project conclusion

Schweizerische Eidgenossenschaft
Confédération suisse
Confederazione Svizzera
Confederaziun svizra

Département fédéral de l'environnement, des transports, de l'énergie et de la communication DETEC
Office fédéral des routes OFROU

RECHERCHE DANS LE DOMAINE ROUTIER DU DETEC

Version du 09.10.2013

Formulaire N° 3 : Clôture du projet

établi / modifié le : 09.06.2026

Données de base

Projet N° : BGT_20_02C_03

Titre du projet : Updated load model for road bridges accounting for current traffic and reliability demand

Echéance effective : 30.06.2026

Textes :

Résumé des résultats du projet :

After selecting the 14 WIM stations with the best performances (representativeness, measurement quality, and long-term stability), the project developed a New Load Model (NLM1) using traffic simulations on typical FEDRO bridge types and using an iterative calibration process combining semi-probabilistic and full probabilistic methods. The methodology involved the creation of the model based on three main load types: concentrated axle loads for local verifications, groups of axle loads for longitudinal and transverse verifications of slabs or slab bridges, and sequences of axles representing vehicle lines for global verifications both for short and long span bridges (up to 80 m).
The NLM1 achieves significantly more uniform safety margins than the current code load model LM1 across all span lengths and bridge types. For single-lane traffic, it eliminates the excessive conservatism observed for short spans (<15 m) and above 30 m spans. For multi-lane traffic, the model covers extreme scenarios including the Repurpose of Emergency Lane (REL) and bidirectional configurations, as well as construction work situations. Despite many similarities, this study extends the one done for doc. ASTRA 82001, namely NLM1 accounts for traffic growth with the increase in number of heavy vehicles in lanes 1 and 2, and for more lanes (3rd, 4th …) by increasing the UDL. This however may lead in certain cases to NLM1 being less favorable than ASTRA 82001. The validity to the horizon 2050 was set because regular review of traffic development need to be made.
Key improvements include: explicit treatment of dynamic amplification factors and multi-lane effects allowing these factors to be adjusted for specific cases or revised as new findings emerge; better coverage of special vehicles such as mobile cranes not sufficiently addressed in the current LM1, and consistent reliability levels across semi-probabilistic and full probabilistic analyses.
Full probabilistic reliability analyses confirmed that the NLM1 provides a more uniform safety margin compared to previous load models and enables further improvements by investigating the reduction in scatter of action effect model uncertainties.
While primarily calibrated for existing bridges, the NLM1 could also serve for designing new bridges with additional validation. A framework based on Levels of Approximation (LoA), compatible with the current SIA 269 stepwise approach, is proposed for quantifying safety reserves between normative load models and actual traffic simulations (the NLM1 corresponding to a LoA II), ensuring practical applicability.

Schweizerische Eidgenossenschaft
Confédération suisse
Confederazione Svizzera
Confederaziun svizra

Département fédéral de l'environnement, des transports, de l'énergie et de la communication DETEC
Office fédéral des routes OFROU

Atteinte des objectifs :

This research project addressed the need to remove unaccounted conservatism in traffic load models, i.e., Load Model 1 (LM1) in SIA 269/1:2011, used for assessing existing road bridges. All research objectives were achieved:
- A comprehensive historical review of the bases and development of LM1 in EN 1991-2:2004 was completed;
- The FEDRO WIM database was thoroughly analyzed including more recent data from 2022, and algorithms were developed for performing traffic simulations to calibrate the new load model;
- Critical traffic load situations were identified probabilistically for one and two lanes across typical FEDRO bridge types;
- The NLM1 was defined and calibrated for both local and global verifications up to 80 m spans, with explicit separation of dynamic amplification factors and model uncertainty of action effects, clarifying which uncertainties are covered by each factor;
- The model was extended to double-lane traffic including REL scenarios with increased heavy traffic;
- A stepwise LoA-based procedure was proposed to quantify safety reserves between normative and simulation-based action effects, applicable to different types of FEDRO structures;
- A framework for regular traffic assumption updates in link with code revisions was established.

Déductions et recommandations :

The NLM1 represents a significant advancement over the current LM1, providing more accurate and uniform reliability levels across bridge types while removing unnecessary conservatism that leads to costly interventions on existing structures. Its explicit treatment of dynamic effects and model uncertainties enables transparent updates as new knowledge becomes available.
The authors think it is important to develop user-friendly tools for practitioners in order to ensure adoption by engineers and policymakers of the semi- and fully probabilistic methods included in the stepwise LoA-based procedure, especially since the LoA-based procedure is suitable for regular evaluation updates considering traffic evolution.
Key recommendations include: extending the NLM1 to fatigue, braking and transversal forces verifications; investigating applicability to retaining walls; expanding the WIM database to additional traffic scenarios and geographic regions, differentiating between traffic regimes; studying the impact of electric and autonomous heavy vehicles; and extending full probabilistic analyses to more bridge types.
Further research should refine dynamic amplification factors for special vehicles, investigate alternative values for the traffic sensitivity factor in semi-probabilistic analyses to reduce conservatism, and extend full probabilistic analyses to a wider range of bridge types and failure modes.

Publications :

Martinolli, S., Taras, A., Xhemsi Malja, X., Miglietta, P., Muttoni, A., Nussbaumer, A., Yu, Q. (2025). “Quantification of hidden safety reserves between different highway traffic load models based on probabilistic calibration analysis.” In: Proc. IABSE Congress Ghent 2025, pp. 58–66. Ghent, Belgium: IABSE, Zurich.
Nussbaumer, A. et al. (2026). "Examen des ponts routiers existants à l'aide de modèles de charge de trafic actualisés". Steelacademy 02/2026. 19 mai 2026 à Lausanne.

Chef/cheffe de projet :

Nom : Nussbaumer Prénom : Alain

Service, entreprise, institut : EPFL, RESSlab

Signature du chef/de la cheffe de projet :

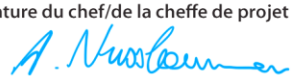

Schweizerische Eidgenossenschaft
Confédération suisse
Confederazione Svizzera
Confederaziun svizra

Département fédéral de l'environnement, des transports, de l'énergie et de la communication DETEC
Office fédéral des routes OFROU

RECHERCHE DANS LE DOMAINE ROUTIER DU DETEC

Formulaire N° 3 : Clôture du projet

Appréciation de la commission de suivi :

Evaluation :

The supervisory committee considers the results of the research project and the conclusions drawn from it as a significant advancement in the determination of traffic loads and their effects for assessment of existing bridges. The proposed new load model for vertical traffic loads, including loads from special vehicles, replicates actual traffic effects from short spans up to 80m spans significantly better than the load model currently in use, and this for single and double lane, cases with use of the emergency lane and construction works situations. The report makes a significant contribution to reducing the current conservatism and providing more uniform reliability in the assessment of existing road bridges. An algorithm is proposed that enables the calibration of the load model using fully probabilistic analyses. The report also outlines an approach for regularly updating traffic behaviour assumptions to account for their evolution, for revising the design and evaluation standards every 25 years.

Mise en oeuvre :

The report provides a detailed explanation of how the new load model was derived, thereby offering a deeper understanding of the key parameters and factors influencing current traffic load models. The report details the application of the new load model for four levels of approximation, applying deterministic, semi-probabilistic, and probabilistic methods which all provide the same reliability levels. Dynamic amplification factors and multilane effects are implemented in an explicit manner, significantly improving the accuracy of action effect predictions. These are essential prerequisites for the effective application of the new load model and the applied calibration methods in practice.

Besoin supplémentaire en matière de recherche :

The report makes nine recommendations for further research, including expanding the applicability of the new load model and developing application rules for other traffic load effects, namely: fatigue, acceleration and braking forces, centrifugal forces, and forces acting transversely. While the new load model was developed with focus on existing bridges, its application to new bridge construction should be investigated.

Influence sur les normes :

The proposed new load model is well-suited for evaluations of existing structures and has good potential for the design of new structures. It should therefore, be considered for implementation in future revisions of standards for traffic actions.

Président/Présidente de la commission de suivi :

Nom : Ganz Prénom : Hans Rudolf

Service, entreprise, institut : Ganz Consulting

Signature du président/ de la présidente de la commission de suivi :